Contribution to the development and validation of wearable-sensor-based methodologies for gait assessment and rehabilitation of people with lower limb amputation

Emeline Simonetti

▶ To cite this version:

Emeline Simonetti. Contribution to the development and validation of wearable-sensor-based methodologies for gait assessment and rehabilitation of people with lower limb amputation. Biomechanics [physics.med-ph]. HESAM Université; Universita degli studi di Roma "Foro Italico", 2020. English. NNT : 2020HESAE052 . tel-03136343

HESAM UNIVERSITÉ

Arts et Métiers
Sciences et Technologies

ÉCOLE DOCTORALE SCIENCES DES MÉTIERS DE L'INGÉNIEUR
[Institut de Biomécanique Humaine Georges Charpak – Campus de Paris]

THÈSE

présentée par : **Emeline SIMONETTI**

soutenue le : **19 novembre 2020**

pour obtenir le grade de : **Docteur d'HESAM Université**

préparée à : **École Nationale Supérieure d'Arts et Métiers**

Spécialité : **Biomécanique**

Contribution to the development and validation of wearable-sensor-based methodologies for gait assessment and rehabilitation of people with lower-limb amputation

---

THÈSE dirigée par :
Mme Hélène PILLET, M. Giuseppe VANNOZZI

et co-encadrée par :
Mme Coralie VILLA, M. Joseph BASCOU

Jury
M. Jean PAYSANT, PUPH, IRR, UGECAM Nord-Est, Nancy	Président
M. Thomas ROBERT, Chargé de recherche, HDR, LBMC, Université Gustave Eiffel	Rapporteur
Mme Laetitia FRADET, Maître de Conférences, HDR, Institut P', Université de Poitiers	Rapportrice
M. Carlo FRIGO, Professeur des Universités, DEIB, Politecnico di Milano	Examinateur
Mme Hélène PILLET, Professeur des Universités, IBHGC, Arts et Métiers Paris	Examinatrice
M. Joseph BASCOU, Directeur de recherche, INI/CERAH	Examinateur
M. Giuseppe VANNOZZI, Professeur des Universités, LBNHM, Université « Foro Italico »	Examinateur
Mme Elena BERGAMINI, Maître de Conférences, LBNHM, Université « Foro Italico »	Examinatrice

T H È S E

Acknowledgments

I wish to thank all the people who contributed directly or indirectly to the completion of this research project.

First and foremost, I am extremely grateful to my supervisors, Hélène Pillet, Elena Bergamini, Coralie Villa, Joseph Bascou and Giuseppe Vannozzi for their invaluable advices and guidance and their continuous support at every stage of this thesis.

> Coralie, thank you for your contagious enthusiasm and your warm-hearted welcome at the beginning of this journey, for your encouragements, and for all the shared moments and laughter

> Hélène, you've always impressed me by your immense experience and knowledge. Thank you for all the time and attention you've devoted to me, especially towards the end of this three-year journey. I don't think that I already expressed my thanks for forcing me out of my comfort zone during this project and helping me building up my self-confidence

> Elena, thank you for your unfailing support and invaluable assistance during this project, for your hospitality in Rome and your presence all along this journey, but most of all for your friendship

> Joseph, thank you for your sound advices and technical support, for your unfailing cheerfulness and your patience,

> Giuseppe, thank you for your insightful comments and suggestions all along this project.

I would also like to thank all the team of the SOCUR project at INI and IRR, especially Isabelle, Christelle, Julie and Hélène. Thanks to all the physiotherapists at INI for your hospitality

I would like to express my gratitude to all members of the IBHGC the (ever-growing) CERAH Team who have crossed my path during these three years, for all the discussions, advices, support and social events. A special thanks to Marine for your invaluable assistance, to Galo and Julie for the coffee breaks and meaningful advices, to Christophe for your trust and encouragements in this last year, to Thomas for the fruitful collaboration during this third year, and to all my fellow PhD students

I would like to extend my thanks to Céline Lansade, from IRMA, and Marie Thomas, from HIA Percy, for their support and the discussions along the PhD, and to everyone at Foro Italico for their warm and friendly welcome in Rome

Thanks also to all the master students that I have cotutored and collaborated with in the course of this PhD, Aude, Aurélien, Jade, Joseph and Julie

Finally, I would like to express my sincere gratitude to Laetitia Fradet and Thomas Robert, for accepting to review my manuscript, and to Carlo Frigo, Jean Paysant, and Julia Facione, for accepting to take part to my PhD committee

On a personal note, I would like to thank my family and friends for their invaluable support with a special thanks to las Chicas, Yona & les Débiles, especially Félix for his encouragements in the moments of doubt during the PhD, and to Fred for his unwavering support and love.

Abstract

English version

One key objective during the rehabilitation of people with lower-limb amputation fitted with a prosthesis is the restoration of a physiological and energy-efficient gait pattern minimizing falling risks due to the loss of balance. Few practical tools are available to provide quantitative data to assist the follow-up of patients in the clinical routine. The development of wearable sensors offers opportunities to quantitatively and objectively describe gait in ecological situations such as during (tele)rehabilitation. In this context, the aim of the thesis is to contribute to the development of wearable tools and protocols to support the functional rehabilitation of lower-limb amputees by providing clinically relevant quantitative data.

Two complementary approaches have been implemented. The first approach consists in developing biomechanical models of the human body in order to retrieve biomechanically founded parameters. An original protocol allowing to accurately estimate the body center of mass acceleration and instantaneous velocity has therefore been proposed based on gait data of ten people with transfemoral amputation and was validated in one person with transfemoral amputation. The second approach consists in identifying patterns in the signals measured by wearable sensors to extract concise descriptors of the quality of gait, with reference to gait symmetry and dynamic balance. The clinical relevance and reliability of these descriptors have been investigated for the first time in people with lower-limb amputation.

The work produced in the course of this thesis has contributed to the clinical transfer of wearable sensors into the clinical practice through the identification of clinically and biomechanically relevant parameters and the validation of original algorithms allowing to quantitatively describe the gait of people with lower-limb amputation.

Key words: Quantitative gait analysis, wearable sensors, center of mass, symmetry, balance, people with lower-limb amputation

French version

Un des objectifs majeurs de la rééducation des personnes amputées de membre inférieur appareillées est le retour à une marche sans défaut ni asymétrie, efficace énergétiquement et minimisant le risque de chutes lié à la perte d'équilibre. Peu d'outils cliniques permettent aujourd'hui de quantifier ces aspects de la locomotion. L'émergence de capteurs embarqués miniaturisés offre des opportunités pour la description quantitative et écologique de la marche lors de la (télé)rééducation. Dans ce contexte, l'objectif de la thèse était de contribuer au développement de protocoles embarqués pour apporter des données quantitatives pertinentes lors de la rééducation à la marche des personnes amputées de membre inférieur.

Deux approches complémentaires ont été adoptées. La première approche consiste à utiliser un modèle biomécanique du corps afin d'extraire des descripteurs quantifiés pertinents. Un protocole original permettant d'estimer l'accélération et la vitesse instantanée du centre de masse à partir de 5 centrales inertielles a ainsi été proposé à partir d'une analyse préliminaire sur les données de marche de dix personnes amputées transfémorales et a été validé chez une personne amputée transfémorale.

La seconde approche consiste à extraire des paramètres concis par traitement du signal des données brutes de capteurs positionnés sur le corps. La fiabilité et la pertinence clinique de la quantification de tels paramètres pour caractériser la symétrie et l'équilibre de la marche ont été étudiées pour la première fois chez les personnes amputées de membre inférieur.

L'ensemble des travaux produits au cours de cette thèse contribue ainsi au transfert vers la clinique des outils embarqués d'analyse du mouvement par l'identification de paramètres biomécaniques et cliniques pertinents et la validation d'algorithmes originaux permettant la quantification de la marche des personnes amputées de membre inférieur.

Mots clés : Analyse quantifiée de la marche, capteurs embarqués, centre de masse, équilibre, symétrie, personnes amputées de membre inférieur

Italian version

Un obiettivo chiave durante la riabilitazione di nella routine clinica di arto inferiore protesizzate è il ripristino di un modello di deambulazione fisiologico e simmetrico, efficiente dal punto di vista energetico, riducendo al minimo i rischi di caduta dovuti alla perdita di equilibrio. Ad oggi tuttavia, sono rari gli strumenti in grado di fornire dati quantitativi e oggettivi per assistere concretamente la valutazione dei pazienti nella routine clinica. Lo sviluppo di sensori indossabili offre un'opportunità per descrivere quantitativamente e oggettivamente la deambulazione in situazioni ecologiche come durante la riabilitazione (domiciliare o no). In questo contesto, la presente tesi si propone di contribuire allo sviluppo di strumenti e protocolli indossabili a supporto della riabilitazione funzionale degli amputati di arto inferiore attraverso l'estrazione di dati quantitativi e clinicamente rilevanti.

Il lavoro si articola secondo due approcci complementari. Il primo approccio consiste nello sviluppo di modelli biomeccanici del corpo umano al fine di recuperare parametri biomeccanicamente rilevanti nel contesto clinico. È stato quindi proposto un protocollo originale che permette di stimare l'accelerazione e la velocità istantanea del centro di massa dell'intero corpo. Il protocollo è stato sviluppato sulla base dei dati di deambulazione di dieci persone con amputazione transfemorale ed è stato validato in una persona con amputazione transfemorale. Il secondo approccio consiste nell'identificare caratteristiche nei segnali misurati dai sensori indossabili per estrarre descrittori concisi della qualità della deambulazione, in termini di simmetria ed equilibrio dinamico. La rilevanza clinica e l'affidabilità di questi descrittori sono state studiate per la prima volta in persone con amputazione di arto inferiore.

Il lavoro svolto nel corso di questa tesi ha contribuito al trasferimento clinico di sensori indossabili nella pratica clinica attraverso l'identificazione di parametri clinicamente e biomeccanicamente rilevanti e la validazione di algoritmi originali che permettono di descrivere quantitativamente la deambulazione di persone con amputazione di arto inferiore.

Parole chiave : Analisi quantitativa della deambulazione, sensori indossabili, centro di massa, simmetria, equilibrio, persone con amputazione

iv

Table of contents

vi

General introduction

In France, the number of people living with a major lower-limb loss in 2012 was estimated to lie between 90,000 to 100,000 people, with an incidence of 8,300 cases per year (Villa, Bascou, *et al.*, 2017). In developed countries, most lower-limb amputations are performed as a result of peripheral vascular diseases (from 80 to 90%), traumatic injuries (10 to 20 %), or tumors (< 5%) (Ziegler-Graham *et al.*, 2008; Carmona *et al.*, 2014). Ageing of the population and increased prevalence of diabetes are predicted to lead to a raise of the number of people living with a lower-limb loss in the next decades (Lamandé *et al.*, 2011). For instance, in the United States, the population of lower-limb amputees is predicted to double between 2005 and 2050 (Ziegler-Graham *et al.*, 2008).

Following an amputation of a lower limb, the objective of the rehabilitation process is the return home of the patient with as much autonomy as possible in the activities of daily living and without pain. Rehabilitation is supervised by a multidisciplinary team whose aim is reducing and supplementing the functional loss induced by amputation. Following surgery, rehabilitation is focused on muscle strengthening and residual limb acceptance. After prosthetic fitting, rehabilitation protocols target the recovery of balance, the ability to perform autonomous transfers and the recovery of a gait pattern as physiological as possible. An important focus of the functional rehabilitation is the reduction of gait limping, asymmetries and compensations such as hip hiking or vaulting in order to prevent the over-solicitation of the preserved articulations, which may introduce long-term disabilities and comorbidities such as arthrosis or low-back pain (Sawers and Hafner, 2013; Villa, Bascou, *et al.*, 2017).

Monitoring the patient's progress relies on regular clinical assessments. Such assessments are usually based upon visual observations performed by the multidisciplinary team in charge of the rehabilitation (doctor, physiotherapist, occupational therapist, ortho-prosthetist...), on the investigation of the patient's perception about the prosthesis (perceived discomfort or pain), and on the assessment of overall patient's performance metrics during specific motor tasks (Cuesta-Vargas *et al.*, 2010; Hafner and Sanders, 2014). Metrics that are associated with a positive evolution of the patient are generally qualitative and subjective; they often depend on the experience of the clinician and, thus, lack inter-rater reliability and specificity. Obtaining objective and quantitative data through rigorous protocols might help clinicians in accurately monitoring their patients' progress or in prescribing a prosthetic component adapted to a specific patient. This is particularly true regarding the prescription of technologically advanced prosthetic components: in France, the public healthcare system reimburses the costs associated to prosthetic fitting and prescribed equipment if the rehabilitation therapists can document that it would truly benefit the patient.

However, few practical tools are available to provide quantitative data to assist the assessment of patients in clinical routine. In fact, although clinical quantitative gait analysis in motion laboratories has been extensively described in the literature, including in people with lower-limb amputation, it is generally hardly accessible in the clinical practice because of a high system cost and portability constraints (Iosa, Picerno, *et al.*, 2016; Benson *et al.*, 2018; Loiret *et al.*, 2019). Miniaturization of sensing technologies and advancement in processing techniques in the last decades have made possible the development of affordable wearable inertial and pressure sensors for motion analysis (Wong *et al.*, 2007, 2015; Benson *et al.*, 2018). Wearable sensors offer the advantages of being

portable and thus located directly onto the patient, enabling to record data outside the laboratory, without limitation of the acquisition volume and without interfering with the clinical routine (Cuesta-Vargas *et al.*, 2010; Tura *et al.*, 2010; Trojaniello, Cereatti, Pelosin, *et al.*, 2014; Maqbool *et al.*, 2015; Iosa, Picerno, *et al.*, 2016; Loiret, 2016; Benson *et al.*, 2018).

In the context of evidence-based practice or medicine, wearable sensors are thus a very attractive solution to provide quantitative data of interest for the rehabilitation of people with lower-limb amputation. Indeed, potential clinical benefits of those sensors include long-term and remote monitoring, real-time feedback, increased implication of the patient in his/her rehabilitation, home-based and telerehabilitation opportunities, and a reduction of global rehabilitation costs (Hafner and Sanders, 2014; Iosa, Picerno, *et al.*, 2016; Villa, Bascou, *et al.*, 2017). However, the transfer of this technology in the clinical routine or for home-based rehabilitation for the assessment of lower-limb represents a challenge (Cutti *et al.*, 2015; Iosa, Picerno, *et al.*, 2016). Indeed, wearable sensors depend on a technology that differs from that of the gold standards gait analysis tools. As a consequence, wearable sensors may not allow to directly quantify all the biomechanical parameters that are usually retrieved in laboratory-based clinical gait analysis. For instance, no currently available wearable sensor can directly provide a measure of its absolute position in an Earth-fixed reference frame.

It is therefore necessary to first identify clinically relevant parameters allowing the quantitative and biomechanical description of lower-limb amputee gait which could be obtained from wearable sensors. These parameters should be synthetic and should allow to globally evaluate gait function and performance while providing an understanding of the underlying mechanical causes. This would indeed allow to use these parameters both as indicators for the evaluation of the rehabilitation and for the implementation of rehabilitation protocols. Once these parameters have been identified, specific algorithms must be developed or adapted for their quantification from wearable sensors data. A special attention must be drawn on limiting the number of sensors required in order to keep the acquisition minimally invasive and as simple as possible so as to facilitate the transfer in clinics (cost and time constraints), or even for home-based applications. Last but not least, the validity and reproducibility of the retrieved parameters in people with lower-limb amputation must be assessed in order to provide clinicians with reliable and easily interpretable data.

This thesis aims at providing a contribution towards the in-field functional assessment of people with lower-limb amputation from wearable sensors. In this framework, the approach chosen consisted in investigating both validated wearable tools and original algorithms with the aim of providing clinicians with relevant quantitative data to support their practice during the functional rehabilitation of people with lower-limb amputation. Although the algorithms developed within the framework of the thesis were specifically developed for people with lower-limb amputation, similar approaches could be adopted in other pathological gait as the use of wearable sensors in the clinical field would similarly benefit both patients and the healthcare system.

The thesis was carried out in the framework of a joint Ph.D. between the IBHGC (*Institut de Biomécanique Humaine Georges Charpak*, Arts et Métiers, Paris, France) and the LBNM *(Laboratory of Bioengineering and Neuromechanics of Movement*, Foro Italico, Rome, Italy). It was financed by a donation from the *Fédération des Amputés de Guerre de France* (FAGF) to INI/CERAH (*Centre d'Etude*

et de Recherches pour l'Appareillage des personnes Handicapées, Antenne de Créteil, France), with the aim to improve care of people with lower-limb amputation. A grant from the Université Franco-Italienne was obtained to finance the mobility between France and Italy.

The research developed within this framework relies on previous collaborative works between the IBHGC and INI/CERAH on the characterization of lower-limb amputee gait[1] and on the expertise of the LBNM on the use of wearable motion sensors for the study of human movement[2]. Furthermore, the joint supervision by IBHGC and LBNM materializes the collaboration between the laboratories, driven by the complementarity of their expertise fields and their common interest for the study of human motion. Finally, the research was supported by the clinical partnerships of INI/CERAH and IBHGC, in particular with INI (*Institution Nationale des Invalides*, Paris, France), IRR (*Institut Régional de Réadaptation*, Nancy France), the military hospital HIA Percy (*Hôpital d'Instruction des Armées Percy*, Clamart, France) and IRMA (*Institut Robert Merle d'Aubigné, Valenton,* France).

The thesis thus benefited from a multidisciplinary environment with the highly valuable collaboration of biomechanical engineers and clinicians for the identification of clinically relevant parameters and the development and/or validation of algorithms allowing their extraction from wearable sensor data.

The first part of the manuscript focuses on the identification of clinically relevant biomechanical parameters for amputee care that could be retrieved from wearable sensor data through a review of the literature. Following a description of the rehabilitation pathway of people with lower-limb amputation (chapter 1), an overview of state-of-the-art descriptors of lower-limb amputee gait is presented (chapter 2). Finally, chapter 3 investigates how wearable sensors, and more especially inertial measurement units and pressure insoles, could benefit both clinicians and people with lower-limb amputation during their rehabilitation by reporting the outcome parameters usually derived from these sensors. Following the conclusion of part 1, the aim of the thesis is further developed with the selection of clinically relevant parameters whose quantification from wearable sensor data will be investigated. These parameters aim at characterizing gait symmetry and balance and at describing the kinematics of the center of mass. The latter indeed appears to be a relevant synthetic biomechanical descriptor of gait performance, providing insight on both energy efficiency and kinematics asymmetries.

The second part of the thesis proposes a framework for the wearable estimation of body center of mass motion in people with lower-limb amputation. First, a review of the literature provides a comprehensive overview of the main methods implemented in diverse populations to estimate the motion of the body center of mass from magneto-inertial measurement units (chapter 1). The review leads to the decision of implementing a multi-sensor approach and the optimal locations of sensors are determined based on an analysis of the segmental contributions to the body center of mass acceleration in ten people with transfemoral amputation (chapter 2). From there, magneto-inertial

---

[1] See the Ph.D. theses of Hélène Pillet (Goujon, 2006), Coralie Villa (Villa, 2014) and Boris Dauriac (Dauriac, 2018).

[2] See the Ph.D. theses of Elena Bergamini (Bergamini, 2011) and Valeria Belluscio (Belluscio, 2020) for instance

measurement units are used to validate the multi-sensor approach in an original framework that allows an almost fully-wearable acquisition of body center of mass motion (chapter 3). Lastly, the impact of errors in the identification of sensors positions relative to the segments on the body center of mass acceleration is investigated (chapter 4).

The last and third part of this thesis proposes an alternative approach to that implemented in the second part and investigates the feasibility of retrieving gait quality indices from wearable sensor data in a rehabilitation set-up. First, five inertial-measurement-units-based gait-event detection algorithms are comparatively assessed in seven people with transfemoral amputation in view of in-the-field quantification of temporal asymmetry from one to two inertial measurement units (chapter 1). The second chapter explores the feasibility and relevance of tracking gait quality indices issued from wearable sensors during the rehabilitation of lower-limb amputees through the instrumentation of the two-minute walking test.

Part 1: Identification of clinically relevant parameters for in-the-field monitoring of the rehabilitation of people with lower-limb amputation through a review of the state-of-the-art

Lower-limb amputation is a life-long handicap, affecting both the psychological and physical integrity of a person and with a definitive impact on ambulation (Samuelsson *et al.*, 2012). Following rehabilitation and definitive prosthetic fitting, gait performance and capacities of the lower-limb amputee are still limited compared to those of asymptomatic people (Bonnet, 2009). Indeed, walking with a prosthesis requires a higher energy cost (Waters *et al.*, 1976) and doesn't always allow walking outdoors on irregular terrain (Van Velzen *et al.*, 2006), in slopes or stairs (Walker *et al.*, 1994). Furthermore, an asymmetrical gait pattern is often observed (Nolan *et al.*, 2003; Sagawa *et al.*, 2011), which not only favors the onset of long-term comorbidities, but also has an impact on the esthetic of walking thus affecting the patient's social life (Gailey *et al.*, 2008).

Obtaining quantitative data to characterize the gait or balance of lower-limb amputees during rehabilitation could help detecting and reducing gait compensations and thus preventing the occurrence of long-term comorbidities. Furthermore, it could assist physicians and prosthetists in the prescription and alignment of prosthetic components. However, current clinical assessment tools do not allow to obtain such quantitative parameters, and optical motion capture systems are inappropriate in most clinical settings (Loiret *et al.*, 2005). Therefore, the use of user-friendly and relatively low-cost wearable sensors is an interesting approach even if they may not allow to quantify the same biomechanical gait descriptors as usually retrieved in laboratory-based quantified gait analysis.

The purpose of the first part of the thesis is thus to identify, from an exhaustive literature review, gait parameters that could be obtained with inertial sensors and pressure insoles and that are clinically relevant for the rehabilitation of people with lower-limb amputation. Following a global overview of contextual elements on the rehabilitation pathway and the gait of people with lower-limb amputation in the first chapter, chapter 2 focuses on the assessment of amputee gait both in clinics and in motion analysis laboratories. Finally, the third chapter introduces inertial measurement units and pressure insoles and provides an overview of their usage in the clinical and research fields.

Chapter 1 – Rehabilitation of people with lower-limb amputation

The number of people living with a major lower-limb loss (that is, amputations above the ankle level) was estimated to lie between 90,000 to 100,000 people, with an incidence of 8,300 new amputations per year in France in 2012 (Villa, Bascou, *et al.*, 2017). Following the amputation of a lower limb, people might be fitted with prosthetic devices to restore gait and balance functions of the lost limb. Transtibial amputation, knee disarticulation and transfemoral amputation (**Figure 1**) account for 99% of major amputations of the lower limbs (Villa, Bascou, *et al.*, 2017), and as a consequence, the present work will focus on these amputation levels.
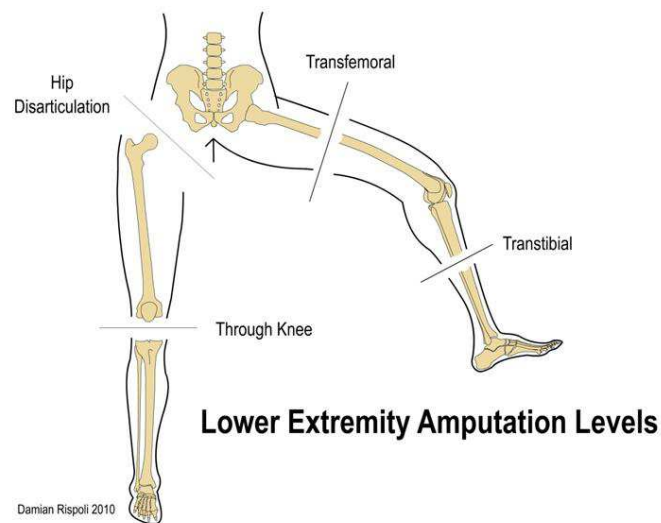
Figure 1: Major lower-limb amputation levels

1.1.   Prosthetic components

Limb amputation entails the loss of bony structures, joint(s) and muscles. Transfemoral and transtibial prosthetic devices aim at replacing the lost limb and are constituted with prosthetic modules manufactured in series production and – except in the cases of osseointegration – a custom-made socket (**Figure 2**). The prosthesist assembles the components and realizes patient- and device-specific settings of the prosthesis to allow an efficient, pain-free and esthetic gait.

The socket constitutes the interface between the residual limb and the prosthesis, and allows prosthetic control through load transmission. As a consequence, a well fitted socket is essential to ensure confort and pain-free use of the prosthesis. The socket is usually manufactured manually by molding the residual limb of the patient. Recently, an alternative computer-aided design and manufacturing process consisting in taking a 3D scan of the patient stump has been proposed. A liner might be worn between the socket and the residual limb to improve comfort and prevent sliding of the socket with respect to the stump.

The generic prosthetic modules consist in a prosthetic knee, for transfemoral amputees, and a prosthetic foot, supplementing both the foot and the ankle. There is a large variety of existing knee and foot devices. The choice of a specific device over another depends on the functional capacities of the amputee as well as on his/her life project.

Figure 2: Components of a transtibial (below knee) and a transfemoral (above-knee) prosthesis (taken from https://www.orthomedics.us/)

The next two paragraphs will briefly introduce the key principles of the prosthetic foot and knee components. For a more detailed presentation of the prosthetic components, the reader can refer to the theses of Xavier Bonnet (Bonnet, 2009) and Boris Dauriac (Dauriac, 2018).

1.1.1. Prosthetic feet

There are three categories of prosthetic feet: "standard" feet, energy storing and returning feet (ESR) and new-generation active feet (Bonnet, 2009). ESR feet have been introduced in 1981 and differ from the rigid standard feet by the inclusion of deformable components, allowing to store energy at the instant of foot contact and to restore it for propulsion. However, the returned energy is still lower than the energy produced by a sound ankle. This partly explains the recent development of active new generation feet. The latter also allow to adapt the behavior of the feet to the terrain or situation encountered (slope, stairs, level ground…). There is a low hindsight on these types of feet, and they are currently not reimbursed by the healthcare system in France.

1.1.2. Prosthetic knees

Similarly, there are three types of prosthetic knees: mechanical, microprocessor-controlled and motorized knees (also called "active" knees). Prosthetic knees must ensure a stable and reliable support when standing on the artificial limb while allowing the required mobility for making a step forward or sitting. Stability during stance is ensured by design, either through a locking system which can be activated manually or because during stance, the ground reaction forces imposes a knee extension torque preventing flexion. In order to control the flexion and extension motion of the prosthetic limb during the swing phase, a friction is applied on the knee. It can be purely mechanical, pneumatic or hydraulic (Hafner and Askew, 2015). Microprocessor-controlled knees adjust the hydraulic or pneumatic friction of the knee along the gait, thanks to sensors embedded in the prosthetic device (Hafner and Askew, 2015; Dauriac, 2018). Finally, active knees include a motor, which allow to actively control the position and motion of the knee joint (Hafner and Askew, 2015). Only one

active knee is commercialized worldwide, and it is not currently reimbursed by the healthcare system in France.

1.2. The rehabilitation pathway

Following surgery, rehabilitation aims at restoring autonomy in the activities of daily living of the amputee person (hygiene and alimentation, displacements, work, …) with the highest quality of life possible. To achieve this aim, a multidisciplinary team composed by physicians, physiotherapists, occupational therapists, prosthetists and any other medical specialists required (for instance, a psychologist) collaborates with the patient, who is also an active member of the team. The rehabilitation and the prescribed prosthetic limb, when applicable, are adapted to the life project and the functional capacities of the amputee person (Villa, Bascou, *et al.*, 2017). The success of the rehabilitation is multifactorial as it depends on the outcomes of the surgery and the amputation level, the prosthetic components, the quality of the prosthesis fitting, the functional capacity of the patient and his/her level of involvement in the rehabilitation. Assessment of the rehabilitation is therefore complex as it requires to identify quantitative indicators corresponding to these multiple factors put in regards with the life-project of the patient. Functional outcomes of the rehabilitation can however be evaluated through biomechanical descriptors of gait, which can be used for therapeutic decision-making along the rehabilitation.

The rehabilitation can be divided in three stages respectively corresponding to the postoperative, pre-prosthetic and prosthetic phase of the rehabilitation (Esquenazi and DiGiacomo, 2001; Kovač *et al.*, 2015; Loiret, 2016). The post-operative and pre-prosthetic rehabilitation have been reported to last about five to six weeks in people with vascular amputation while a minimum of three to four weeks following surgery has been reported for wound healing in traumatic amputation (Kovač *et al.*, 2015). The duration of the prosthetic phase of the rehabilitation then lasts four to six weeks in people with transtibial amputation, six-to-eight weeks in people with transfemoral amputation and is prolonged in case of bilateral amputation (Kovač *et al.*, 2015). It should be noted that the overall rehabilitation duration depends on each patient and in particular on the scar healing process of the residual limb of the person.

1.2.1. Post-operative and pre-prosthetic rehabilitation

Immediately after surgery, post-operative rehabilitation mainly focuses on wound healing and pain management. Limb loss acceptance is also a major focus of this early stage of the rehabilitation.

As soon as the patient is medically stable, mobility exercises involving both the residual and contralateral legs are proposed by the physiotherapists in order to preserve the range of motion of the residual and sound leg articulations, to avoid contractures and to strengthen the muscles that will be solicited during prosthetic gait. Muscle training of the upper limbs must not be neglected to prepare the patient to the temporal use of manual wheelchair or walking aids, such as crutches or a walker. Early mobility is paramount for the success of the rehabilitation. Aided

Figure 3: Preparation for prosthetic ambulation

8

ambulation training, without a prosthesis (**Figure 3**), is initiated to prepare the patient for prosthetic gait training; muscle strengthening is accentuated.

The pre-prosthetic rehabilitation stage ends when the temporary prosthesis is delivered by the prosthetist. It consists of a temporary socket made of plastic, molded on the residual limb, and of prosthetic component(s) of simple design.

1.2.2. Prosthetic rehabilitation

Prosthetic training can be divided in two subphases. The ultimate aim of this stage is gait recovery with a prosthesis.

First, unspecific training focuses on residual limb self-care, learning to don and doff the prosthesis, and reaching a stable residual limb volume. At the beginning of this stage, special care is addressed to skin monitoring. Balance and weight-bearing exercises are initiated, as well as prosthetic gait training on level ground using the temporary prosthesis. First, the patient learns to walk between parallel bars, and then walking aids are incrementally removed (Wilhoite *et al.*, 2019).

The prosthetic components can evolve during this stage as the amputee person retrieves a consistent gait pattern. Specific training aims at learning *i)* to control the prosthesis through the socket and residual limb proprioception, and *ii)* to use the specific functionalities of the prosthetic components. Muscle strengthening, endurance and balance are still trained along with gait on level ground. Once the amputee person masters prosthetic gait on level ground, training on slopes and stairs is addressed. Ultimately, the functional capacity of the amputee person and his or her life project will drive the choice of the definitive prosthetic components. During this stage of the rehabilitation, an important focus is the reduction of gait asymmetries or limping, which may arise from an insufficient loading of the prosthetic lower limb, a lack of confidence on the prosthesis, muscle atrophy resulting from the surgery, etc. Typical gait compensations observed in people with lower-limb amputation are described in the next section (1.3).

During this stage, the volume of the residual limb reaches a (relatively) stable state, allowing to replace the temporary socket with a "definitive" lighter and sturdier one, made of carbon.

1.2.3. Long-term clinical follow-up

Following discharge from the rehabilitation center, almost 90% of people with lower-limb amputation return home (Villa, Bascou, *et al.*, 2017) where they keep learning how to use their prosthetic device in their daily-living environment. In the first months following discharge, several appointments may be needed, for instance, to adapt the socket to the residual limb. Then, regular appointments for patient follow-up and prosthetics adjustments are required all along the life of the patient, generally on an annual basis (Kovač *et al.*, 2015). Eventually, when a prosthetic component is changed, there might be a need for specific rehabilitation sessions to assist the amputee in learning how to control and to use the specific functionalities of the new prosthesis (Paradisi, 2016).

1.3.   Typical gait compensations and asymmetries observed in people with lower-limb amputation

Due to muscle loss following lower-limb amputation and to limitations inherent to prosthetic components, several adaptations of the gait pattern can be observed in transtibial and transfemoral amputees (Michaud *et al.*, 2000; Goujon-Pillet *et al.*, 2008; Villa, 2014). The aim of this section is to propose an overview of some of the major compensations identified in the gait of people with lower-limb amputation. In particular, the loss of ankle flexor muscles in both transtibial and transfemoral amputation leads to a reduced propulsion (or *push-off*) at the end of the stance phase and an absence of active dorsiflexion during the swing phase. This contributes to a decrease in power generation (Seroussi *et al.*, 1996) and in toe clearance (that is, a decreased distance between the foot and the ground, see **Figure 4**) during the prosthetic swing phase. This phenomenon is even accentuated in people with transfemoral amputation who cannot control knee flexion due to the loss of the knee joint and of atrophied hip musculature.
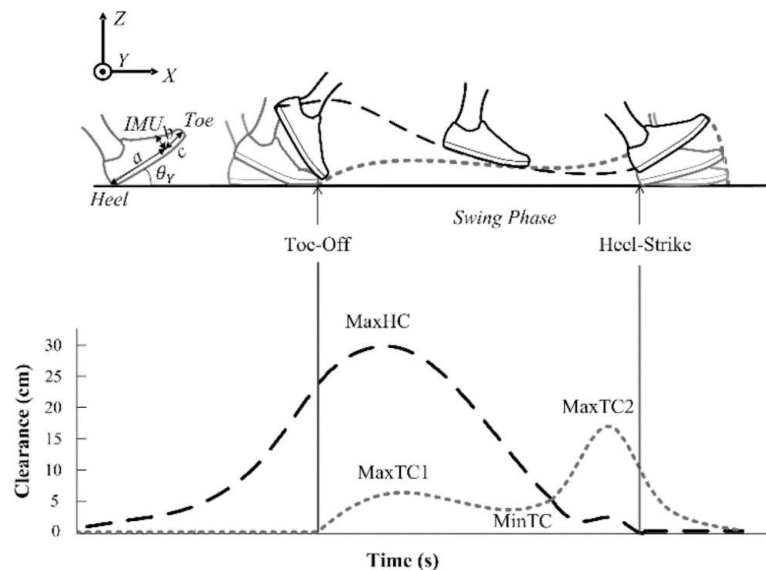
Figure 4: Foot clearance during the swing phase (taken from (Dadashi *et al.*, 2013))

Several compensatory strategies are thus implemented to increase toe clearance and avoid tripping during the prosthetic swing phase. These compensations include hip circumduction, hip hiking, and vaulting and are mostly observed in people with transfemoral amputation (Villa, 2014) :

- Hip circumduction (**Figure 5**a) consists in simultaneously abducting and rotating the residual hip during the swing phase. This allows to maintain a reasonable toe clearance without flexing the knee joint.
- Hip hiking (**Figure 5**b) consists in tilting the pelvis towards the stance leg in the frontal plane to increase toe clearance. This strategy is observed during the prosthetic swing phase in both people with transtibial and transfemoral amputation (Michaud *et al.*, 2000; Goujon-Pillet *et al.*, 2008). In people with transfemoral amputation, hip hiking also occurs during the sound swing phase, and it is assumed to result from a lateral trunk bending strategy to compensate for weak hip abductors (Jaegers *et al.*, 1995; Michaud *et al.*, 2000; Goujon-Pillet *et al.*, 2008).

- Vaulting (**Figure 5**c) is a compensation strategy consisting in a premature propulsive plantar flexion of the sound ankle during the sound stance phase. It allows to improve toe clearance by increasing the functional length of the sound leg.
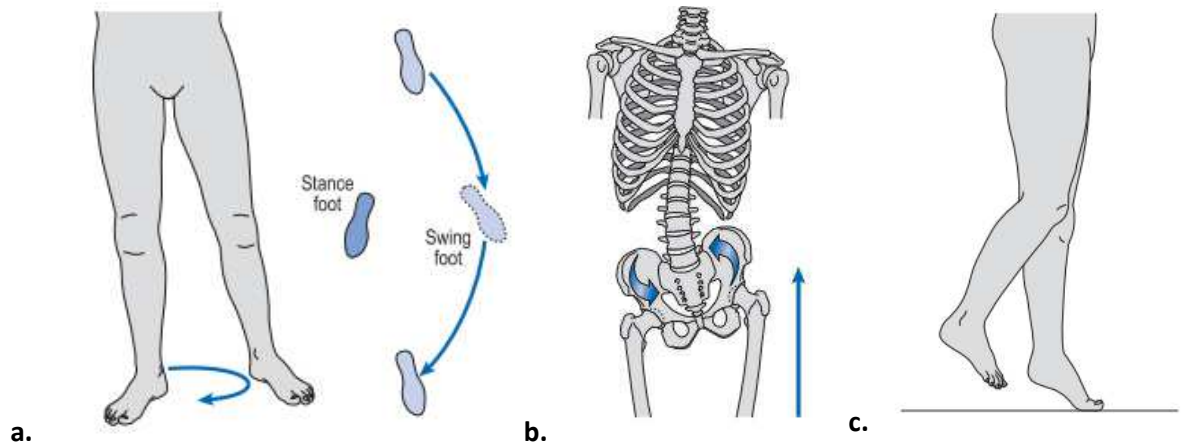
Figure 5: Most common gait deviations observed in amputee gait (Whittle, 2007)
a.   Hip circumduction; b. Hip hiking; c. Vaulting

These compensations can often be detected, although not quantified, by the experienced eyes of clinicians. As they result in over-solicitation of muscles and joints, leading to osteoarticular comorbidities (Gailey *et al.*, 2008; Esposito *et al.*, 2015), they are targeted by the rehabilitation team.

Chapter 2 – Current modalities for the assessment of the rehabilitation

2.1. Usefulness of quantitative data

Although most patients are fitted with a prosthesis and regain the ability to walk (Van Velzen *et al.*, 2006), recent systematic reviews found out that less than 62% of lower-limb amputees are able to walk outdoors (Van Velzen *et al.*, 2006) and that only 50 to 72% of people with transfemoral amputation actually walk with their prosthesis (Sawers and Hafner, 2013). These difficulties may arise from back pain and socket discomfort, due to ill-adapted prosthetic components or poor alignment settings (Gailey *et al.*, 2008), from limited functionalities of the prosthetic components (Dauriac, 2018), from lack of confidence in the prosthetic devices (Miller *et al.*, 2001) or from insufficient functional capacities of the person with amputation (Sawers and Hafner, 2013). Furthermore, gait deviations such as increased loading of the intact limb or abnormal efforts or moments at the contralateral joint may lead to severe comorbidities such as osteoarthrosis, osteopenia and back pain (Gailey *et al.*, 2008; Dauriac, 2018), resulting in a poorer quality of life and activity participation in the community of people with lower-limb amputation.

Being able to monitor amputees' gait during the rehabilitation and long-term follow-up appointments is therefore of paramount importance. Indeed, obtaining quantitative data to characterize the gait or balance of lower-limb amputees during rehabilitation can help detecting and reducing gait compensations and thus preventing the occurrence of long-term comorbidities (Hafner and Sanders, 2014; Paradisi, 2016). Furthermore, such data can assist physicians and prosthetists in the prescription and alignment of prosthetic devices as they can provide evidence-based reports to compare different prosthetic devices or alignment settings (Sagawa *et al.*, 2011; Boone *et al.*, 2012; Hafner and Sanders, 2014; Thomas-Pohl *et al.*, 2019; Zhang *et al.*, 2020). Systematic and objective gait analysis of lower-limb amputees during rehabilitation could therefore assist both patients and clinicians by providing evidence supporting and facilitating the rehabilitation (Heinemann *et al.*, 2014), or justifying the prescription of specific prosthetic components (Hawkins and Riddick, 2018). Healthcare systems could also benefit from evidence-based practice as it could help identifying rehabilitation strategies, facilitating home-based rehabilitation or assessing rehabilitation performance earlier and, thus, could reduce treatment-related costs (Agrawal, 2016).

In order to be relevant during the rehabilitation, gait-characterizing quantitative data should be synthetic and comprehensible – in order to be interpretable by both the patient and the clinician – and should have a valid biomechanical basis. To simplify the interpretation of such quantitative data, a limited number of parameters should be retrieved. A major difficulty lies within the tradeoff between complexity, biomechanical-relevance and accuracy. Indeed, obtaining biomechanical accurate quantitative data often implies to use a complex and high-cost system, requiring specific acquisition protocols and technical skills for data post-processing, which is often not compatible with the constraints in the clinical field.

The next two paragraphs aim at providing an overview of the clinical tools currently used for rehabilitation assessment and of the biomechanical parameters that have been presented in the literature to quantify lower-limb amputee gait.

2.2. Quantitative gait assessment in current clinical practice

During rehabilitation, gait evaluation is mostly based on observational gait assessment and on inputs from patients, such as capacity or comfort perception and retrospective self-reports of potential incidents (Perry, 1992; Calmels *et al.*, 2002; Hafner and Sanders, 2014; Heinemann *et al.*, 2014). In addition of being only qualitative, such assessments are subjective as they strongly depend on the clinician's interpretation (Hafner and Sanders, 2014; Muro-de-la-Herran *et al.*, 2014) and on self-reports from patients which might be biased by (in)voluntary omissions (Hafner and Sanders, 2014).

To complete clinical gait assessment with quantitative measures, various self-administered questionnaires and performance-based clinical tests are available (Arch *et al.*, 2016). Although a few questionnaires quantifying perceived mobility, function, satisfaction, or quality of life of people with lower-limb amputation have been validated in people with lower-limb amputation (Calmels *et al.*, 2002; Condie *et al.*, 2006; Resnik and Borgia, 2011; Hawkins *et al.*, 2014), responsiveness to change was not always evaluated (Deathe *et al.*, 2009; Heinemann *et al.*, 2014). Furthermore, due to the nature of the questions, most questionnaires are more suited for community-dwelling amputees (Calmels *et al.*, 2002; Condie *et al.*, 2006). On the other hand, performance-based tests provide objective or semi-objective assessments of the ability of patients to perform specific tasks (Hawkins and Riddick, 2018). They consist either in summary scores or in walking tests.

Summary scores are obtained by aggregating scores from a set of tasks that aim at assessing several aspects related to gait and/or balance. For instance, the *Amputee Mobility Predictor* (AMP) score was designed specifically for people with lower-limb amputation to predict ambulation ability after rehabilitation. It consists in 21 items, testing gait ability, transfer or balance. Each item is graded between 0 and 2 depending on the use of assistive device and on the patient's ability to perform the task (can't, partially can, can do) (Condie *et al.*, 2006; Deathe *et al.*, 2009). This test allows to estimate the functional K-level of people with lower-limb amputation and is used for prosthesis prescription during or after rehabilitation (Loiret *et al.*, 2005).

Walking tests aim at assessing the mobility of a person and result in a single measure. They are declined either in timed tests, where the distance covered within a specific duration is measured, or in distance-based tests, where the time taken to perform an ambulation task along a specific circuit is measured. In addition to being reliable and valid in multiple populations (Hawkins *et al.*, 2014), these tests are easy to implement and quick to administer, which allow their regular use for rehabilitation assessment (Loiret *et al.*, 2005; Condie *et al.*, 2006; Agrawal, 2016). Furthermore, timed tests allow the estimation of walking speed, which is a prominent descriptor of gait function (Perry, 1992; Fritz and Lusardi, 2009; Batten *et al.*, 2019). The two-minute walking test (2MWT) and the Timed-Up and Go (TUG) test are among the most frequently administered and most recommended tests in the literature (Condie *et al.*, 2006; Hawkins *et al.*, 2014; Hawkins and Riddick, 2018). Both tests provide valid assessments of mobility in people with amputation (Deathe *et al.*, 2009). During the 2MWT, participants are asked to walk back and forth at their self-selected speed along a long straight-corridor

or along a square path for two minutes. The achieved distance, and thus, the average walking speed, is used to assess the global function of the participant. The TUG test (**Figure 6**) has been used to quantify balance ability in addition to mobility, as it consists in several motor-tasks: rising from a chair, walking 3 meters, turning back and sitting back on a chair. The time taken to complete this circuit is measured during the test, and it has been shown to be well correlated to the Berg Balance Scale (Loiret *et al.*, 2005). The latter evaluates balance ability but requires a minimum of 15 minutes (Heinemann *et al.*, 2014), contrary to the TUG which takes only up to two minutes to complete (Calmels *et al.*, 2002; Condie *et al.*, 2006).
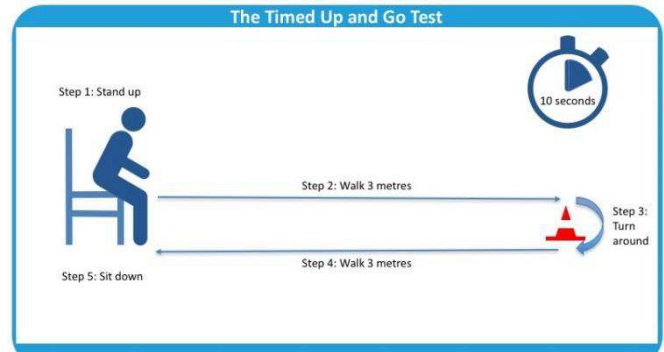
Figure 6: Timed-Up and Go test
(from https://www.frailtytoolkit.org)

A recent study has assessed test-retest validity of the most current performance-based and self-reported outcome measures used in the population of people with lower-limb amputation, and found that the AMP, 2MWT and TUG tests are reliable, while the authors reported that the minimally detectable changes observed were higher than expected (Resnik and Borgia, 2011). However, reproducibility assessment was based on a sample of 44 lower-limb amputees without distinction of amputation level or etiology, while both these factors have been shown to significantly influence gait performance and overall quality of life (Waters *et al.*, 1976; Miller *et al.*, 2001; Gailey *et al.*, 2008). Furthermore, responsiveness and minimal clinically-significant differences of the tests were not reported (Resnik and Borgia, 2011; Hawkins and Riddick, 2018).

While these scores can provide relevant information on the gait of people with lower-limb amputation, they are not self-sufficient (Calmels *et al.*, 2002); for instance, an indication of high performance to the 2MWT does not provide information regarding the quality of gait (symmetry, articular range of motion, …) or the ability to fully use the prosthetic components. Complete and objective evaluation of gait through reliable and valid quantitative descriptors is possible using biomechanical gait analysis which is most frequently performed with optical motion capture systems and force plates in motion analysis laboratories. A large body of literature has thus focused on the study of lower-limb amputees' gait in motion analysis laboratories. Therefore, the next section aims at identifying the most reported descriptors of gait in people with lower-limb amputation through an overview of the main findings of the literature on amputees' locomotion.

2.3.   Quantitative gait assessment in motion analysis laboratories

Gait analysis aims at analyzing *how* and *how* well a person walks (Cappozzo, 1984). As a consequence, two categories of gait descriptors studied in motion analysis laboratories can be defined:

- Function assessment parameters, whose aim is to describe motion and its origin. This category of descriptors can be put in relation with the parameters describing impairments of body

functions according to the International Classification of Functioning, Disability and Health (ICF)[3].

- Performance assessment parameters, aiming at assessing and describing the quality of motion (such as gait symmetry or efficiency)

Since gait is a cyclical motion, these parameters are generally assessed over a stride, or gait cycle. This allows to interpret them and to identify normal/pathological gait patterns by comparing, for instance, the parameters' evolution or peak values at different instants of the gait cycle (**Figure 7**).

Paragraph 2.3.1 introduces the gait cycle and derived spatiotemporal parameters. Then, the following paragraphs provide an overview of the characterization of amputee gait through function and performance assessment parameters quantified in motion analysis laboratories.

2.3.1. *Gait cycle and spatiotemporal parameters*

Gait segmentation is the process of dividing gait into cycles. Conventionally, the instant of initial foot contact is generally used for this purpose. The prosthetic gait cycle thus corresponds to the period between two successive contacts of the prosthetic foot (**Figure 7**).

Several terminologies can be found in the literature to describe the different events composing the gait cycle; the denominations "initial contact" (also *heel strike* or *heel contact* in the literature) and "final contact" (also *terminal contact, foot off* or *toe off*) will be used in this thesis due to the absence of proper heel strike or toe off in some pathological gait (Tunca *et al.*, 2017). Initial and final contact events are of interest because they respectively mark the beginning and the end of the stance phase. Stride length and duration are defined as the distance covered or the elapsed time between two successive initial contacts of the same foot (during a cycle). Their determination allows to estimate walking velocity. Another relevant spatiotemporal parameter is step length (resp. duration), which is defined as the distance between both feet (resp. elapsed time) between two consecutive initial contacts of two subsequent feet.

| Double Stance | Prosthetic Stance Phase | Double Stance | Prosthetic Swing Phase |
| | Controlateral Swing Phase | | Sound Stance Phase |

| Prosthetic Initial Contact (IC) | Controlateral Final Contact (FC) | | Controlateral IC | Prosthetic FC | Prosthetic IC |
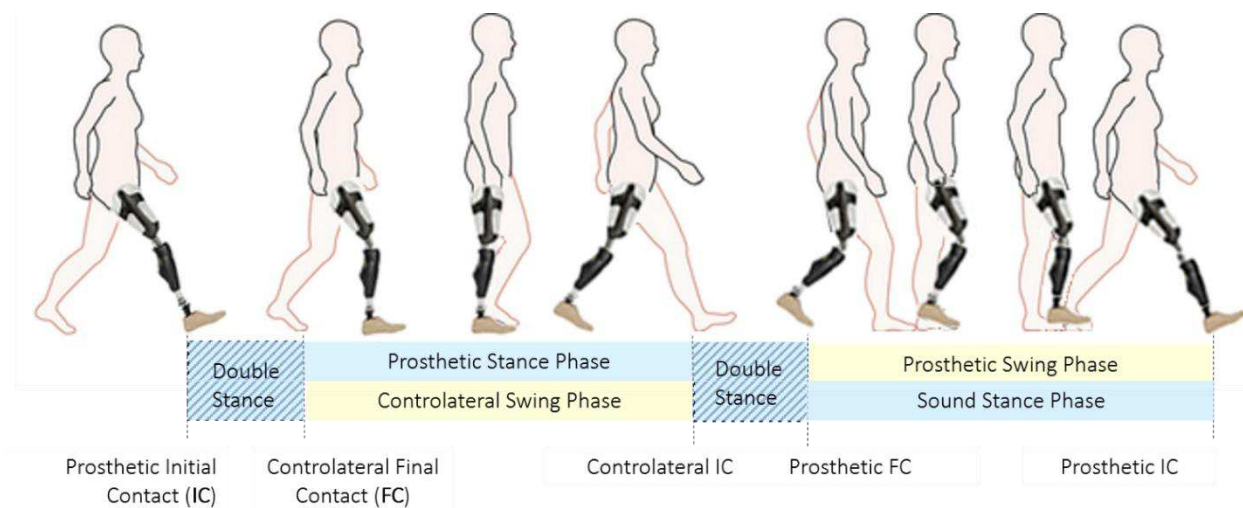
Figure 7: Prosthetic gait cycle and main gait events

---

[3] The ICF is a framework developed by the WHO (https://www.who.int/classifications/icf/en/)

In a systematic review in 2011, Sagawa and coworkers found that gait velocity, cadence, stride and step length are the most common parameters used to describe the gait of people with lower-limb amputation (Sagawa *et al.*, 2011). These parameters are easy to measure and interpret and are considered as global gait descriptors (Sagawa *et al.*, 2011). They indeed allow to detect the presence and quantify gait impairment but do not provide information regarding the cause of impairment.

2.3.2. Function assessment parameters

Following lower-limb amputation, the loss of articular and muscle complexes results in significant changes in the gait pattern, whether at the kinematic or the kinetic levels. Important kinematic adaptations (segments orientation, joint range of motion, …) may be observed with the naked eyes. However, the use of dedicated instruments, such as optoelectronic systems, is required for their quantification or for refined assessments, for instance when aiming at assessing the evolution of a joint angle within a patient following the prescription of a new prosthetic device or a new rehabilitation protocol. Furthermore, laboratory-based biomechanical gait analysis allows to quantify kinetic parameters that cannot be estimated without instrumentation, such as intersegmental moments, or the contributions of each joint in the generated mechanical power. Function assessment parameters have been extensively studied in people with lower-limb amputation and this paragraph aims at providing an overview of the relevant literature. Detailed description of the acquisition of such parameters using optical motion capture systems and force plates can be found in the literature (Cappozzo *et al.*, 2005; Goujon, 2006).

a. Kinematic gait analysis

The use of optical motion capture data allows to retrieve curves describing the evolution of segment orientations and joint angles during a gait cycle. Comparing the curve patterns of people with lower-limb amputation to that of an asymptomatic population has allowed to identify some specificities of lower-limb amputee gait (Sagawa *et al.*, 2011). Similarly, comparing the angle patterns of a person in a pre/post configuration may allow to identify the impact of a prosthetic device or rehabilitation procedure on gait.

Gait compensations typically observed in the gait of people with lower-limb amputation (see section 1.3 in Chapter 1) can often be evidenced using such kinematic parameters. Hip circumduction has for instance been characterized with the measure of the maximal value of the hip abduction angle during swing (Dauriac, 2018), hip hiking with elevation of the pelvis in the frontal plane. An increase in trunk motion was also observed in the frontal plane in people with transtibial amputation and in all the three anatomical planes in people with transfemoral amputation compared to sound subjects (Jaegers *et al.*, 1995; Goujon-Pillet *et al.*, 2008; Rueda *et al.*, 2013).

Additional kinematic adaptations are observed at the hip joint in people with transfemoral amputations for prosthetic knee control. For instance, swing phase knee flexion is initiated by the premature recruitment of hip flexor muscles (Bonnet *et al.*, 2014). Furthermore, instead of maintaining a constant hip flexion at early stance as in sound subjects, the residual hip tends to have an extension

motion from prosthetic initial contact to secure the knee in extension (Jaegers *et al.*, 1995; Villa, 2014). During prosthetic stance, differently from what is observed in sound subjects, the knee remains in extension in people with transfemoral amputation (**Figure 8**), even when the prosthetic knee allows some flexion (Detrembleur *et al.*, 2005; Sagawa *et al.*, 2011). As a result, the knee cannot be used as a shock absorber during stance. This phenomenon is also observed, at a lesser degree, in people with transtibial amputation (Sagawa *et al.*, 2011).
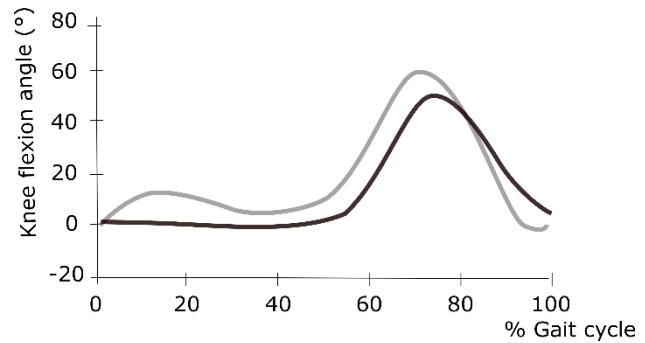
Figure 8: Knee flexion angle in asymptomatic subjects (grey curve) and in transfemoral amputees (black curve). Taken from (Detrembleur et al. 2005)

The characterization of such kinematic adaptations provides accurate information on specific body segments or joints. Therefore, the study of a large number of parameters or features extracted from curve patterns (e.g. maximal flexion angle) of various body segments or joints is required to obtain a global description of gait.

Kinematics of the body center of mass

From a mechanical standpoint, locomotion can also be described by the motion of the body center of mass, resulting from the summation of forces and moments exerted on each body segment (Saunders *et al.*, 1953; Detrembleur *et al.*, 2000; Pavei *et al.*, 2017; Tesio and Rota, 2019). Interestingly, the study of the body center of mass motion provides global information regarding the gait of a person from a single parameter. Indeed, kinematic alterations at the segment or joint level have repercussion on the body center of mass motion (Saunders *et al.*, 1953). For instance, the absence of prosthetic knee flexion results in an increased amplitude of the body center of mass excursion during the gait cycle of people with transfemoral amputation (Tesio *et al.*, 1998; Detrembleur *et al.*, 2005) which was shown to reach up to 4.1 times that of asymptomatic subjects in (Detrembleur *et al.*, 2005). Asymmetries in the gait pattern can also be detected in the 3D path of the body center of mass (Minetti *et al.*, 2011; Pavei *et al.*, 2017; Askew *et al.*, 2019), and a high degree of asymmetry of the 2D body center of mass path in the horizontal plane has been evidenced in people with transtibial amputation (Askew *et al.*, 2019). The vertical components of the excursion and velocity of the center of mass (Strutzenberger *et al.*, 2019; Ochoa-Diaz and Padilha L. Bó, 2020) also allow to evidence some degree
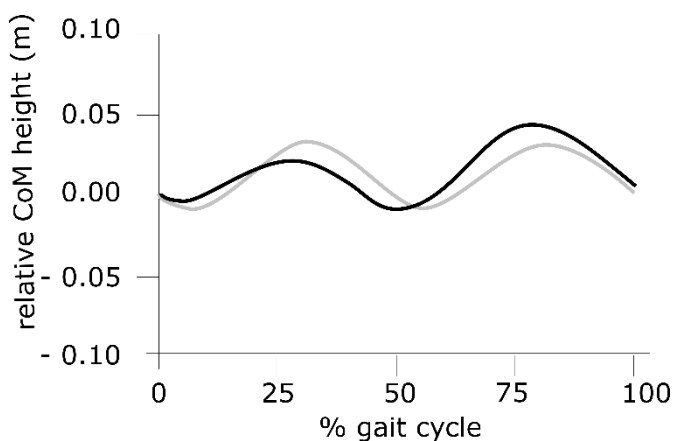
Figure 9: Body center of mass vertical relative excursion during the prosthetic limb gait cycle in people with transfemoral amputees (black curve) and asymptomatic subjects (grey curve), adapted from (Strutzenberger et al. 2019).

of asymmetry (**Figure 9**). It was for instance shown that the vertical displacement of the body center of mass was lower during the prosthetic stance than the sound limb stance (Tesio *et al.*, 1998; Agrawal *et al.*, 2009) in both people with transtibial and transfemoral amputation, possibly due to prosthetic feet design, and in particular, to the lower effective foot length ratio of prosthetic feet compared to physiological feet (Agrawal *et al.*, 2009).

Biomechanical gait analysis allows the estimation of body center of mass motion from two approaches: either from force plates data (using the second law of Newton) or from segmental analysis, that is, from the weighted summation of the motion of each individual segment center of mass. In the first case, using force plates data, the acceleration of the body center of mass is computed from the measured ground reactions forces as well as body weight. Obtaining the body center of mass trajectory or instantaneous velocity requires to integrate the acceleration, and therefore to formulate hypotheses on the integration constants. In the second case, when estimating the body center of mass motion from segmental analysis, the measure of the positions of optical motion capture markers must be coupled with an inertial model in order to obtain the mass of each segment (required for the weighted sum) and the position of each segment's center of mass in its respective anatomical frame. Therefore, different inertial models may yield different estimates of the body center of mass trajectory (Pavei *et al.*, 2017). To obtain the velocity or the acceleration of the body center of mass, its position must be differentiated. The use of a low-pass filter to remove signal noise inherent to the differentiation process may result in an over-smoothed signal. In both these laboratory-based approaches, the retrieval of body center of mass motion is not as straightforward as the retrieval of segment orientation or joint angle, but it provides a synthetic parameter for gait evaluation.

b. Kinetic gait analysis

Kinetic gait analysis focuses on parameters that explain the origin of motion. For instance, ground reaction forces and moments, measured by force plates, allow to measure the external forces applied on a body. Ground reaction forces exerted under each limb individually are of particular interest for the rehabilitation of people with lower-limb amputation (Loiret *et al.*, 2019). Indeed, the latter allows
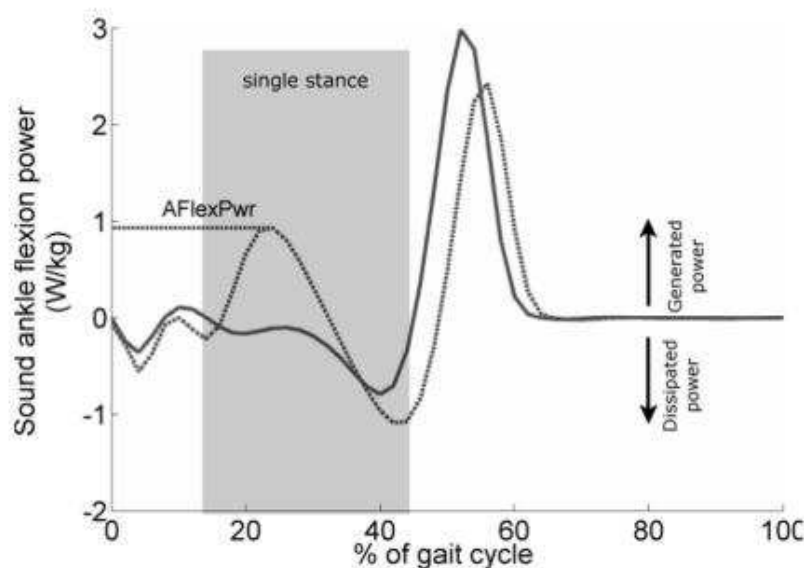
Figure 10: Flexion power at the ankle in asymptomatic subjects (solid line) and in a person with transfemoral amputation with vaulting (dotted line). Taken from (Drevelle *et al.*, 2014)

to quantify how a person loads his/her prosthesis. Inverse dynamics approaches allow to retrieve the articular moments, forces and power at each joint from the measured ground reaction forces and moments as well as joint kinematics. Similar as for kinematic parameters, a multitude of joint kinetic parameters can be retrieved from biomechanical gait analysis, resulting in a complete and accurate description of "localized" gait kinetics. The flexion power peak measured at the sound ankle during stance (**Figure 10**) was for instance shown to allow the quantification of vaulting (Drevelle *et al.*, 2014). In early stance at the intact limb of both transtibial and transfemoral amputees, the increase in the sound hip extensor muscles work and the resulting hip moment have been assumed to facilitate the forward translation of the pelvis in absence of propulsion from the prosthetic ankle (Seroussi *et al.*, 1996; Silverman *et al.*, 2008; Prinsen *et al.*, 2011; Sagawa *et al.*, 2011).

Kinetics of the body center of mass

Some mechanical parameters offering a global overview of gait kinetics have also been proposed and are computed at the body center of mass. The net mechanical work at the body center of mass, which results from the mechanical work generated or dissipated by each joint for the translation of the body center of mass, is a synthesized global gait descriptor. The net mechanical work can be computed as the time integral of the body center of mass power. The former is itself computed as the time derivative of the sum of the kinetic and potential energies. Neglecting the kinetic energy due to the rotations of the body segments relative to the body center of mass, the power of the body center of mass (P_{BCoM}) can be calculated as the dot product of the external forces applied on the body center of mass ($\boldsymbol{F_{ext}}$) with the body center of mass velocity ($\boldsymbol{v_{BCoM}}$) :

$$P_{BCoM} = \sum \boldsymbol{F_{ext}} . \boldsymbol{v_{BCoM}}$$

It is therefore a relatively simple parameter to compute and can be estimated from force platforms data alone (Donelan *et al.*, 2002b). Furthermore, the external mechanical work represents the mechanical component of the metabolic energy required for locomotion, explaining the contributions of the musculoskeletal body structures without considerations of a person's metabolism or anthropometric measures.

However, the external mechanical work was found not to allow the discrimination of people with transfemoral amputation from sound participants (Gitter *et al.*, 1995; Askew *et al.*, 2019) and therefore, not to explain the 27 % increase of metabolic energy required when walking with a prosthesis in transfemoral amputees (Gitter *et al.*, 1995). This might be explained by compensations in the generated and dissipated power by each leg during the double stance of walking. The individual limb method was therefore proposed to estimate the mechanical energy produced by each lower-limb individually (P_{left} and P_{right} for the left and right limbs respectively) including during the double stance phase of a gait cycle (Donelan *et al.*, 2002b) :

$$P_{BCoM} = \boldsymbol{F_{left}} . \boldsymbol{v_{BCoM}} + \boldsymbol{F_{right}} . \boldsymbol{v_{BCoM}} = P_{left} + P_{right}$$

Using this approach, several authors have also evidenced that the loss of mechanical energy production due to prosthetic components is compensated by an increase in power generation at the intact limb (Houdijk *et al.*, 2009; Bonnet *et al.*, 2014). This asymmetry in power generation was found to increase with amputation level, with, for instance the affected limb generating 0.09 J/kg and 0.16 J/kg in people with transfemoral and transtibial amputation in late stance compared to work production of 0.34 J/kg and 0.27 J/kg respectively by the intact limb (Houdijk *et al.*, 2009; Bonnet *et*

al., 2014) and to increase with walking speed. The compensation of the decreased power generation of the intact limb by the increased power generation of the prosthetic limb may therefore explain why total external mechanical energy fails to account for the increased metabolic energy consumption observed in lower-limb amputee gait (Donelan *et al.*, 2002a; Houdijk *et al.*, 2009; Bonnet *et al.*, 2014). Based on these findings, an index of asymmetry between the external work generated by the intact and the prosthetic limbs was therefore proposed in (Agrawal *et al.*, 2009) to compare different prosthetic feet and was found to differentiate different designs of feet. The asymmetry in external work was also found to be more sensitive than the asymmetry in vertical body center of mass displacement and step length asymmetry in nine people with transtibial amputation (Askew *et al.*, 2019), corroborating previous findings according to which the study of the mechanical work generated by lower-limb amputees might allow to identify asymmetries that are not detected using mere kinematic analyses (Tesio *et al.*, 1998; Tesio and Rota, 2019). All in all, the analysis of the external mechanical work using the individual limb method allows to provide insight on gait deficiencies (asymmetries, energetic consumption).

c.   Synthesis on the function assessment parameters

To sum up, the study of kinematic and kinetic parameters during locomotion allows to describe alterations and functional adaptations adopted by people with lower-limb amputation while walking. Most of the compensatory motions adopted were shown to involve the intact limb and the residual hip joint, especially in people with transfemoral amputation. These abnormal solicitations are evidenced by analyses of joint and segment ranges of motion and joint moments and powers, which require to analyze the curve patterns of multiple joints or segments. Alternatively, the study of the body center of mass motion and mechanical energy *via* the individual limb method have been shown to provide synthetic information regarding the gait of people with lower limb amputation, although at the cost of complexification of interpretation (evaluating the body center of mass motion being less tangible than that of a physical point of the body, such as the knee joint).

2.3.3.   *Performance assessment parameters*

Motion performance can be evaluated using criteria related to the quality and the efficiency of the locomotor act. In this thesis, the notion of "gait quality" will be used to describe parameters relative to gait symmetry (homogenous solicitation of the prosthetic and the sound limb, aesthetic gait) and to gait balance, while the notion of "gait efficiency" will be related to the metabolic cost of ambulation, cognitive demand associated with walking and to the actual activity performance in the community (walking speed, activity level and participation).

a. Gait quality indices

i.   Symmetry

Gait symmetry is relative to the similarity of successive contralateral limb strides or steps. Symmetry indices are generally computed to characterize three aspects of gait: limb loading (loading symmetry), step length (spatial symmetry) and stance phase duration (temporal symmetry - see **Figure 7**). Prosthetic gait has been shown to be highly asymmetrical with, in general, more time spent in stance phase on the intact limb than on the prosthetic limb, longer prosthetic steps than contralateral steps and higher loading of the intact limb than the prosthetic limb (Jaegers *et al.*, 1995; Nolan *et al.*,

20

2003; Goujon, 2006; Sagawa *et al.*, 2011; Roerdink *et al.*, 2012; Cutti *et al.*, 2018). Asymmetry has been also shown to be more variable than in people without orthopedic disorders (Dingwell *et al.*, 1996; Nolan *et al.*, 2003; Hof *et al.*, 2007). Visual and auditive feedback have been shown to improve stance time and loading symmetry in people with transtibial amputation (Dingwell *et al.*, 1996; Yang *et al.*, 2012) and thus constitute an interesting track for rehabilitation. Indeed, spatiotemporal and loading asymmetries may lead to long-term comorbidities and are thus targeted in rehabilitation protocols (Nolan *et al.*, 2003; Loiret, 2016; Villa, Bascou, *et al.*, 2017). However, several authors have hypothesized that step length and duration asymmetries might be implemented for increasing gait stability, and that functional rehabilitation should not solely focus on the restoration of spatiotemporal symmetry (Hof *et al.*, 2007; Roerdink *et al.*, 2012; Hak *et al.*, 2014). Similarly, in a recent study based on the gait of only two people with knee disarticulation, stance duration asymmetry was assumed to be an efficient compensation to insufficient prosthetic push off and work generation (Mohamed *et al.*, 2019). Therefore, while such global parameters are useful to rapidly assess the overall gait performance or quality, they do not provide an understanding of the underlying mechanical causes. These parameters should thus be completed with mechanical descriptors in order to both quantify and mitigate gait deviations.

Gait symmetry can also be quantified through body center of mass-derived parameters. Indeed, various abnormal kinematic patterns (for instance, in knee flexion) are reflected in an asymmetric pattern of the body center of mass motion (Tesio *et al.*, 1998; Agrawal *et al.*, 2009; Askew *et al.*, 2019; Strutzenberger *et al.*, 2019) or in the external work done by each lower-limb (Agrawal *et al.*, 2009; Houdijk *et al.*, 2009; Bonnet *et al.*, 2014; Askew *et al.*, 2019). Asymmetry in external work has been shown to discriminate different prosthetic feet (Agrawal *et al.*, 2009; Askew *et al.*, 2019) and to be positively correlated with the metabolic cost of walking (Askew *et al.*, 2019).

ii.   Balance

The term "gait stability", widely found in the literature on human motion analysis, is often used to describe a "gait that does not lead to fall", while stability, in a mechanical standpoint, relates to the ability of a system to develop forces or moments in order to restore a state of equilibrium after a perturbation (Bruijn et al. 2013; Robert 2019). Most parameters describing "gait stability" in the literature are in fact parameters which aim at quantifying the risk of falling while parameters describing the mechanisms implemented by the body as a whole (seen as a mechanical system) preventing the occurrence of falling following a perturbation are rarely described. In what follows, the terminology "balance control" will be used to describe parameters associated with the risk of falling during gait.

People with lower-limb amputation are more prone to falling than the asymptomatic age-matched population. One in two people with transfemoral amputation reports falling at least once a year, and a third of lower-limb amputees report avoiding activities due to fear of falling (Miller et al. 2001; Frossard et al. 2010). Thus, quantifying and understanding the underlying mechanisms of balance is paramount for the rehabilitation of lower-limb amputees and for prostheses design.

Postural balance

Postural balance is studied in gait analysis laboratories using force-platform derived measurements, such as the center of pressure sway during stance (Winter, 1995). Control of balance during stance relies on the processing of multiple sensory inputs and results in sway that increases when some sensory inputs are disrupted (Najafi *et al.*, 2012), for instance when somatosensory

feedback is impaired, such as in people with amputation. The latter thus exhibit a wider center of pressure path at the intact foot than at the prosthetic foot or compared to sound subjects. New generation feet provide control over the ankle mobility and are thus assumed to increase balance. The benefits of new generation prosthetic feet were recently investigated through the analysis of center of pressure excursions while standing on level ground and in slopes (Thomas-Pohl *et al.*, 2019).

Balance control during gait

In 2005, Hof and coworkers have introduced new parameters to quantify dynamic stability: the "extrapolated center of mass" and "margin of stability" (**Figure 11**). These notions allow to expand to
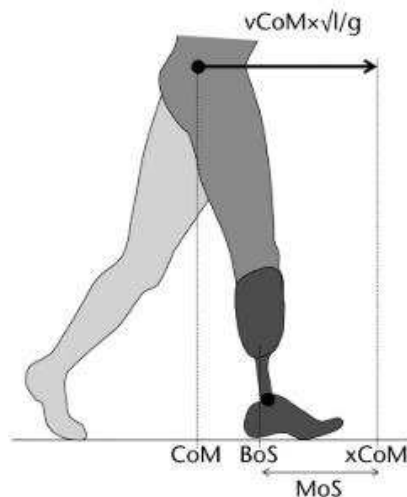
Figure 11: Definition of the Margin of Stability (MoS) as the backward distance between the extrapolated center of mass (xCoM) and the posterior limit of the base of support (BoS). The xCoM is calculated as the addition of the position of the center of mass (CoM) and its velocity (vCoM) divided by the eigenfrequency of an inverted pendulum of length l (leg length). From (Hak *et al.*, 2014)

gait the stability criterion defined in stance (according to which the projection of the body center of mass should lie within the base of support) by taking into account the velocity of the body center of mass (Hof *et al.*, 2005). Since then, multiple studies have focused on the study of these parameters, in particular in people with lower-limb amputation who were shown to have a reduced margin of stability compared to asymptomatic people (Hof *et al.*, 2007; Hak *et al.*, 2014). Using the concept of the extrapolated center of mass, the authors demonstrated that decreasing step length allows to compensate for the reduction of margin of stability induced by the decreasing velocity of the body center of mass following prosthetic push off (Hak *et al.*, 2014). Therefore, they conclude that step length asymmetry might be a functional adjustment for increased stability.

b. Gait efficiency

i. Metabolic energy cost

Energy expenditure allows to measure gait efficiency. Indeed, locomotion aims at translating the body in space while minimizing energy expenditure (Saunders *et al.*, 1953; Waters and Mulroy, 1999). Metabolic energy expenditure is estimated through the measure of oxygen uptake during the steady state of a physical task (Waters *et al.*, 1976; Perry, 1992). Metabolic energy rate is the amount of energy demand per unit time and was shown to be similar for people with lower-limb amputation and sound subjects, except for people with vascular transfemoral amputation (Waters *et al.*, 1976). However, metabolic energy cost, computed as the ratio of metabolic energy rate per walking speed, was shown to increase with amputation level for a given etiology and with etiology for a given amputation level (Waters *et al.*, 1976; Waters and Mulroy, 1999; Schmalz *et al.*, 2002; Detrembleur *et al.*, 2005). This raise in energy expenditure as a function of the walking speed is supposed to be caused

by kinematic compensations and by the increase of power generated by the residual and sound joints to cope with the reduced or the absence of power provided by prosthetic components (Sagawa *et al.*, 2011; Piazza *et al.*, 2017; Askew *et al.*, 2019). Reduction of metabolic energy cost following rehabilitation or modifications to prosthetic components is used to demonstrate the efficiency of an intervention or a new prosthetic design (Waters and Mulroy, 1999; Schmalz *et al.*, 2002; Askew *et al.*, 2019). Indirect calorimetry is not always available in motion analysis laboratories (Bonnet *et al.*, 2014). Furthermore, metabolic energy consumption is highly dependent on physiological parameters (gender, obesity, fatigue, digestion…) and its measure with spirometry devices suffers from calibration errors which might alter sensitivity (Ghillebert *et al.*, 2019). Therefore, the computation of mechanical energy, very accessible in laboratory-based motion analysis, can allow to retrieve the mechanical determinants of metabolic energy (van de Walle *et al.*, 2012). In particular, the work done during step-to-step transition was shown to correlate well and to partially explain metabolic energy cost (Donelan *et al.*, 2002a; Houdijk *et al.*, 2009).

ii. Cognitive load

While self-reports and questionnaires indicate that prosthetic gait is often associated with a significant cognitive load (Miller *et al.*, 2001; Morgan *et al.*, 2018), the dual-task paradigm implemented in research hasn't allowed to consistently refute or accept this hypothesis (Morgan *et al.*, 2018). In recent studies, cognitive and gait performance were observed to significantly decrease in both experienced and newly prosthetic ambulators during dual tasks (Frengopoulos *et al.*, 2018; Hunter *et al.*, 2018), confirming that walking represent a cognitive load in people with lower-limb amputation. However, based on the literature, concurrent dual task while walking didn't differentially affect people with amputation and sound participants (Morgan *et al.*, 2018). In a recent review investigating dual task paradigm in people with lower-limb amputation, the authors suggest that in-lab level walking may not be sufficiently challenging to be representative of the cognitive load encountered in daily living and that the chosen outcome measures (gait velocity, spatiotemporal and loading asymmetry, step width) may not be sensitive enough to discriminate groups (Morgan *et al.*, 2018).

iii. Activity level

Physical activity level in the community cannot be assessed in motion analysis laboratories using conventional measuring systems. However, gait walking speed has been shown to increase with the K-level which is used to predict community-based mobility (Batten et al. 2019). This global functional outcome is quantified both in research settings and in rehabilitation due to its reliability, sensitivity and ability to predict overall health status and quality of life (Fritz and Lusardi, 2009). The lower self-selected speed of people with lower-limb amputation compared to sound subjects might therefore be interpreted as decreased ambulatory performance (Frengopoulos *et al.*, 2018). Furthermore, comfortable walking speed can be seen as a measure of gait efficiency loss (Waters and Mulroy, 1999): indeed, it seems to be regulated in people with lower-limb amputation so that metabolic energy rate of walking remains in the range of that of sound subjects (Waters *et al.*, 1976; Waters and Mulroy, 1999).

2.4. Limitations of clinical and laboratory-based gait analysis and perspectives

The aim of this chapter was to provide an overview of the available tools/parameters for gait assessment of people with lower-limb amputation during the rehabilitation and subsequent follow-up visits in clinics and in motion analysis laboratories. Objective gait analysis allows to accurately characterize and evaluate gait function and performance. However, administering laboratory-based biomechanical gait analysis in clinical practice is not always possible due to high system costs, time-consuming protocols and analysis complexity (Perry, 1992; Calmels *et al.*, 2002; Cuesta-Vargas *et al.*, 2010; Loiret *et al.*, 2019). Thus, clinicians mostly rely on their experienced eyes and on validated clinical tests to identify the degree of impairment of their patients, to evaluate their progression or to plan new rehabilitation strategies. Therefore, few quantitative data are available to support the assessment of the functional rehabilitation of people with lower-limb amputation.

In the last two decades, miniaturization of sensing technologies and advancement in processing techniques and communication protocols have made wearable technology accessible to gait analysis (Wong *et al.*, 2007, 2015). Wearable sensors have the advantages of being portable – they can be worn by patients without hindering or constraining their motion – and are not limited to a predefined acquisition volume, which allows recording data outside of laboratories. Therefore, their use in clinical and research gait analysis offers multiple perspectives such as ecological measurements, simplified protocols, real-time feedback, long-term and remote monitoring or home-based and telerehabilitation opportunities (Hafner and Sanders, 2014; Iosa, Picerno, *et al.*, 2016; Villa, Bascou, *et al.*, 2017).

Chapter 3 – Wearable motion analysis

As introduced in the previous section, wearable sensors are a very attractive alternative to laboratory-based instruments for gait analysis. However, they differ from gold standard optical motion capture systems and force plates by the nature of the measured data. Therefore, obtaining relevant gait descriptors with wearable sensors may not be straightforward (Cutti *et al.*, 2015; Iosa, Picerno, *et al.*, 2016). The objective of this chapter is to introduce the most common wearable sensor technologies and to provide an overview of their outputs. This will allow to introduce the challenges faced regarding the use of wearable sensors for the rehabilitation of people with lower-limb amputation and therefore, the issues that will be addressed in this thesis.

3.1. Presentation of wearable sensors

Different sensing technologies have been described in the literature on wearable gait analysis. They include, but are not limited to, electrogoniometers, magnetic and inertial sensors (accelerometers, gyroscope, or their combination – also known as inertial measurement units or magneto-inertial measurement units when a magnetometer is included), pressure sensors, force sensors, surface EMGs, and sensing fabric (Wong *et al.*, 2007, 2015; Patel *et al.*, 2012; Muro-de-la-Herran *et al.*, 2014). **Table 1** summarizes their main properties and applications, as well as challenges associated with their use.

Inertial sensors consist in the most used technology in wearable gait analysis (Wong *et al.*, 2007, 2015; Muro-de-la-Herran *et al.*, 2014). For instance, 62.5% of the published literature on wearable gait analysis in 2012-2013 dealt with inertial sensors (Muro-de-la-Herran *et al.*, 2014). Together with pressure insoles, inertial sensors are the wearable technology the more susceptible to capture kinematic and kinetic parameters that are usually retrieved using optical motion capture and force plate systems (Muro-de-la-Herran *et al.*, 2014). Therefore, the next two paragraphs will provide a more detailed description of inertial and pressure sensors and the literature review in section 3.2 will focus on gait descriptors that can be measured or estimated using these two categories of sensors.

Table 1: Measured quantities and challenges   encountered when using wearable sensors
MIMU = (Magneto-)Inertial Measurement Unit; ECG = Electro-cardiogram

	Sensor	Measured quantity	Estimated / Computed data	Biomechanical model	Challenges
	Electrogoniometer	Flexion angle	Relative joint angle (Muro-de-la-Herran *et al.*, 2014)	/	- High sensitivity, requires careful placement (Wong *et al.*, 2015) - Complex setup procedures (Wong *et al.*, 2015) - May hinder motion (Wong *et al.*, 2015)
Inertial sensors	Accelerometer	Linear acceleration	- Segment velocity, displacement (Muro-de-la-Herran *et al.*, 2014) - Joint angle (Iosa, Picerno, *et al.*, 2016) in static, posture (Redfield *et al.*, 2013b; Iosa, Picerno, *et al.*, 2016)	/	- Noisy measurement (Wong *et al.*, 2015) - Integration drift (Iosa, Picerno, *et al.*, 2016) ; might be compensated for using kinematic models - Sensor-to-segment calibration required (Wong *et al.*, 2015; Poitras *et al.*, 2019)
			- Gait event detection and spatiotemporal parameters (Pacini Panebianco *et al.*, 2018) - Number of steps (Patel *et al.*, 2012; Benson *et al.*, 2018)	Kinematic models for spatial parameters	- Gait alterations and low speed may compromise the identification of events from acceleration signals in pathological gait (Trojaniello, Cereatti and Della Croce, 2014)
			- Gait stability (Guaitolini *et al.*, 2019)	Inverted pendulum model: extrapolated center of mass theory	- Integration drift (Iosa, Picerno, *et al.*, 2016) - Orientation inconsistency (Picerno *et al.*, 2011; Guaitolini *et al.*, 2019)
			- Fall-risk prediction & balance assessment (Wong *et al.*, 2007; Iosa, Picerno, *et al.*, 2016; Ghislieri *et al.*, 2019)	/	- Removal of gravity necessary (orientation) (Benson *et al.*, 2018) - Lack of information regarding sensitivity (Ghislieri *et al.*, 2019) and validity of original parameters (Benson *et al.*, 2018)
			- Symmetry indices (Iosa, Picerno, *et al.*, 2016; Benson *et al.*, 2018)	/	- Original parameters that may lack validity (Benson *et al.*, 2018)

Sensor	Measured quantity	Estimated / Computed data	Biomechanical model	Challenges
		- Energy expenditure (Ladlow *et al.*, 2017)	Regression between measured acceleration, physiological parameters & oxygen consumption	- Regression equations are specific to populations (Ladlow *et al.*, 2017)
Gyroscope	Angular velocity	- Segment angular acceleration, orientation - Joint angles (Poitras *et al.*, 2019)	Kinematic models might be used to limit drift	- Integration drift (Iosa, Picerno, *et al.*, 2016) - Sensor-to-segment calibration required (Wong *et al.*, 2015; Poitras *et al.*, 2019)
		- Gait event detection and spatiotemporal parameters (Pacini Panebianco *et al.*, 2018)	Kinematic model for spatial parameters	- Gait alterations may compromise the identification of events from gyroscope signals in pathological gait (Jasiewicz *et al.*, 2006) - Symmetry assumption for spatial parameters estimation (Aminian *et al.*, 2002)
MIMU	Linear acceleration, angular velocity (and magnetic field)	*Same as accelerometer and gyroscope* +	/	- Easy set up (Wong et al. 2015) - May require complex algorithms (Muro-de-la-Herran *et al.*, 2014) - Sensitive to magnetic disturbances when magnetometer is included (Picerno *et al.*, 2011; Wong *et al.*, 2015)
		- Walking speed (Li *et al.*, 2010; Benson *et al.*, 2018)	Kinematic model	- Integration drift (Iosa, Picerno, *et al.*, 2016)
		- Ground reaction forces (Shahabpoor and Pavic, 2017; Ancillao *et al.*, 2018)	Inertial model + force distribution between feet during double stance	- Double stance indetermination (Shahabpoor and Pavic, 2017; Ancillao *et al.*, 2018)
		- Articular joints and moments (Karatsidis *et al.*, 2017)	Inertial model + kinematic chain + contact detection	
Force sensor	3D force	3D GRF (Liu *et al.*, 2011)	/	- Cumbersome to wear (Guo *et al.*, 2017; Ancillao *et al.*, 2018) - Modification of footwear (Ancillao *et al.*, 2018)

27

	Sensor	Measured quantity	Estimated / Computed data	Biomechanical model	Challenges
Pressure sensors	Foot switch (force-sensing resistors)	Pressure applied	Gait event detection / cycle segmentation (Maqbool *et al.*, 2017)	/	- Nonlinear response (Wong *et al.*, 2015)
	Pressure insoles	Pressure applied	- Gait event detection (Loiret *et al.*, 2019) - Temporal parameters, asymmetry in stance phase duration (Cutti *et al.*, 2018; Loiret *et al.*, 2019)	/	- Requiring size adapted to patient's shoes (Wong *et al.*, 2015) - Requiring calibration for threshold-based gait event detection (Loiret *et al.*, 2019)
			- Pressure distribution (Wong *et al.*, 2015), center of pressure path - Stability measures derived from pressure distribution (Howcroft, Lemaire, *et al.*, 2016)	/	- Wear (Wong *et al.*, 2015) - Requiring calibration to mitigate wear effects / hysteresis (Abdul Razak *et al.*, 2012; Wong *et al.*, 2015)
			- Vertical component of the ground reaction force, asymmetry in limb loading (Cutti *et al.*, 2018; Loiret *et al.*, 2019)	/	- Requiring subject-specific calibration (Wong *et al.*, 2015) - Complex algorithm (nonlinearities) to derive force estimations (Wong *et al.*, 2015)
Surface EMG		Muscle activation patterns	- Muscle activity and muscle fatigue (Frigo and Crenna, 2009)	/	- Highly dependent on placement (training required) (Wong *et al.*, 2015) - Only superficial muscles can be measured (Wong *et al.*, 2015)
			- Motion intention (Wentink *et al.*, 2013; Wong *et al.*, 2015)	/	- Motion hindrance (Frigo and Crenna, 2009; Wong *et al.*, 2015) - Cross-talk of muscles / interferences (Frigo and Crenna, 2009; Wong *et al.*, 2015)
Sensing fabric		Strain measurement	- Segment orientation (Wong *et al.*, 2007; Fleury *et al.*, 2015)	/	- Sensitivity to temperature and humidity (Wong *et al.*, 2007; Fleury *et al.*, 2015)
		ECG	- Physiological parameters (Patel *et al.*, 2012; Fleury *et al.*, 2015)	/	- Motion artifact (Fleury *et al.*, 2015) - User discomfort (Fleury *et al.*, 2015)
Ultrasonic sensor		Distance between sensors	- Stride length, step length (Muro-de-la-Herran *et al.*, 2014)	/	- Sensitivity to sensor placement (Muro-de-la-Herran *et al.*, 2014) - Low accuracy compared to inertial sensors (Wong *et al.*, 2015)

3.1.1. Inertial sensors

Inertial measurement units (IMUs) consist of a combination of uni-, two- or three-axial orthogonally mounted accelerometer and gyroscope in a single case. They may also include a magnetometer; in that case they are generally called "Magneto-Inertial Measurement Units" (MIMUs). M/IMUs provide the values of angular velocity, linear acceleration and – when magnetometers are included – magnetic field components along the axes of the orthonormal coordinate system of the MIMU case (referred to as the "MIMU local frame" in this thesis). Each sensor included in a MIMU provides information about the 3D orientation of the MIMU local frame in a global Earth-fixed frame (**Figure 12**): accelerometers output can be used to determine the inclination of the sensor case compared to gravity, angular velocities provided by gyroscopes can be integrated to orientation angles and, when available, magnetic field measures can provide the heading, or magnetic North direction.
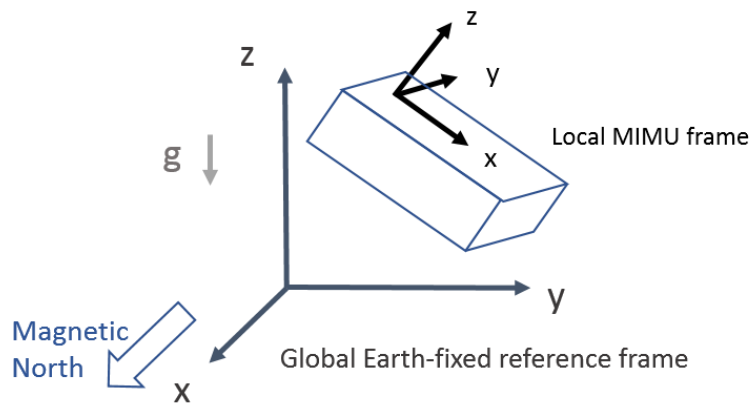
Figure 12: MIMU local frame and global Earth-fixed reference frame sensed by the MIMU (vertical z-axis aligned with gravity (g), x-axis aligned with the magnetic North)

However, each orientation estimate is affected by errors and must therefore be used under specific assumptions. Indeed, the accelerometer output contains both linear accelerations due to sensor motion and to gravity. Accelerometer-derived orientation estimates are thus more reliable in static or slow-motion conditions, when the gravity component can be isolated (Sabatini, 2011; Iosa, Picerno, *et al.*, 2016). Even in such conditions, accelerometers may only be used to estimate the inclination relative to the gravity vector, but not relative to the heading. Magnetometer readings can be used as a complementary information but are perturbated in the presence of ferromagnetic materials (Picerno *et al.*, 2011; Wong *et al.*, 2015; Iosa, Picerno, *et al.*, 2016). Conversely, gyroscopic data can be integrated to provide relative 3D orientation. However, gyroscope signals are generally biased, which results in drift when integrating angular velocity (Bergamini *et al.*, 2014). Sensor fusion is therefore used to combine the advantages and mitigate the weaknesses of each sensor so as to provide accurate estimates of the orientation of the MIMU local frame relative to a global Earth-fixed frame (Bergamini *et al.*, 2014; Ligorio *et al.*, 2016; Poitras *et al.*, 2019). Two main categories of fusion filters have been implemented: stochastic and complementary filters (Bergamini *et al.*, 2014). Kalman filters, which belong to the first category, use the measured signals at an instant and a representation of each sensor and its associated noise to predict the orientation at a further instant. The predicted and measured orientation are then fused. Complementary filters take advantage of the specificities of each sensor's

spectral characteristics (known *a priori*) to estimate the orientation, without modeling the noise characteristics of each sensor (**Figure 13**). For instance, they associate more trust to gyroscope readings in the high frequency domain and more trust to accelerometer/magnetometer readings in the low frequency range (Lopez-Nava and Angelica, 2016). Kalman filters and complementary filters were shown to equally mitigate the integration drift in locomotion tasks lasting up to 3 minutes (Bergamini *et al.*, 2014). Most of the commercially available MIMUs integrate a fusion filter.
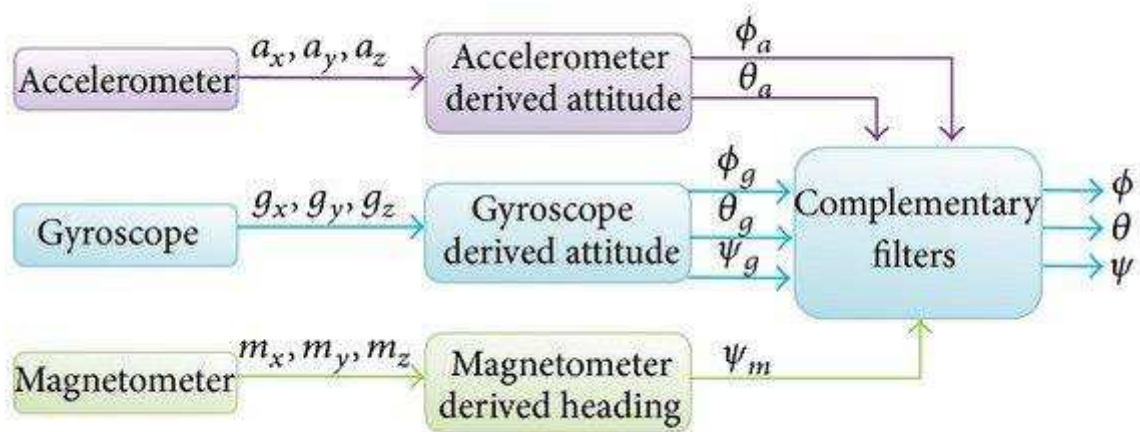
Figure 13: Working principle of complementary filters. Estimation of MIMU local frame orientation (roll ϕ, pitch θ, yaw ψ) in a global Earth-fixed reference frame from triaxial accelerometer (a_x, a_y, a_z), gyroscope (g_x, g_y, g_z) and magnetometer (m_x, m_y, m_z) readngs. Taken from (Amin *et al.*, 2014)

3.1.2. Pressure insoles

Various sensing technologies are used in pressure insoles, the most common being resistive (as in foot switches), capacitive, piezoelectric and piezoresistive sensors (Abdul Razak *et al.*, 2012). Depending on the technology and number of embedded sensors, pressure insoles provide either the pressure distribution or the normal load applied on the insole or both (Abdul Razak *et al.*, 2012; Wong *et al.*, 2015; Loiret *et al.*, 2019) (**Figure 14**). Insole designs whose output is the pressure distribution may also provide the path of the center of pressure and allow to estimate the normal component of the ground reaction force, which is non-linearly related to the applied pressure (Wong *et al.*, 2015). Whatever the design, insoles have to be rigorously calibrated before interpreting force data (Wong *et al.*, 2015; Loiret *et al.*, 2019).
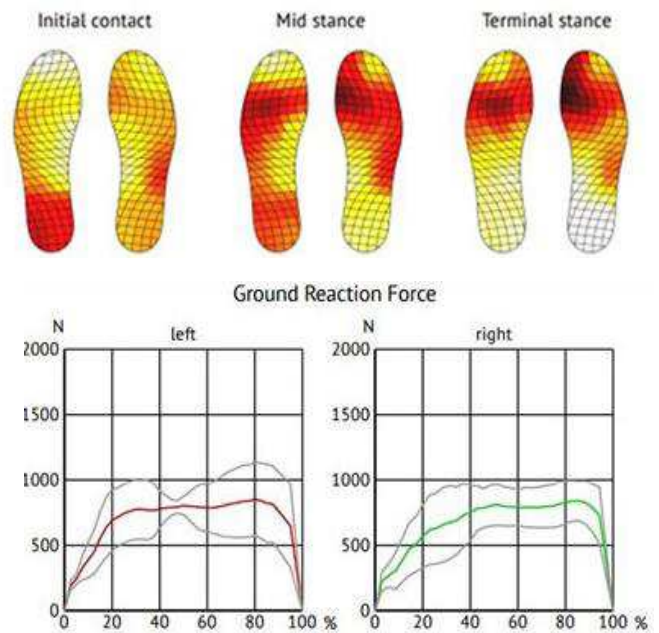
Figure 14: Example of pressure insoles output (from https://peakpodiatry.com.au)

3.2. Outcome parameters derived from wearable sensors

This section aims at describing to which extent pressure insoles and inertial measurement units can be used to monitor functional and performance outcomes of people with lower-limb amputation.

3.2.1. Spatiotemporal parameters

As reported in section 2.3.1, spatiotemporal parameters are paramount to describe gait function. Temporal parameters can be directly derived from gait events detection. This can be achieved with insoles, using a threshold on the pressure or force detected (Maqbool *et al.*, 2015; Loiret *et al.*, 2019), or with inertial sensors, by identifying key features within the output signals. A large body of literature has focused on inertial sensors-based gait events detection (Pacini Panebianco *et al.*, 2018), with some attempts in comparison (Trojaniello, Cereatti and Della Croce, 2014; Trojaniello *et al.*, 2015; Storm *et al.*, 2016; Pacini Panebianco *et al.*, 2018) and few applications in people with lower-limb amputation (Selles *et al.*, 2005; Maqbool *et al.*, 2017; Ledoux, 2018). It should be noted that alterations in the gait pattern of people with lower-limb amputation or other pathologies may compromise the validity of the algorithms that were not developed for this specific population (Trojaniello *et al.*, 2015; Tunca *et al.*, 2017).

While both inertial sensors and pressure insoles can be used for temporal parameters assessment, only inertial sensors allow to quantify spatial parameters. Two different approaches have been reported in the literature. In any case, the detection of either one or several events pertaining to the gait cycle is paramount.

The first approach consists in defining a kinematic model of gait (**Figure 15**). Two models based on a single inverted pendulum have been proposed for people with lower limb amputation from a gyroscope located on the thigh (Miyazaki, 1997) or an accelerometer located at the lower-back (Zijlstra and Hof, 2003; Houdijk *et al.*, 2008). The accuracy of prosthetic and sound step length estimates was not discussed (Miyazaki, 1997; Houdijk *et al.*, 2008). Aminian and coworkers have developed a more
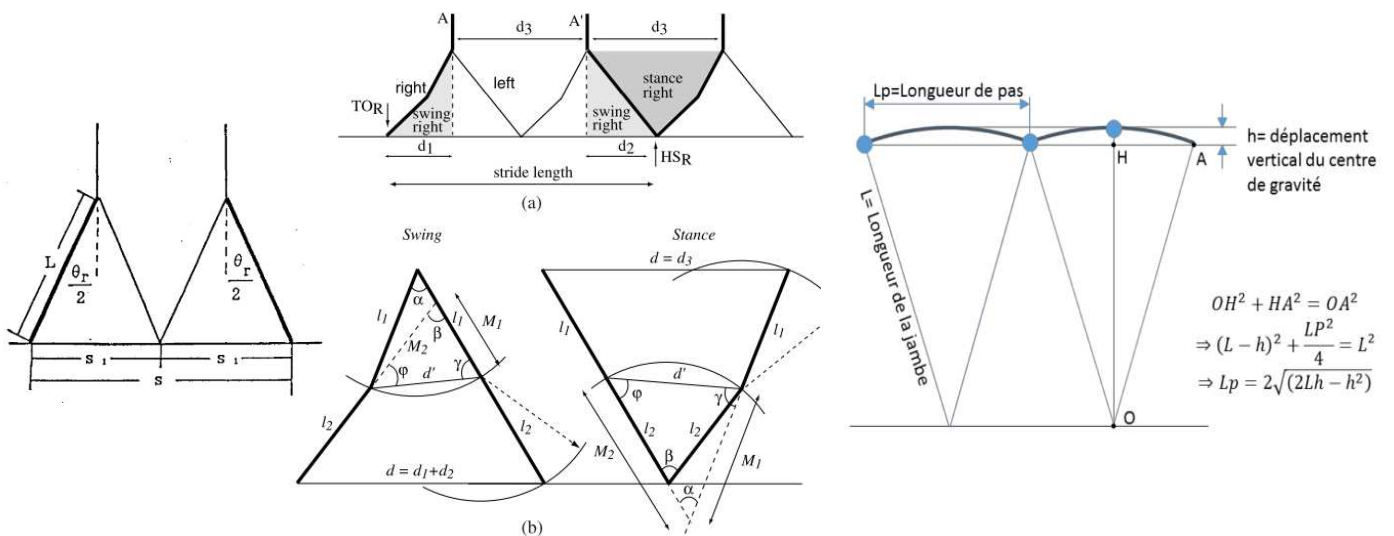
Figure 15: From left to right: Miyazaki's gait kinematic model (Miyazaki, 1997) ; Aminian's kinematic model (Aminian *et al.*, 2002) ; Inverted pendulum model used by Zijlstra and Hof (Zijlstra and Hof, 2003) to estimate step length. Image from Dauriac, 2018

complex model including both shanks and thighs which allows gait event detection using three gyroscopes (Aminian *et al.*, 2002). Swing phase is modeled as a double pendulum while stance phase is modeled as an inverted pendulum model. Integration of angular rates of the gyroscopes and knowledge of thighs and shanks lengths enable to obtain an estimate of stride length by trigonometry. All the developed models assume that gait is symmetrical, which is not the case in people with lower-limb amputation, especially those undergoing rehabilitation.

The second methodological approach to obtain spatial parameters with inertial sensors consists in the direct integration of the anteroposterior acceleration measured at the trunk (Köse *et al.*, 2012), shank (Li *et al.*, 2010; Trojaniello, Cereatti, Pelosin, *et al.*, 2014; Bertoli *et al.*, 2018) or foot (Sabatini *et al.*, 2005; Mariani *et al.*, 2010) between successive gait events. Hypotheses on the velocity of the foot (Sabatini *et al.*, 2005; Jasiewicz *et al.*, 2006; Mariani *et al.*, 2010) or shank (Li *et al.*, 2010; Yang and Li, 2012a; Trojaniello, Cereatti, Pelosin, *et al.*, 2014; Bertoli *et al.*, 2018) at specific instants of the cycle have to be assumed in order to correct the integration drift. Since the relative position of two inertial sensors is not known, methods based on sensors mounted on shank or foot only provide spatial parameters relative to strides, but not to steps. Conversely, using a waist-mounted MIMU, Köse and coworkers obtained an estimate of step length, with the assumption of equal speed at the beginning and end of the gait cycle (Köse *et al.*, 2012). None of these methods have been validated on people with lower-limb amputation.

3.2.2. Function assessment parameters

Function assessment parameters can be divided in kinematic and kinetic gait descriptors. The first category of parameters can exclusively be estimated with MIMUs, while both pressure and inertial sensors can be used to estimate the kinetics of human motion using wearable sensors.

a. Kinematic parameters

There is an extensive literature on the validity of using MIMUs to estimate kinematic parameters such as segment orientation, joint angles and range of motion (Picerno *et al.*, 2008; Cuesta-Vargas *et al.*, 2010; Seel *et al.*, 2014; Lebel *et al.*, 2017; Poitras *et al.*, 2019). Indeed, since sensors included in a MIMU can be fused to estimate the orientation of the MIMU local frame in a global Earth-fixed reference frame (see section 3.1.1), MIMUs have quickly emerged as a promising wearable alternative to optical motion capture systems (Wong *et al.*, 2007, 2015; Iosa, Picerno, *et al.*, 2016). However, noisy measurements and drift entailed in the numerical integration of sensor data does not make the estimation of such parameters trivial (Bergamini *et al.*, 2014; Iosa, Picerno, *et al.*, 2016). Furthermore, it must be noted that, to derive clinically-relevant information, the orientation of MIMU local frames with respect to the underlying segments, also known as sensor-to-segment alignment, has to be obtained (Iosa, Picerno, *et al.*, 2016; Picerno, 2017; Poitras *et al.*, 2019).

Four types of sensor-to-segment calibration methods have therefore been proposed in the literature: manual, static, functional and anatomical calibrations (**Figure 16**) (Pacher *et al.*, 2020). Manual calibration procedures consist in aligning the MIMUs case (and hence the MIMU local frame) with at least one segment axis. Although easy to set-up and time-efficient, this method is highly dependent on the operator and its reliability has not been assessed (Pacher *et al.*, 2020). For static calibration, the participant is required to take specific static postures in which a segment axis is assumed to be aligned with the gravity vector or joint angles are assumed to be known (in general: 0°

or 90°). This hypothesis may be a bit strong, especially in pathological gait (Zabat *et al.*, 2019). Cutti and coworkers have proposed to measure the residual joint angles using a goniometer (Cutti *et al.*, 2010) to the cost of increased calibration duration (Pacher *et al.*, 2020). Functional calibrations require the participants to realize single-plane rotations in order to estimate the segment axis in the MIMU frame. For applications in pathological gait, passive motions can be induced by an operator (Cutti *et al.*, 2010; Pacher *et al.*, 2020). These methods are more complex to set up as the operators must ensure that there is no out-of-plane motion (Pacher *et al.*, 2020) and depend on the biomechanical model assumed to represent joint motion (Poitras *et al.*, 2019). Finally, anatomical calibration relies on the determination of anatomical landmarks to construct anatomical frames similarly to what is done in optical motion capture analysis (Picerno *et al.*, 2008). Due to the complex additional instrument and longer set up, this calibration method is less prevalent in the literature (Pacher *et al.*, 2020). Sensor-to-segment calibration methods have been developed and validated for different populations, tasks, and sensor locations. Therefore, in the absence of comparative studies, there is currently no consensus on the most adapted method (Pacher *et al.*, 2020).
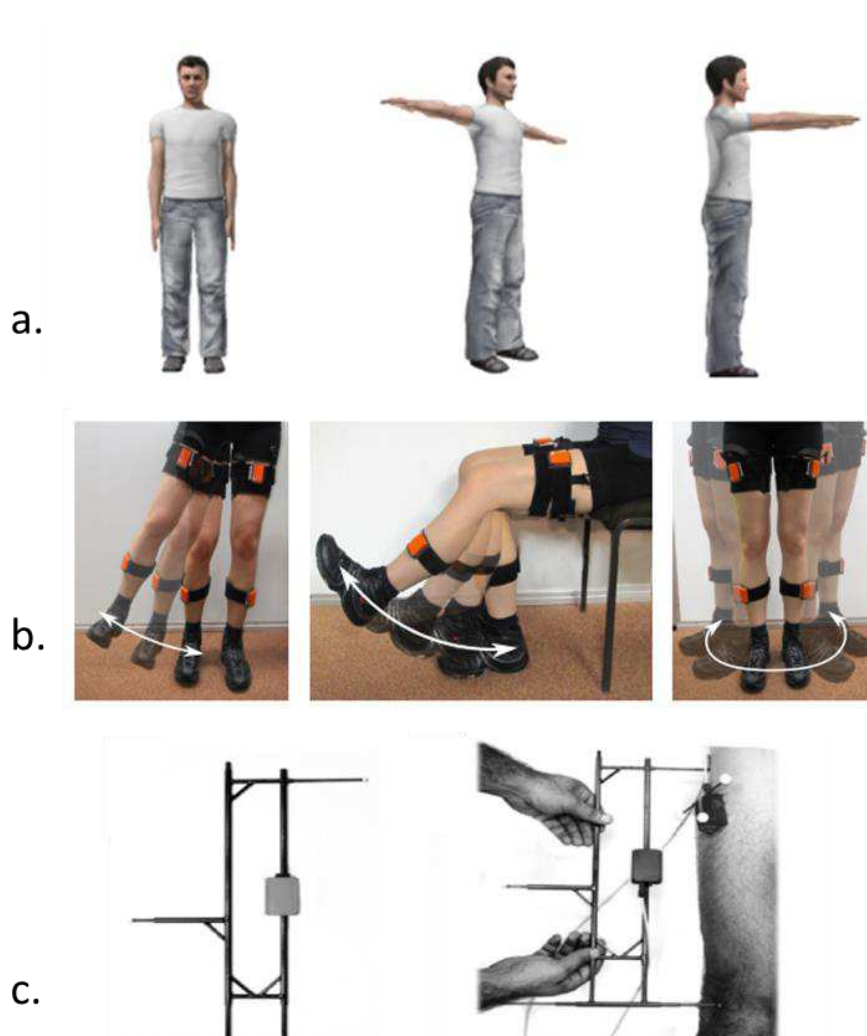
Figure 16: Example of sensor-to-segment calibration procedures
a. Static calibration (taken from (Liu *et al.*, 2019));
b. Functional calibration (taken from (Seel *et al.*, 2014)),
c. Anatomical calibration (taken from (Picerno *et al.*, 2008))

Assuming segments to be rigid solids, segment-to-sensor calibration provides the constant transformation between MIMUs and anatomical frames and, thus, allows to deduce segment orientations and joint angles in the global Earth-fixed reference frame associated to MIMUs (**Figure 17**). The validity of MIMU-based joint angles and segment orientations appear to depend on the joint or segment considered as well as on the task performed (Cuesta-Vargas *et al.*, 2010; Lebel *et al.*, 2017; Poitras *et al.*, 2019). Furthermore, joint angles appear to be less accurately estimated than segment orientations (Lebel *et al.*, 2017; Poitras *et al.*, 2019), possibly due to summation of orientation errors (Lebel *et al.*, 2017) and to soft-tissue artefact impacting MIMUs alignments on segments of both sides of a joint (Zabat *et al.*, 2019). This could also result from inconsistencies between the global Earth-fixed

Figure 17: Knee joint angle estimation using a thigh and a shank MIMU. Taken from (Favre *et al.*, 2008).

reference frames sensed by different MIMUs (Picerno *et al.*, 2011), in particular in the presence of non-homogeneous magnetic field (Picerno *et al.*, 2008; Lebel *et al.*, 2018). Nevertheless, while conflicting evidence has been reported for upper-limbs and complex motions, fair-to-excellent reliability and strong validity has been reported in sound subjects for joint angles estimated during walking (Poitras *et al.*, 2019). In particular, flexion/extension angles are best estimated, probably due to the higher range of motion of joints and segments in the sagittal plane while walking (Iosa, Picerno, *et al.*, 2016; Poitras *et al.*, 2019). Most of the literature on MIMU-based kinematics have focused on asymptomatic subjects (Iosa, Picerno, *et al.*, 2016) and methods have rarely been validated for people with pathological gait (Poitras *et al.*, 2019) or adopted in clinical research (Iosa, Picerno, *et al.*, 2016). It is to be noted that Cutti and coworkers have devised a protocol for kinematic gait analysis of people with lower-limb amputation (Cutti *et al.*, 2010). While reliability has been reported in people with transtibial amputation, construct validity was not investigated (Cutti *et al.*, 2015). Furthermore, equal to higher accuracy levels were reported for lower-limb flexion/extension angles estimated visually by orthopedic surgeons and other clinical specialists in quasi-static conditions (Kianifar *et al.*, 2019). Therefore, although MIMUs appear promising, more studies are required to confirm the added value of MIMUs for dynamic joint angle assessment in the clinical field.

b. Kinetic parameters

MIMUs and pressure insoles have also been investigated for the estimation of ground reaction forces (Shahabpoor and Pavic, 2017; Ancillao *et al.*, 2018). Pressure insoles only provide the vertical component of the ground reaction force, while MIMUs are susceptible to allow the retrieval of all three components. Using single or multi-segment biomechanical models, MIMUs have been used to estimate the body center of mass acceleration (Karatsidis *et al.*, 2017; Shahabpoor *et al.*, 2018; Mohamed Refai *et al.*, 2020). From there, application of the Newton's second law leads to the estimation of the total ground reaction force, in the absence of other external forces (for instance, when carrying a load). The vertical component of ground reaction force was shown to be accurately estimated in most cases, but poorer validity was found for mediolateral and anteroposterior

components (Ancillao *et al.*, 2018). Furthermore, only few models have been proposed to distribute the force between the right and left foot during the double stance of the gait cycle of asymptomatic subjects (Ren *et al.*, 2008; Villeger *et al.*, 2014; Yang and Mao, 2015; Ancillao *et al.*, 2018; Erfan Shahabpoor and Pavic, 2018), with some attempts using machine learning approaches (Leporace *et al.*, 2015; Tan *et al.*, 2019; Arumukhom Revi *et al.*, 2020).

Several attempts to estimate intersegmental forces and moments in asymptomatic participants have been reported combining kinematics and ground reaction forces estimated with MIMUs (Yang and Mao, 2015; Faber *et al.*, 2016; Karatsidis *et al.*, 2017). One study reported the joint use of MIMUs and insoles for the estimation of intersegmental forces and moments in asymptomatic subjects (Khurelbaatar *et al.*, 2015) and another proposed an inverse dynamic approach based on inertial sensing and musculoskeletal modeling (Karatsidis *et al.*, 2019). In all studies, poorer accuracy was reported for the non-vertical components of the forces and non-sagittal components of the moments.

Finally, few studies investigated the feasibility of using MIMUs to estimate work or power, with limited to poor accuracy achieved (Zijlstra *et al.*, 2010; Pavei *et al.*, 2020).

3.2.3. Performance assessment parameters

While MIMUs and insoles may not be as valid as the gold standard for function assessment parameters, a large number of applications to monitor locomotion quality and efficiency have emerged with wearable sensors. In particular, monitoring of daily-living ambulatory performance and of upright balance has been facilitated with the introduction of inertial sensors in the field of motion analysis, and original parameters have been proposed for gait quality assessment (Iosa, Picerno, *et al.*, 2016; Benson *et al.*, 2018). The following overview of the literature on performance assessment parameters aims at identifying those that might be relevant to support the biomechanical and clinical assessment of the rehabilitation of people with lower-limb amputation.

a. Gait quality indices

i. Symmetry

Spatiotemporal and loading symmetry have been investigated using both MIMUs and pressure insoles. In particular, loading and temporal symmetry can be easily monitored with pressure insoles (Nolan *et al.*, 2003; Cutti *et al.*, 2018; Loiret *et al.*, 2019), whose use was validated against force plates in people with transfemoral amputation for this specific purpose (Loiret *et al.*, 2019). Regarding MIMUs, although a large number of studies have focused on gait events detection and temporal parameters quantification (see section 3.2.1), none reported the use of MIMUs to compute a symmetry index based on gait cycle temporal parameters.

However, several parameters based on MIMU signal processing have emerged from the literature for symmetry assessment (Benson *et al.*, 2018). Thus, a coefficient based on the autocorrelation of the anteroposterior acceleration measured at the trunk has been proposed to quantify temporal asymmetry (Moe-Nilssen and Helbostad, 2004). A statistically significant but moderate correlation was found between the autocorrelation coefficients and insoles-based temporal asymmetry in people with transfemoral amputation (Tura *et al.*, 2010). Similarly, a global parameter has been proposed and widely adopted in recent literature to quantify global gait symmetry through spectral analysis of upper-body acceleration data: the harmonic ratio (Smidt *et al.*, 1971; Menz *et al.*, 2003). Based on the

observation that, in asymptomatic gait, the pelvis, trunk and head segments move symmetrically with respect to the anatomical planes with a periodicity of a step along the direction of progression and the vertical direction, and with a period of a stride (two steps) along the mediolateral direction (**Figure 18**), the Fourier decomposition of the displacement or acceleration signal measured at the upper body within each stride is expected to contain even harmonics in the anteroposterior and vertical directions and odd harmonics in the mediolateral direction (Smidt *et al.*, 1971; Cappozzo, 1981). These harmonics are considered to describe the stereotype pattern of locomotion, and are called 'intrinsic', while other
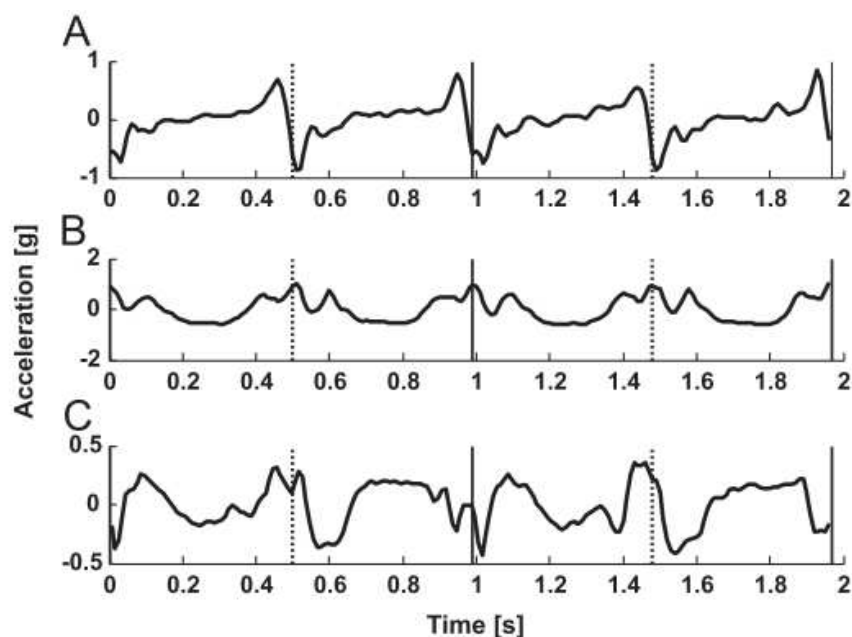
Figure 18: Lower-back acceleration of an asymptomatic person while walking with right (vertical solid line) and left (vertical dotted line) heel contacts. Taken from (Bellanca *et al.*, 2013)
A – anteroposterior direction; B – vertical direction; C – mediolateral direction

harmonics are considered to disturb the inherent locomotion pattern and are called 'extrinsic' (Cappozzo, 1981). The harmonic ratio was first introduced as the ratio of the sum of the amplitudes of intrinsic harmonics to the sum of the amplitudes of extrinsic harmonics of the acceleration signal measured at pelvis level (Smidt *et al.*, 1971; Menz *et al.*, 2003). The improved harmonic ratio (Pasciuto *et al.*, 2017) was then introduced to overcome limitations in the calculations of the harmonic ratio (Bellanca *et al.*, 2013) and is expressed as a percentage of total symmetry. Both the harmonic and improved harmonic ratios have been studied in people with lower-limb amputation (Iosa *et al.*, 2014; Pasciuto *et al.*, 2017) and were reported to be related to dynamic balance and fall risk in amputees and stroke patients respectively (Iosa *et al.*, 2014; Bergamini *et al.*, 2017).

ii. Balance

Postural balance

Postural balance has been described in gait analysis laboratories using the center of pressure (CoP) sway path during stance (see section 2.3.3). The use of wearable sensors such as pressure insoles (Lemaire *et al.*, 2006; Kendell *et al.*, 2010) or inertial sensors located near the center of mass (Betker *et al.*, 2006; Najafi *et al.*, 2012; Al-Jawad *et al.*, 2013; Noamani *et al.*, 2020) may allow to retrieve the sway path of the CoP or of the projection of the body center of mass while standing. Parameters

extracted from the sway path, such as sway velocity and the lateral or anteroposterior range of the CoP can be used to characterize postural balance (Kendell *et al.*, 2010; Al-Jawad *et al.*, 2013; Hsu *et al.*, 2014) (**Figure 19**).
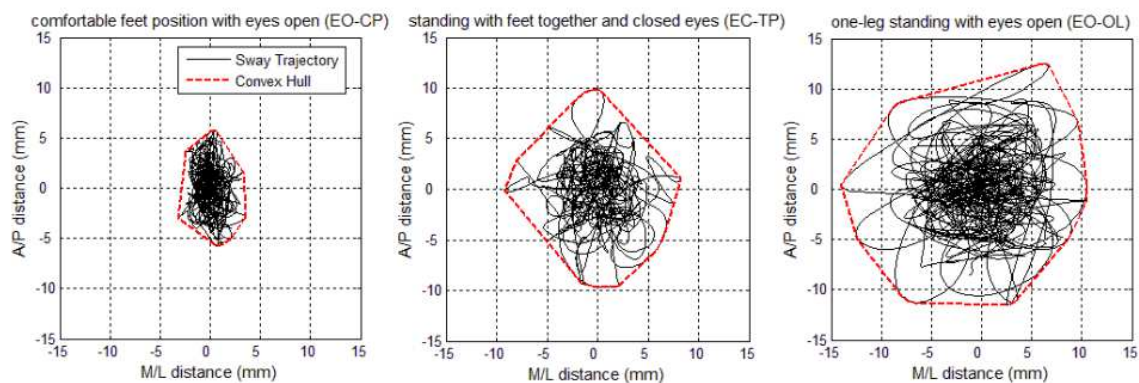
Figure 19: Example of body center of mass sway trajectory retrieved with MIMUs for three equilibrium tasks with increasing difficulty, from (Al-Jawad et al. 2013)

Alternatively, the root-mean-square (RMS) of accelerations, after subtraction of the gravity component, were proposed as estimators of postural balance as they quantify the dispersion of the accelerations while no motion is supposed to occur (Mancini *et al.*, 2012; Al-Jawad *et al.*, 2013). Although not directly comparable to the CoP sway path, the RMS accelerations in the horizontal plane were shown to provide reliable and clinically relevant information regarding postural balance in both sound participants and participants with Parkinson's disease (Mancini *et al.*, 2012; Ghislieri *et al.*, 2019).

Balance control during gait

In the literature, balance control during gait has been defined either as the ability to maintain continuous motion despite internal small perturbations (Kendell *et al.*, 2010, 2016; Lamoth *et al.*, 2010; Iosa *et al.*, 2014), the ability to minimize oscillations transferred from the lower-limbs to the upper-body (Iosa *et al.*, 2014; Summa *et al.*, 2016; Bergamini *et al.*, 2017), or, in a simpler manner, as "gait that do not lead to fall" (Bruijn *et al.*, 2013). A variety of parameters has been proposed in the literature to quantify gait balance based on those definitions. They are either parameters derived from the center of pressure or center of mass trajectory, parameters extracted from dynamical system theory and derived from raw signals, or coefficients directly extracted from root-mean-square (RMS) of accelerations. Therefore, two approaches can be identified: a biomechanical-model based approach and a signal processing approach which consists in proposing parameters based on the measured signals rather than processing the signals to derive *a priori* defined parameters.

Regarding the first approach, balance control has been assessed through the analysis of parameters derived from the center of pressure (CoP) trajectory estimated with pressure insoles (Lemaire *et al.*, 2006; Kendell *et al.*, 2010, 2016). A set of parameters derived from the CoP path were proposed to characterize dynamic balance and compensatory adjustments: unexpected anteroposterior and mediolateral direction changes or deviations, maximal lateral position of the CoP and cell trigger frequency. They have been analyzed in the population with lower-limb amputation and were shown to predict classical clinical balance scores (Kendell *et al.*, 2010, 2016; Howcroft, Lemaire, *et al.*, 2016). Higher values were obtained for all parameters quantified on the intact limb compared

to the prosthetic limb, suggesting that adjustments for balance mostly occur with the intact limb on both transtibial and transfemoral amputee groups (Kendell *et al.*, 2010, 2016; Howcroft, Lemaire, *et al.*, 2016). This could be expected given that the prosthetic limb lacks functional neuromuscular structures due to the amputation. The theory of dynamic margin of stability developed by Hof and coworkers has also recently been transposed to wearable gait analysis in asymptomatic young and elderly participants (Arvin *et al.*, 2016; Guaitolini *et al.*, 2019; Fino *et al.*, 2020). Only one proof-of-concept study provided an estimate of the margin of stability that was validated against a gold standard, but the method is complex as it requires seven MIMUs and the use of an optical motion capture system for sensor-to-segment calibration and anthropometric measurements (Guaitolini *et al.*, 2019).

The second approach implemented for balance control assessment allows to compute parameters or indices directly from the signals measured by wearable sensors. This ensures a high accuracy to the detriment of hindsight on the retrieved parameters and therefore, a lower understanding of these parameters. However, a large number of studies have proposed to analyze dynamic balance using such an approach and MIMUs (Benson *et al.*, 2018; Ghislieri *et al.*, 2019)

The measurement of RMS of upper body accelerations, especially at lower-back level, is one of the most reported parameter reported for dynamic balance assessment with inertial sensors (Kavanagh and Menz, 2008; Howcroft *et al.*, 2013; Iosa, Picerno, *et al.*, 2016). High RMS of upper body accelerations have been shown to be associated with higher risk of falls and decreased balance (Howcroft *et al.*, 2015; Summa *et al.*, 2016; Bergamini *et al.*, 2017; Paradisi *et al.*, 2019). Furthermore, RMS of upper body accelerations have been shown to discriminate levels of walking ability in people with lower-limb amputation (Iosa *et al.*, 2014).
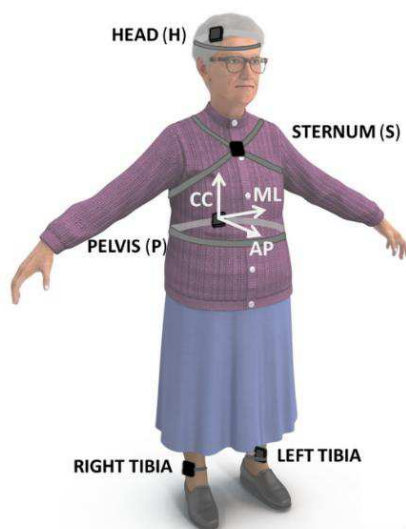
Figure 20: Set-up of IMUs for the analysis of accelerations transmission from lower-limbs to the upper body, from (Bergamini *et al.*, 2017). IMUs located on the right and left tibia were used for gait segmentation

Attenuation coefficients (Mazzà *et al.*, 2009), based on the ratio of RMS of accelerations measured at successive levels of the trunk (pelvis, sternum, head), have been computed to quantify the ability to minimize upper body accelerations in people with transtibial amputation (Paradisi *et al.*, 2019) (**Figure 20**). An amplification of the acceleration variability was observed from the sternum to the head. The resulting head instability might explain the impaired balance in people with lower-limb amputation (Paradisi *et al.*, 2019). Indeed, head stability is essential to ensure a steady optical flow and a trustworthy processing of vestibular signals which contribute to the control of equilibrium (Berthoz and Pozzo, 1994; Kavanagh and Menz, 2008; Iosa, Picerno, *et al.*, 2016; Summa *et al.*, 2016).

The maximum Lyapunov exponent, a parameter extracted from dynamical systems theory, has been extensively used in recent years in different populations (Bruijn *et al.*, 2013). This parameter characterizes the resistance of a system to internal perturbations (which are, when the system is the body, perturbations inherent to the neuromuscular system). It quantifies the divergence rate between initially similar "trajectories" in a multi-dimensional state space, the latter being reconstructed from the pelvis accelerations and their time-delayed copies for instance (**Figure 21**). Larger values of Lyapunov exponent correspond to larger variability and lower gait stability. Although the Lyapunov exponent could differentiate people with lower-limb amputation from healthy controls (Lamoth *et al.*, 2010), it might not be sensitive enough to detect changes within a subject (van Schooten *et al.*, 2013) during his/her rehabilitation or following a modification of his/her prosthetic devices. Indeed, in a test-retest study, the smallest detectable difference found between-session was higher than the difference between elderly fallers and non-fallers (van Schooten *et al.*, 2013). Thus, this parameter does not seem to be adequate to monitor patients' progression during their rehabilitation.
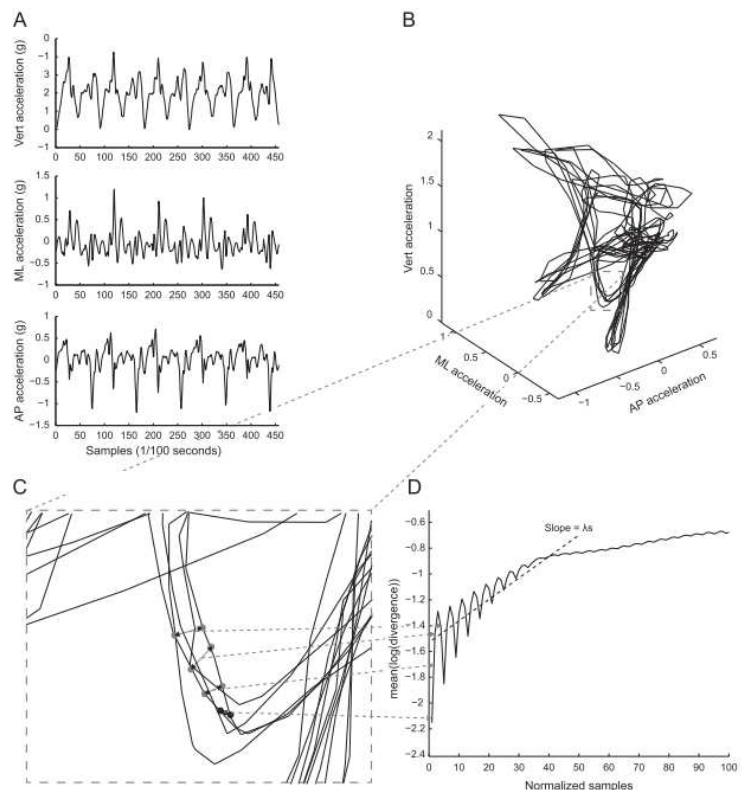
Figure 21: Computation of the Lyapunov exponent, from (van Schooten *et al.*, 2013)
A) Original time-series (trunk accelerations).
B) State space reconstruction of the time-series.
C) Identification of the nearest neighbours for each point in the state-space.
D) The Lyapunov exponent is the slope of the logarithmic curve of the divergence between neighbouring points.

b. Gait efficiency

When considering parameters related to gait efficiency (ambulatory capacity in the community, energy cost, cognitive demand associated with gait) obtained through wearable protocols, those have been exclusively obtained with MIMUs or accelerometers.

i. Actimetry

Actimetry literally means the measure of activity. This term encompasses the detection of the nature of the activity, but also the estimation of its intensity. Recently, accelerometers have been

39

extensively used for the measure of activity, with several commercial solutions developed (Kavanagh and Menz, 2008; Hafner and Sanders, 2014).

In quasi-static situations, accelerometers can be used as inclinometers to estimate the orientation of the body segment to which they are attached. Using this principle, accelerometers located on the residual limb and/or on the prosthesis of a lower-limb amputee can be used to detect donning and doffing of the prosthesis and to classify postures between standing and sitting (Redfield *et al.*, 2013a; Gardner *et al.*, 2016). More recently, manufacturers have shown interest in recognizing the situation encountered by the prosthetic user (stairs – slopes – level ground) in order to adapt the behavior of the prosthesis to its environment (Dauriac, 2018). These classification schemes could also benefit rehabilitation, as they could provide reliable information regarding the between-session exercises performed by people with amputation (Preece *et al.*, 2009; Hafner and Sanders, 2014).

Regarding physical activity level, it can first be estimated through the number of steps performed, which can be extracted from features in the acceleration signals. In the context of people with lower-limb amputation, a distal attachment of the accelerometer on the prosthetic limb seems to be more appropriate as sharper peaks will be detected than at the pelvis, even if the accelerometer would only detect prosthetic steps (Rosenbaum Chou *et al.*, 2009; Redfield *et al.*, 2013a; Dauriac, 2018). Intensity levels of the performed physical activity can be estimated based on the amount of steps performed during a specific time or based on thresholds on the acceleration magnitude summed over a specific time window (Santos-lozano *et al.*, 2014). Furthermore, energy expenditure has been estimated using accelerometry: indeed, linear regressions based on acceleration features and anthropomorphic measurements have been validated against indirect calorimetry for several populations, including lower-limb amputees (Santos-lozano *et al.*, 2014; Ladlow *et al.*, 2017). The most appropriate position of the accelerometer was found to be the waist on the side of the residual limb, possibly due to hip hiking (Ladlow *et al.*, 2017). However, no further analysis enabled to establish a relationship between gait compensations and the increased accuracy of the energy expenditure regression with the accelerometer at this location.

ii.   Cognitive load

In order to evidence higher cognitive demand associated with walking in transfemoral amputee gait, Lamoth and coworkers assessed the evolution of the sample entropy of the pelvis acceleration signals while performing a dual-task compared to single-task or when walking outdoors on irregular terrains compared to indoors (Lamoth *et al.*, 2010). Sample entropy is a measure of similarity between two asynchronous time-series taken within the same original time-series (Richman and Randall Moorman, 2000). It was found to decrease while performing a dual-task and to increase while walking outdoors, meaning that acceleration signals measured at the pelvis are less repeatable and predictable when performing a dual task compared to a single task but more repeatable when walking on irregular terrain than indoors. This might be associated with an increased voluntary control of walking in constraining conditions, reflecting the need of the person with amputation to concentrate on where to position his/her prosthetic leg to prevent falls – and a decreased control when performing simultaneously another demanding task (Lamoth *et al.*, 2010). The authors also investigated the scaling exponent, which indicates the presence of long-range correlations within a signal through Detrended Fluctuation Analysis (DFA). This exponent had been shown to evolve in children as they grow up and in people with cognitive impairment (Hausdorff *et al.*, 2001). However, no difference were found

between the scaling exponents of experienced transfemoral amputees and asymptomatic people (Lamoth *et al.*, 2010). It should be noted that the scaling exponent has not been investigated in people with lower-limb amputation during their rehabilitation, when they have not yet completed prosthetic gait training.

3.3. Synthesis of the literature and limitations

This literature overview on wearable sensors highlighted the diversity of quantitative parameters describing locomotion that can be obtained with MIMUs and/or pressure insoles. Attention shall be drawn on the fact that most methods to get those parameters were developed and validated on healthy subjects, and that they often rely on specific features of MIMUs raw data signals. Thus, they might not be directly applicable to people with lower-limb amputation, especially those undergoing rehabilitation. Indeed, slow walking speed and three- or four-points gait, such as when using crutches or other walking aids, have been shown to modify gait patterns or attenuate signal features.

Furthermore, due to the nature of the signals obtained with MIMUs and pressure insoles, obtaining classical gait analysis parameters such as intersegmental moments, power, or position, is not straightforward and may not achieve a sufficient accuracy (section 3.2.2). However, these sensors have been extensively used to evaluate locomotion quality through balance and symmetry indices, introducing new parameters that are usually not measured in motion laboratory-based gait analysis (section 3.2.3). The relevance and validity of these indices for the assessment of lower-limb amputee gait quality remains to be verified.

In the few studies focusing on the gait of people with lower-limb amputation, recruited participants were generally experienced walkers, who did not require the use of assisting devices. Only two studies were conducted with non-experienced walkers. The first one monitored their daily physical activity, in term of number of steps, in the six weeks following the amputation with a device that had not been validated in this context (Samuelsen *et al.*, 2017). The second evaluated gait quality of people with transtibial and transfemoral amputation at dismissal from the rehabilitation center, in terms of stability (using RMS of accelerations) and symmetry (using indices of temporal symmetry and harmonic ratio) (Iosa *et al.*, 2014). Before clinical implementation to monitor patient's progression during rehabilitation, the methods shall be both adapted and validated on this specific population, and test-retest reliability shall be assessed in order to measure the sensitivity of the method and its ability to detect clinically-relevant changes.

Conclusion

The purpose of this first part was to identify gait parameters that could be obtained with inertial sensors and pressure insoles and that are clinically relevant for the rehabilitation of people with lower-limb amputation.

The first two chapters have introduced contextual elements on amputee care, in particular regarding the tools used in clinics for gait evaluation. It appears that simplicity and rapidity of implementation are critical for an assessment tool to be adopted in clinical routine. For instance, walking tests are often performed as they are reliable and easy to set up. Several authors have therefore proposed the instrumentation of TUG and timed-tests with wearable sensors in order to extract additional parameters (Nguyen *et al.*, 2017; Belluscio *et al.*, 2018). Chapter 2 has also allowed to identify relevant parameters used to assess the gait of people with lower-limb amputation in motion analysis laboratories. In addition to joint angles and segment orientations – which allow to quantify gait deviations that are visible to the clinicians – the study of the body center of mass motion appears relevant as it is a synthetic parameter that may reflect gait asymmetries and that is related to the mechanical energy, and hence, the energy expenditure. Monitoring asymmetry in spatiotemporal and loading parameters also appears to be critical as it is correlated with the onset of comorbidities. Interestingly, few studies investigate balance of lower-limb amputee gait, probably due to the lack of dynamic balance descriptors proposed with optical motion capture systems and force plates.

The third chapter has introduced wearable sensors and, most particularly, pressure insoles and MIMUs, as well as their applications for human motion analysis. An extensive body of literature has investigated the use of MIMUs for kinematic analysis, including in pathological gait, but, comparatively, few studies have investigated the ability of MIMUs to track kinetic parameters and the body center of mass motion. Most of the literature proposing wearable methods for ground reaction forces and moments estimation were published in the last five years and developed and validated on asymptomatic participants. Finally, MIMUs and pressure insoles were also found to capture a large diversity of original gait quality parameters, characterizing, in particular, gait balance and symmetry. These gait quality descriptors can be obtained from a limited number of sensors and are compatible with clinical walking tests. Interestingly, two distinct approaches seem to emerge when using wearable sensors for gait analysis. The first approach aims at retrieving biomechanical parameters, similarly as with laboratory-based instruments. In most cases, these parameters can be quantified with complex algorithms requiring several synchronized sensors and a model of the human body (see for instance the kinematic models and assumptions required for deriving full body joint kinematics or for ground reaction force distribution during double stance phase). The second approach proposes quantitative parameters derived from the measure of raw signals from a limited number of wearable sensors and allows to quickly retrieve concise parameters able to quantify global aspects of gait related with dynamic balance or symmetry. These parameters should therefore be easily intelligible although they may differ from the usually derived parameters from laboratory-based biomechanical gait analysis.

The purpose of the thesis could be further defined based on these findings and will be specified in the next section.

Aim of the thesis

The aim of this thesis is to contribute in the development of wearable tools to support the assessment of the functional rehabilitation of people with lower-limb amputation.

Based on the findings of the literature review presented in the first part of this thesis, it appears that, to be relevant, such tools must allow to quickly retrieve quantitative and intelligible parameters describing the gait of people with lower-limb amputation and its alterations. For instance, the acquisition set up should allow to instrument clinical tests that are currently performed during the rehabilitation or to obtain relevant data within a few steps in order not to interfere with the rehabilitation. Ideally, a minimal number of sensors should be used to reduce as possible the set-up duration. Furthermore, a limited number of output parameters should be retrieved in order to facilitate interpretation and limit the duration of the analysis.

Dynamic balance and gait symmetry seem to be of particular interest for clinical assessment as these aspects of locomotion are able to quantify gait deficiency. However, these parameters alone do not allow to get a complete picture of gait functional alterations and performance. The analysis of the body center of mass motion appears therefore relevant to complete gait assessment. Indeed, it allows to identify the presence of kinematic alterations and may provide insight on the metabolic cost of walking without requiring the analysis of individual joint motions or intersegmental forces, therefore limiting the number of quantified parameters.

The **aim of the thesis** is therefore to develop algorithms allowing the wearable characterization of these different aspects of gait following two approaches which were identified in the literature.

The first approach aims at retrieving biomechanically relevant parameters from wearable sensors through modeling of the human body as a set of rigid body segments, similar as what is done in laboratory-based gait analysis. This approach allows to retrieve biomechanical parameters that have demonstrated their usefulness in quantitative gait analysis at the cost of complex algorithms development. Thus, the second part of the manuscript proposes an original wearable framework to estimate 3D motion (acceleration and instantaneous velocity) of the body center of mass from a limited number of sensors. The framework will be developed and validated on the data of a person with transfemoral amputation taking laboratory-based instruments and a full-body inertial model as criterion measurements.

The second approach aims at processing wearable sensors' signals and at identifying features in the retrieved signals that may relate to gait descriptors. A large amount of studies has thus proposed to quantify gait balance and symmetry using this approach. In particular, the analysis of acceleration signals measured at the pelvis, trunk or head levels in different populations was proposed to quantify gait balance. Temporal parameters and symmetry were computed from the analysis of pressure insoles signals or from the detection of gait events instants of occurrence, identified as specific features in the signals of a single-pelvis or two lower-limb-mounted MIMUs. Such parameters issued from signal processing have not always been studied in people with lower-limb amputation while they might be relevant for this specific population. The third part of the thesis therefore aims at contributing to the creation of knowledge regarding these recent parameters by providing reference values for the

43

population of lower-limb amputees. In addition, a comparative evaluation of MIMU-based gait events detection algorithms taken from the literature will be proposed to investigate their validity for temporal symmetry assessment in people with lower-limb amputation.

These two complementary approaches allow to contribute to the development of wearable gait analysis protocols for the in-field assessment of the rehabilitation of people with lower-limb amputation. The first approach allows the development of an original framework and contributes to fundamental research on wearable gait analysis. The second approach contributes to the creation of knowledge and aims at better characterizing recently developed gait indices. This approach is therefore closer to the clinical transfer of wearable tools for rehabilitation. However, further validation steps are required prior to implementing these methods in the rehabilitation process.

In order to develop both these approaches, several data sets, which have been either collected in the course of the PhD or which had already been collected in the context of previous work, were post-processed. **Figure 22** provides an overview of the data that has been used during the thesis for the development of algorithms and creation of knowledge.
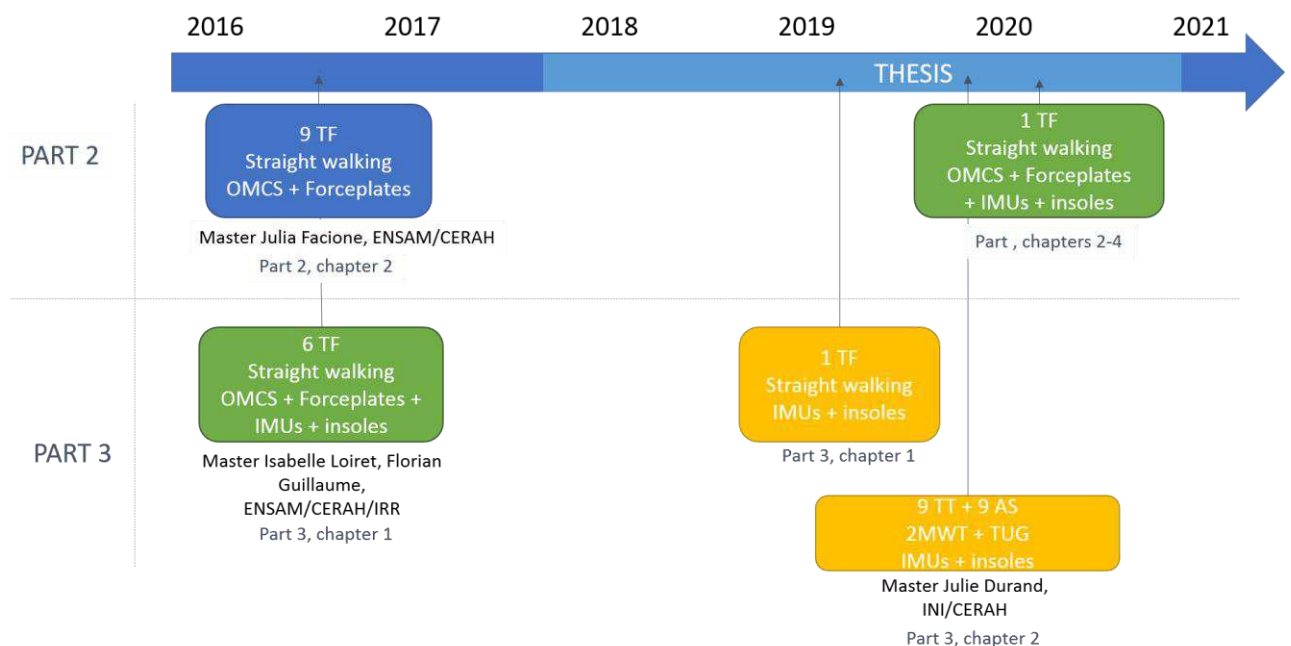
Figure 22: Graph of the experimental data used in the course of the thesis for the development of the original framework (Part 2) or the creation of knowledge regarding recently developed wearable sensor-base gait quality indices (Part 3). Each framed box corresponds to a data collection and indicates the number of participants, the nature of the trials and the acquisition systems used.
Two datasets that had been collected during masters occurring in 2016 were processed in the course of the present thesis and were partially completed by acquiring supplementary data in the course of the PhD.
The dataset in blue box correspond to data collected using only laboratory-based instruments while datasets in yellow boxes were collected using only wearable sensors. Protocols involving both laboratory-based and wearable capture systems are framed in green boxes.
TF = people with transfemoral amputation; TT = people with transtibial amputation; AS = asymptomatic subjects; OMCS = Optical Motion Capture Systems; IMUs = (magneto-)Inertial Measurement Units; 2MWT = 2-minute walking test; TUG = Timed-Up-and-Go test

The thesis benefited from the availability of data from a cohort of nine people with transfemoral amputation, recorded with laboratory-based instruments. This data (used in Chapter 2 Part 2) allowed the development of the wearable framework proposed in the third chapter of Part 2.

44

Part 2: Development of a wearable framework for the estimation of the body center of mass 3D motion during gait of people with lower-limb amputation

This part of the thesis aims at retrieving, from the analysis of wearable sensors' signals, biomechanically relevant parameters that have proven to be meaningful for the analysis of lower-limb amputee gait: the 3D motion of the body center of mass (BCoM). Indeed, the study of the BCoM path may allow to characterize gait alterations that are not visible to the naked eyes of clinicians and has been shown to evidence an asymmetrical gait pattern (Askew *et al.*, 2019; Tesio and Rota, 2019). Furthermore, BCoM velocity can be combined with ground reaction forces under each foot to estimate mechanical work and energy, providing insight on gait efficiency (Donelan *et al.*, 2002a). Eventually, the combination of ground reaction forces and kinematic parameters would allow to obtain intersegmental kinetics. As a consequence, the estimation of 3D BCoM motion and individual limb ground reaction force is of particular relevance for gait analysis of people with lower-limb amputation (see Part 1, section 2.3.2). To the author's knowledge, the feasibility of quantifying these parameters using wearable sensors has never been investigated in people with lower-limb amputation.

From a mechanical standpoint, the kinematics and dynamics of the body center of mass (BCoM) are important parameters of the locomotion which directly result from the application of external forces (Tesio and Rota, 2019). The application of the fundamental principles of dynamic indeed yields the following equations for linear and rotation motions:

$$m_{body}\, \boldsymbol{a_{BCoM}} = \Sigma_i\, \boldsymbol{F_{i_{ext}}} + m_{body}\boldsymbol{g} \quad (1)$$

$$\boldsymbol{\delta_A} = \frac{d\sigma_A}{dt} + m_{body}\boldsymbol{v_A} \times \boldsymbol{v_{BCoM}} = \Sigma_i\, \boldsymbol{M_{i_{A,ext}}} \quad (2)$$

Where all the following quantities are expressed in an Earth-fixed reference frame:

$\begin{cases} \boldsymbol{a_{BCoM}} \text{ is the BCoM acceleration} \\ m_{body} \text{ is the mass of the body} \\ \boldsymbol{g} \text{ is the gravitational acceleration} \\ \boldsymbol{F_{i_{ext}}} \text{ are the external forces applied on the body} \\ \boldsymbol{\delta_A} \text{ is the dynamical moment of the body expressed at the point A} \\ \boldsymbol{\sigma_A} \text{ is the angular momentum of the body expressed at the point A} \\ \boldsymbol{v_A}, \boldsymbol{v_{BCoM}} \text{ are the linear velocity computed of the points A and the BCoM respectively} \\ \boldsymbol{M_{i_{A,ext}}} \text{ are the external moments exerted on the body, applied at the point A} \end{cases}$

The first equation indicates that the linear motion of the body is explained by the external forces that are exerted on the body and can be used to describe the translation motion of the body. The second equation, less frequently used to describe human motion (Herr and Popovic, 2008), indicates that the rotation motion of the body around a point A is explained by the external moments applied at this point. Equation 2 can be simplified as follows when expressed at the BCoM:

$$\boldsymbol{\delta_{BCoM}} = \frac{d\sigma_{BCoM}}{dt} = \sum_i \boldsymbol{M_{i_{BCoM,ext}}}$$

When no external moments are applied on a body, the angular momentum is a conserved quantity. While this is not the case in human legged locomotion, several authors have demonstrated that the

angular momentum takes small values during gait in spite of prominent segmental contributions. Therefore, the angular momentum has been assumed to be highly regulated by the central nervous system in order to minimize angular excursions of the body (Popovic *et al.*, 2004; Herr and Popovic, 2008). Fluctuations of the angular momentum are evidenced by the dynamic momentum and have been shown to be a promising indicator of gait balance, in particular in stroke and in lower-limb amputee patients (Silverman *et al.*, 2008; Nott *et al.*, 2014; Neptune and Vistamehr, 2019). Therefore, the study of the angular momentum appears relevant for the rehabilitation of people with lower-limb amputation. Developing algorithms allowing to estimate the angular momentum and its fluctuations from wearable sensors is a relevant track of research for future works (Neptune and Vistamehr, 2019).

In this part of the thesis, however, only the first equation of the fundamental principles of dynamics will be investigated. It indeed allows to retrieve the 3D motion of the BCoM and provides hindsight on gait asymmetry and mechanical energy parameters, which could be used to support the functional rehabilitation of people with lower-limb amputation. Therefore, the feasibility of estimating the 3D acceleration, velocity or displacement of the BCoM in people with lower-limb amputation from wearable sensors appears highly relevant.

In motion analysis laboratories, BCoM acceleration can be immediately retrieved from force plates using equation (1). Integration of the BCoM acceleration with proper initial conditions yields the instantaneous velocity of the BCoM, which can be further integrated to estimate the trajectory of the BCoM. When force plates are not available, an optical motion capture system coupled with an inertial model providing, for each segment, its mass and the position of its center of mass (SCoM) in the anatomical frame defined by segment-mounted markers can be used instead. Indeed, using a representation of the body as a chain of linked rigid segments of mass m_i, the BCoM position can be retrieved using equation (3) from the positions r_{SCoM_i} of the segments' center of mass:

$$r_{BCoM} = \sum_i \frac{m_i}{m_{body}} \, r_{SCoM_i} \quad (3)$$

Then, by differentiating equation (3), the velocity or the acceleration of the BCoM can be retrieved from optical motion capture data:

$$a_{BCoM} = \sum_i \frac{m_i}{m_{body}} \, a_{SCoM_i} \quad (4)$$

Eventually, the ground reaction force can be estimated using equation (1), providing that the person is not carrying extra weight and no other external forces are applied on the body.

When using wearable sensors such as MIMUs, the output data is not the same as the one provided by force plates or optical motion capture system. Indeed, MIMUs provide the acceleration of the origin of the sensor case, the angular velocity and the magnetic field in the MIMU local frame but do not provide the absolute position of the sensor in a global Earth-fixed frame. Furthermore, even if a full body MIMU set could be adopted to track the kinematics of all body segments, similarly to what is done with optical motion capture systems, instrumenting the whole body with sensors is not advisable for clinical transfer of the protocol. Indeed, a trade-off between accuracy and complexity of the acquisition protocol is essential for applications in the clinical field, where clinicians may only have a limited time to spend with the patient (Huntley *et al.*, 2017). Therefore, a specific protocol must be developed for the estimation of the 3D motion of the BCoM from wearable sensors.

This part of the thesis therefore aims at contributing to the development of a wearable gait analysis protocol for the estimation of 3D BCoM acceleration and instantaneous velocity. The first chapter

46

provides an overview of the existing wearable methods for the estimation of 3D BCoM motion, as well as their validity. Then, the second chapter aims at identifying contributions of each body segment to the BCoM acceleration so as to identify optimal combinations of sensors and their positioning for an accurate estimation of BCoM acceleration in people with transfemoral amputation while limiting the number of required sensors. The study implemented in this second chapter was based on the data of a cohort of ten people with transfemoral amputation for which only force plates and optical motion capture data were available. Chapter 3 consists in a proof-of-concept study regarding the application of the identified combinations of sensors for the estimation of 3D BCoM acceleration and velocity in a wearable framework, using magneto-inertial measurement data. Challenges associated to the use of MIMUs will be identified and tackled in this chapter. Finally, a sensitivity analysis investigating the impact of sensors mispositioning on the estimation of the BCoM acceleration will be proposed in chapter 4. The methodology developed in this last chapter could be applied to other segment models or to other BCoM derived parameters, such as the instantaneous velocity of the center of mass.

Chapter 1 – 3D motion of the body center of mass: state-of-the-art of wearable sensor-based methods

1.1. Overview of wearable-sensor based methods

In the last decade, the number of studies investigating the feasibility of acquiring 3D ground reaction forces (GRF) or 3D motion of the body center of mass (BCoM) through its acceleration, velocity or displacement using wearable sensors has considerably increased. To facilitate the transfer of methods for the in-field assessment of 3D BCoM motion or total GRF, it is essential to keep the number of required sensors as low as possible while obtaining sufficient accuracy (Ancillao *et al.*, 2018).

Table 2 presents an overview of the published literature where developed methods for the acquisition of total GRF or 3D BCoM motion were validated against a gold standard and involved the sole use of MIMUs and/or pressure insoles. It should be noted that methods developed and compared to a gold standard for the estimation of GRF under each foot independently were not included if the comparison between total GRF and the gold standard was not provided. However, two recent reviews investigated the validity of such methods and reported that, in general, poor accuracy for the anteroposterior and mediolateral component of GRF was achieved when using pressure insoles and/or MIMUs (Shahabpoor and Pavic, 2017; Ancillao *et al.*, 2018). Better results were achieved using machine learning paradigm, although these methods were in their infancy at the time of the reviews (Ancillao *et al.*, 2018; Tan *et al.*, 2019). Recently, promising mixed inertial and musculoskeletal approaches were developed (Dorschky *et al.*, 2019, 2020; Karatsidis *et al.*, 2019). Readers are advised to refer to the abovementioned reviews for more details on single-limb GRF estimation (Shahabpoor and Pavic, 2017; Ancillao *et al.*, 2018).

Regarding methods investigating the 3D path of the BCoM or the total GRF, 17 studies (reported in **Table 2**) were retrieved in the literature. All methods involved from 1 to 17 MIMUs with only one study combining pressure insoles to MIMUs for stance phase detection (Yuan and I. M. Chen, 2014). Eleven studies involved the use of a MIMU at pelvis or trunk level as an approximation of the BCoM (Meichtry *et al.*, 2007; Esser *et al.*, 2009; Floor-Westerdijk *et al.*, 2012; Yuan and I. Chen, 2014; Regterschot *et al.*, 2014; Myklebust *et al.*, 2015; Najafi *et al.*, 2015; Sabatini and Mannini, 2016; E. Shahabpoor and Pavic, 2018; Lintmeijer *et al.*, 2018; Mohamed Refai *et al.*, 2020), with two studies using other MIMUs to complete or correct the estimation (Yuan and I. Chen, 2014; Sabatini and Mannini, 2016) and two studies simultaneously evaluating multi-sensor configurations and concluding on their superiority (Najafi *et al.*, 2015; Lintmeijer *et al.*, 2018). The remaining six studies investigated only multi-sensor configurations for the 3D BCoM motion (Zijlstra *et al.*, 2010; Faber *et al.*, 2016; Fasel, Spörri, *et al.*, 2017; Karatsidis *et al.*, 2017; Shahabpoor *et al.*, 2018; Pavei *et al.*, 2020). Three main categories of biomechanical models could be identified based on the approach chosen: models based on single-sensor approximation of the BCoM, on multi-segment inertial models, or on kinematic chain. Two methods consisted on mixed approaches involving machine learning methodology (Sabatini and Mannini, 2016; E. Shahabpoor and Pavic, 2018).

The developed methods were validated on asymptomatic populations, either for straight walking (9 studies), for sports motion (4 studies: golf swing, cross-country skiing, alpine skiing, rowing), for jumping (1 study), for sit-to-stand transfer (2 studies), or trunk bending motion (1 study). Regarding

the BCoM outcome parameters, studies investigated either the accuracy of the estimation of the acceleration (9 studies: 4 studies investigated 3D motion, 4 studies validated only the vertical component and the study on rowing only investigated the accuracy in the estimation of the anteroposterior component), the velocity (6 studies: half investigated the 3D velocity and the other half the vertical component) and/or the displacement (8 studies: 7 investigated the 3D component and the last one the vertical component). Optical motion capture data, force plates or instrumented treadmill were used for validation, except in one study where tri-axial force sensors were used under each foot (Mohamed Refai *et al.*, 2020). Among the seven studies using an optical motion capture system for validation, two used a full-body inertial model (Floor-Westerdijk *et al.*, 2012; Myklebust *et al.*, 2015; Fasel, Spörri, *et al.*, 2017) while the other used markers directly on top of MIMUs for validation.

The next two paragraphs will discuss the accuracy achieved respectively using single-sensor and multi-sensor approaches.

Table 2: Estimation of 3D motion of the body center of mass (BCoM) from wearable sensors.
Acc. = acceleration; Vel. = velocity; Disp. = displacement; Traj.= trajectory; AP = anteroposterior; ML = mediolateral; CC = craniocaudal; M/IMU =(Magneto-)Inertial Measurement Units; OMCS = Optical Motion Capture Systems; AS = Asymptomatic subjects; BW = Body Weight; (N)RMSE = (Normalized) Root Mean Square Error.
BCoM Approximation = method where a single MIMU was used and assumed to be representative of the BCoM motion

| Authors | BCOM motion | | | Method | | Validation | |
	Acc.	Vel.	Disp.	Method type	Wearable sensor	Reference, situation, population	Results
(Esser *et al.*, 2009)	CC	CC	CC	Biomechanical model (BCoM approximation)	1 MIMU at lower-back (L4)	- OMCS (marker on top of MIMU) - Straight walking - 5 AS	High correlations of peak-to-peak vertical acceleration, velocity and displacement (ICC > 0.78). Significant difference in vertical velocity (< 2.5%)
(Faber *et al.*, 2016)	3D	-	-	Biomechanical model (Inertial model)	MVN suit: 17 MIMUs	- Force plates - Trunk bending - 9 AS	CC: RMS ~ 10 N ~ 1% peak value, Pearson r^2>0.98 AP, ML: RMS ~ 10N ~ 0.12 ms^{-2}, r^2~0.6
(Fasel, Spörri, *et al.*, 2017)	-	-	3D traj.	Biomechanical model (kinematic chain)	7 to 11 MIMUs (shanks, thighs, sacrum, sternum, head + arms, wrists)	- OMCS (full body inertial model) - Sloped skiing - 11 skiers	Overall accuracy < 26 mm for full body model. When arms are not taken into account, decreased accuracy in 3D (-3mm), AP and CC direction (up to 8 mm), but no impact on precision
(Floor-Westerdijk *et al.*, 2012)	-	-	3D	Biomechanical model (BCoM approximation)	3 MIMUs (Sacrum + Right & Left shanks for gait segmentation)	- OMCS (full body inertial model) - Straight walking - 8 AS (50-75 years)	Full body vs general compensated single sensor ICC: AP: 0.68; ML: 0.77; V: 0.96 RMS (mm): AP: 5.52; ML: 4.44; V: 3.17
(Karatsidis *et al.*, 2017)	3D	-	-	Biomechanical model (BInertial model)	MVN suit: 17 MIMUs	- Force plates - Straight walking - 11 AS	Estimation of individual limb GRF. During single stance (GRF = mass * acceleration of BCoM): NRMSE(%): AP=10.0; ML=35.4; V=9.0
(Lintmeijer *et al.*, 2018)	AP	-	-	Biomechanical model (inertial model vs BCoM approximation)	13 MIMUs + single pelvis MIMU	- Force plates - Rowing - 9 rowers	single-pelvis MIMU: good reliability (ICC > 0.91) but elevated mean NRMSE (9.15%). Full body standardized model should be preferred (ICC > 0.98%, NRMSE < 3.7 %)
(Meichtry *et al.*, 2007)	-	3D	3D	Biomechanical model (BCoM approximation)	3D accelerometer at L3	- Force plates - Straight walking - 12 AS	- L3 leads the CoM in AP direction - larger acceleration amplitudes but significant correlations in RMS accelerations - larger vertical excursions but high correlations (> 0.9)

Authors	BCOM motion			Method		Validation	
	Acc.	Vel.	Disp.	Method type	Wearable sensor	Reference, situation, population	Results
(Mohamed Refai *et al.*, 2020)	3D	-	-	Biomechanical model (BCoM approximation)	3 MIMUs (sacrum + feet for reference frame)	- Force sensors under each foot - Walking tasks including turns - 8 AS	- Significative correlations in all directions (AP > 0.7 except for asymmetric walking, CC > 0.75 except for slow walking, ML < 0.55) - RMS < 7.4 % BW in all directions - NRMSE: Horizontal plane: 12.1% +/- 3.3% Vertical 10.2 +/- 1.2%
(Myklebust *et al.*, 2015)	-	-	3D	Biomechanical model (BCoM approximation)	1 MIMU at S1	- OMCS (full body inertial model) + 1 marker at S1 level - cross-country skiing - 6 skiers	IMU captures CC excursion of S1 marker with accuracy < 2% RMS error ~ 5% in ML but up to 72% in AP and CC excursions
(Najafi *et al.*, 2015)	-	-	3D	Biomechanical model (comparison of 3 x-link models)	1 to 3 MIMUs (shank, thigh, back)	- Pressure platform / 5 OMCS markers - Golf swing - 4 AS + 18 golfers	- 2-link model optimal accuracy/simplicity ratio (r > 0.93 in AP and ML ; but up to 14,6% error in ML motion) - High correlations with OMCS-based CoM during dynamic swing (0.91 in AP and 0.71 in ML; RMSE 12% and 15.52 % in AP and ML)
(Pavei *et al.*, 2020)	-	-	3D	Biomechanical model (Inertial model)	MVN suit: 17 MIMUs	- Force plates - Straight walking - 12 young AS	- 3D contour : good reliability (ICC = 0.86) but poor shape agreement (3D RMSD = 17 mm), especially in AP and ML directions- Very poor accuracy in BCOM displacement (mean RMS > 37% in AP and ML and up to 98% of RMS error in AP direction)
(Regterschot *et al.*, 2016),	CC	CC	-	Biomechanical model (comparison of 2 BCoM approximation)	2 MIMUs (sternum, right waist)	- Force plates - Sit-to-stand transfers - 27 older adults	- Time-series were not compared. - Strong to very strong association between hip sensor and platforms but only maximal acceleration was within 10% of the reference value. Systematic overestimation of all other measures => adequate validity of hip MIMU but insufficient accuracy
(Sabatini and Mannini, 2016)	-	3D	-	Mixed machine learning approach and biomechanical model (BCoM approximation)	2 MIMUs (L5, right shank)	- OMCS (rigid clusters of markers on top of MIMUs) - treadmill / straight-walking - 12 AS / 5 AS	-LoA of cyclical component (+/- 1.96 std): - ML = 0,07 m/s (+/- 0.10 m/s) - AP = 0.03 m/s (+/- 0.05 m/s) - CC = 0.06 m/s (+/- 0.10 m/s) -RMS error of average velocity : 0.06 m/s (0.07 m/s) (Average RMSE about 4% above 4km/h if task-specific training vs 5% when non-task specific training)
(E. Shahabpoor and Pavic, 2018)	CC	-	-	Mixed machine learning approach (dynamic-time warping) & biomechanical model (BCoM approximation)	1 MIMU at C7	- Force plates / insoles - treadmill / outdoor free-walking - 6 AS / 10 AS	- in-lab validation NRMSE vGRF = 5.6 % +/- 1.5% with dynamic time warping vs 7.5% +/- 1.7 % without - outdoor validation range NRMSE = 7-11%

| Authors | BCOM motion | | | Method | | Validation | |
	Acc.	Vel.	Disp.	Method type	Wearable sensor	Reference, situation, population	Results
(Shahabpoor *et al.*, 2018)	3D	-	-	Biomechanical model (Inertial model: comparison of different models)	3 MIMUs: C7, L5, right thigh (located the closest possible to SCoM)		- 3-IMU model: NRMSE 16% in AP, 18% in ML and 7% in V => NRMSE can be decreased by 3-5 % with subject training (12 MIMUs) => Non-linear model by including 1-lagged term improved NRMSE by 2% - Outodoor validation => Model 2 NRMSE 8.7 % for vertical GRF
(Yuan and I. M. Chen, 2014)	-	3D	3D	Biomechanical model (fusion of kinematic chain + BCoM approximation)	3 MIMUs (pelvis, thigh, shank) & pressure insoles (stance phase)	- OMCS - Marker on top of pelvis MIMU - Jumping forward - 1 AS	- RMSE AP 0,051 m/s (< 3 % of max velocity) / 3.8 cm (total length: 3.6 m) - RMSE V 0,029 m/s / 3.2 cm - RMSE ML 0,13 m/s (lack of accuracy) / 5.2 cm
(Zijlstra *et al.*, 2010)	CC	CC	-	Biomechanical model (comparison of inertial models)	3 MIMUs (sternum, pelvis, right waist)	- Force plates - Sit-to-stand transfers - 5 AS + 12 elderly	- weighted average of sternum and waist sensor achieved highest correlations (mean 0.99 / 0.94 for young/elderly) and good accuracy (NRMSE from 11.5 to 13%). - Pelvis MIMU achieved good accuracy (NRMSE < 13.4%) but correlations as low as 0.56 for slow motion. Sternum MIMU highly correlated (r > 0.85) but high NRMSE (> 24%)

1.2.   Single-sensor approach

In general, single-segment approaches are based on the assumption that a single sensor positioned at pelvis level allows to capture BCoM motion with great accuracy (Gard *et al.*, 2004; Floor-Westerdijk *et al.*, 2012; Huntley *et al.*, 2017). The underlying hypotheses within this theory are that the BCoM is fixed in the pelvis reference frame – and therefore, that it is not influenced by the other body segments motions relative to the pelvis' (Eames *et al.*, 1999; Floor-Westerdijk *et al.*, 2012) – and that pelvis rotations can be considered as sufficiently small so that the relative motion of a skin-mounted marker compared to the BCoM due to these rotations are negligible (Gard *et al.*, 2004). Although these assumptions can be valid in people with asymptomatic gait at self-selected or slower speeds (Gard *et al.*, 2004), they were shown not to be acceptable in pathological gait where the single-marker method implemented in laboratory-based gait analysis was shown to result in significant overestimations in the estimated BCoM excursion (average error of up to 5 cm within a step in the anteroposterior direction in post-stroke participants) compared to a full body inertial model (Eames *et al.*, 1999; Huntley *et al.*, 2017). BCoM excursions were also shown to be overestimated using a single marker at pelvis level in the asymptomatic population, especially when performing dynamical motion (Pavei *et al.*, 2017).

Despite this conflicting evidence, the single-marker approach remains attractive because it offers a simple and quick estimate of BCoM motion with a good agreement in the motion patterns compared to force plates or full body data (Gard *et al.*, 2004; Huntley *et al.*, 2017). Therefore, several authors have investigated the validity of using a single MIMU at pelvis level to approximate BCoM motion (Meichtry *et al.*, 2007; Esser *et al.*, 2009; Floor-Westerdijk *et al.*, 2012; Yuan and I. Chen, 2014; Regterschot *et al.*, 2014; Myklebust *et al.*, 2015; Najafi *et al.*, 2015; Sabatini and Mannini, 2016; E. Shahabpoor and Pavic, 2018; Lintmeijer *et al.*, 2018; Mohamed Refai *et al.*, 2020).

In three studies (Esser *et al.*, 2009; Yuan and Chen, 2012; Sabatini and Mannini, 2016), the single-MIMU-based BCoM motion was compared to that obtained with reflective markers positioned above the sensor and not to a gold standard (full body inertial model or force plate data). However, the methods were applied in asymptomatic subjects, where the sacral approximation of the BCoM can be considered valid during straight walking and comfortable speed (Gard *et al.*, 2004). In (Esser *et al.*, 2009), vertical peak-to-peak acceleration, velocity and excursion of the BCoM obtained with a MIMU positioned at L4 were compared to that derived from a MIMU-mounted marker. Although high agreement was found for these three parameters against marker data, the amplitude of vertical velocity motion was slightly (< 0.04 m.s^{-1}), but significantly, underestimated with the MIMU (Esser *et al.*, 2009). Errors might have been introduced during the integration process of acceleration data. Both other methods, which provide results in the three directions of motion, rely on additional sensors to improve the integration and the estimation of BCoM velocity (Yuan and I. Chen, 2014; Sabatini and Mannini, 2016). Furthermore, these methods provide the instantaneous walking velocity while the former only provided an estimate of the mean-subtracted walking velocity.

The remaining single-sensor-based studies investigated the validity of the single-MIMU approach against either force plate data or full body inertial models in different situations. When the considered situation included significant upper body motion, such as when skiing (Myklebust *et al.*, 2015), performing golf swing (Najafi *et al.*, 2015) or rowing (Lintmeijer *et al.*, 2018), a significant decrease in

accuracy was observed, in particular in the anteroposterior direction. This might be explained by higher range of motion of the trunk and arms, compared to walking. Furthermore, decreased agreement of the anteroposterior and mediolateral acceleration were observed in asymptomatic subjects walking with a forced asymmetrical gait pattern compared to normal walking (Mohamed Refai *et al.*, 2020). These results seem to indicate that including a sensor on the trunk, rather than solely on the pelvis, might be necessary for pathological gait, in particular in people with lower-limb amputation who were shown to present wider range of motion of the trunk segment (Goujon-Pillet *et al.*, 2008). This proposition was already underlined in (Meichtry *et al.*, 2007) where the anteroposterior acceleration measured at L3 was found to precede the BCoM acceleration in the asymptomatic population. This phase difference, which was not observed in the vertical direction, might explain the overestimation of mechanical energy parameters when using the sacral method compared to full body or force plate data (Meichtry *et al.*, 2007; Pavei *et al.*, 2017). Higher excursions of the BCoM were found in all three directions when using the single sensor approximation compared to a gold standard during sit-to-stand transfer (Regterschot *et al.*, 2016) and straight walking (Meichtry *et al.*, 2007; Floor-Westerdijk *et al.*, 2012), similarly as when using a single optical motion capture marker (Pavei *et al.*, 2017).

As introduced in the first paragraph, pelvis rotations and in particular pelvis tilt may be accountable for the increased range of motion of a skin-mounted device compared to a fixed point within the pelvis (Gard *et al.*, 2004; Floor-Westerdijk *et al.*, 2012). In order to mitigate the effect of pelvis rotations on the BCoM displacement estimated with the single sensor approach, Floor-Westerdijk and coworkers used a generic translation vector to transfer the acceleration measured at the sacrum to a point within the pelvis, considered to be the BCoM (Floor-Westerdijk *et al.*, 2012). This resulted in a significative improvement of the accuracy and agreement of the displacement of the BCoM in the mediolateral direction as evidenced by the reduction of root mean square error by 40% (RMS = 4.27 mm instead of 7.16 mm) and the increase of the intraclass correlation coefficient (ICC going from 0.64 to 0.77) between the MIMU-based and the segmental analysis-based BCoM. Agreement in the anteroposterior direction remained moderate (ICC = 0.68) as the method didn't correct for the lag observed between pelvis and BCoM motion.

Finally, Shahabpoor and Pavic proposed a machine learning approach to increase the accuracy of the vertical component of the BCoM acceleration estimated using a single MIMU (E. Shahabpoor and Pavic, 2018). The vertical BCoM acceleration was estimated using the acceleration measured at C7 corrected by a time-varying factor. The former was derived from a dynamic time warping approach that was applied to the average time-series of difference between C7 and BCoM vertical accelerations. This approach allowed to reduce the error achieved when using a constant coefficient by up to 25 %, yielding an average error of 5.6 %. The validity of this approach was not investigated for the anteroposterior and mediolateral components of the acceleration or of any other BCoM kinematic descriptor, therefore, the added value of the complex machine learning approach compared to a constant coefficient method applied at pelvis level is questionable.

1.3.   Multi-sensor approach

Two main approaches are described in the literature when dealing with multiple sensors. The most common approach consists in the wearable version of the full body inertial model (Faber *et al.*, 2016; Karatsidis *et al.*, 2017; Lintmeijer *et al.*, 2018; Pavei *et al.*, 2020), possibly simplified using a reduced

number of sensors (Zijlstra *et al.*, 2010; Najafi *et al.*, 2012; Shahabpoor *et al.*, 2018) while the second approach relies on a kinematic chain (Yuan and I. Chen, 2014; Fasel, Spörri, *et al.*, 2017).

1.3.1. Inertial model

Methods based on the inertial model paradigm rely on the fact that the 3D BCoM kinematics can be retrieved through the weighted sum of the kinematics of the body segments centers of mass (SCoM). First, segment-mounted MIMUs allow to retrieve the acceleration of the SCoM which are then fused to estimate BCoM acceleration, and, after integration, BCoM velocity or trajectory. An inertial model provides, for each included segment, the position of its center of mass in the segment anatomical frame as well as the mass of the segment.

Four studies have investigated the accuracy of a full-body inertial model associated with MIMUs for the estimation of BCoM motion. The first three studies use the xSens MVN suit (consisting of 17 MIMUs positioned at specific locations on the body), therefore, unknown proprietary algorithms allowed to retrieve the SCoM accelerations from MIMU measurements. Two of these studies compared the 3D BCoM acceleration retrieved from the xSens MVN suit to force plates data during straight walking (Karatsidis *et al.*, 2017) and a trunk bending task (Faber *et al.*, 2016). In both cases, poorer accuracy was achieved for the anteroposterior and mediolateral directions than for the vertical direction and only moderate correlations were found between the lateral component estimated with the MIMU-based inertial model and the force plates (average of 35% of errors in the mediolateral direction during single stance in straight walking in (Karatsidis *et al.*, 2017)). Another study investigated the accuracy of the 3D BCoM trajectory output of the MVN suit compared to force plate and optical motion capture (OMC) data (Pavei *et al.*, 2020). The MIMU-based 3D BCoM path was found to have a different shape than that obtain with force plate or OMC data, with significant errors. Average errors were in fact above 35% in both the anteroposterior and mediolateral directions and leaded to an overestimation of the external work of more than 100%. In the fourth study, Lintmeijer and coworkers investigated the use of a 13-segment inertial model to track the BCoM acceleration in the anteroposterior direction while rowing. Each of the thirteen MIMUs was manually positioned at the longitudinal position of the SCoM of the underlying segment and was considered to directly provide the SCoM acceleration. Contrary to when using a single sensor at the pelvis, the 13-MIMU set allowed to estimate accurately the anteroposterior acceleration of the BCoM (Lintmeijer *et al.*, 2018). Such results may not be achieved in different motions such as walking.

The four above-mentioned studies involved a full-body inertial model and the use of 13 to 17 MIMUs. For the sake of simplicity and time-efficiency, a wearable protocol intended for the clinical field should include the minimal number of sensors possible (Najafi *et al.*, 2015; Ancillao *et al.*, 2018; Jeong *et al.*, 2018). Therefore, three authors proposed a reduced set of MIMUs for the estimation of BCoM kinematics.

For instance, a model combining the trunk and pelvis segments was proposed to estimate BCoM kinematics and the vertical power exerted at the BCoM to lift the body (or "lifting power") during sit-to-stand transfers of elderly people from only two MIMUs (Zijlstra *et al.*, 2010). Although this model resulted in a significant overestimation of the vertical acceleration of the BCoM (about 11%), the simple MIMU-based estimation was found to be highly correlated with the vertical BCoM motion and allowed to predict the peak of lifting power estimated with force plate data. Najafi and coworkers

55

proposed a two-link model, integrating MIMUs rigidly attached to a shank and the trunk for the evaluation of BCoM motion during golf swing. High correlations were obtained with errors in the horizontal BCoM displacement below 16% (Najafi *et al.*, 2015). The model developed could be used to estimate postural stability in clinics (Najafi *et al.*, 2015) but may not be transferable to gait. Last but not least, Shahabpoor and coworkers proposed a methodology to identify the optimal locations of MIMUs for the estimation of 3D BCoM acceleration (Shahabpoor *et al.*, 2018). In a population of young asymptomatic subjects, a weighted average of the SCoM accelerations of the trunk, pelvis and a thigh SCoMderived from an OMC system were shown to estimate the 3D BCoM acceleration with good accuracy in the vertical direction (7% of errors), and moderate accuracy in the anteroposterior and mediolateral directions (respectively 16 and 18%). Subject-specific training of the model and/or the use of non-linear relationship were shown to improve the results in the horizontal plane (< 15%). The validity of the method when using acceleration data derived from MIMUs and for outdoor ambulation was investigated in the vertical direction using pressure insoles and MIMUs rigidly mounted on each segment, near the underlying SCoM. Mean errors of 8.7% were achieved in the vertical BCoM acceleration with subject-specific training (Shahabpoor *et al.*, 2018).

1.3.2. Kinematic chain

Kinematic chain approaches allow to retrieve the trajectory of segments and joint centers of rotation based on the knowledge of the length and orientation of segments, as well as the localization of joint centers of rotation in the anatomical frames.

In (Yuan and I. Chen, 2014), the center of mass is assumed to lie at the pelvis level. Under the assumption of ankle null velocity during stance phase, velocity at the knee joint can be estimated assuming that the tibia is a rigid solid, that its orientation is correctly captured by a MIMU positioned on the tibia, and knowing the distance between the ankle and the knee joints. The same process in then applied to obtain the velocity as the hip joint and ultimately at the pelvis. This estimation of the velocity is fused with that obtained by direct integration of the acceleration measured by the pelvis MIMU in order to correct the drift inherent to the integration. During swing phase, the assumption of null velocity does not hold and the velocity is estimated only by the direct integration of the pelvis MIMU acceleration. This allows to estimate the velocity of the BCoM with three MIMUs, located at the shank, thigh and pelvis of one leg (**Figure 23**). The method was validated on a single asymptomatic subject, performing a forward jump. While the method was proven to be accurate in the vertical direction, relatively low accuracy was achieved for the mediolateral component and errors in the anteroposterior direction reached 3% of the maximal velocity. The absence of other segment-to-sensor calibration than manual alignment may partially explain the inaccuracies, especially in the mediolateral direction.
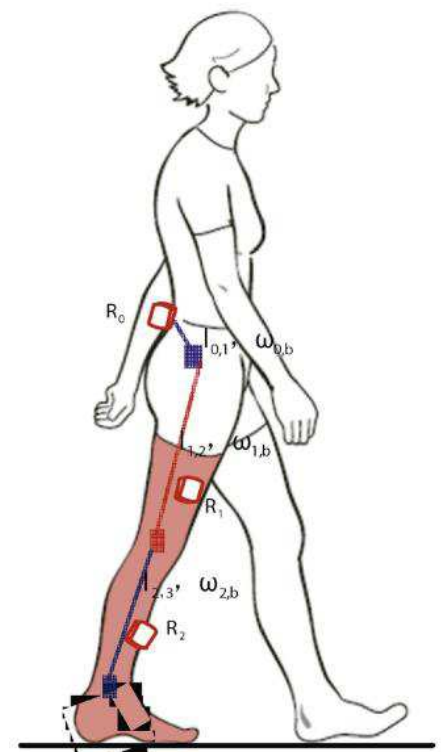
Figure 23: Kinematic chain, taken from (Yuan and I. Chen, 2014). R_j are the orientation outputs of MIMUs j, $l_{j,k}$, are the vector linking joint j to k, $\omega_{j,b}$ is the angular velocity vector of segment j in the global reference frame

1.3.3.   Fusion of inertial model and kinematic chain approaches

The method proposed by Fasel and coworkers requires to define both a kinematic chain and a full-body inertial model (Fasel, Spörri, *et al.*, 2017). The anthropometric inertial model is used to retrieve, for each segment, its mass and dimensions as well as the position of its center of mass in its anatomical frame. The position of the SCoM in the reference global frame are then retrieved using a kinematic chain approach. This subsequently allows to obtain an estimate of the BCoM position as the weighted sum of the SCoM positions, similar as when using an optical motion capture system. To achieve this aim, the first step consists in computing the orientation of 11 MIMUs mounted on the body relative to the underlying segments using functional and/or static calibrations. During the skiing trials, the application of the kinematic chain allows to retrieve the trajectory of the joint centers of rotations relative to the root point of the kinematic chain (here, the lumbar joint center) using the segment orientations (known thanks to the MIMUs rigidly mounted on the segments) and the segments dimensions (obtained using anthropometric tables). The inertial model provides the position of each SCoM relative to their respective joint centers of rotation in the segment frame. Therefore, using the rigid body assumption and the trajectory of the joints center of rotations thanks to the kinematic chain, it allows to compute the SCoM trajectory. Finally, a weighted average of SCoM positions at each timestamp was computed to estimate BCoM trajectory. The position of the BCoM relative to the lumbar joint center was tracked with better accuracy in the vertical and mediolateral than in the anteroposterior directions, with a 3D accuracy of less than 26 mm (Fasel, Spörri, *et al.*, 2017). In the perspective of model simplification, the authors evaluated the accuracy achieved with seven sensors, removing the arms from the model. Accuracy and precision did not change significantly, suggesting that the arms contribution to the BCoM motion in the investigated situation was negligible. Interestingly, the method was shown to achieve a decreased accuracy in the kinematics of the most distal segments, due to errors accumulation with the kinematic chain paradigm.

1.4.   Synthesis and selection of the most appropriate methods for the wearable estimation of BCoM kinematics in people with lower-limb amputation

None of the methods identified in the literature were applied to the gait of people with lower-limb amputation. Therefore, the advantages and drawbacks of each of the retrieved methods should be weighted and put in regards with the specificities of the lower-limb amputee gait pattern in order to identify the most promising methods for BCoM kinematics estimation in amputee gait. In particular, it should be kept in mind that a trade-off between simplicity (number of sensors, calibration procedures) and accuracy is essential for clinical transfer of wearable protocols.

Three categories of methods have emerged from the literature regarding the estimation of BCoM derived parameters: single-sensor approaches, multi-segment inertial models and kinematic chains.

Single sensor approaches are attractive because of their simplicity (Gard *et al.*, 2004; Esser *et al.*, 2009; Jeong *et al.*, 2018). However, they were shown to overestimate BCoM range of motion and to lack accuracy in the mediolateral and anteroposterior directions, similar as their optical motion capture counterpart. Indeed, significant differences were found between the BCoM displacement and acceleration in the mediolateral direction retrieved with the sacral method compared to the multi-segment analysis in asymptomatic subjects (Jeong *et al.*, 2018). Furthermore, when analyzing movements involving a wide upper body range of motion or an asymmetrical gait pattern, the sacral

method was deemed inappropriate (Meichtry *et al.*, 2007; Myklebust *et al.*, 2015; Huntley *et al.*, 2017; Lintmeijer *et al.*, 2018; Mohamed Refai *et al.*, 2020). Therefore, this method is not likely to allow the accurate capture of 3D BCoM motion in amputee gait. Indeed, people with lower-limb amputation were shown to display an increased range of motion of the pelvis and the trunk (Michaud *et al.*, 2000; Goujon-Pillet *et al.*, 2008).

Multi-sensor inertial models allow to retrieve the BCoM acceleration from a weighted sum of accelerations measured by a set of MIMUs. A large variety of MIMU sets has been retrieved from the literature, including from two to 17 MIMUs when using the commercialized MVN suit. This approach assumes that MIMUs rigidly attached to body segments can allow to estimate the accelerations of the underlying SCoMs. Therefore, a large number of MIMUs should be employed in order to capture the accelerations of all the segments pertaining to the body. In general, MIMUs are carefully positioned as closely as possible to the underlying SCoM and the accelerations measured by the MIMUs are used as proxy measurements of the SCoM accelerations (Lintmeijer *et al.*, 2018; Shahabpoor *et al.*, 2018). As MIMUs provide the acceleration in the MIMU local frame, their output must be transferred in a global reference frame prior to computing their weighted average (Lintmeijer *et al.*, 2018; Shahabpoor *et al.*, 2018). Care must be taken to ensure that the orientation output is not influenced by magnetic disturbances (Lintmeijer *et al.*, 2018; Shahabpoor *et al.*, 2018). In order to reduce the number of sensors required, several authors have investigated the feasibility of simplifying inertial models by considering only the motion of up to three segments (Zijlstra *et al.*, 2010; Najafi *et al.*, 2015; Shahabpoor *et al.*, 2018), with one approach implemented in a walking task.

The last approach is that of the kinematic chain. It can either be used with the estimation that the BCoM lies within a segment pertaining to the kinematic chain, such as the pelvis (Yuan and I. Chen, 2014) or it must be coupled with an inertial model in order to estimate SCoM motion from the motion of the joint centers of rotation (Fasel, Spörri, *et al.*, 2017). In any case, the kinematic chain method imposes to use MIMUs on all adjacent segments pertaining to the kinematic chain. Furthermore, accurate sensor-to-segment alignments are crucial since the method relies on the orientation of segments to estimate the segments' trajectories and since errors build up along the kinematic chain (Fasel, Spörri, *et al.*, 2017). The coupled kinematic chain and inertial model proposed by Fasel and coworkers yielded an accurate estimation of the BCoM excursion but required 7 MIMUs and didn't provide the absolute kinematics of the BCoM in an Earth-fixed reference frame since the root point of the kinematic chain was the lumbar joint center.

Based on this overview of the literature, single-sensor approaches do not seem relevant for lower-limb amputee gait as BCoM trajectory and acceleration estimated using this approach or its laboratory-based counterpart were shown to be overestimated in pathological and asymmetrical gait. However, since a trade-off between accuracy and simplicity of the protocol is crucial, full-body inertial models or complete kinematic chain neither appear relevant. Therefore, the multi-sensor approach consisting in simplifying inertial models represents an interesting track for the estimation of BCoM kinematics from MIMUs for the gait of people with lower-limb amputation. In particular, the method developed by Shahabpoor and coworkers could be adapted in the population of people with lower-limb amputation in order to identify the optimal segments network required for the estimation of 3D BCoM motion. The next chapter thus aims at investigating the feasibility of deriving an optimal sensor network for the estimation of BCoM acceleration in people with transfemoral amputation, using optical motion capture data.

Chapter 2 – Optimal sensor network for the estimation of 3D body center of mass acceleration in people with transfemoral amputation

This chapter will be submitted as an article. Part of the validation study, with a slightly different post-processing, was submitted as an abstract for the 45th Congress of the Société de Biomécanique. The work of Joseph Basel, Msc, is duly acknowledged.

2.1. Introduction

The study of biomechanical parameters derived from body center of mass (BCoM) motion may reveal crucial information about gait impairment (Minetti *et al.*, 2011; Pavei *et al.*, 2017; Tesio and Rota, 2019), especially in people with lower-limb amputation (Agrawal *et al.*, 2009; Bonnet *et al.*, 2014; Askew *et al.*, 2019; Tesio and Rota, 2019). Indeed, from a mechanical standpoint, the kinematics and dynamics of the body center of mass (BCoM) are important parameters of the locomotion which directly result from the application of external forces (Tesio and Rota, 2019). The 3D path of the BCoM allows to describe the displacement of the body as a whole (Pavei *et al.*, 2020). BCoM acceleration, velocity and displacement have been shown to provide insight on dynamical stability (Hof *et al.*, 2005; Hak *et al.*, 2014; Al Abiad *et al.*, 2020), gait efficiency (Donelan *et al.*, 2002a; Bonnet *et al.*, 2014; Askew *et al.*, 2019), and gait asymmetries (Agrawal *et al.*, 2009; Minetti *et al.*, 2011) both in the asymptomatic population and in the population of lower-limb amputees. Although 3D BCoM motion is of particular interest to describe pathological gait, it is scarcely studied in clinical routine (Tesio and Rota, 2019), partly due to the high cost and complexity of optoelectronic motion capture systems and force plates which allow the acquisition of BCoM-derived parameters.

Recently, the use of magneto-inertial measurement units (MIMUs) has been proposed as an alternative to the gold standards for the capture of BCoM derived parameters (Floor-Westerdijk *et al.*, 2012; Ancillao *et al.*, 2018; Shahabpoor *et al.*, 2018; Pavei *et al.*, 2020). MIMUs are indeed small, light, and low-cost wearable sensors, embedding orthogonally mounted accelerometers, gyroscopes and magnetometers. The latter provide the linear acceleration, angular velocity and local magnetic field along the axes of an inertial frame defined by the MIMU case ("MIMU local frame") and their fusion allows to estimate the orientation of the MIMU local frame relative to a global Earth-fixed frame (Bergamini *et al.*, 2014). Therefore, provided MIMUs are securely attached to segments and carefully aligned with the underlying anatomical frames, they can be used to estimate segmental orientation and motion and ultimately, similarly as optoelectronic systems, segments' centers of mass (SCoM) and 3D BCoM motion.

For the sake of simplicity, most wearable protocols developed for 3D BCoM motion tracking involve a single sensor at pelvis level (Meichtry *et al.*, 2007; Floor-Westerdijk *et al.*, 2012; Ancillao *et al.*, 2018). Yet, several works evidenced that the sacral method tends to overestimate the 3D path of the BCoM (Meichtry *et al.*, 2007; Pavei *et al.*, 2017). In particular, the mediolateral (Jeong *et al.*, 2018; Mohamed Refai *et al.*, 2020) and anteroposterior (Meichtry *et al.*, 2007; Myklebust *et al.*, 2015; Najafi *et al.*, 2015) components of BCoM trajectory and acceleration were shown not to be accurately captured when using the sacral method in the asymptomatic population, especially when adopting an asymmetrical gait pattern or performing motion involving the upper body (amplitude of the sacral marker displacement compared to that of BCoM displacement of 124 mm vs 46 mm in the

anteroposterior direction in cross-country skiers - Myklebust et al. 2015 ; correlations of the sacral-method-based acceleration with the BCoM acceleration inferior to 0.56 in the anteroposterior and mediolateral directions in sound participants mimicking an asymmetrical gait pattern - Mohamed Refai et al. 2020). As a consequence, multi-segment analyses, including 11 to 17 MIMUs, have also been proposed (Fasel, Sporri, *et al.*, 2017; Karatsidis *et al.*, 2017; Lintmeijer *et al.*, 2018; Pavei *et al.*, 2020). In (Fasel, Spörri, *et al.*, 2017), the BCoM trajectory was for instance estimated using 11 MIMUs with high 3D accuracy (25.7 mm for the norm and errors < 8.6 mm along each axis) in 11 athletes performing indoor alpine skiing. Similarly, in (Lintmeijer *et al.*, 2018), the anteroposterior component of the BCoM acceleration was estimated accurately compared to force plates (NRMSE = 3.8 %, intraclass correlation coefficient > 0.988) using thirteen MIMUs located on the body segments of nine rowers.

To the authors' knowledge, no study investigated the feasibility of estimating 3D BCoM motion with MIMUs in people with lower-limb amputation. While single-sensor approaches may not be accurate enough for pathological gait, finding a balance between the number of MIMUs and accuracy is essential (Ancillao *et al.*, 2018; Jeong *et al.*, 2018). In this prospect, Shahabpoor and coworkers recently proposed a method to select a reduced number of MIMUs for the estimation of 3D BCoM acceleration in the asymptomatic population (Shahabpoor *et al.*, 2018). Three MIMUs located on the trunk, pelvis and one thigh allowed to accurately estimate the vertical component of BCoM acceleration (normalized root mean square errors NRMSE < 8.7% of the reference BCoM acceleration amplitude). While the need to consider the 3D nature of BCoM movement has been widely acknowledged (Minetti *et al.*, 2011; Pavei *et al.*, 2017; Tesio and Rota, 2019), moderate accuracy was achieved in the mediolateral and anteroposterior components (NRMSE > 16 %) when adopting this configuration with an optical motion capture system (Shahabpoor *et al.*, 2018). Nonetheless, the method developed appears promising and could be adapted in people with lower-limb amputation.

The aim of the present study was therefore to identify optimal sensor networks for the estimation of 3D BCoM acceleration in people with transfemoral amputation. First, segmental contributions to the BCoM acceleration will be investigated using optical motion capture system data and a full body inertial model. Based on these results, the accuracy of 3D BCoM acceleration estimated using different combinations of the most contributing segments will be investigated.

2.2. Methods

2.2.1. Participants

The study was designed according to the Declaration of Helsinki and was granted ethical approval (Comité de Protection des Personnes CPP NX06036). Ten people with traumatic transfemoral amputation (age: 41.5 ± 11.3 years; mass: 68.8 ± 15.2 kg; height: 1.73 ± 0.07 m; 8 males) gave written informed consent to participate in the study (**Table 3**). Inclusion criteria were people with transfemoral unilateral amputation due to trauma or tumor, fitted with a definitive prosthesis, able to walk at various speeds without any assistance. Participants walked with their usual passive microprocessor-controlled knee with an energy storing and return foot, the alignment of which was controlled by a prosthetist prior to data collection.

2.2.2. Measurement protocol

Each participant was equipped with a full-body marker set (Al Abiad *et al.*, 2020 - see Appendix A – Marker set used in Part 2 details). An optoelectronic system (VICON, Oxford, UK, 200 Hz) recorded markers positions while the participant was keeping a static standing posture and four photographs (front, back, both sides) were being taken (**Figure 24**). Following the static calibration trial, participants had

Figure 24: Static standing posture

to walk at self-selected speed along an 8 m pathway, with 3 force plates (AMTI, 1000 Hz) in the middle. Only trials with three successive foot contacts on the force plates (i.e. a complete stride) were considered for further analysis.

Table 3: Participants' characteristics

Participant	Gender	Age (years)	Height (m)	Mass (Kg)	BMI	Amputation delay (years)	Amputation level	Prosthetic knee	Prosthetic foot
TF1	M	58	1,8	68	21,9	31	TF	Mauch SNS	Variflex
TF2	M	48	1,8	64	19,7	1	TF	C-leg	Triton
TF3	M	54	1,8	85	25,9	7	TF	C-leg	1C40
TF4	M	43	1,6	72	26,7	3	KD	Rheo knee	Variflex
TF5	F	49	1,7	53	19,4	25	KD	Total Knee	Elation
TF6	M	44	1,7	47	16,6	18	TF	C-leg	Silhouette
TF7	F	26	1,7	65	23,9	2,5	Gritti	Rheo knee	Elation
TF8	M	26	1,8	56	17,3	1,5	TF	C-leg	Pro-Flex
TF9	M	32	1,8	95	29,3	7	TF	Rheo knee XC	Pro-Flex
TF10	M	35	1,7	83	29,1	9,5	KD	C-leg	Triton
Mean		*41,5*	*1,73*	*68,8*	*23,0*	*10,5*			
SD		*11,3*	*0,07*	*15,2*	*4,7*	*10,6*			

BMI, body mass index; F, female; M, male; TF, Transfemoral amputation; KD, Knee disarticulation, SD, standard deviation.
The prosthetic devices are from Ottobock (C-Leg, Triton, and 1C40) from Ossür (Rheo Knee, Mauch SNS, Total knee TK200, Variflex, Elation and Pro-Flex) and from Freedom Innovation (Silhouette).

2.2.3. Data processing

A 15-segment hybrid inertial model defined according to Pillet and coworkers (Pillet *et al.*, 2010), was used to obtain body segmental inertial parameters. Prosthetic limbs were represented by a concentrated mass estimated from the manufacturers' notices similarly to (Al Abiad *et al.*, 2020). Markers and force plate data were filtered using a zero-phase fourth order Butterworth low-pass filter, with a cut-off frequency of 5 Hz. Each segment's center of mass (SCoM) and inertial-model based BCoM accelerations were computed from marker data. Before each differentiation, marker-based signals were low pass filtered using the abovementioned Butterworth filter. Additionally, reference BCoM acceleration ($\boldsymbol{a_{BCoM,ref}}$) was derived from ground reaction force time-series ($\boldsymbol{GRF}$) following Newton's second law (equation 1, with m_{body}, the mass of the body and $\boldsymbol{g}$ the gravitational acceleration). Gait cycles were segmented using a 20 N threshold on the ground reaction force data and acceleration data was time-normalized to percent of the gait cycle.

$$\boldsymbol{GRF} = m_{body}\left(\boldsymbol{a_{BCoM,ref}} - \boldsymbol{g}\right) \quad (1)$$

a. Segmental contributions

Segmental contributions to the BCoM accelerations were defined according to two criteria as defined in (Shahabpoor *et al.*, 2018): the relative weight of SCoM accelerations in BCoM acceleration and the similarity of SCoM acceleration patterns with that of the BCoM derived from the inertial model.

The weight of the contribution of each segment ($\boldsymbol{Contrib_{seg_i}}$) in BCoM acceleration was defined as the SCoM acceleration ($\boldsymbol{a_{SCoM_i}}$) weighted by the relative mass of the segment in the body (equation 2, m_{seg_i} being the ith segment mass). Contribution weights were normalized by peak-to-peak BCoM acceleration and expressed as a percentage of total contributions. Segmental contribution weights were then averaged for each segment over all the participants.

$$\boldsymbol{Contrib_{seg_i}} = \frac{m_{seg_i}}{m_{body}} \, \boldsymbol{a_{SCoM_i}} \quad (2)$$

Regarding the similarity of SCoM accelerations, the Pearson's cross-correlation coefficient was computed between each pair of segment accelerations as well as between each SCoM acceleration and the inertial model based BCoM acceleration, for the anteroposterior (AP), mediolateral (ML) and vertical (V) directions, yielding three 16x16 symmetric cross-correlation matrices per gait cycle. For each direction and for each subject, the retrieved cross-correlation matrices were averaged over all the retrieved gait cycles to yield subject-specific cross-correlation matrices. Finally, the cross-correlation matrices were averaged over all subjects.

The most relevant contributing segments were then identified based on their respective weight and similarity to the BCoM acceleration derived from the inertial model.

b. Optimal sensor networks

The identification of the most contributing segments to the BCoM acceleration allowed to define several MIMU-based sensor networks with a minimal number of sensors for the estimation of BCoM acceleration, including three to six sensor locations. Furthermore, two methods were investigated for the construction of optimal sensor networks (OSN). In the first method, the OSN-based BCoM acceleration was computed as the sum of the segmental contributions for the N included segments (OSN type 1, equation 3):

62

$$a_{BCoM,OSN_1} = \sum_{i=1}^{N} Contrib_{seg_i} = \sum_{i=1}^{N} \frac{m_{seg_i}}{\sum_{j=1}^{N} m_{seg_j}} a_{SCoM_i} \quad (3)$$

The second method was based on the model proposed in (Shahabpoor *et al.*, 2018). In order to account for the whole-body mass, the mass of each of the non-selected segments (m_{seg_j}) was attributed to the main contributor whose acceleration was the more correlated to that of the non-selected segment, based on the average cross-correlation matrix (OSN type 2, equation 4).

$$a_{BCoM,OSN_2} = \sum_{i=1}^{N} \alpha_i \; Contrib_{seg_i} = \sum_{i=1}^{N} \frac{m_{seg_i} + \sum_{j=1}^{15-N} r_{j,i} \, m_{seg_j}}{m_{body}} a_{SCoM_i} \quad (4)$$

with $\begin{cases} r_{j,i} = 1, \text{ if included segment } i \text{ was the more correlated with segment } j \\ r_{j,i} = 0, \text{ if included segment } k \neq i \text{ was the more correlated with segment } j \end{cases}$

The inertial-model-based and the OSN-models-based BCoM acceleration were compared to the force plates-based reference BCoM acceleration. A leave-one-out methodology was used for the validation of the second type of OSN-based BCoM acceleration (equation 4) so that, for each participant, cross-correlation coefficients used to build the model were not used in the validation dataset. Reference and models-based BCoM accelerations were compared over the central prosthetic gait cycle of each trial using Pearson's linear correlation coefficients and their p-value as well as peak-to-peak normalized root-mean square errors (NRMSE) as proposed in (Ren *et al.*, 2008), averaged over all patients. An alpha-level of 0.05 was used for assessing the correlations significance. The results achieved with a single sensor at the pelvis center of mass ($a_{BCoM,pelvis} = a_{SCoM,pelvis}$) are also provided as an indication of the performance of the single sensor method. Given the low sample size, only descriptive statistics was provided.

2.3.   Results

A total of 25 complete prosthetic gait cycles were retrieved for the analysis, with an average of 3 gait cycles per participant (range 1-6).

a. Segmental contributions

Both absolute and relative average segmental contribution weights were represented as stacked bar plots every 2% of the prosthetic gait cycle (**Figure 25**). These representations allow to observe the weight of individual segments as well as the between-segments compensations. For instance, the upper-limbs were shown to contribute for less than 20% in the BCoM acceleration in all directions (**Figure 25** d.-f.) and contributions from the right and left sides to cancel each other in the anteroposterior direction (**Figure 25** a.). The trunk contributes to an average of about 30 % of BCoM acceleration in the vertical and mediolateral directions and to 16 % of the anteroposterior direction, which makes it the major contributor of BCoM acceleration.

In the anteroposterior direction, BCoM acceleration results from opposite actions of the different segments. In particular, prosthetic and sound limbs contributions are opposed in signs to each other. However, lower-limb actions do not cancel each other. On average, during the prosthetic gait cycle, the sound leg contributes to 47.4 % of the anteroposterior acceleration while the prosthetic leg contributes to 18.7 % of the BCoM anteroposterior acceleration, with most of each leg's contribution occurring in their respective swing phase.

63

In the mediolateral direction, the percentage contribution of upper and lower limbs appears to be near constant along the full gait cycle. The upper limbs contribute to 13.6 %, the sound lower limb to 26.0 % and the prosthetic lower limb to 15.5 % of the BCoM acceleration. Thus, the head, trunk and pelvis segments contribute to an average of 45.0 % of BCoM acceleration. The average head contribution in the mediolateral direction (9.3 %) is almost as high as that of a thigh (sound thigh: 13.9 %, prosthetic thigh: 11.0 %). It is interesting to note that the average contributions of the prosthetic shank and foot are below 2.5 % over the gait cycle.

In the vertical direction, the trunk and the thigh in swing phase appear to be the major contributors of BCoM acceleration, contributing for about 50 % of the latter. Over the full prosthetic gait cycle, the HAT (head, upper-limb, trunk and pelvis) segments contribute to 54 %, the prosthetic lower limb to 16 % and the sound lower limb to 30 % of the vertical acceleration. The prosthetic thigh contribution in swing phase (8 % on average) was found to be less than that of the sound thigh (about 22.5 %). During prosthetic midstance, the sound foot also appears to contribute to the vertical acceleration by up to 24.5 % while its contribution is below 3 % during sound-limb stance phase.

SCoM and BCoM accelerations cross-correlations matrices in the anteroposterior, mediolateral and vertical directions along the prosthetic gait cycle are displayed in **Figure 26**.

While significant and strong correlations were found between the accelerations of the BCoM, and that of centers of mass of the trunk, pelvis, prosthetic thigh and both shanks in the anteroposterior direction, the strong correlation of the head center of mass acceleration with the BCoM acceleration in the anteroposterior direction was found to be non-significant for at least one participant, but the correlation was significant on average. Interestingly, the anteroposterior accelerations of the centers of mass of the sound thigh and shank were negatively correlated with that of the BCoM. Moderate to strong correlations were found between the accelerations of the centers of mass of the sound upper limb and the BCoM acceleration. Strong and significative correlations were found between the accelerations of the BCoM and that of the centers of mass of the pelvis, trunk and sound thigh in the mediolateral direction while moderate correlations were found for the prosthetic thigh. For the latter segment, correlations were not significant for all participants, although significant on average (p-value < 0.05).

Eventually, very strong and significant correlations were found between the BCoM acceleration and that of the HAT SCoM in the vertical direction. The acceleration of the centers of mass of both thighs was also strongly and significantly correlated with the BCoM.
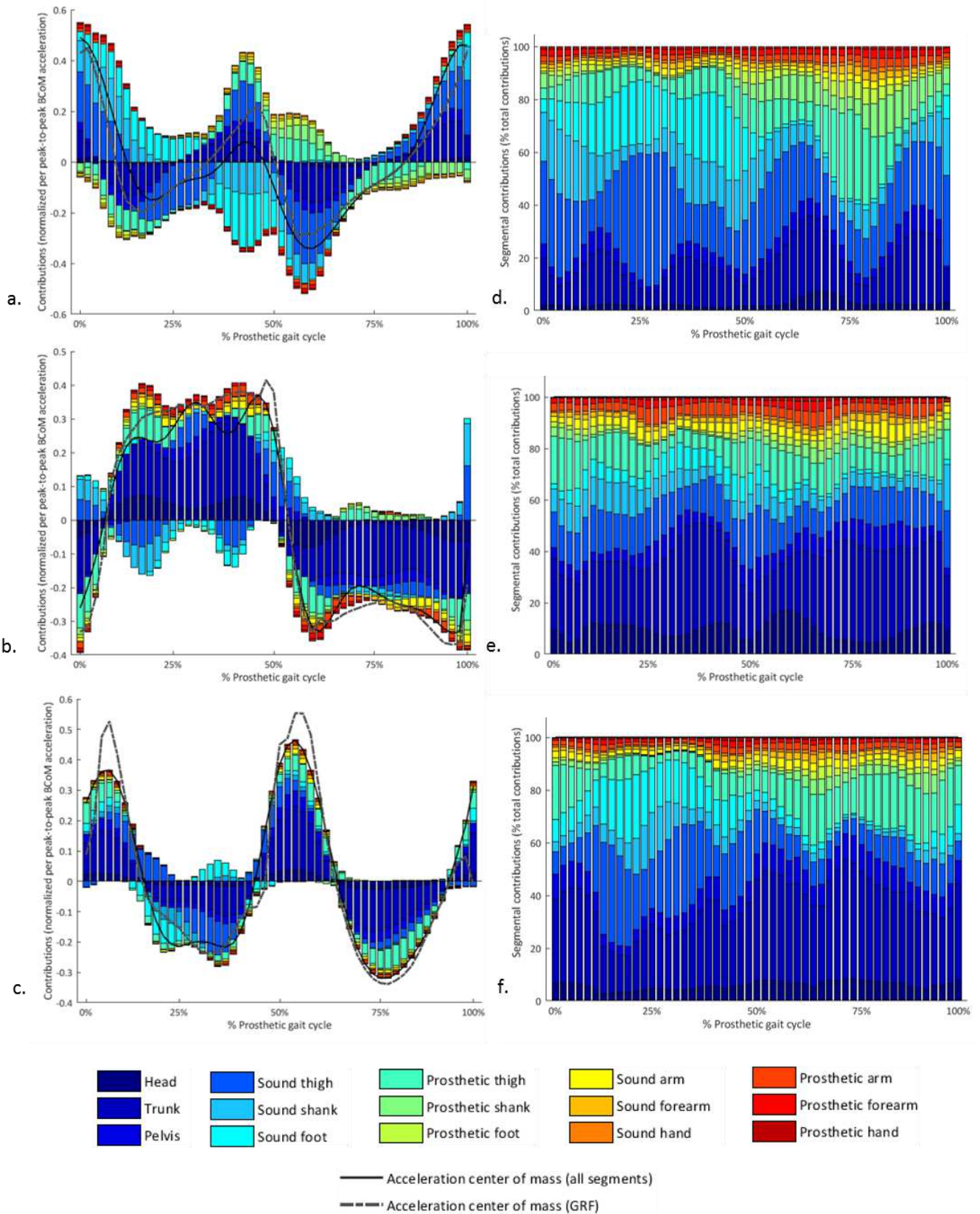
Figure 25: Segmental contributions in the body center of mass (BCoM) acceleration compared to total contributions and /or inertial-model based acceleration and reference acceleration (GRF) in the anteroposterior direction (**a.** and **d.**), in the mediolateral direction (**b.** and **e.**) and in the craniocaudal direction (**c.** and **f.**).

(**a.-c.**) Segmental contributions normalized per axial BCoM peak-to-peak acceleration;
(**d.-f.**) Segmental contributions expressed as percent of total absolute contribution;

65
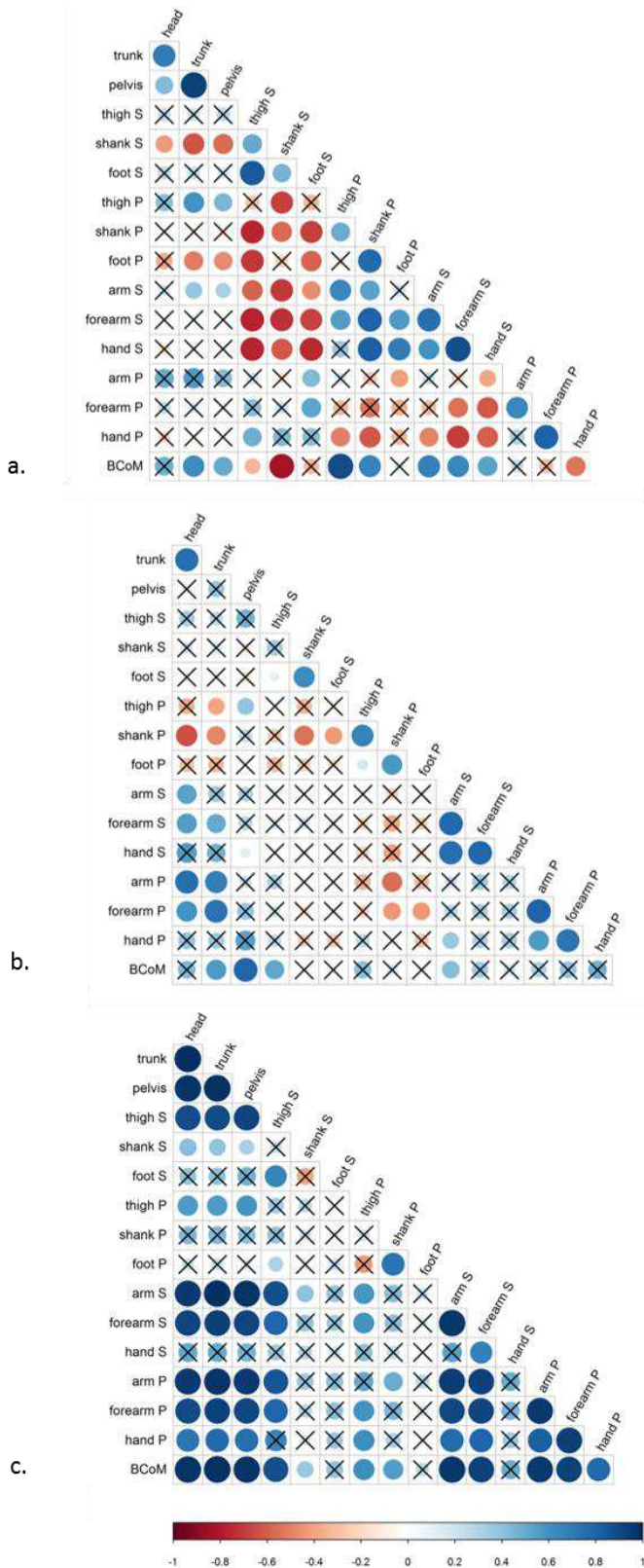
Figure 26: Average cross-correlation matrices of segments (P stands for Prosthetic side, and S for Sound side), inertial model-based Body center of mass acceleration (BCoM) and reference BCoM (from ground reaction force, BCoM GRF) along the prosthetic gait cycle in the (**a.**) anteroposterior, (**b.**) mediolateral, and (**c.**) vertical directions. Crossed correlations indicate that the correlation was non-significative for at least one participant. The darker an bigger the circle, the stronger the correlation (blue tones: positive correlation, red tone: negative correlations)

To conclude, the trunk, the pelvis and both thighs appear to be the main contributors of the BCoM in all three directions both in terms of similarity and weight. The head is also a prominent contributor of BCoM acceleration in the mediolateral direction, but head motion may be voluntarily uncorrelated to whole body motion, as evidenced by the non-significant correlations between the acceleration of the center of mass of the head and the BCoM acceleration in the anteroposterior and mediolateral direction. For both the prosthetic and sound limbs, ipsilateral shank and foot segments were found to have their SCoM accelerations significantly and highly correlated with each other, and to be significant contributors in the anteroposterior and vertical direction of the BCoM acceleration during the contralateral stance phase.

Based on these observations, the trunk, pelvis, and segments from both lower limbs were considered as promising sensor locations for BCoM acceleration estimation.

b. Optimal sensor networks

Several networks combining from three to six segment locations were considered for further analysis (**Table 4**). Estimated BCoM accelerations with these models or using single-segment paradigms were compared to reference BCoM acceleration, using the leave-one-out paradigm for OSN models of type 2. It should be noted that the inertial-model-based BCoM acceleration achieved mean errors of 10.6 ± 1.3 %, 10.7 ± 3.2 % and 11.2 ± 6.4 % in the anteroposterior, mediolateral and vertical directions respectively. All models achieved higher accuracy and agreement in the vertical than in the anteroposterior or mediolateral directions, with higher variability achieved along the mediolateral axis. The redistribution of the masses of excluded segments to those included in the model according to equation 4

didn't result in a significant improvement compared to the weighted sum method (equation 3) and generally led to a slight decrease in the correlation with the reference BCoM acceleration in the anteroposterior direction. For two models including the trunk and the shanks or feet, OSN type 2 models even resulted in a significant decrease of accuracy (up to -21 % of NRMSE in the anteroposterior direction) and agreement. All models including three sensors or more estimated the BCoM acceleration with higher accuracy and agreement than the sacral method in the anteroposterior and mediolateral directions. Only models including five segments or more achieved NRMSE below 15% in all three directions, except for one model with three sensors which resulted in NMRSE below 16.3 % in all directions.

Table 4: Comparison of body center of mass (BCoM) acceleration derived from various optimal sensor network (OSN) models to the reference acceleration issued from force plates. OSN of type 1 correspond to models where BCoM acceleration was estimated as the weighted sum of contributions of the included segments (see equation 3), while type 2 OSN models take into account the excluded segments' masses by redistributing them to their most correlated included segments (equation 4). Results are provided as **mean (standard deviation)**
Green shaded cases correspond to NRMSE < 15% and/or Pearson's linear correlation coefficient r ≥ 0.80
NRMSE = Normalized root mean square error; AP = Anteroposterior; ML = Mediolateral; CC = Craniocaudal

Number of segments	Included segments	OSN type	NRMSE (%)			Pearson's r		
			AP	ML	CC	AP	ML	CC
1	Pelvis	N/A	25.3 (2.4)	26.2 (8.0)	11.2 (2.0)	0.65 (0.07)	0.60 (0.28)	0.91 (0.05)
1	Trunk	N/A	20.0 (2.8)	20.8 (3.1)	10.6 (2.0)	0.74 (0.08)	0.84 (0.07)	0.92 (0.04)
3	Pelvis, thighs	1	23.3 (2.8)	24.8 (6.6)	14.4 (2.8)	0.84 (0.04)	0.62 (0.19)	0.84 (0.10)
		2	21.0 (2.8)	21.4 (6.1)	11.3 (2.5)	0.81 (0.04)	0.73 (0.15)	0.90 (0.05)
3	Trunk, thighs	1	18.0 (1.8)	13.0 (3.6)	11.3 (2.5)	0.87 (0.03)	0.91 (0.08)	0.90 (0.07)
		2	18.1 (1.9)	13.9 (2.7)	10.5 (2.4)	0.85 (0.03)	0.89 (0.06)	0.91 (0.05)
3	Trunk, shanks	1	15.0 (2.8)	16.3 (3.9)	11.0 (2.4)	0.82 (0.06)	0.86 (0.07)	0.91 (0.04)
		2	36.5 (4.1)	21.1 (5.7)	10.4 (2.2)	-0.08 (0.26)	0.74 (0.18)	0.92 (0.04)
3	Trunk, feet	1	25.6 (4.4)	18.3 (4.1)	12.3 (2.4)	0.51 (0.15)	0.84 (0.09)	0.88 (0.07)
		2	34.4 (3.7)	20.2 (6.7)	11.1 (2.2)	0.18 (0.20)	0.75 (0.17)	0.91 (0.05)
4	Trunk, pelvis, thighs	1	18.0 (1.8)	13.0 (3.5)	11.1 (2.4)	0.86 (0.03)	0.91 (0.08)	0.90 (0.06)
		2	18.6 (2.1)	12.9 (3.1)	10.6 (2.4)	0.84 (0.03)	0.91 (0.07)	0.91 (0.05)
5	Trunk, thighs, shanks	1	13.3 (1.8)	14.1 (5.1)	11.2 (2.3)	0.92 (0.02)	0.89 (0.10)	0.90 (0.06)
		2	10.3 (1.3)	13.0 (3.6)	10.5 (2.5)	0.93 (0.02)	0.91 (0.06)	0.91 (0.05)
5	Trunk, thighs, feet	1	11.9 (1.9)	13.5 (3.9)	10.7 (2.6)	0.91 (0.02)	0.90 (0.08)	0.91 (0.05)
		2	13.7 (2.6)	13.9 (4.1)	10.3 (2.5)	0.86 (0.06)	0.89 (0.09)	0.92 (0.04)
6	Trunk, pelvis, thighs, shanks	1	12.7 (1.5)	14.2 (4.9)	11.0 (2.4)	0.93 (0.02)	0.90 (0.10)	0.91 (0.06)
		2	10.5 (1.4)	13.4 (3.9)	10.6 (2.5)	0.93 (0.02)	0.91 (0.08)	0.91 (0.05)
6	Trunk, pelvis, thighs, feet	1	11.8 (2.1)	13.5 (3.7)	10.5 (2.6)	0.91 (0.03)	0.90 (0.07)	0.92 (0.05)
		2	13.5 (2.6)	13.6 (4.0)	10.4 (2.5)	0.86 (0.05)	0.90 (0.09)	0.92 (0.04)

The estimated BCoM acceleration with the pelvis sacral method, and two OSN models (OSN type 1 including the trunk and shanks segments, which is the only model achieving errors < 16.3% in all three directions while including less than 4 sensors and the OSN type 2 including the trunk, pelvis, both thighs and both shanks which yielded the better results) are represented in **Figure 27** against the reference BCoM acceleration derived from force plates data.

67

2.4. Discussion

a. Segmental contributions

The first objective of the study was to investigate segmental contributions to the BCoM acceleration in people with transfemoral amputation.

Similarly as in asymptomatic gait (Gillet *et al.*, 2003), the trunk was found to be the major contributor of BCoM acceleration in the vertical and mediolateral directions while the lower limbs, and more especially the thighs, the prime force generator in the direction of progression in people with transfemoral amputation. The accelerated masses of the trunk and both thighs were found to contribute to more than 50% of BCoM acceleration in all three directions, and up to 59% in average
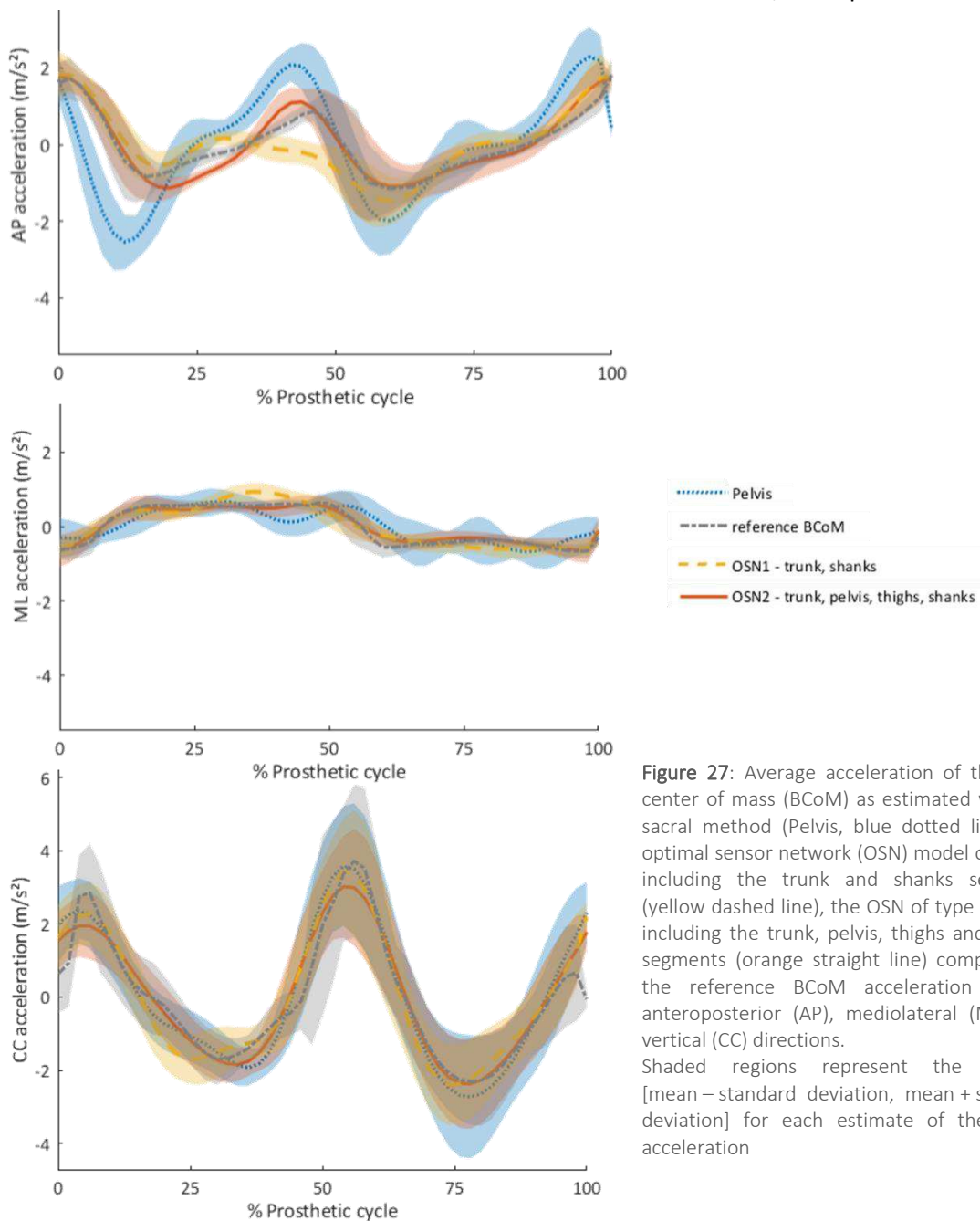
Figure 27: Average acceleration of the body center of mass (BCoM) as estimated with the sacral method (Pelvis, blue dotted line), the optimal sensor network (OSN) model of type 1 including the trunk and shanks segments (yellow dashed line), the OSN of type 2 model including the trunk, pelvis, thighs and shanks segments (orange straight line) compared to the reference BCoM acceleration in the anteroposterior (AP), mediolateral (ML) and vertical (CC) directions.
Shaded regions represent the interval [mean − standard deviation, mean + standard deviation] for each estimate of the BCoM acceleration

for the vertical direction. These segments happen to be the heaviest of the body, which may explain their significant weight in the BCoM acceleration.

The analysis of trunk and pelvis contributions in BCoM acceleration was of particular interest as they are often used in the literature as proxy measures of the BCoM motion (Gard *et al.*, 2004; Pavei *et al.*, 2017; E. Shahabpoor and Pavic, 2018). Trunk acceleration correlations with BCoM acceleration were shown to be stronger than that of the pelvis in the anteroposterior and mediolateral directions (Pearson r > 0.79 for the trunk while 0.66 > r > 0.63 for the pelvis). In both cases, stronger and significative correlations were found in the vertical direction (r > 0.9). These results support previous findings regarding the sacral method, which might be accurate enough for the study of vertical BCoM motion (Gard *et al.*, 2004) while unsuited to accurately track BCoM motion in the mediolateral or anteroposterior direction (Meichtry *et al.*, 2007; Jeong *et al.*, 2018).

Interestingly, contrary to what was observed in asymptomatic subjects (Shahabpoor *et al.*, 2018), segmental percent contributions in the vertical direction were not found to be near-constant during the prosthetic stance phase (**Figure 25f.**). Increased weight of sound leg accelerations is indeed observed at the beginning of the prosthetic gait cycle, following sound-limb push-off. This might result from ankle plantarflexion at terminal stance which was shown to be a major determinant of vertical BCoM motion (Hayot *et al.*, 2013). In the anteroposterior direction, the lower limbs were found to constitute the primary contributor of BCoM acceleration, with the sound limb accounting for almost half of total BCoM acceleration. This asymmetry in contribution weight might be partly explained by the lower mass of the prosthetic leg compared to the contralateral limb. An alternative explanation might lie with the specific gait compensations implemented by people with transfemoral amputation. Indeed, compensatory mechanisms at the sound limb, especially involving the hip and ankle joints, are common in this population (Sagawa *et al.*, 2011; Bonnet *et al.*, 2014; Drevelle *et al.*, 2014) and may contribute to increased accelerations of the contralateral thigh, shank and foot segments during gait. However, it was beyond the scope of the present study to investigate kinematic compensations adopted by the participants. Shanks and feet accelerations were shown to be highly correlated with each other in all directions, and shanks to be significantly and strongly correlated with BCoM acceleration in the anteroposterior direction. Furthermore, the sound lower-limb segments contribute in average to 34% of BCoM acceleration during the first half of the gait cycle. In light of these results, the inclusion of either shank or foot sensors seems relevant for the construction of OSN for BCoM acceleration estimation. Although the interest of including shank sensors was not reported for the asymptomatic population (Shahabpoor *et al.*, 2018), shank sagittal angles were previously shown to predict BCoM displacement along with thigh and HAT segments in the asymptomatic population (Mohan Varma and Sujatha, 2017; Arumukhom Revi *et al.*, 2020).

Similarly as in (Shahabpoor *et al.*, 2018), the head and upper limbs were discarded from the list of potential sensor locations for the wearable estimation of BCoM acceleration. Indeed, while the head was shown to be a prominent contributor of BCoM acceleration in the mediolateral direction, head motion can often be decorrelated from whole-body motion as pointed out by the non-significant correlation of its accelerations with that of the BCoM. Eventually, the upper limbs were found to be minor contributors in terms of weight (< 10% for each limb). This might be due both to their reduced mass relative to the body's (Dumas *et al.*, 2007) or to the fact that arms have a limited range of motion during straight walking. Furthermore, in a study investigating the feasibility of wearable tracking of BCoM displacement while skiing, Fasel and coworkers showed that accuracy and precision of BCoM

displacement was not much impacted by the removal of upper-limbs sensors due to the out-of-phase motion of the arms (Fasel, Spörri, *et al.*, 2017). However, it should be kept in mind that the upper limbs may play a more important role in other ambulation situations and should therefore not be systematically discarded.

b. Optimal sensor networks

Following the identification of the major contributors to BCoM acceleration, several OSN were devised including from three to six segments. The higher weight and agreement of trunk acceleration with BCoM acceleration compared to the pelvis one favored the investigation of three and five-sensor models involving the trunk and lower-limb segments. Relevance of this choice was confirmed by the achieved results: poorer accuracy was achieved when using the pelvis in a single-segment paradigm compared to when using the trunk and adding the pelvis to a trunk-based OSN model improved the NRMSE by less than 1 % (**Table 4**). Thus, our results advocate for the inclusion of the trunk segment when tracking body motion in people with transfemoral amputation. This is in agreement to previous literature reporting significant trunk 3D motion in this population (Goujon-Pillet *et al.*, 2008).

The added-value of including several segments compared to the trunk-only or pelvis-only models for the anteroposterior and mediolateral components of BCoM acceleration is demonstrated in **Table 4** and **Figure 27**. This confirms previous findings showing that the single sensor paradigm is not suited to accurately capture 3D BCoM motion, especially in pathological or voluntary asymmetrical gait (Gard *et al.*, 2004; Meichtry *et al.*, 2007; Pavei *et al.*, 2017; Jeong *et al.*, 2018; Mohamed Refai *et al.*, 2020). In particular, increased range of motion of the upper body in people with transfemoral amputation, especially of the pelvis in the sagittal plane (Goujon-Pillet *et al.*, 2008), may explain the limited agreement and higher excursions of the BCoM acceleration estimated with a single sensor compared to the reference BCoM acceleration in the anteroposterior direction . To the contrary, the pattern of 3D BCoM acceleration estimated using a 6-segment OSN-type 2 model including the trunk, pelvis, both thighs and shanks was found to closely match reference BCoM acceleration (**Figure 27**).

Following a similar procedure for the selection of segments in the asymptomatic population, Shahabpoor and coworkers developed an OSN model of type 2 including the trunk, the pelvis and a thigh. Errors achieved on the training set (four asymptomatic participants, 20 trials) in the anteroposterior, mediolateral and vertical directions were respectively 16 ± 2.0 %, 18 ± 6.7 % and 7 ± 1.7 %, and increased up to 32% in the mediolateral direction on the inter-subject validation set (two asymptomatic participants, 2 trials). While higher errors were achieved in the vertical direction by all the developed models within the present study, all the proposed OSN models including at least 5 segments and one 3-sensor model achieved higher accuracy in the anteroposterior and mediolateral directions. In particular, the 5-segment OSN-type 1 models, which did not require to compute segmental acceleration cross-correlation coefficients for mass redistribution, achieved the same error as Shahabpoor's with subject-specific training (Shahabpoor *et al.*, 2018). In the authors' opinion, instrumenting a participant with 5 MIMUs is less cumbersome than performing a 17-MIMU calibration to obtain the subject-specific cross-correlation matrix required for the development of OSN-type 2 models. The number of sensors included can be further reduced to three MIMUs when aiming at capturing only the anteroposterior (respectively, mediolateral) component of BCoM acceleration where enough accuracy is achieved with the instrumentation of trunk and shanks (respectively, thighs) segments (**Table 4**).

70

Karatsidis and coworkers investigated the accuracy of the ground reaction force estimated using a 17-MIMU model. During the single-stance phase of the gait cycle, their model yielded lower errors in the anteroposterior and vertical directions (NRMSE of 10.0 % and 9.0 % respectively) but low accuracy (35.4% NRMSE) and agreement (r = 0.61) were achieved for the mediolateral component (Karatsidis *et al.*, 2017). They achieved similar accuracy when using MIMUs and optical motion capture systems, indicating that high mediolateral errors might be due to the anthropometric model implemented rather than to the use of MIMUs.

c. Perspectives

In order to further reduce the number of sensors included in OSN models, an interesting track of research would be to propose kinematic models of groups of segments. For instance, the shanks and feet segments were shown to similarly contribute to the BCoM acceleration and their SCoM accelerations were significantly correlated. Therefore, a kinematic model representing the shank and foot as a rigid segment, such as proposed in (Hansen *et al.*, 2000, 2004), might allow to retrieve the acceleration of the center of mass of the foot/shank complex and therefore may contribute to an increase of accuracy of the OSN models without requiring supplementary sensors. Similarly, a kinematic model linking the pelvis and thigh segments may allow to capture the motion of both the pelvis and the thighs from a single sensor attached to the pelvis. Indeed, the rotation of the pelvis (captured through the angular velocity measured by a pelvis sensor) may provide indications on the thighs motion. However, it was not in the scope of this study to investigate such kinematic models and these merely constitute interesting path of reflection for future work.

d. Limitations and sources of errors

The contribution analysis presented in this study was performed by comparing individual SCoM accelerations to that of the BCoM using an hybrid geometric and proportional model (Pillet *et al.*, 2010). Since anthropometric models were shown to influence the BCoM motion pattern (Catena *et al.*, 2017; Pavei *et al.*, 2017), different results may have been achieved using other body segmental inertial parameters. Nevertheless, the present analysis provided the same major contributors of BCoM acceleration as in the literature on asymptomatic population (Gillet *et al.*, 2003; Shahabpoor *et al.*, 2018), with specificities that appear to be related to the specific gait pattern of people with transfemoral amputation. The inertial model used to compute SCoM and BCoM accelerations achieved mean NRMSE of 10.6 ± 1.3 %, 10.7 ± 3.2 % and 11.2 ± 6.4 % in the anteroposterior, mediolateral and vertical directions respectively (**Figure 25**c). This may explain why no further improvement in accuracy was achieved by the different OSN models-based estimations when adding segments, in particular in the vertical direction. Errors of the OSN-based and inertial model-based vertical BCoM accelerations may have resulted from the filtering and differentiation processes of marker data.

OSN models presented within this study were developed and validated with data derived from optical motion capture rather than wearable sensors. Therefore, their validity should be verified when using MIMUs. The latter provide raw acceleration and angular velocity measured at the origin and along the axes of the MIMU local frame as well as orientation data in a global reference frame. To transfer the measured accelerations at the SCoM, the position of each MIMU relative to the underlying SCoM must be obtained and angular velocity differentiated. These processes may introduce errors compromising the accuracy of BCoM estimates (Iosa, Picerno, *et al.*, 2016; Karatsidis *et al.*, 2017).

71

Furthermore, the orientation output estimated from MIMU signals have been shown to be affected by ferromagnetic perturbations (Lebel *et al.*, 2018), that may result from the ground within buildings or prosthetic components. In such conditions, different MIMUs may sense different global Earth-fixed frames (Picerno *et al.*, 2011), which may introduce new errors when computing BCoM acceleration from a weighted average of estimated SCoM acceleration. However, similar accuracy achieved with optical motion capture systems compared to MIMUs in (Karatsidis *et al.*, 2017) is promising and tend to indicate that transferring the OSN models developed within this study in a wearable framework might achieve similar accuracy.

2.5. Conclusions

This study investigated the feasibility of estimating BCoM acceleration in people with transfemoral amputation from the acceleration of a limited number of segment-mounted wearable sensors. Including a minimum of five segments provided an accurate estimation of 3D BCoM acceleration compared to the literature while only three segments were necessary for the estimation of 2D acceleration. The trunk segment was shown to be crucial for the estimation of BCoM acceleration and should be instrumented along with a minimum of two lower-limb segments. The models were developed using data from optical motion capture system associated with an inertial model. Thus, applicability of the method with wearable sensors will be verified in future works. Indeed, MIMUs might be affected by higher signal noise and ferromagnetic perturbations, which may compromise the accuracy of the estimated BCoM acceleration. Furthermore, the method relies on the correct estimation of SCoM accelerations. Therefore, the investigation of the impact of MIMUs positioning relative to the center of mass of underlying segments and the development of wearable methods allowing the identification of these relative positions represent research tracks of interest. Finally, the suitability of the proposed OSN models to accurately capture BCoM velocity and displacement, which are relevant parameters for motion analysis in people with transfemoral amputation, should also be investigated in the future. Future works will therefore investigate the transfer of the best OSN models to a wearable framework, the sensitivity of BCoM acceleration estimation to MIMUs positioning and the applicability of the models to track other BCoM-derived parameters.

Chapter 3 – Estimation of 3D body center of mass kinematics in a fully wearable framework

The previous chapter investigated the feasibility of using a reduced number of sensors for the estimation of the body center of mass (BCoM) acceleration in people with transfemoral amputation. The study allowed to select various optimal sensor networks (OSN) which provided accurate estimates of the BCoM acceleration using the acceleration measured at the centers of mass of three to six segments. However, the results obtained for the selected OSN were derived from optical motion capture (OMC) data. Therefore, the suitability of the OSN networks and of the overall methodology should be verified when using MIMUs. In particular, several challenges, that will be detailed in section 3.1, arise with the use of MIMUs. Indeed, for each MIMU, the acceleration is measured at the origin of the MIMU local frame and must be transferred to the center of mass of the underlying segment (SCoM), which is not immediate since MIMUs do not provide an estimation of their position. Furthermore, the obtained acceleration must be fused in a consistent Earth-fixed reference frame to estimate BCoM acceleration. Yet, the Earth-fixed reference frames sensed by several MIMUs may not be consistent across MIMUs (Picerno *et al.*, 2011; Lebel *et al.*, 2018; Guaitolini *et al.*, 2019), which might lead to errors when fusing data from multiple sensors. These problems are not encountered when using OMC data. Indeed, while OMC markers do not directly provide the trajectory of the SCoM, their coordinates allow to define the segment anatomical frames position and orientation in the OMC Earth-fixed reference frame. Thus, a full body inertial model coupled with OMC data allows to retrieve the SCoM position in the OMC reference frame. Using MIMUs therefore imposes to develop a specific framework prior to estimating BCoM acceleration from the OSN models selected in the previous section.

Once BCoM acceleration is accurately estimated from wearable sensors, obtaining the instantaneous velocity of the BCoM appears relevant. Indeed, the instantaneous velocity of the BCoM can provide insight on the energy cost of walking (Donelan *et al.*, 2002b; Detrembleur *et al.*, 2005) as well as on gait balance (Hof *et al.*, 2005, 2007). Furthermore, the average BCoM velocity or "walking speed" is a key descriptor of health status and gait function in pathological gait, including in people with lower-limb amputation (Batten *et al.*, 2019). While OMC-based BCoM position is differentiated to obtain BCoM instantaneous velocity, computing the instantaneous BCoM velocity from MIMU-based BCoM acceleration is not straightforward. Indeed, integration of MIMU signals leads to drift due to the presence of noise in the raw signal and must therefore be corrected to obtain an accurate estimation of BCoM instantaneous velocity.

The aim of this chapter is therefore to propose and validate a wearable framework to use MIMUs in the selected OSN configurations for the estimation of BCoM acceleration and instantaneous velocity. The first section of this chapter will provide an overview of the methods implemented in the literature to tackle the abovementioned issues and to justify the choices made for the development of a wearable framework. The former should be as compatible as possible with clinical constraints in order to allow its transfer in the field: setup and acquisition durations should be as short as possible, with a minimal number of sensors, simple calibration procedures and minimal operator implication in the post-processing. In the subsequent sections, the framework will be introduced and validated as a

proof-of-concept in one person with transfemoral amputation against force platforms (BCoM acceleration) and optical motion capture data (BCoM acceleration and velocity).

3.1. State-of-the-art: scientific challenges associated with the use of optimal MIMU networks for BCoM acceleration and velocity estimation

The aim of this section is to provide an overview of the scientific challenges associated with the estimation of BCoM acceleration and instantaneous velocity from a network of connected MIMUs.

In the study presented in the previous chapter, various optimal segment networks allowing an accurate estimation of BCoM acceleration from a set of segment-mounted markers were identified. The suitability of these OSN must be verified when using segment-mounted MIMUs instead of markers. Using equation 5, where N is the number of MIMUs included in the OSN, β_i is the weight associated to the SCoM acceleration estimated with the ith MIMU ($a_{SCoM_i}^G$) in an Earth-fixed global reference frame R_G, the acceleration of the BCoM can be estimated in R_G as follows:

$$a_{BCoM}^G = \sum_{i=1}^N \beta_i \, a_{SCoM_i}^G \quad (5)$$

The acceleration of each SCoM of the segments included in the OSN can be estimated in the MIMU local frame R_{MIMU_i} following equation 6, where all the mechanical quantities are expressed in R_{MIMU_i} (as indicated by the exponent $\boldsymbol{MIMU_i}$):

$$a_{sCoM_i}^{MIMU_i} = a_{oIMU_i}^{MIMU_i} + \Omega_{oIMU_i}^{MIMU_i} \wedge \left(\Omega_{oIMU_i}^{MIMU_i} \wedge r_{oIMU_i-sCoM_i}^{MIMU_i}\right) + \left(\Omega_{oIMU_i}^{\dot{MIMU_i}}\right) \wedge r_{oIMU_i-sCoM_i}^{MIMU_i} \quad (6)$$

with

$\begin{cases} a_{sCoM_i}^{MIMU_i} \text{ is the } i^{th} \text{ SCoM acceleration} \\[4pt] a_{oIMU_i}^{MIMU_i} \text{ is the acceleration measured by the } i^{th} \text{ MIMU rigidly attached to the } i^{th} \text{ segment} \\ \qquad \text{(expressed at the origin of the MIMU local frame)} \\[4pt] \Omega_{oIMU_i}^{MIMU_i} \text{ is the angular velocity measured by the } i^{th} \text{ MIMU rigidly attached to the } i^{th} \text{ segment} \\[4pt] \left(\Omega_{oIMU_i}^{\dot{MIMU_i}}\right) \text{ is the angular acceleration of the } i^{th} \text{ MIMU obtained from differentitation of } \Omega_{oIMU_i}^{MIMU_i} \\[4pt] r_{oIMU_i-sCoM_i}^{MIMU_i} \text{ is the the translation vector from the origin of the } i^{th} \text{MIMU to the underlying} \\ \qquad \text{SCoM in the MIMU local frame} \end{cases}$

In the former equation, all quantities can be retrieved or computed from MIMUs raw signals except for the translation vector from the origin of the MIMU to the underlying SCoM: $r_{oIMU_i-sCoM_i}^{MIMU_i}$. Indeed, MIMUs do not provide information about their absolute position. Therefore, several authors have proposed alternative ways to estimate SCoM acceleration from MIMU signals without using equation 6. The objective of section 3.1.1 is thus to provide an overview of the methods proposed in the literature for the estimation of SCoM accelerations from MIMU signals with a special attention on wearable methods that allow to retrieve MIMUs positions relative to the center of mass of the underlying segment.

Then, in order to estimate BCoM acceleration from the fusion of SCoM accelerations (equation 5), the formers must be expressed in a common global Earth-fixed reference frame (equation 7):

$$a_{SCoM_i}^G = P_{G-MIMU_i} \, a_{SCoM_i}^{MIMU_i} \qquad (7)$$

The relative orientation of each MIMU local frame in this global reference frame P_{G-MIMU_i} must be obtained, which implies to first resolve the inconsistencies between the Earth-fixed reference frames sensed by each MIMU. Section 3.1.2. provides an overview of the literature dealing with the definition of a consistent Earth-fixed reference frame across MIMUs.

Eventually, an overview of the methods proposed in the literature for the computation of BCoM instantaneous velocity from BCoM acceleration will be provided in section 3.1.3.

3.1.1. Estimation of SCoM acceleration from MIMU signals

Several approaches have been retrieved in the literature regarding the estimation of SCoM motion from MIMU signals and are summarized in the following subsections.

a. Approximation of the relative MIMU/SCoM position

The first approach, implemented in two studies, consists in using MIMUs manually positioned at the longitudinal location of the SCoM (as reported in anthropometric tables) and in considering that the acceleration of the segment-mounted MIMUs correspond to the SCoM accelerations (Lintmeijer *et al.*, 2018; Shahabpoor *et al.*, 2018). This approximation is equivalent to writing $\vec{r}_{oIMU_i-sCoM_i} = \vec{0}$ in equation 6, which necessary yields to errors since the SCoM lies inside the segment and the MIMU on the skin surface. The impact of this approximation has never been investigated on the estimated SCoM accelerations or velocities.

b. Kinematic chain approach

Several authors have associated a kinematic chain model to an inertial model in order to recover SCoM positions in a global Earth-fixed frame from MIMUs measurements. This approach does not require to obtain the relative positions between each pair of MIMU and SCoM but requires computing the relative orientation between each segment anatomical frame and its respective MIMU local frame (sensor-to-segment calibration). Indeed, the kinematic chain approach (**Figure 28**) consists in representing the segments as rigid bodies connected by joints and at successively computing the trajectory of each joint $J_{i,i+1}$ linking the segments S_i and $S_{i+1} (r_{J_{i,i+1}}^G)$ from the known trajectory of the previous joint center of rotation $J_{i-1,i}$ ($r_{J_{i-1,i}}^G$), the known orientation of the segment S_i (P_{G-S_i}), and the dimensions of the segment S_i (given by the vector linking the successive joints $J_{i-1,i}$ and $J_{i,i+1}$ in the segment anatomical frame: $r_{J_{i-1,i}-J_{i,i+1}}^{S_i}$):
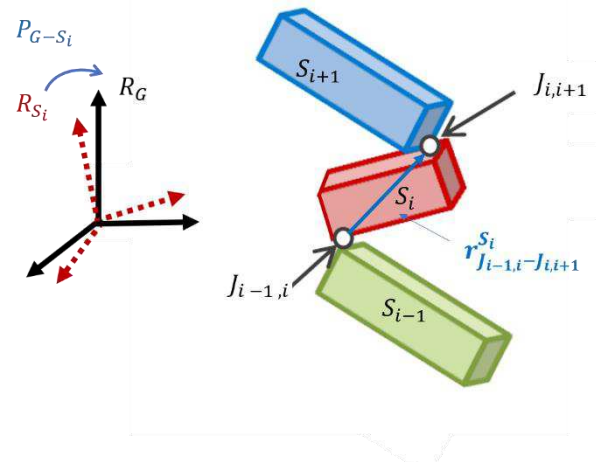
Figure 28: Kinematic chain approach. Example of a 3-segment chain. Segment S_i is linked with segments S_{i-1} and S_{i+1} at the joints $J_{i-1,i}$ and $J_{i,i+1}$ respectively. S_i segment orientation in the global reference frame R_G is given by the transformation matrix P_{G-S_i}.

$$r^G_{J_{i,i+1}} = r^G_{J_{i-1,i}} + P_{G-S_i} \times r^{S_i}_{J_{i-1,i}-J_{i,i+1}} \quad (8)$$

The rigid body assumption allows to derive the trajectory of any point pertaining to any segment of the kinematic chain, and hence, to any SCoM, using equation 9, provided that its position relative to one of the joints ($r^{S_i}_{J_{i-1,i}-SCoM_i}$) is known in the segment anatomical frame (which is possible using anthropometric tables such as (Dumas *et al.*, 2007).

$$r^G_{SCoM_i} = r^G_{J_{i-1,i}} + P_{G-S_i} \times r^{S_i}_{J_{i-1,i}-SCoM_i} \quad (9)$$

Therefore, provided that the sensor-to-segment calibration gives an accurate estimate of the relative orientation of the segment anatomical frame in the MIMU local frame ($P_{MIMU_i-S_i}$), the orientation of the MIMU local frame in the global Earth-fixed reference frame can be used (P_{G-MIMU_i}) to estimate the SCoM trajectory in the global frame:

$$r^G_{SCoM_i} = r^G_{J_{i-1,i}} + P_{G-MIMU_i} \times P_{MIMU_i-S_i} \times r^{S_i}_{J_{i-1,i}-SCoM_i} \quad (10)$$

In (Fasel, Spörri, *et al.*, 2017), a full-body MIMU set was used to estimate the BCoM displacement while skiing. A kinematic chain was designed, taking the orientation of MIMUs to derive segment orientations and using segments dimensions from anthropometric tables, scaled to the participants body height. This step allowed to estimate the position of each joint center of rotation relative to the root point of the kinematic chain (in this case, the lumbar joint center) in a global frame. Using an inertial model derived from anthropometric tables, the position of the center of mass of each segment was estimated in its respective segment anatomical frame. Then, using the rigid body assumption, SCoM positions were finally deduced in the global frame. Finally, a weighted average of SCoM positions at each timestamp was computed to estimate the BCoM trajectory in the global frame. All in all, the association of a 7-segment kinematic chain and an inertial model allowed to estimate the BCoM displacement relative to the lumbar joint center with good accuracy and precision (< 11.2 mm for each axis) without requiring the knowledge of MIMU positions relative to their respective underlying SCoM (Fasel, Spörri, *et al.*, 2017). However, the method requires the use of MIMUs on all the body segments pertaining to the kinematic chain, compromising the development of models with a limited number of sensors while this was shown to be paramount for clinical applications. Furthermore, the accuracy of kinematic chain outputs is highly dependent on an accurate sensor-to-segment calibration. Indeed, pose estimation derived from kinematic chains was shown to be highly sensitive to MIMU orientation on the underlying segment (Kianifar *et al.*, 2019).

The 17-MIMU MVN suit developed by Xsens uses proprietary kinematic and inertial models that seem similar to those described above (Schepers *et al.*, 2018). Indeed, a static posture calibration associated with anthropometric measurements allows to define a kinematic chain for the estimation of joint angles and segment orientations. A proportional inertial model then allows to recover SCoM positions in the segment anatomical frames and thus to compute BCoM trajectory in a global reference Earth-fixed frame (Karatsidis *et al.*, 2017; Pavei *et al.*, 2020). Validity of SCoM accelerations issued from the MVN framework were not reported in the literature, but the BCoM trajectory was shown to be affected by large errors (3D root mean square error of 17 ± 5 mm, overestimation of the anteroposterior amplitude by 89 ± 47 %) which were assumed to result from signal drift, magnetic perturbations or biomechanical models inaccuracies (Pavei *et al.*, 2020).

c. Approaches implemented for the retrieval of MIMU absolute positions

Several authors have developed approaches to retrieve the absolute positions of MIMUs in a global Earth-fixed frame for the estimation of joint angles, either to predict acceleration and angular velocity signals and fuse them with the measured ones for drift and noise correction (Kianifar *et al.*, 2019) or to reconstruct segment pose using a redundant formulation and an optimization procedure (Miezal *et al.*, 2016; Teufl *et al.*, 2018, 2019). These approaches could be adapted in order to retrieve both MIMU and SCoM positions and therefore, compute the relative MIMU and SCoM position in the global Earth-fixed frame.

In order to initialize MIMUs position in the global Earth-fixed reference frame, Teufl and coworkers used marker position data acquired during a static posture with optical motion capture system (Teufl *et al.*, 2019). Similarly, Dejnabadi and coworkers took photographs of participants equipped with MIMUs while ensuring that the camera field of view was aligned with the body sagittal plane. This allowed to *a posteriori* estimate MIMUs' positions and orientations relative to the underlying body segments (Dejnabadi *et al.*, 2006). In both studies, the aim of the authors was to recover MIMUs' positions in a global Earth-fixed reference frame which required the use of an external device. It is interesting to note that the external device was only needed for the initialization of MIMUs positions and orientations. Such procedures could be adapted in order to obtain for MIMUs and SCoM positions in a common reference frame ($r^G_{oIMU_i-sCoM_i}$), as well as MIMUs orientation in the global frame (P_{G-MIMU_i}). The relative position of the SCoM in the MIMU local frame could then be computed ($r^{MIMU_i}_{oIMU_i-sCoM_i} = P^{-1}_{G-MIMU_i} \times r^G_{oIMU_i-sCoM_i}$), allowing to estimate the acceleration of the SCoM in the MIMU local frame using equation 6. It has to be noted that SCoM positions are defined in their own segment anatomical frames. Thus, to derive SCoM positions in a common global frame, either segment orientation in the same global frame as that sensed by MIMUs or MIMU-to-segment calibration must be computed.

d. Synthesis of the literature

From this overview of the literature, it seems that no study has estimated the acceleration of a SCoM from a segment-mounted MIMU by using the rigid body assumption and the distribution of accelerations (equation 6). Indeed, retrieving the relative position of MIMU and SCoM does not seem trivial and seems to require the use of external devices, such as optoelectronic motion capture systems or photographs. Therefore, some authors have assumed that the MIMUs directly lie at the SCoM.

An alternative approach allows to estimate SCoM accelerations without having to obtain MIMUs and SCoM relative positions. However, it requires to model human gait with a kinematic chain. This not only imposes to use MIMUs positioned on each segment of the kinematic chain but also to perform accurate sensor-to-segment calibration in order to retrieve the orientation of the segments' anatomical frames in the global reference frame.

3.1.2. Definition of a consistent global frame across MIMUs
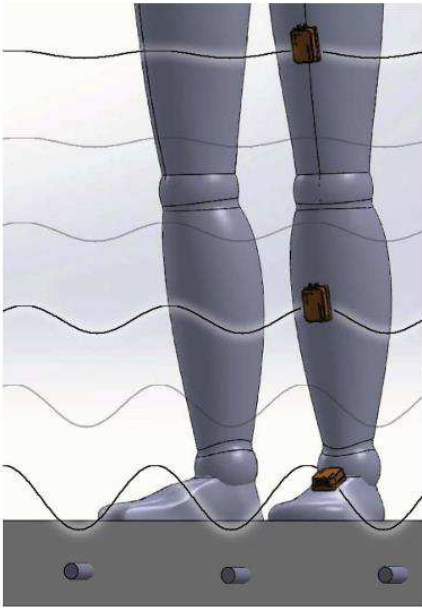
Figure 29: Magnetic field distortions due to construction materials within buildings. Taken from (**Lebel** et al. 2018)

When estimating the BCoM acceleration from a weighted sum of MIMU-based SCoM accelerations, it is crucial to ensure that all SCoM accelerations are expressed in a consistent global Earth-fixed reference frame prior to performing data fusion. Theoretically, angular velocity, linear acceleration and magnetic field sensed by a MIMU can be fused to obtain MIMU orientation in a Earth-fixed global reference frame (Madgwick *et al.*, 2011; Sabatini, 2011; Bergamini *et al.*, 2014) (refer to section 3.1.1 in Part 1). Magnetic perturbations, which may arise from objects in the acquisition environment (Picerno *et al.*, 2011; Sabatini, 2011), from prosthetic components (Garofalo, 2010) and from construction materials within buildings (Picerno *et al.*, 2011; Sabatini, 2011; Lebel *et al.*, 2018), have been shown to inconsistently affect the reference frame sensed by each MIMU (Picerno *et al.*, 2011; Lebel *et al.*, 2018). For instance, MIMUs that are the farthest from the ground were shown to be the less affected by magnetic perturbations in indoor environments (Miezal *et al.*, 2016; Lebel *et al.*, 2018) (see **Figure 29**) . As a consequence of magnetic field distortion, several MIMUs may point to different "magnetic North", and thus, may sense different Earth-fixed reference frames (Picerno *et al.*, 2011; Lebel *et al.*, 2018; Guaitolini *et al.*, 2019) (**Figure 30**). Although a large body of literature has focused on
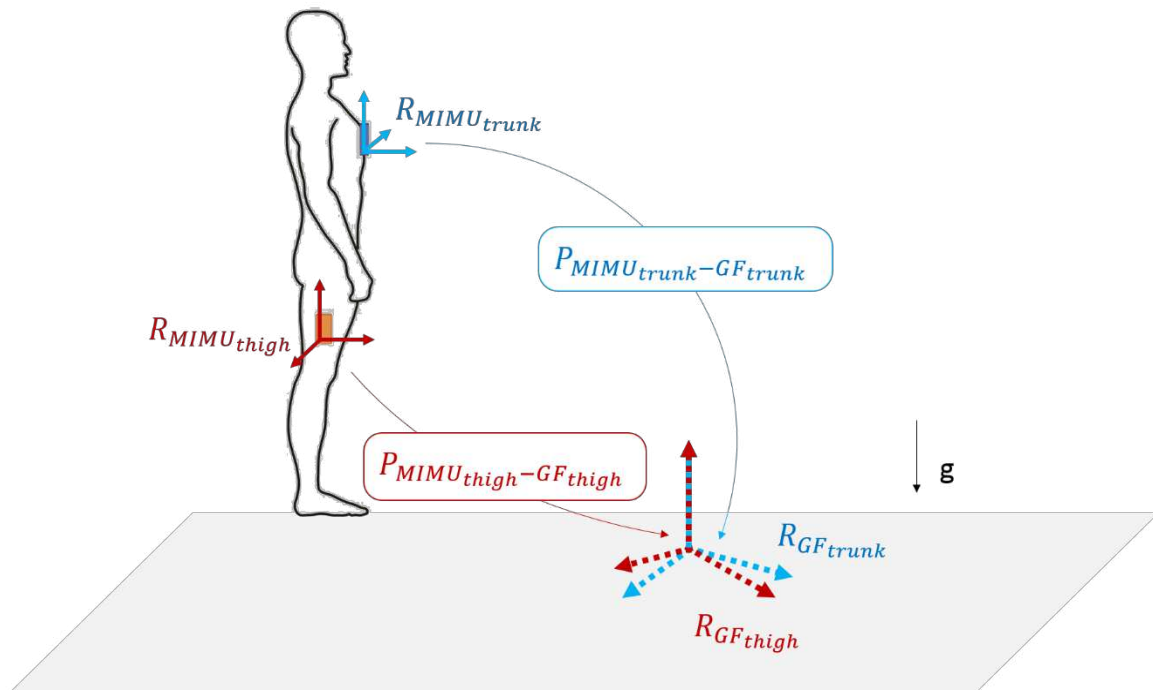
Figure 30: Inconsistencies of the Earth-fixed global frames sensed by two MIMUs – Example for MIMUs located on the thigh and trunk.
R_{MIMU_i} is the MIMU local frame, $P_{MIMU_i-GF_i}$ the transformation matrix from the MIMU local frame to the global reference frame R_{GF_i} sensed by the MIMU ($i = trunk, thigh$)

78

the development/comparison and validation of orientation filters (Sabatini, 2011; Bergamini *et al.*, 2014; Caruso *et al.*, 2019), very few studies investigated the (in)consistency of the reference frames sensed by several MIMUs.

a. Correction of MIMU-sensed Earth-fixed reference frame inconsistencies using an external device

Several authors have shown that correcting for the global frame inconsistency between MIMUs at the beginning of a trial may allow to decrease the errors in joint accuracy estimation during the whole trial (Palermo *et al.*, 2014; Lebel *et al.*, 2015, 2018). This correction was performed either with an optical motion capture system or using photographs but required in any case the use of an external device.

Increased accuracy in joint angle estimation was observed when using an optical motion capture system to determine the initial orientation of MIMUs in a common consistent global frame (Palermo *et al.*, 2014) or to *a posteriori* correct initial orientation errors (Lebel *et al.*, 2015). Similarly, when validating a MIMU-based algorithm, some authors have preferred to use orientation outputs from an optical motion capture system so as to isolate the errors due to inconsistencies in the Earth-fixed reference frames sensed by different MIMUs from those inherent to the model/algorithm (Teufl *et al.*, 2018; Guaitolini *et al.*, 2019). However, these corrections impose to use an optical motion capture system, which compromises the transfer of the method in the field due to high system cost and limited portability.

In (Lebel *et al.*, 2018), the initial relative orientation of two segment-mounted MIMUs is derived from a camera pose estimation algorithm which compares the dotted pattern on MIMU-fitting boxes from a photograph taken while standing in a static posture. Then, this initial relative orientation is used to correct for both MIMUs their orientation computed with proprietary algorithm outputs. Although this method also imposes the use of an external system and is incompatible with real-time processing, it was shown to significantly increase the accuracy in MIMU-based ankle angle estimation (error decreased from 6.7° to 2.4° for all planes of motion) and to drastically reduce the effect of magnetic perturbations occurring in the starting environment (maximum difference explained by the starting environment remained statistically significant but decreased from 8° to 0.6°) (Lebel *et al.*, 2018). Furthermore, taking a photograph is not as cumbersome and constraining as capturing a full body static acquisition with an optical motion capture system.

b. Correction of MIMU-sensed Earth-fixed reference frame inconsistencies using hypotheses relative to segment orientations in the global Earth-fixed reference frame

In a recent study, a magnetometer-free approach was proposed to estimate joint angles from IMUs (Ligorio *et al.*, 2020). First, participants are asked to stand in a static posture (the N-pose), in which the segments orientations are assumed to be known in a global Earth-fixed reference frame (longitudinal axes of the segment anatomical frames aligned with the vertical direction). Sensor-to segment calibration is performed in two steps. First, using the accelerometers readings in the N-pose allows to retrieve the longitudinal axis of all segments' anatomical frames in the MIMU local frame during the static posture. Then, functional motion allows to retrieve the mediolateral functional axis of all segments in the MIMU local frame. Using the triad algorithm, segments orientations in the MIMU local frame is computed. Using the N-pose configuration, MIMU orientation can be deduced in the global

79

reference frame which therefore allows to correct the inconsistencies between the Earth-fixed reference frames sensed by the segment-mounted MIMUs. While the algorithm displayed similar tilt errors than a MIMU-based Kalman filter compared to an optical motion capture system, higher errors were achieved for the estimation of the heading (6.8 degrees against 4.6 degrees).

c.   Synthesis of the literature

Two approaches have been proposed in the literature to compute segment orientation from MIMUs in a consistent global frame. One approach relies on external devices to compute the relative orientation between the MIMU-sensed Earth-fixed reference frame R_{GF} and a global Earth-fixed reference frame R_G using an external device (photographs, optical motion capture). The alternative approach, presented in a recent study, relies on assumptions regarding the position of body segments in the global Earth-fixed reference frame R_G at a given instant and uses the sensor-to-segment calibration to deduce the MIMU or segment orientation at all instants in R_G.

3.1.3.   Computation of the instantaneous velocity of the BCoM from MIMUs

The third issue when dealing with MIMUs is the drift resulting from integration of noisy signals. If the actual velocity is known at certain instants t_n, the drift can be compensated for *a posteriori*: the computed velocity is compared to the known velocity and the difference is used for the correction of the velocity between t_{n-1} and t_n. Generally, a linear drift function is defined (Hannink *et al.*, 2017). Taking advantage of the cyclical nature of gait, the instantaneous velocity of the BCoM can be computed for each stride and further decomposed into two components: an average component in the direction of progression ("average walking speed") and a 3D cyclical component with null mean velocity.

a.   3D cyclical component of the BCoM velocity

The cyclical component of the instantaneous velocity of the BCoM is generally estimated from numerical integration of the lower-back acceleration, followed by a high-pass filter (Pfau *et al.*, 2005; Meichtry *et al.*, 2007; Köse *et al.*, 2012). More recently, an analytical integration method, based on the Fourier series decomposition of the pelvis acceleration signal, was shown to yield promising results with limits of agreement < 0.10 m/s as compared with optical motion capture (Sabatini *et al.*, 2015; Sabatini and Mannini, 2016). These integration methods were validated for the estimation of lower-back velocity in asymptomatic subjects and remain to be tested for the integration of BCoM acceleration in people with lower-limb amputation.

b.   Average BCoM velocity

Regarding the average BCoM velocity, or walking speed, three methods have been described in the literature for its estimation from MIMUs: abstraction models, human gait models, and direct integration of linear acceleration (Yang and Li, 2012b).

Abstraction models consist in machine learning frameworks: a relationship is learnt between MIMU signals and a reference walking speed, without support of a biomechanical model. This type of methods allows to estimate the average walking speed from raw MIMU data without introducing error from signal integration. For instance, using the angular velocity and acceleration signals from shank MIMUs, average root mean square errors below 5 % were achieved for the average walking speed

(speed ≥ 4 km/h) when walking on treadmill or overground (Sabatini and Mannini, 2016). Higher errors were obtained at slower walking speeds (9 % at 3 km/h). Although no such study was found in the literature, machine learning frameworks could be designed to estimate the instantaneous velocity of the BCoM. In (Betker *et al.*, 2006), the authors developed an abstraction model for the estimation of BCoM trajectory from trunk and shank accelerations in quasi-static conditions (body sway). While encouraging results were achieved, the method was not transposed to gait nor to instantaneous velocity computation.

Contrary to abstraction models, human gait models and direct integration methods aim at estimating the average walking speed through the ratio of stride length by stride duration.

In general, human gait models use inverted pendulum for gait representation and estimate the average walking speed (for more details, see Part 1, section 3.2.1. or refer to (Yang and Li, 2012b)). One such model, developed and validated in seven people with transfemoral amputation, achieved relative errors within +/- 15 % (Miyazaki, 1997). Recently, Dauriac and coworkers have proposed a kinematic model specific to people with transfemoral amputation for the estimation of the average walking speed from a single MIMU on the prosthetic shank (Dauriac *et al.*, 2019). The model takes advantage of the absence of knee flexion during early stance of people with transfemoral amputation to represent the prosthetic lower limb as a single rigid body. Furthermore, the model assumes that the BCoM velocity is the same as the one of the residual hip center of rotation. Combining an inverted pendulum representation and roll-over-shapes characteristics of the foot-shank complex (**Figure 31**), the sagittal plane instantaneous walking speed of the body center of mass is estimated during the first half of the cycle. Averaging the anteroposterior component over the first half of the gait cycle, the average walking speed is estimated with a root mean square error of 0.09 m/s (9%).

Lastly, the average walking speed has been estimated through direct double integration of the linear acceleration of the foot (Mariani *et al.*, 2010; Kitagawa and Ogihara, 2016) or shank (Li *et al.*, 2010; Yang and Li, 2012a) in the direction of progression, using the zero-velocity update paradigm
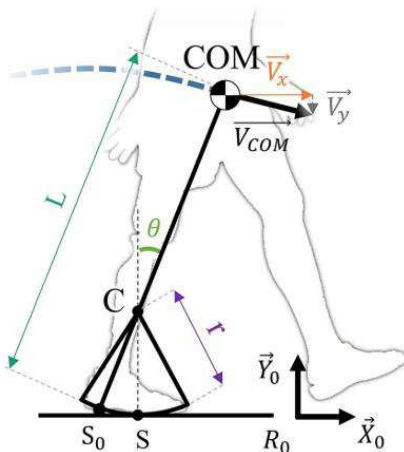
Figure 31: Kinematic model for body center of mass (CoM) velocity estimation in people with transfemoral amputation. C, r are the characteristics of the roll over shape, S is the contact point of the foot with the ground (S_0 when the shank is vertical), θ is the shank angle, and L the CoM height. V_x and V_y are the projections of the CoM velocity (V_{CoM}) in the global frame R_0. From (Dauriac *et al.*, 2019)
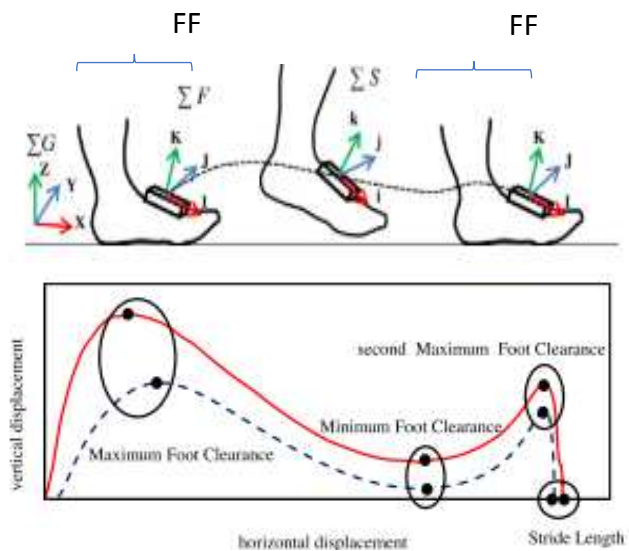
Figure 32: Double integration of linear acceleration of the foot in the direction of progression between two successive foot flat (FF) events. Adapted from (Kitagawa and Ogihara, 2016)

81

(**Figure 32**). Taking advantage of the null velocity of the foot at mid-stance (detected through the foot-flat event or shank-vertical event depending on MIMU position), the acceleration is double integrated between two detected events and drift can be compensated for after the first integration. The average walking speed is then computed as the distance covered between two detected events, divided by the duration between those two events. Using foot-mounted MIMUs, Mariani and coworkers reported stride velocity values within 1.5 ± 5.8 % of stride velocity in the asymptomatic population (Mariani *et al.*, 2010). Yang and Li estimated the walking speed from shank mounted MIMUs with an average root mean square error of 4.2 % in people walking on a treadmill (Yang and Li, 2012a).

c. Instantaneous velocity of an anatomical point

A kinematic model recently developed by Duraffourg and coworkers allows to estimate the instantaneous velocity and the trajectory of the knee joint from a shank mounted MIMU in people with transfemoral amputation ambulating overground (Duraffourg *et al.*, 2019). The method could be adapted for the estimation of walking speed from the distance covered by the shank within a stride. Stride length was found to be underestimated by 5.1 % of its nominal value in 3 people with transfemoral amputation. The method consists in estimating the knee joint velocity from the foot roll-over-shape characteristics while in unipodal stance, similarly as in (Dauriac *et al.*, 2019), and at double integrating the knee joint acceleration derived from the acceleration measured by the shank-mounted MIMU (using rigid body assumption) during the swing phase (**Figure 33**).

Figure 33: Knee joint center (K) trajectory estimation from a shank mounted MIMU (positioned at I) using the roll over shape paradigm (C representing the center of the foot roll-over-shape). Taken from (Duraffourg *et al.*, 2019)

It is worth noting that the instantaneous walking speed of the BCoM in an Earth-fixed global frame (both the average and the cyclical components) could also be estimated directly from kinematic chain gait models, with the assumption that the BCoM lies within the pelvis (Yuan and I. M. Chen, 2014). However, such kinematic chain models do not include the trunk, and impose to use MIMUs on all the segments pertaining to the kinematic chain. Such a model would therefore not be compatible with the selected OSN (see Chapter 2, Part 2) and was not investigated.

d. Synthesis of the literature

Table 5 below summarizes the results achieved in the literature for the estimation of the average walking speed and instantaneous BCoM velocity. The studies that only indicated results regarding the accuracy of stride length estimation are not reported.

Authors	Population	Sensors	Method	Results	Reference for the average walking speed
(Aminian et al., 2002)	20 AS	4 gyroscopes (both thighs and shanks)	Kinematic model (average walking speed)	RMSE = 0.06 m/s (6.7 %)	Stopwatch (time to cover 20 m)
(Dauriac et al., 2019)	9 TF	1 shank-mounted IMU	Kinematic model (average walking speed)	RMSE = 0.09 m/s (9 %)	Treadmill speed
(Mariani et al., 2010)	20 AS	2 feet mounted IMUs	Double integration (average walking speed)	Average error = 0.014 ± 0.056 m/s (1.5 ± 5.8 %)	Optical motion capture system (feet markers)
(Miyazaki, 1997)	7 TF	1 thigh-mounted gyroscope	Kinematic model (average walking speed)	RMSE +/- 15 %	Stopwatch (time to cover 40 m)
(Sabatini and Mannini, 2016)	17 AS	1 pelvis-mounted MIMU	Double integration (cyclical component) + abstraction model (average walking speed)	LoA of cyclical component (± 1.96 std) overground walking: - ML = ± 0.10 m/s - AP = ± 0.05 m/s - CC = ± 0.10 m/s RMS error of average velocity : 0.06 m/s (0.07 m/s) (Average RMSE about 5% above 4km/h)	Treadmill speed
(Sabatini et al., 2005)	5 AS	1 foot-mounted IMU	Double integration (average walking speed)	RMSE = 0.05 m/s	Treadmill speed
(Yang and Li, 2012a)	7 AS	1 shank-mounted IMU	Double integration (average walking speed)	RMSE = 4.2 %	Treadmill speed

Table 5: Synthesis of the methods for BCoM instantaneous velocity and average walking speed estimation in the literature. *TF = people with transfemoral amputation, AS = Asymptomatic participants; RMSE = root mean square error; AP = Anteroposterior; ML = mediolateral; CC = craniocaudal; LoA = Limits of agreement*

3.1.4. *Towards the implementation of an OSN-based framework for the estimation of BCoM acceleration and velocity: how to tackle the challenges associated with MIMUs*

The aim of this section is to introduce the choices made for the implementation of a fully wearable protocol for the estimation of 3D BCoM acceleration and velocity, based on the state-of-the-art (sections 3.1.1 to 3.1.3).

The first step requires to estimate the acceleration of SCoM from MIMUs mounted on selected body segments. From the literature (see section 3.1.1), it appears that, for each segment, the translation vector from the origin of the MIMU to the SCoM in the MIMU local frame ($r_{oIMU_i-sCoM_i}$) could be first obtained in an Earth-fixed reference frame during a static calibration using an external device such as a photo camera (Dejnabadi *et al.*, 2006) or an optical motion capture system (Teufl *et al.*, 2018; Guaitolini *et al.*, 2019). The obtained translation vector could then be computed in the MIMU local reference frame using the MIMU orientation in the same global Earth-fixed reference frame R_G as the one in which the relative positions are known (**Figure 34**). The advantage of the method is that it does not require to obtain an accurate sensor-to-segment calibration, and therefore, does not rely on an accurate sensor positioning nor on the need to perform calibration motions which might be too demanding for people with gait impairment or untrained users.

83
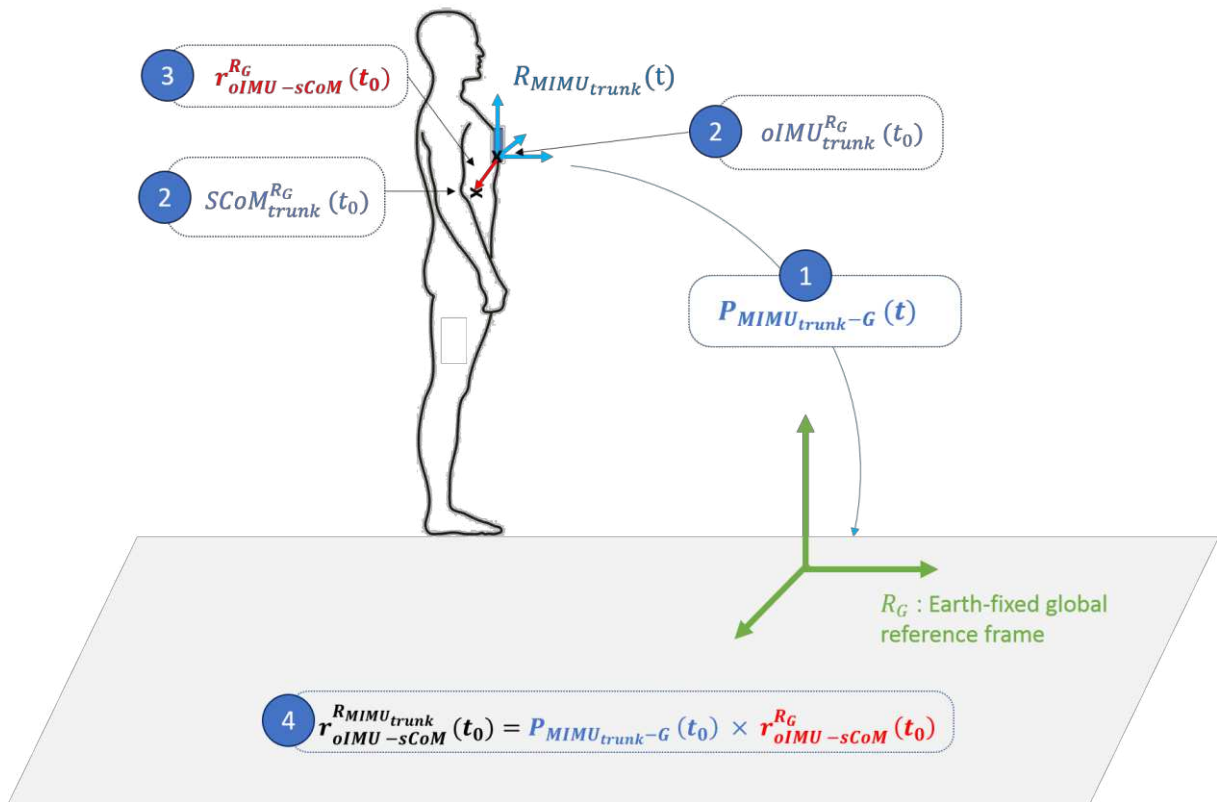
Figure 34: Retrieval of the relative position of segment center of mass (SCoM) and the segment-mounted MIMU in the MIMU local frame - example for the trunk MIMU.

1 – MIMU orientation in the Earth-fixed global reference frame R_G is known (transformation matrix $P_{MIMU_{trunk}-G}$)

2 – The positions of the SCoM and of the origin of the MIMU (o_{IMU}) are known in R_G at t_0, during the static calibration thanks to an external device (calibrated photographs, optical motion capture)

3 – The relative position of the MIMU and the underlying SCoM is deduced in R_G at t_0: $r^{R_g}_{oIMU_{trunk}-SCoM_{trunk}}$

4 – Using the knowledge of MIMU orientation in R_G, the relative position of the MIMU and the underlying SCoM is computed in the MIMU local frame $R_{MIMU_{trunk}}$ at t_0 : $r^{R_g}_{oIMU_{trunk}-SCoM_{trunk}}(t_0)$. With the rigid body assumption, this vector is constant and $r^{R_g}_{oIMU_{trunk}-SCoM_{trunk}}(t)$ is known for all timestamps t

In (Choe *et al.*, 2019), the authors propose to perform a static posture sensor-to-segment calibration while the participants are facing the magnetic North direction, as indicated by a compass, in order to ensure that the segments orientations are known in the same Earth-fixed reference frame as the one sensed by MIMUs. This implies that the formers consistently sense the magnetic North direction. However, such ideal conditions are not often encountered, especially indoors (Picerno *et al.*, 2011; Lebel *et al.*, 2018). Indeed, the Earth-fixed reference frames sensed by several MIMUs are generally different (Guaitolini *et al.*, 2019) (see also **Figure 30**), which results in errors when fusing data from several MIMUs (Lebel *et al.*, 2018). As reported in the literature (see section 3.1.2), *a posteriori* correction of inter-MIMU inconsistency using the static part at the beginning of data acquisition allows to significantly reduce the influence of magnetic perturbations on the output biomechanical parameters all along the acquisition. Therefore, identifying a common global Earth-fixed reference frame R_G in which the orientation of each MIMU local frame R_{MIMU_i} can be assumed to be known at a specific instant t_0, and then computing the relative orientation of the Earth-fixed reference frames R_{GF} sensed by each MIMU in this consistent common global Earth-fixed reference frame (P_{GF_i-G}) at

the same instant represents an interesting solution. The transformation matrices P_{GF_i-G} being constant (as they describe the relative orientation of a pair of Earth-fixed reference frames) (Lebel *et al.*, 2018), this allows to compute the orientation of each MIMU local frame R_{MIMU_i} in R_G at all time (**Figure 35**). Finally, using the transformation matrix from R_G to R_{MIMU_i}, the relative position of each MIMU and its underlying SCoM is known in the MIMU local frame, which subsequently allows to estimate the SCoM acceleration in the MIMU local frame using equation (6). Then, using the transformation matrix from R_{MIMU_i} to R_G allows to express each SCoM acceleration in a consistent global reference frame to finally estimate the BCoM acceleration from an OSN (equation 5).
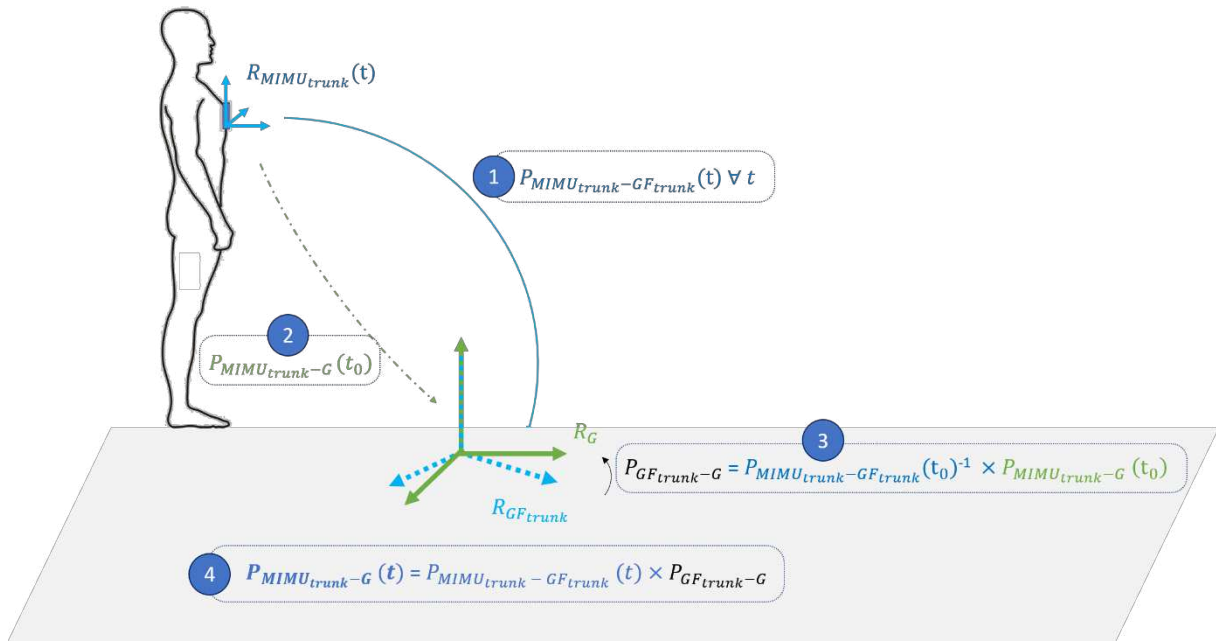
Figure 35: Computation of the orientation of a MIMU local frame in a global Earth fixed reference frame, using a static calibration - example for the trunk MIMU

1 – Known orientation of MIMU local frame $R_{MIMU_{trunk}}$ in its associated Earth-fixed reference frame $R_{GF_{trunk}}$ at all instants t of the acquisition (transformation matrix $P_{MIMU_{trunk}-GF_{trunk}}$ obtained from sensor fusion)

2 – In a predefined static posture taken at t_0, the orientation of the MIMU local frame in the Earth-fixed global frame R_G can be assumed to be known ($P_{MIMU_{trunk}-G}(t_0)$)

3 – The constant relative orientation $P_{GF_{trunk}-G}$ between the MIMU-sensed Earth fixed reference frame $R_{GF_{trunk}}$ and the Earth-fixed global frame R_G is computed using the knowledge of $P_{MIMU_{trunk}-G}$ and $P_{MIMU_{trunk}-GF_{trunk}}$ at $t = t_0$

4 – Using (1) and (3), the orientation of the MIMU local frame in the global Earth-fixed reference frame R_G can be computed at all timestamps t of the acquisition

Once the BCoM acceleration has been computed in an Earth-fixed global reference frame, the instantaneous BCoM velocity can be estimated from a combination of direct integration of the BCoM acceleration (cyclical component) and a kinematic model of the shank (average component).

In the next section, the framework development and implementation will be presented in detail.

3.2. Material and Methods

3.2.1. Framework overview

The development of the framework can be divided in three steps aiming at:

a)   computing the 3D acceleration of each segment's center of mass (SCoM) from MIMUs data,

b)   merging SCoM accelerations in a consistent common global frame R_G, and

c)   estimating the 3D BCoM acceleration and velocity from a weighted average of selected SCoM accelerations.

From chapter 2, the trunk, thighs, shanks and feet were identified as the major contributors in 3D BCoM acceleration in people with transfemoral amputation and several promising OSN were identified for the estimation of BCoM acceleration from the acceleration of these segments. Therefore, 7 MIMUs, manually aligned with the longitudinal axes of the segments, are adopted.

a. Computing 3D SCoM acceleration

Following Pillet et al. (2010), a 15-segment subject-specific inertial model, personalized using calibrated photographs in a static posture, is used to obtain the SCoM positions in an optical motion capture system (OMCS) reference frame R_{OMCS}. For each MIMU, the position of its origin is manually identified on the photographs, which allows to compute its relative position with respect to the underlying SCoM ($r_{oIMU_i-sCoM_i}$) in R_{OMCS}.

Multiple synchronized MIMUs may be inconsistently affected by sustained distortions of the magnetic field (Picerno *et al.*, 2011; Picerno, 2017; Lebel *et al.*, 2018), leading to MIMUs sensing a different direction of the Magnetic North. Therefore, although the vertical axis/attitude of the reference global frames R_{GF_i} sensed by each MIMU coincides with that of the OMCS, the heading is inconsistent across MIMUs and differs to that of the OMCS. Therefore, the orientation output provided by each MIMU $P_{GF_i-MIMU_i}$ cannot be directly used to estimate the transformation matrix $P_{OMCS-MIMU_i}$ from R_{MIMU_i} to R_{OMCS} in static. Instead, knowledge of MIMUs alignment on the underlying segments and hypotheses on the orientation of segments during the initial static posture are used. Indeed, the static posture in which the participant is being photographed has been defined such that he is standing facing the direction of progression. As a first approximation, it is assumed that, in this position, the axes of the segment local frames are aligned with the axes of R_{OMCS}, and thus, that, for each MIMU, the axes of the local frame (R_{MIMU_i}) are aligned with those of R_{OMCS} in static. A first approximation of $P_{OMCS-MIMU_i}$ can therefore be derived. This approximation is then corrected for each MIMU using the attitude output issued by the MIMU and ensuring that an orthonormal reference frame is built. **Figure 36** details this procedure for the MIMU positioned on the trunk.

In the end, this allows to express the vector $r_{IMU_i-sCoM_i}$ in R_{MIMU_i}, and to compute SCoM accelerations in their respective sensor frame as follows:

$$a_{sCoM_i} = a_{oIMU_i} + \Omega_{IMU_i} \wedge \left(\Omega_{IMU_i} \wedge r_{IMU_i-sCoM_i}\right) + \dot{\Omega}_{IMU_i} \wedge r_{IMU_i-sCoM_i}$$

where a_{oIMU_i} and Ω_{IMU_i} are respectively the acceleration and the angular velocity measured by the MIMU$_i$ in the sensor frame R_{MIMU_i} and $\dot{\Omega}_{IMU_i}$ is obtained using a 5-point stencil differentiation.
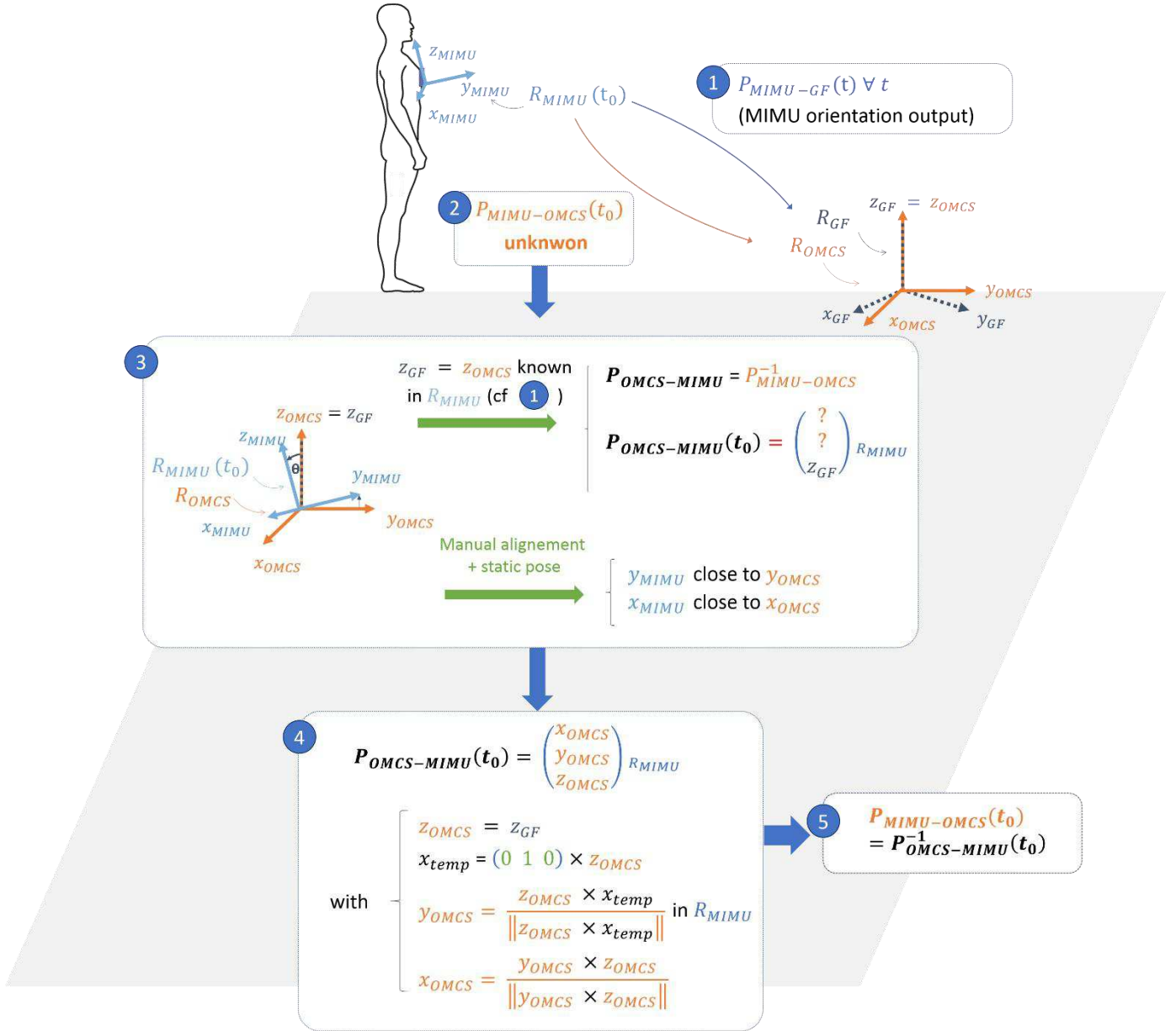
Figure 36: Approximation of the orientation of a MIMU local frame in the optical motion capture system (OMCS) global reference frame during the initial static posture at $t = t_0$ – Example for the trunk MIMU.

- $P_{MIMU-GF}$ is retrieved from the orientation output of the MIMU at $t = t_0$ (1)
- $P_{MIMU-OMCS}$ is unknown at $t = t_0$ (2) but it might be approximated using (3):
  Using the orientation output of the MIMU, the vertical direction z_{GF} of the MIMU-sensed Earth-fixed frame is known in R_{MIMU}. Furthermore, since MIMUs attitude is not affected by magnetic perturbations, the vertical direction detection by MIMUs is robust and is consistent with that of the OMCS global frame R_{OMCS}. Therefore, $z_{GF} = z_{OMCS}$ in R_{MIMU}. Furthermore, the manual alignment of the MIMU on body segments and the static posture taken by the participant ensures that the x and y axes of the MIMU local frame are close to that of the OMCS. This allows to use the cross-product to compute the x and y axes of the OMCS in R_{MIMU} (4).
- Lastly, $P_{MIMU-OMCS}$ is obtained at $t = t_0$ as the inverse of $P_{OMCS-MIMU}$ (5)

b. Merging SCoM accelerations in a consistent common global frame

Since MIMUs sense inconsistent Earth-fixed reference frames (R_{GF_i}), a common global reference frame R_G must be defined consistently for each MIMU. The reference frame sensed by the trunk MIMU $R_{GF_{trunk}}$, rotated so that one axis is coincident with the direction of progression, is chosen as

the common global reference frame ($R_G = R_z(\theta) \times R_{GF_{trunk}}$, see **Figure 37**). This arbitrary choice is supported by the fact that all the best performing OSN models identified in Chapter 2 include a sensor at the trunk. Furthermore, the trunk MIMU is less susceptible to magnetic perturbations than the other MIMUs, as it lies farther from the ground (Lebel *et al.*, 2018) and it endures low height variation while walking (Miezal *et al.*, 2016). Lastly, the direction of progression can be inferred from the orientation output of the trunk MIMU since it is positioned such that its z-axis is oriented towards the direction of
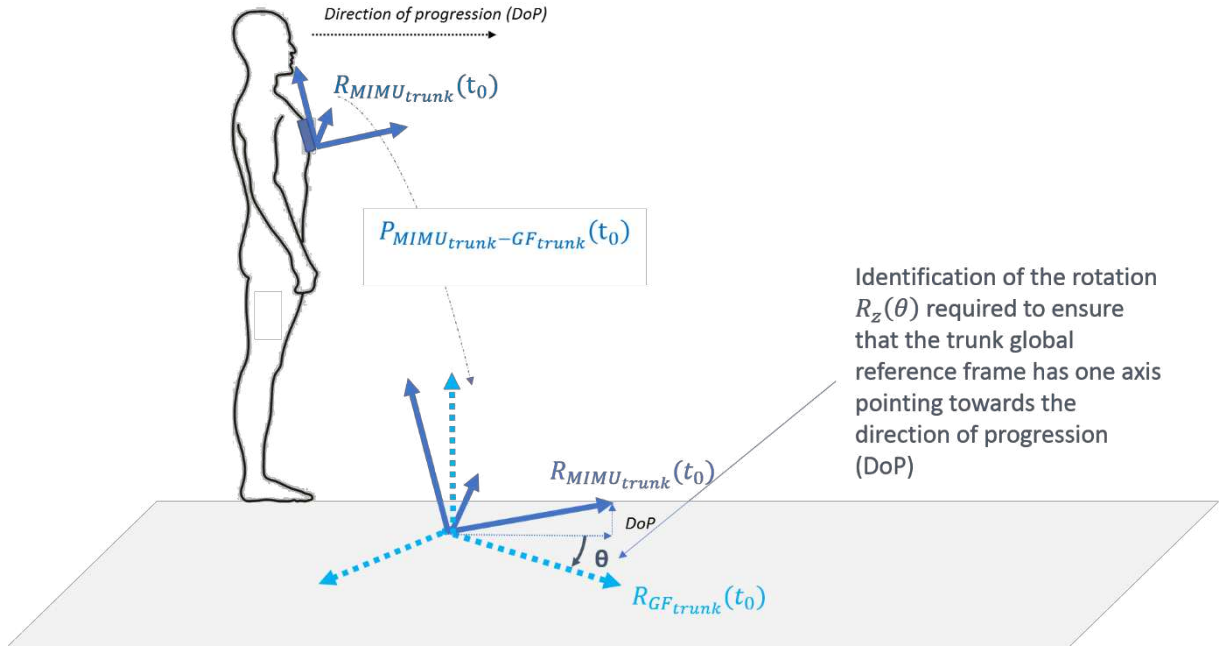
Figure 37: Rotation $R_z(\theta)$ of the trunk-MIMU sensed Earth-fixed frame ($R_{GF_{trunk}}$) to align one of its axis with the direction of progression, using the orientation of the trunk MIMU local frame ($R_{MIMU_{trunk}}$)

progression.

For each MIMU$_i$, the constant transformation matrix P_{G-GF_i} between the MIMU's sensed reference frame R_{GF_i} and the common global reference frame $R_G = R_z(\theta) \times R_{GF_{trunk}}$ is obtained during the initial static posture at the beginning of each acquisition using the known orientation in R_{OMCS} of both the trunk MIMU ($P_{OMCS-MIMU_{trunk}}$) and MIMU$_i$ ($P_{OMCS-MIMU_i}$) (**Figure 36**, cf paragraph a), as well as their known orientation outputs ($P_{MIMU_{trunk}-GF_{trunk}}$, $P_{MIMU_i-GF_i}$):

$$P_{G-GF_{trunk}} = R_z(\theta)$$

$$P_{G-GF_i} = P_{G-GF_{trunk}} \times P_{GF_{trunk}-GF_i} = R_z(\theta) \times P_{GF_{trunk}-GF_i}$$

$$P_{G-GF_i} = R_z(\theta) \times P_{GF_{trunk}-MIMU_{trunk}}(t_0) \times P_{MIMU_{trunk}-OMCS}(t_0) \times P_{OMCS-MIMU_i}(t_0) \times P_{MIMU_i-GF_i}(t_0)$$

Using the constant transformation matrix P_{G-GF_i}, and the orientation output provided by each MIMU ($P_{MIMU_i-GF_i} = P_{GF_i-MIMU_i}^{-1}$), the acceleration of each SCoM can be expressed in a consistent global reference frame at all timestamps:

$$\boldsymbol{a}^G_{sCoM_i}(\boldsymbol{t}) = P_{G-GF_i} \times P_{GF_i-MIMU_i}(t) \times \boldsymbol{a}^{MIMU_i}_{sCoM_i}(\boldsymbol{t})$$

i. Selected OSN

Based on the results of chapter 2, three OSN models including 3 to 5 segments are considered as good candidates for the estimation of BCoM acceleration and velocity (**Table 6**). BCoM acceleration and velocity estimated using a unique MIMU at the trunk level will also be analyzed to demonstrate the added value of using multiple sensors instead of a single sensor.

Table 6: List of the optimal sensor networks (OSN) implemented for the estimation of 3D BCoM acceleration and velocity

Number of segments	Included segments
5	Trunk, thighs, shanks
5	Trunk, thighs, feet
3	Trunk, shanks
1	Trunk

ii. 3D BCoM acceleration

For each OSN model, SCoM accelerations of the included segments are expressed in R_G and fused to compute 3D BCoM acceleration, with m_{Seg_i} the mass of the ith segment derived from the personalized inertial model, and N the number of segments included in the OSN:

$$\boldsymbol{a_{BCoM}} = \sum_{i=1}^{N} \frac{m_{seg_i}}{\sum_{j=1}^{N} m_{seg_j}} \boldsymbol{a_{SCoM_i}}$$

iii. 3D BCoM velocity

The 3D BCoM velocity is computed stride-per-stride as the sum of the average walking speed and the cyclical component. Stride segmentation is performed at the prosthetic heel strike from shank MIMU readings (Trojaniello, Cereatti, Pelosin, *et al.*, 2014). Subsequently, the average component of 3D BCoM velocity is computed from a prosthetic shank-mounted MIMU following (Duraffourg *et al.*, 2019) and will be designated as the "average walking speed" in the following paragraphs. The cyclical component was computed from direct numerical integration of 3D OSN-derived BCoM linear acceleration followed by high-pass filtering (Steins *et al.*, 2014).

3.2.2. Framework implementation

a. Experimental protocol

One male individual with transfemoral amputation (mass: 83 kg, stature: 1.69 m) gave his written informed consent to participate in the study. He was instrumented with a full-body marker set (Al Abiad et al., 2020) and 7 MIMUs (Xsens, 100 Hz) on the feet, shanks, thighs and trunk, each mounted on a 3D-printed plastic support with housings for 4 reflective markers. An OMCS (VICON, 200 Hz) recorded the markers' positions while 4 photographs (front, back, both sides) were taken. Then, starting from a static standing posture, the participant walked at self-selected speed along an 8 m pathway, with 3 force plates (AMTI, 1000 Hz) in the middle. Synchronization between instruments was achieved by an electronic trigger signal. Only trials with three successive foot contacts on the force plates (i.e. a complete stride), were considered for further analysis.

b. Data processing

Data were filtered using a zero-phase 4th-order Butterworth filter. Cut-off frequencies were identified using a trial-and-error approach (5 Hz for marker and MIMU raw data, 10 Hz for force plates). Reference SCoM accelerations were obtained by double derivation of OMCS-based SCoM positions. Each differentiation step was followed by a zero-phase low-pass Butterworth 4th order filter with cut-off frequencies 8 Hz (velocity) and 10 Hz (acceleration). Reference 3D BCoM acceleration was computed from the force plates' signal while reference 3D BCoM velocity was computed from the inertial model, to avoid error propagations due to ill-chosen integration constants when estimating the velocity from force platforms. For each OSN, reference and MIMU-based SCoM and BCoM accelerations/velocities were compared using Pearson's correlation coefficient ρ, root mean square error (RMSE) and peak-to-peak normalized RMSE (NRMSE) averaged over the trials. Errors in the estimation of BCoM velocity was also quantified in percent of the average walking speed in the direction of progression (ARMSE). The average and standard deviation of the (normalized) RMSE respectively indicate the accuracy and precision of the methods.

3.3.   Results

Seven trials, resulting in thirteen strides, were analyzed. Only the middle strides occurring entirely on the force plates were analyzed for the investigation of BCoM acceleration accuracy, whereas the whole set of strides was analyzed for the SCoM acceleration and BCoM velocity.

i.   SCoM and BCoM acceleration

Results of the comparison between MIMU-derived and inertial-model based SCoM accelerations are provided in **Table 7**. Correlations between MIMU-based and reference SCoM acceleration were small at both feet and moderate at the sound shank in the mediolateral direction but were strong otherwise (ρ > 0.7).

Table 7: Accuracy of segments' center of mass accelerations estimated with MIMU compared to the optical motion capture reference in terms of root mean square errors (RMSE), normalized RMSE, and Pearson's correlation coefficients (ρ)

Segment	RMSE (m.s⁻²)			NRMSE (%)			Pearson's ρ		
	Antero-posterior	Medio-lateral	Vertical	Antero-posterior	Medio-lateral	Vertical	Antero-posterior	Medio-lateral	Vertical
	Mean (standard deviation)								
Prosthetic foot	2.94 (0.61)	2.74 (0.65)	2.00 (0.21)	5.2 (1.1)	26.1 (4.0)	6.6 (0.7)	0.97 (0.01)	0.27 (0.14)	0.96 (0.01)
Sound foot	3.64 (1.10)	3.99 (0.70)	3.31 (1.05)	6.3 (1.9)	22.1 (5.4)	8.4 (1.4)	0.96 (0.03)	0.19 (0.18)	0.90 (0.06)
Prosthetic shank	1.58 (0.33)	1.21 (0.39)	1.38 (0.08)	5.0 (1.0)	16.7 (5.3)	12.4 (0.8)	0.97 (0.01)	0.71 (0.16)	0.88 (0.02)
Sound shank	2.08 (0.43)	1.49 (0.43)	1.56 (0.19)	8.9 (1.6)	18.9 (4.1)	12.4 (1.9)	0.93 (0.03)	0.42 (0.20)	0.83 (0.05)
Prosthetic thigh	1.94 (0.07)	0.50 (0.11)	0.79 (0.02)	18.5 (0.6)	7.6 (1.7)	7.5 (0.4)	0.83 (0.03)	0.94 (0.04)	0.96 (0.00)
Sound thigh	2.10 (0.66)	0.72 (0.12)	0.94 (0.33)	10.5 (1.5)	14.6 (1.8)	9.5 (1.7)	0.85 (0.10)	0.74 (0.08)	0.90 (0.07)
Trunk	0.95 (0.05)	0.48 (0.04)	0.43 (0.22)	12.8 (1.1)	12.9 (1.1)	5.7 (2.4)	0.73 (0.04)	0.89 (0.02)	0.97 (0.03)
Average (all segments)	**2.04 (0.99)**	**1.47 (1.25)**	**1.39 (0.95)**	**10.0 (4.6)**	**16.6 (6.3)**	**9.1 (2.8)**	**0.87 (0.10)**	**0.62 (0.30)**	**0.92 (0.06)**

90

Results of the comparison between MIMU-derived OSN-based and force platform-based BCoM accelerations are provided in **Table 8**. Correlations between MIMU-based and reference BCoM acceleration were strong for all OSN models in all directions ($\rho > 0.7$). The added value of using multiple sensors instead of a single sensor at trunk level is demonstrated by the increased accuracy and the better fit of reference BCoM acceleration in the anteroposterior and mediolateral directions when using OSN (**Table 8**, **Figure 38**).

Table 8: Accuracy of Optimal sensor network (OSN)-based MIMU-derived BCoM acceleration as compared with force platform-based acceleration in terms of root mean square errors (RMSE), normalized RMSE, and Pearson's correlation coefficients (ρ)

OSN (included segments)	RMSE (m/s²)			NRMSE (%)			Pearson's ρ		
	Antero-posterior	Medio-lateral	Vertical	Antero-posterior	Medio-lateral	Vertical	Antero-posterior	Medio-lateral	Vertical
	Mean (standard deviation)								
Trunk, thighs, shanks	0.54 (0.02)	0.32 (0.03)	0.57 (0.06)	13.7 (0.9)	14.0 (2.1)	8.5 (0.5)	0.93 (0.01)	0. 89 (0.04)	0.95 (0.01)
Trunk, thighs, feet	0.33 (0.02)	0.37 (0.03)	0.51 (0.05)	9.7 (0.7)	13.7 (0.7)	7.4 (0.4)	0.93 (0.01)	0.88 (0.02)	0.96 (0.01)
Trunk, shanks	0.40 (0.06)	0.50 (0.05)	0.54 (0.04)	11.6 (2.1)	21.5 (2.7)	7.7 (0.4)	0.89 (0.03)	0.74 (0.08)	0.96 (0.00)
Trunk	0.66 (0.05)	0.70 (0.05)	0.63 (0.06)	17.0 (1.2)	23.5 (2.0)	8.8 (0.6)	0.78 (0.02)	0.76 (0.05)	0.95 (0.00)

ii. BCoM velocity

Accuracy of OSN-derived BCoM velocity compared to the reference inertial model is presented in **Table 9**. OSN-derived and reference BCoM velocity averaged over the thirteen prosthetic strides are displayed in **Figure 39**. Interestingly, the OSN models that achieved the best estimation of BCoM velocity were different from those that achieved the best fit for BCoM acceleration. The five-MIMU OSN model including the shanks performed better than that including the feet in all directions, as displayed by the higher Pearson's correlation coefficients and the lower RMSE. BCoM velocity estimated with the trunk SCoM acceleration achieved a good fit of BCoM velocity with excellent correlations in the mediolateral and vertical direction ($\rho > 0.90$), but only a moderate agreement in the anteroposterior direction. Furthermore, high errors were achieved by this model in the anteroposterior and mediolateral direction (RMSE > 0.08 m.s^{-1}).

Table 9: Accuracy of body center of mass (BCoM) velocity derived from the optimal sensor network (OSN)-based BCoM acceleration compared to the reference velocity computed from optical motion capture in terms of root mean square error (RMSE), RMSE normalized to average walking speed (ARMSE) and peak-to-peak normalized RMSE (NRMSE)

OSN (included segments)	RMSE (m.s^{-1})			ARMSE (%)	NRMSE (%)			Pearson's ρ		
	Antero-posterior	Medio-lateral	Vertical	Antero-posterior	Antero-posterior	Medio-lateral	Vertical	Antero-posterior	Medio-lateral	Vertical
Trunk, thighs, shanks	0.05 (0.02)	0.05 (0.01)	0.03 (0.00)	4.1 (1.2)	16.7 (5.1)	13.2 (3.0)	6.0 (0.8)	0.94 (0.04)	0.96 (0.03)	0.99 (0.00)
Trunk, thighs, feet	0.05 (0.01)	0.06 (0.02)	0.03 (0.01)	4.2 (1.0)	20.8 (6.2)	15.6 (3.9)	6.0 (0.6)	0.85 (0.05)	0.90 (0.04)	0.99 (0.01)
Trunk, shanks	0.04 (0.02)	0.05 (0.01)	0.03 (0.01)	3.5 (1.3)	15.1 (6.1)	13.7 (2.4)	6.7 (1.0)	0.92 (0.02)	0.94 (0.01)	0.99 (0.00)
Trunk	0.08 (0.01)	0.09 (0.01)	0.04 (0.01)	6.7 (0.7)	27.7 (3.3)	20.8 (1.7)	7.6 (0.8)	0.57 (0.06)	0.92 (0.02)	0.99 (0.00)
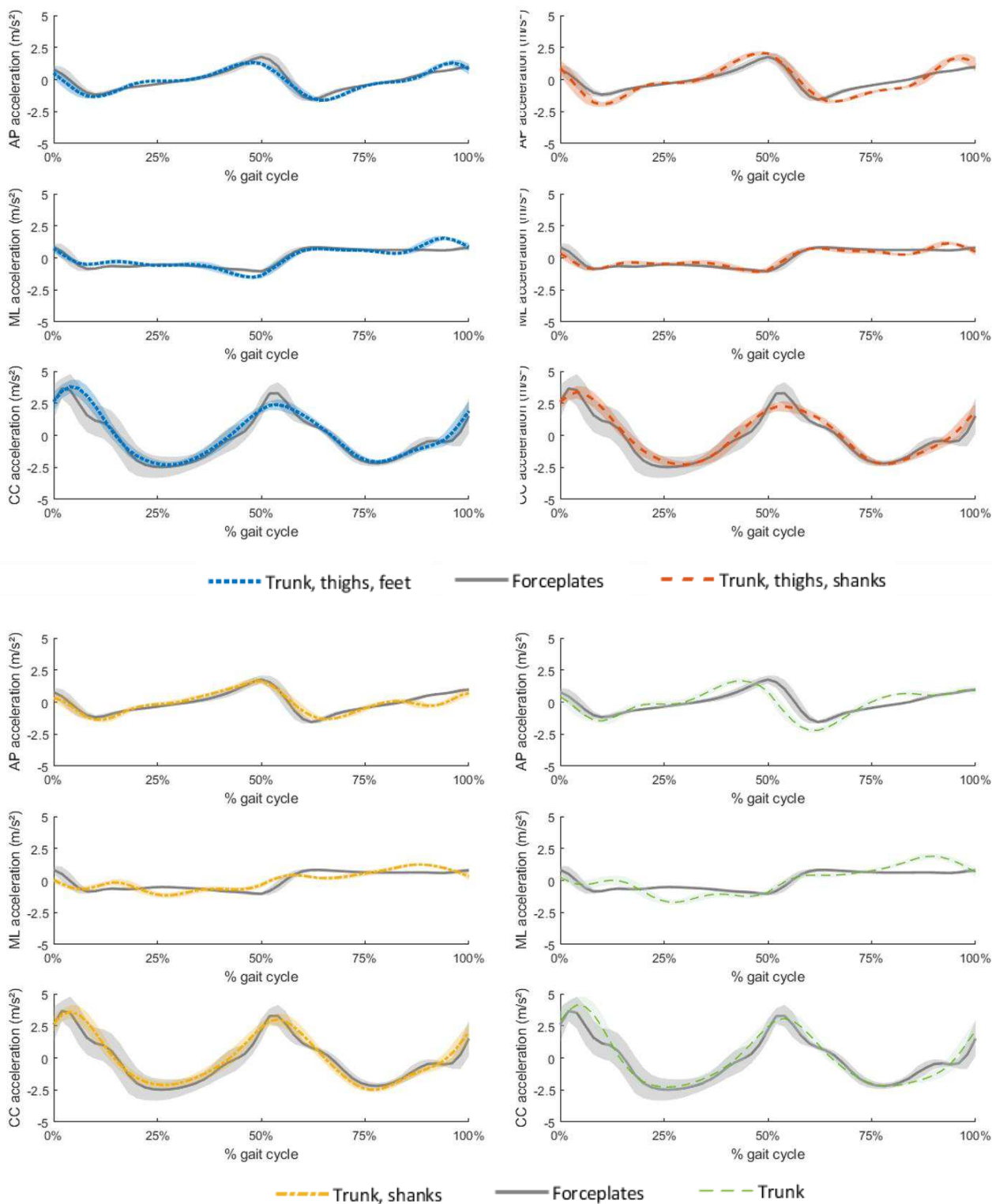
Figure 38: Acceleration of the body center of mass derived from force platforms measures (gray straight line), optimal sensor networks consisting in the weighted sum of center of mass accelerations of the included segments (colored dashed and dotted lines), in the anteroposterior direction (AP), mediolateral direction (ML) and vertical direction (CC). Shaded regions represent the interval [mean – standard deviation ; mean + standard deviation] for the estimates of the BCoM acceleration averaged over the 7 gait cycles of the participant.
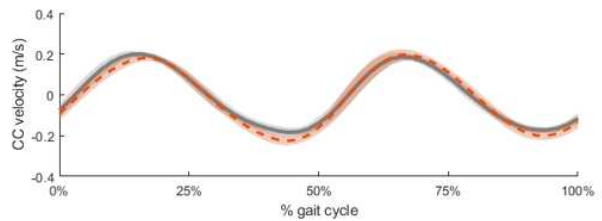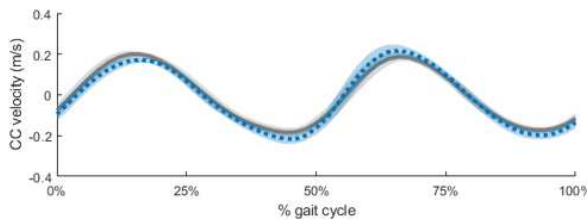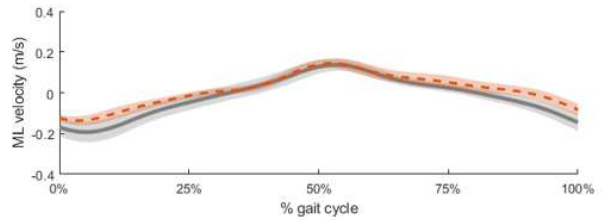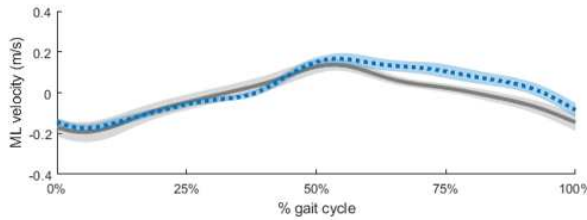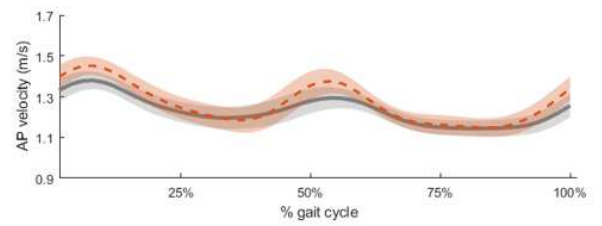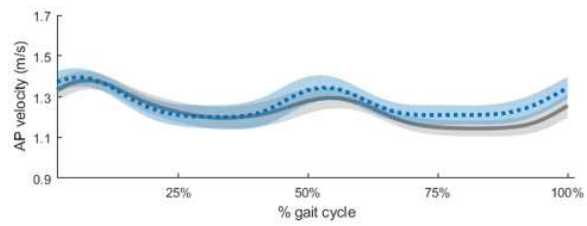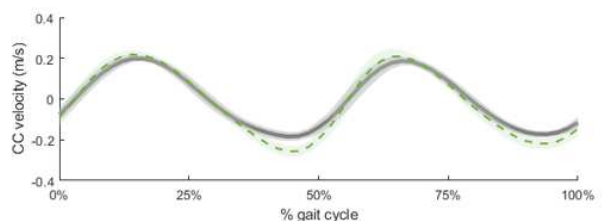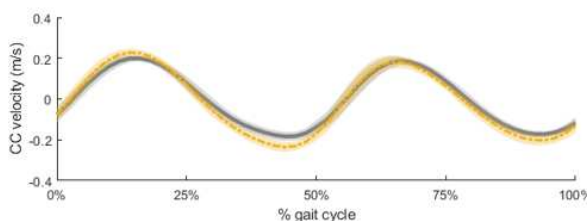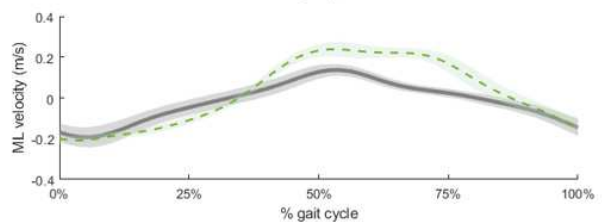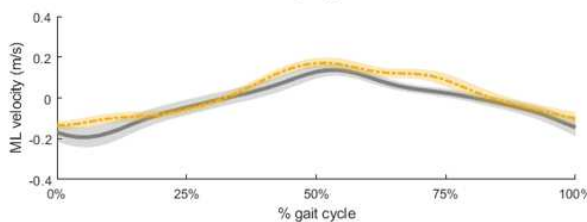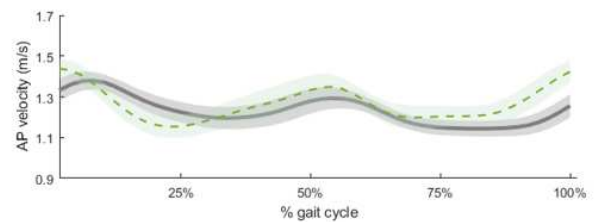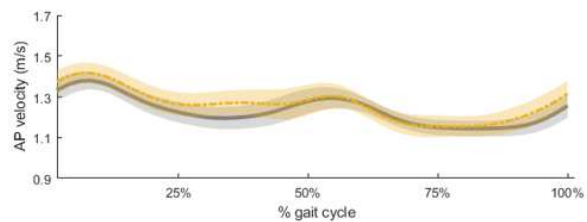
Figure 39: Body center of mass (BCoM) velocity as estimated by OSN-derived models [upper-left corner (blue dotted lines): trunk, thighs, feet; upper-right corner (orange dashed-lines): trunk, thighs, shanks; lower-left corner (yellow dashed lines): trunk and shanks; lower-right corner (green dashed lines): trunk] in comparison with the reference BCoM velocity obtained by optical motion capture (gray straight line). Shaded regions represent the interval [mean – standard deviation, mean + standard deviation] for each estimate of the BCoM velocity averaged over the thirtheen prosthetic gait cycles of the participant in the anteroposterior (AP), mediolateral (ML) and vertical (CC) direction.

3.4.   Discussion

This proof-of-concept study aimed at proposing and validating a framework for the estimation of BCoM acceleration and velocity from an optimal network of MIMUs. Based on the results of an optical motion capture-based study (Chapter 2), several OSN were investigated, including from 3 to 5 MIMUs positioned on the trunk and on either a pair or more of the following segments: thighs, shanks and feet. The added value of using an optimal network of sensors instead of a single sensor at trunk level was also investigated by comparing the accuracy of the various OSN estimates to that obtained with the trunk MIMU. This pilot study demonstrated the feasibility of accurately estimating the 3D BCoM instantaneous walking velocity and acceleration using five MIMUs in people with transfemoral amputation. The fact that the protocol was validated in a single case study should however be kept in mind before generalization of the achieved results to the population of transfemoral amputees.

i.   SCoM and BCoM acceleration

In the developed framework, the BCoM acceleration is estimated through a weighted average of SCoM accelerations. To the author's knowledge, this is the first study that reported accuracy results for the estimation of SCoM accelerations from MIMUs.

Interestingly, when more than 3 sensors were used for BCoM accelerations, higher errors were achieved on average for the estimation of accelerations at the SCoMs than at the BCoM. Accelerations estimated at the shanks and feet were shown to have the highest errors and to poorly (sound limb) or moderately (prosthetic limb) fit the reference SCoM acceleration in the mediolateral direction. A possible reason for this discrepancy lies on the assumptions made regarding the alignment of segment anatomical axes with those of the global reference frame in static. Indeed, the participant was not specifically asked to stand with his feet parallel, which would have justified this hypothesis for the feet segments. Natural outward alignment of the feet of 20° have been reported in the literature (Tunca *et al.*, 2017) and would have necessarily an impact on the orientation of both the feet and the shanks. However, OSN that included feet and thighs segments were shown to be superior to their counterparts using shank-mounted MIMUs in terms of accuracy with the BCoM acceleration (**Table 8**).

BCoM acceleration estimated using a single sensor at trunk level in the present study resulted in lower accuracy in the anteroposterior and mediolateral directions than reported by Mohamed Refai and coworkers with a single MIMU at pelvis level in eight asymptomatic participants (Mohamed Refai *et al.*, 2020). However, the presented framework achieved higher accuracy in the vertical direction and higher consistency with the reference acceleration pattern in the mediolateral and vertical directions, as demonstrated by higher correlation coefficients. When estimated using several sensors, OSN-derived BCoM acceleration results were in agreement with those reported in healthy subjects using optical motion capture system-based accelerations (Shahabpoor et al., 2018). Indeed, using three sensors (trunk and shanks mounted MIMUs), our method achieved similar to improved accuracy (mean NRMSE) and better precision (standard deviation of the NRMSE) compared to the one proposed by Shahabpoor and coworkers using the acceleration of three different segments (trunk, pelvis and a thigh) in sound participants (present study vs sound-participants : 11.6 ± 2.1% vs 16 ± 2.0 % in the anteroposterior direction, 21.5 ± 2.7 % vs 18 ± 6.7 % in the mediolateral direction and 7.7 ± 0.4 % vs 7 ± 1.7 % in the vertical direction). The increased precision in the present study may have resulted from the validation of the method on a unique participant whereas six asymptomatic subjects ambulating

at different walking speeds were recruited in (Shahabpoor *et al.*, 2018). It is worth noting that, in the former study, BCoM acceleration was estimated from a weighted average of SCoM accelerations derived from optical motion capture measurement. Therefore, decreased accuracy and precision is expected when transposing the method with MIMUs. The validity of the method presented in (Shahabpoor *et al.*, 2018) when using wearable sensors was only investigated in the vertical direction, where a mean accuracy of 8.7 % was achieved in the vertical direction (1.7 % decreased in accuracy). Therefore, the results achieved in the current study using a 3-MIMU configuration are very promising.

Increasing the number of MIMUs allowed to improve the accuracy of the estimated BCoM acceleration, in particular in the mediolateral direction (**Table 8**). Interestingly, the five-MIMU OSN including the thighs and shanks sensors resulted in an improved accuracy only in the mediolateral direction compared to the three-MIMU OSN, while an increase accuracy in the anteroposterior direction was also observed when considering the five-MIMU OSN including the thighs and feet sensors. High consistency between reference and MIMU-based 3D BCoM acceleration patterns was observed with all the OSN models investigated, with perceivable deviations in the mediolateral direction for the three-MIMU model (**Figure 38**, **Table 8**).

In the light of these results, the three-segment OSN model including both shanks and the trunk appears to be optimal when the sagittal plane BCoM acceleration is targeted (anteroposterior and vertical directions). When the 3D BCoM acceleration must be estimated with high accuracy, a five-sensor model including the trunk, both thighs and either both feet or both shanks is to be preferred.

ii.   BCoM velocity

BCoM velocity was computed stride per stride using the sum of a cyclical component and an average walking speed in the direction of progression. The average walking speed was estimated as the ratio of the shank MIMU displacement along the direction of progression within a stride to the stride duration, using the kinematic model specifically developed for people with lower-limb amputation in (Duraffourg *et al.*, 2019). The use of this model imposes the use of a MIMU mounted on the prosthetic shank, even when considering OSN models for BCoM acceleration estimation that did not include a sensor at the shank. In order to keep the number of sensors at a minimal, it is therefore preferred, with this integration method, to use OSN models including the shanks segments rather than the feet. Otherwise, integrating the foot acceleration between successive foot flat periods could allow to estimate the average walking speed (Kitagawa and Ogihara, 2016). However, reliable detection of foot flat events from inertial sensors may not be straightforward in people with lower-limb amputation.

BCoM velocity estimated from a single sensor at trunk level was shown to be slightly in advance of phase in the anteroposterior direction (**Figure 39**) and to lack accuracy in the anteroposterior and mediolateral directions (average RMSE > 0.08 m.s^{-1}) (**Table 9**). The use of multiple sensors arranged in OSN allowed to improve the estimated velocity by up to 12.6 % in the anteroposterior direction. Interestingly, the three-MIMU OSN including the trunk and shanks provided the most accurate estimate of BCoM velocity in the anteroposterior direction, with errors in the order of 3.5 ± 1.3 % of the average walking speed (average RMSE = 0.04 m.s^{-1}). Adding supplementary sensors at the thighs resulted in a better fit of curve pattern in the anteroposterior and mediolateral directions (**Figure 39**) but in a slight decrease of accuracy in the anteroposterior direction (RMSE of 0.05 ± 0.01 m.s^{-1}, corresponding to 4.1 ± 1.0 % of the average walking speed), due to the overestimation of BCoM

velocity peaks in that direction (**Figure 39**). Therefore, although 3 MIMUs allowed to estimate BCoM acceleration and velocity with a good accuracy index, using 5 MIMUs on the trunk, thighs and shanks should be preferred if a strong accuracy is required especially in the mediolateral direction. The model including the feet sensors achieved lower accuracy in the anteroposterior and mediolateral direction than the models including the shanks. This might be a consequence of the assumption of parallel feet required for computing the relative orientation of the reference frames sensed by the feet MIMUs in the global reference frame (see equations in part 3.2.1b).

Few studies in the literature have focused on the estimation of the instantaneous BCoM velocity, compromising the comparison of our results. Furthermore, all former studies investigating the instantaneous BCoM velocity used the assumption that the BCoM was fixed in the pelvis anatomical frame. Sabatini and Mannini investigated a method for the estimation of the instantaneous velocity of a MIMU positioned at the pelvis compared to the velocity of an optical motion capture marker positioned on top of the MIMU (Sabatini and Mannini, 2016). Validation results are proposed separately for the cyclical component (limits of agreement [$\pm$ 1.96 standard deviation] of $\pm$ 0.10 m.s^{-1} in the anteroposterior and mediolateral direction, and $\pm$ 0.05 m.s^{-1} in the vertical direction) and average component (RMSE = 0.07 m.s^{-1} when ambulating overground). A smaller dataset was used in the present study but higher accuracy was achieved for the cyclical component ($\pm$ 1.96 standard deviation of the RMSE: $\pm$ 0.01 m.s^{-1} in all directions, including when using a single sensor at the trunk level).

Regarding the average walking speed, multiple authors have proposed algorithms for its estimation using inertial sensors (Yang and Li, 2012b). Only two studies reported an estimate of the average walking speed within less than 4.1 % of its nominal value. In (Mariani *et al.*, 2010) the average walking speed was estimated from double integration of the acceleration of a foot mounted MIMU in twenty sound participants (young and elderly) and achieved higher accuracy but lower precision (1.5 $\pm$ 5.8 % of the actual walking velocity) than the proposed method. Using a shank MIMU and a kinematic model relying on stance knee flexion, which is absent in people with transfemoral amputation, Yang and coworkers estimated the average walking speed within 4.0 % of its nominal value.

iii.   Limitations and perspectives

The developed framework allowed to estimate the instantaneous walking speed and acceleration of the body center of mass from five MIMUs positioned on the trunk, thighs and shanks segments of one person with transfemoral amputation. Results should be confirmed in a larger cohort prior to generalization.

The aim of the present study was to propose a wearable framework as compatible as possible with clinical use. Currently, the framework requires the use of a camera and an optoelectronic system for the personalization of the geometric inertial model and the estimation of the relative position of each MIMU to the center of mass of the underlying segment in the intermediary global frame (static). The use of these external devices, and especially of the optical motion capture system, compromises the transfer of the framework in the clinical field. The optical motion capture system was used for the calibration of photographs and for the construction of an initial geometric inertial model based on anatomical landmarks. Projections of the initial volumes on face and profile photographs were manually reshaped so as to fit the participant's body contours based on face and profile photographs (Pillet *et al.*, 2010). Therefore, using an alternate system for the calibration of photographs – or a method that does not require to take photographs at all – would facilitate the transfer of the

framework in the clinical field. Regarding the first solution, using a device of known shapes and dimensions may allow to calibrate photographs. Regarding a possible alternative to taking photographs, body segmental inertial parameters and positions of anatomical landmarks and MIMUs could be retrieved from body meshes obtained with a 3D scanner. A semi-automatic method, requiring less than 1 minute of acquisition, has been proposed and validated in nine sound participants (Robert *et al.*, 2017). Its validity in impaired people, in particular in people with a lower-limb prosthesis, remains to be verified. All in all, making the framework fully wearable does not appear to be a major issue even if it would require some further development and validation. It should be noted that the method would still rely on an external portable device (camera/3D scanner) in order to retrieve the SCoM and MIMU positions in a consistent intermediary global frame (the scanner or camera frame). The impact of errors in the estimations of the relative positions of MIMUs and SCoM on the output parameters (SCoM and BCoM acceleration, BCoM velocity) should therefore be investigated in a further study.

It should be noted that, in order to obtain the relative position of MIMUs and SCoM in the MIMU local frame, the framework uses a static calibration during which both the relative SCoM/MIMU positions and the orientations of MIMUs are estimated in an intermediary global frame. To do so, MIMUs were aligned with the longitudinal axes of segments while the latter were supposed to have their axes aligned with that of the intermediary reference frame. It should be stressed that this sensor-to-segment calibration was required only to derive the position of SCoM in their respective MIMU local frames and was not directly used for the fusion of SCoM accelerations. Furthermore, inclination of MIMUs with respect to the vertical were corrected using the orientation output provided by the MIMUs. Therefore, the impact of misorientation of MIMUs on segment is believed to be minimal, which would not have been the case if the aim of this study was to derive joint angles (Miezal *et al.*, 2016; Kianifar *et al.*, 2019). Verification of this hypothesis should also be investigated in further studies.

The framework could finally be enhanced in order to obtain complementary biomechanical parameters. A growing interest for the estimation of individual limb ground reaction forces from MIMUs can be inferred from recent literature. In people with lower-limb amputation, in particular, receiving/giving feedback on the load distributed to each lower limb represents an interesting track for the rehabilitation (Loiret *et al.*, 2019). Several models proposing a smooth transition of the weight from one limb to another have been investigated in the literature (Ren *et al.*, 2008; Karatsidis *et al.*, 2017) but may not be adapted for impaired gait. Therefore, developing a method allowing to estimate the ground reaction force under each foot from MIMU-based BCoM acceleration in people with transfemoral amputation represents a relevant track for future works. Furthermore, when combined with the instantaneous BCoM velocity, the individual ground reaction force can provide insight on mechanical energy exchanges (Donelan *et al.*, 2002b; Bonnet *et al.*, 2014).

3.5.   Conclusions

The framework's results are encouraging and suggest that MIMUs may be a valid alternative to lab-based instruments when the 3D BCoM acceleration or velocity is targeted. Indeed, using a set of five MIMUs on the trunk, thighs and shanks allowed to estimate 3D BCOM acceleration and velocity in a person with transfemoral amputation with a strong agreement with reference data obtained from force platforms (acceleration: $\rho > 0.89$) and an optical motion capture (velocity: $\rho > 0.94$) and high

accuracy (NRMSE in the anteroposterior, mediolateral and vertical directions of 11.6 ± 2.1 %, 14.0 ± 2.1 %, 7.7 ± 0.4 % for the acceleration and 16.7 ± 5.1 %, 13.2 ± 3.0 %, 6.0 ± 0.8 % for the velocity). Results of this proof-of-concept study still need to be confirmed on a larger cohort.

In medium-term, future studies will aim at assessing *i)* the accuracy achieved when a fully wearable framework (that is, without an optical motion capture system) is implemented and *ii)* the impact of MIMU misplacement on the estimation of SCoM and BCoM kinematic parameters. In the long term, suitability of the OSN to estimate the ground reaction force under each foot should be investigated.

Chapter 4 – The impact of inertial measurement units positioning error on the estimated accelerations of body and segments' centers of mass: a sensitivity analysis

The previous chapters indicate that, in people with transfemoral amputation, body center of mass (BCoM) acceleration can be estimated from a weighted average of the accelerations of the centers of mass of a set of 5 segments. The formers can be estimated from the signals measured by MIMUs rigidly mounted on each of the segments using the following equation – provided that the SCoM position in the MIMU local frame $r_{oIMU-SCoM}$ is known:

$$a_{SCoM} = a_{oIMU} + \Omega_{oIMU} \wedge (\Omega_{oIMU} \wedge r_{oIMU-sCoM}) + \dot{\Omega}_{oIMU} \wedge r_{oIMU-SCoM}$$

With a_{SCoM}, the acceleration of the SCoM, a_{oIMU} and Ω_{oIMU} the acceleration and angular velocity measured by the MIMU and $\dot{\Omega}_{oIMU}$ the angular acceleration obtained from differentiation of the angular velocity. All the quantities are expressed in the MIMU local frame.

With the hypothesis that MIMUs are rigidly mounted on each segment, the relative position of MIMUs and the underlying SCoM is constant in the MIMU local frame. Therefore, its retrieval at a specific instant, for example, during a static calibration, is enough. In light of the above, it is clear that the accurate determination of the position of each MIMU with respect to the relevant SCoM is crucial to obtain an accurate estimation of SCoM and BCoM accelerations.

In the framework presented in chapter 3, SCoM and MIMUs' positions are retrieved in a consistent intermediary global frame using calibrated photographs taken with the participant in a static standing posture. SCoM positions are obtained along with other body segmental inertial parameters by fitting a geometric inertial model on face and profile photographs while the positions of MIMUs are recovered by clicking on the locations of MIMUs origins on the same calibrated photographs. The vector describing the relative position of each pair of SCoM and MIMU origin must then be transferred in the MIMU local frame, which requires the knowledge of the MIMU orientation in the intermediary global frame. Thus, two main sources of errors may impact the accuracy of the vector $r_{oIMU-SCoM}$ in MIMU local frame when using the presented framework: mislocation errors (due to errors in calibrating the photographs or clicking on the wrong position) and orientation errors, due to the assumptions made regarding MIMUs orientation in the intermediate global frame. When estimating BCoM acceleration, the accelerations estimated at each SCoM must then be fused in a consistent global reference frame.

The sensitivity of MIMU-derived biomechanical parameters to MIMU positions and orientations has recently been studied in the literature for the estimation of joint angles and of ground reaction forces (Kianifar *et al.*, 2019; Tan *et al.*, 2019). In both cases, sensor-to-segment orientations were found to be more critical than MIMUs positions on segments (Kianifar *et al.*, 2019; Tan *et al.*, 2019). Regarding the study that focused on ground reaction forces (Tan *et al.*, 2019), the formers were estimated with a machine learning approach using raw acceleration and angular velocity data, expressed in their respective MIMU local frames, as inputs. No sensor-to-segment calibration procedure was used to pre-process raw MIMU data and expressed them in a common global reference frame prior to using them for the estimation of SCoM acceleration. Modifying the orientation of MIMUs on segments necessarily impacted both angular velocity and acceleration raw data used as inputs, while modifying the position

of a MIMU on a segment had only repercussions on the acceleration signals. Therefore, the greater impact of orientation errors compared to position errors could be expected in their study.

When investigating SCoM or BCoM acceleration following the framework proposed in Chapter 2, sensor-to-segment orientation is not critical, since only the orientations of MIMUs in an intermediary global frame during a static posture is required to define a between-MIMU consistent global frame. Orientation errors of two natures could occur with the framework implementation. During the static posture, the hypotheses of manual alignments of the MIMUs on the segments could lead to errors and should be quantified. During the dynamic trials, there could be residual errors due to the orientation computation from sensor data leading to inconsistencies between the reference frames sensed by multiple MIMUs, which would impact the acceleration of the BCoM. However, it is believed that these errors are not as critical as those made when clicking on MIMUs on photographs. Therefore, in this chapter, we focused solely on the impact of MIMUs mislocation on SCoM and BCoM accelerations. The impact of orientation errors due to the hypotheses of manual alignment of sensors and due to the computation of orientation from sensor data should nonetheless be investigated in future studies.

The impact of the MIMUs location errors on SCoM and BCoM accelerations of an ambulating transfemoral amputee was analyzed through a sensitivity analysis. First, the potential range of localization error was investigated by two independent operators, who retrieved five times the position of MIMUs origins after having recalibrated the photographs. Then, a simulation-based sensitivity analysis was performed. It consisted in estimating SCoM and BCoM accelerations when introducing errors in the relative position of MIMUs and their respective SCoM. Estimated SCoM and BCoM accelerations were then compared to the reference value, which allowed to assess the impact of MIMUs mispositioning on SCoM and BCoM acceleration. Finally, the sensitivity analysis allowed to identify the MIMUs whose accurate location is critical for the estimation of SCoM and BCoM accelerations. This work was produced during the master internship of J. Basel, whose contribution is duly acknowledged. The content of this chapter will be submitted as an article in IEEE Transactions on Biomedical Engineering.

4.1. Definition of the possible magnitude of errors in the identification of MIMUs positions

The MIMU-based framework presented in the previous chapter allows to estimate the relative position of each segment-mounted MIMU with respect to the underlying SCoM in the optical motion reference frame using calibrated photographs. Errors made when identifying MIMU positions on the photographs would inevitably impact the estimation of SCoM acceleration. To properly define the magnitude of error to be used in the sensitivity analysis performed in this study, namely the amount of position variation to be simulated for each segment-mounted MIMU, the range of errors that could be made when identifying MIMU positions on photographs was calculated.

To this aim, four back, face and profile photographs (**Figure 40**) were taken with the participant standing in a static posture while optical motion capture (OMC) recorded the position of 59 markers attached to the body and 20 markers positioned on five 3D printed boxes embedding MIMUs mounted on the trunk, thighs and shanks. MIMU positions were retrieved by clicking on their locations on the photographs, calibrated following (Pillet *et al.*, 2010) by two operators who repeated the whole process five times (calibration + position identification). Photograph-based and OMC-based positions of each MIMU origin were calculated for each operator and results are reported in **Table 10**.

Figure 40: Left side photo of the subject equipped with MIMUs and optoelectronic markers. Zoom on the CAD-designed structure on the subject's sound thigh. On the photo, the MIMU and CAD structure are covered with strap band

Absolute errors in the identification of MIMU positions were found to reach up to 0.02 m (**Table 10**). This value was thus considered for the sensitivity analysis. It should be noted that errors in MIMU identification could be reduced by improving the visibility of the MIMU origins on the photographs/scan (see **Figure 40**), for instance, by positioning a colored sticker on top of the MIMU origin when positioning the MIMU on the participants. Furthermore, this could pave the way for automatic detection of MIMU positions, thus reducing the post-processing time and inter-operator errors.

Table 10: Mean and range of errors (in m) observed following the five repetitions performed by the two operators for the identification of each MIMU origin.
P: prosthetic; S: sound, ML: medio-lateral, AP: anteroposterior, V: vertical

	Mean error (m)			Min error (m)			Max error (m)		
	AP	ML	V	AP	ML	V	AP	ML	V
	Operator 1								
ShankP	0.012	0.007	0.012	-0.018	-0.010	-0.020	-0.001	0.010	0.005
ShankS	0.009	0.003	0.004	-0.017	-0.003	-0.005	-0.005	0.004	0.005
ThighP	0.016	0.005	0.007	-0.021	0.002	-0.010	-0.010	0.008	0.000
ThighS	0.015	0.005	0.006	0.008	-0.010	-0.004	0.018	-0.001	0.010
Trunk	0.007	0.007	0.012	0.003	0.001	0.005	0.010	0.011	0.020
All Segments	0.012	0.005	0.008	-0.021	-0.010	-0.020	0.018	0.011	0.020

101

	Mean error (m)			Min error (m)			Max error (m)		
	AP	ML	V	AP	ML	V	AP	ML	V
Operator 2									
ShankP	0.009	0.004	0.003	-0.018	-0.007	-0.003	0.006	0.005	0.004
ShankS	0.009	0.008	0.011	-0.014	-0.004	-0.016	0.004	0.011	0.006
ThighP	0.016	0.005	0.011	-0.020	-0.002	-0.014	-0.012	0.009	0.013
ThighS	0.005	0.010	0.012	-0.009	-0.015	-0.018	0.006	0.013	0.006
Trunk	0.006	0.015	0.008	-0.009	0.008	0.003	0.001	0.020	0.011
All Segments	0.009	0.008	0.009	-0.02	-0.015	-0.018	0.006	0.020	0.013
Operator 1 + Operator 2									
ShankP	0.011	0.006	0.009	-0.018	-0.010	-0.020	0.006	0.010	0.005
ShankS	0.009	0.006	0.008	-0.017	-0.004	-0.016	0.004	0.011	0.006
ThighP	0.016	0.005	0.009	-0.021	-0.002	-0.014	-0.010	0.009	0.013
ThighS	0.011	0.008	0.009	-0.009	-0.015	-0.018	0.018	0.013	0.010
Trunk	0.006	0.012	0.010	-0.009	0.001	0.003	0.010	0.020	0.020
All Segments	0.011	0.007	0.009	-0.021	-0.015	-0.020	0.018	0.020	0.020

4.2. Sensitivity analysis: impact of MIMUs localization errors on the accuracy of the estimated accelerations of body and segments centers of mass

4.2.1. Material and Methods

a. Experimental method

This study was approved by the local ethical committee. A transfemoral amputee subject (mass: 83.1 kg, height: 1.69 m) gave written informed consent to participate to the study. He was equipped with a set of 5 MIMUs (Xsens Technologies B.V., Enschede, The Netherlands, 100 sample·s-1) located on the trunk (over the sternum), both prosthetic and sound thighs (ThighP, ThighS) and shanks (ShankP, ShankS). Each MIMU was inserted in a customized 3D-printed rigid support equipped with 4 reflective markers (**Figure 40**). Additionally, as described in (Al Abiad *et al.*, 2020), 59 reflective markers were positioned on the patient's anatomical landmarks and an optical motion capture system (OMC) was used to record the 3D trajectory of the set of markers (Vicon system, Oxford Metrics, UK, 100 Hz). The participant was asked to walk in a straight line at his natural speed along an 8 m pathway with three force plates (AMTI, Advanced Mechanical Technology, Inc, Massachussets, USA, 1000 Hz) in its middle. OMC, force plates and MIMU data were synchronized with an electronical trigger. Data acquisition was performed over a total of seven trials. For each trial, only the prosthetic stride performed at steady state walking speed and occurring on the force plates was considered in the analysis.

b. Data Processing

All raw data from the acquisition were filtered using a Butterworth zero-lag 4th order low pass filter with cut-off frequencies set at 5 Hz (MIMUs and markers) and 10 Hz (force plates).

i. Reference accelerations

SCoM 3D positions were estimated from OMC measurements using a 15-segment inertial model as reported in (Pillet *et al.*, 2010). These positions were differentiated and low-pass filtered using the

same filter as described above and cut off frequencies set at 8 Hz and 10 Hz for the first and second differentiation respectively to obtain the reference SCoM accelerations. Reference BCoM acceleration was extracted from the filtered force plates data. Reference accelerations were expressed in the OMC inertial reference frame R_{OMC} such that the y-axis was aligned with the direction of progression (anteroposterior, AP), the z-axis vertical and opposing gravity (vertical, V) and the x-axis orthonormal to both (mediolateral, ML).

ii. MIMU-based accelerations

3D orientation and position of each MIMU local frame R_{MIMU} with respect to R_{OMC} were computed using the markers located on the 3D-printed rigid cluster. The transformation matrix from R_{MIMU} to R_{OMC} was obtained and allowed to express both gravity-free accelerations and angular velocities measured by each MIMU in R_{OMC}.

Afterwards, the vector going from MIMU origin to the center of mass of the underlying segment, $\overrightarrow{MIMU-SCoM}$, was obtained and expressed in R_{OMC} for each MIMU. MIMU-based estimation of the SCoM accelerations in R_{OMC}, a_{SCoM}^{MIMU}, were then computed as follows:

$$\overrightarrow{a_{SCoM}^{MIMU}} = \overrightarrow{a_{MIMU}} + \frac{\overrightarrow{d\Omega_{MIMU}}}{dt} \wedge \overrightarrow{MIMU-sCoM} + \overrightarrow{\Omega_{MIMU}} \wedge \left(\overrightarrow{\Omega_{MIMU}} \wedge \overrightarrow{MIMU-SCoM}\right) \quad (1)$$

with $\overrightarrow{a_{MIMU}}$ and $\overrightarrow{\Omega_{MIMU}}$ being the MIMU-measured gravity-free linear acceleration and angular velocity signals expressed in R_{OMC}.

Finally, BCoM acceleration was estimated as a weighted average of the estimated SCoM accelerations ($\overrightarrow{a_{SCoM}^{MIMU}}$) using:

$$\overrightarrow{a_{BCoM}^{MIMU}} = \sum_{i=1}^{n} \frac{m_i}{m_{body}} \overrightarrow{a_{SCoM_i}^{MIMU}} \quad (2)$$

Where: n is the number of segments considered and m_{body} and m_i are respectively the masses of the body and of the ith segment.

The accelerations $\overrightarrow{a_{SCoM}^{MIMU}}$ and $\overrightarrow{a_{BCoM}^{MIMU}}$ were compared to reference data using the normalized root-mean square error (NRMSE) (Ren et al., 2008) and the Pearson's correlation coefficient averaged over the seven analyzed strides along the R_{OMC} directions.

iii. Sensitivity analysis

A sensitivity analysis was performed to investigate the impact of an erroneous identification of each MIMU location, and thus an error on the components of the vector $\overrightarrow{MIMU-SCoM}$ on the NRMSE between MIMU-based and reference SCoM and BCoM accelerations.

To achieve this aim, errors in the identification of MIMU positions on the relevant body segments reaching up to 0.02 m in all three directions (AP, ML and V) were introduced. This range of errors was estimated experimentally (see section 4.1). Simulations were performed where each MIMU position was varied from its actual position (**p₀ML p₀AP p₀V**) by ±0.02 m along each R_{OMC} axis. The resulting SCoM accelerations were estimated using equation (3):

$$\overrightarrow{a_{SCoM}^{MIMU}} = \overrightarrow{a_{MIMU}} + \frac{\overrightarrow{d\Omega_{MIMU}}}{dt} \wedge \overrightarrow{(MIMU-SCoM)+\Delta}$$
$$+ \overrightarrow{\Omega_{MIMU}} \wedge \left(\overrightarrow{\Omega_{MIMU}} \wedge \overrightarrow{(MIMU-SCoM)+\Delta}\right) \quad (3)$$

103

Where: $\overrightarrow{a_{MIMU}}$ and $\overrightarrow{\Omega_{MIMU}}$ are the linear acceleration and angular velocity measured by the MIMU and expressed in R_{OMC}, whereas an erroneous term $\vec{\Delta} = (\Delta_{AP}, \Delta_{ML}, \Delta_V)$ was added to the vector $\overrightarrow{MIMU - sCoM}$ with $\Delta_i \in \{-0.02\ m, 0\ m, 0.02\ m\}$ for $i = AP, ML, V$.

The NRMSE between reference and MIMU-based SCoM and BCoM accelerations, referred hereafter as Y^{sCoM_i} and Y^{bCoM}, were then computed. This allowed to construct a so-called mechanical model for each SCoM or BCoM acceleration linking the NRMSE (outputs) to the input errors.

Using the experimental design methodology (Goupy, 2016), the relation between each component of the NRMSE (AP, ML, V) and the simulated mislocation of MIMUs along the AP, ML, and V axes (hereafter designated as "factors") can also be modelled with a polynomial model of degree up to 2 as described in equation (4), resulting in three models per MIMU (for the AP, ML, V components of the relevant SCoM acceleration) and for the BCoM:

$$Y_{stat}^{acc_i}(X) = b_0 + \sum_{i=1}^{n} b_i x_i + \sum_{i=1}^{n}\sum_{j>i} b_{ij} x_i x_j + \sum_{i=1}^{n} b_{ii}(x_i)^2 \quad (4)$$

where: $Y_{stat}^{acc_i}$ is the estimated NRMSE between reference and MIMU-based accelerations in the i direction (acc) and X is a vector containing the $n = 3N$ factors x_i corresponding to the positions of the N MIMUs used for the estimation (N = 1 for SCoM acceleration and N = 5 for BCoM acceleration).

Sensitivity of SCoM accelerations estimations

For each MIMU, three polynomial models were devised to emulate the SCoM acceleration along each axis of the OMC, following equation (4) with three input factors x_i: **p$_{AP}$, p$_{ML}$, p$_V$**, describing the MIMU position along the three axes of R_{OMC}. Then, after normalization of the factors' values into [- 1 ; 1], a three-level full factorial design allowed to choose the experimental points resulting in 3^3 combinations of the factors (i.e. 27 different position simulations) per MIMU (**Table 11**).

Choice of the polynomial model's complexity

The model complexity corresponds to the degree of the polynomial model and therefore depends on the inclusion of the interaction and/or quadratic terms in equation (4). The choice of polynomial model complexity is determined based on the residual variance of the polynomial model with respect to the mechanical model and will be justified in section 4.2.2.b.i.

Table 11 : Levels of the factors used for each polynomial model emulating a component of a SCoM acceleration

Factors	Level of the factors		
	Low-level (-1)	Mid-level (0)	High-level (+1)
p$_{AP}$ (m)	p$_{0AP}$ − 0.02	p$_{0AP}$	p$_{0AP}$ + 0.02
pML (m)	p0ML − 0.02	p0ML	p0ML + 0.02
p$_V$ (m)	p$_{0V}$ − 0.02	p$_{0V}$	p$_{0V}$ + 0.02

Quantification of the sensitivities

Based on the experimental design methodology, the influence of each factor (i.e., the coordinate of the simulated MIMU origin along each axis of R_{OMC}) on the accuracy of the SCoM acceleration estimate is defined as the total percentage of variance of the output due to this factor (Goupy, 2016). First, the sensitivity of the output $Y_{stat}^{acc_i}$ to each monomial (i.e., linear ($b_i x_i$), interaction ($b_{ij} x_i x_j$) or

quadratic term ($b_{ii}x_i^2$)) of the polynomial model is computed. With the input factors considered as independent and uniformly distributed in [-1, 1], the following equations can be written:

$$\begin{cases} s_i = var(b_i x_i) = b_i^2 var(x_i) = b_i^2 \times \frac{1}{3} \\ s_{ii} = var(bx_i^2) = b_{ii}^2 var(x_i^2) = b_{ii}^2 \times \frac{4}{45} \\ s_{ij} = var(b_{ij}x_i x_j) = b_{ij}^2 var(x_i)var(x_j) = b_{ij}^2 \times \frac{1}{9} \\ var(Y_{stat}^{acc_i}) = \sum_{i=1}^{6} s_i + \sum_{i=1}^{6} s_{ii} + \sum_{i=1}^{6}\sum_{j>i}^{6} s_{ij} \end{cases}$$

The sensitivity to the ith factor x_i can be obtained as follows:

- $S_i = s_i + \sum_j s_{ij}$ for the linear model with interactions
- $S_i = s_i + \sum_j s_{ij} + s_{ii}$ for the quadratic model with interactions

The sensitivities S_i were then expressed as a percentage of the total variance ($var(Y_{stat}^{acc_i})$)

Sensitivity of BCoM accelerations estimations

Three polynomial models of the highest complexity defined for the SCoM models were built for the BCoM accelerations sensitivity analysis following equation (4) with n = 15 factors corresponding to the three position factors of each of the five MIMUs. In order to limit the number of simulations (k^{15} with k the number of levels per factor), a two-level factorial design (factors taking the levels ± 1) was considered sufficient if the model was linear with interactions whereas a three-level factorial design (factors taking the levels ± 1 and 0) was implemented if the model was quadratic with interaction (Goupy, 2016). As for SCoM acceleration models, the suitability of the complexity chosen will be verified using an analysis of the residual variance of the polynomial models compared to the mechanical models.

4.2.2. Results

a. Reference and MIMU-based accelerations

Reference and MIMU-based estimations of the BCoM acceleration components in ML, AP and V directions are reported in **Figure 41**. Accuracy of the MIMU-based BCoM and SCoM accelerations in
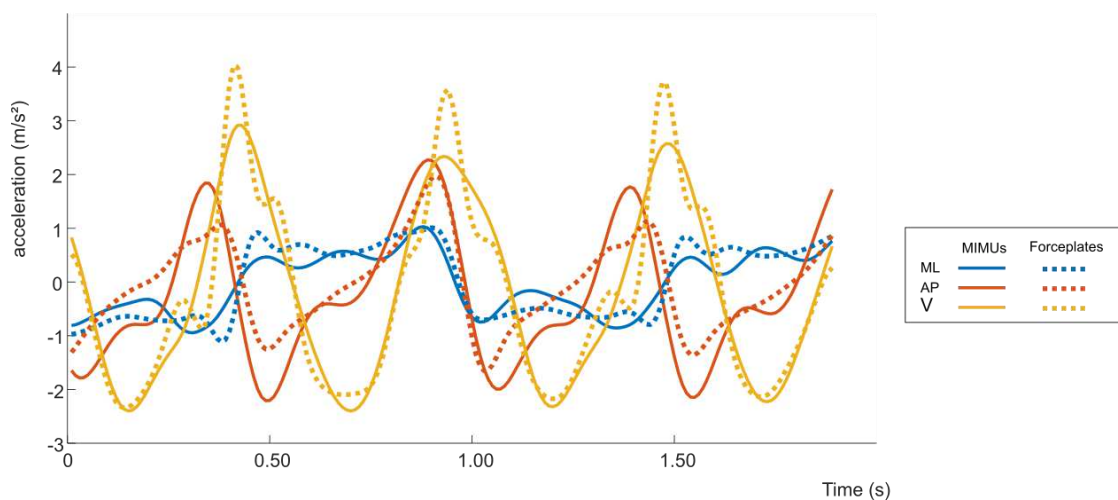
Figure 41: Comparison of BCoM accelerations obtained with MIMU (straight lines) and force plates (dotted lines) during one trial in the anteroposterior (AP), mediolateral (ML) and vertical (V) directions

terms of NRMSE values and correlation coefficients compared to the reference accelerations are presented in **Table 12**. It should be stressed that the MIMU-based estimations presented in **Figure 41** and **Table 12** were obtained with the correct identification of the sensor position, i.e. with $\mathbf{p_{0ML}}$, $\mathbf{p_{0AP}}$ and $\mathbf{p_{0V}}$ as defined with the rigid marker clusters (**Figure 40**). Results show relatively low errors (< 15.4 ± 2.5 % in AP, < 11.8 ± 1.3 % in ML, < 12.5 ± 2.0 % in V) and mostly good correlations between reference and MIMU-based accelerations (r > 0.77).

Table 12: Comparison of the computed SCoM and BCoM accelerations to reference values, quantified using the average and standard deviation of the NRMSE (%) and average Pearson's r correlations over the 6 trials.

			AP	ML	V
SCoM	Trunk	NRMSE (%)	14.1 (1.9)	9.8 (1.2)	5.2 (2.3)
		Pearson's r	0.77 (0.03)	0.94 (0.02)	0.98 (0.03)
	ThighS	NRMSE (%)	9.9 (2.2)	10.2 (1.3)	7.5 (2.0)
		Pearson's r	0.85 (0.10)	0.83 (0.08)	0.93 (0.06)
	ThighP	NRMSE (%)	12.5 (1.5)	5.7 (1.9)	5.5 (1.2)
		Pearson's r	0.89 (0.03)	0.96 (0.03)	0.97 (0.01)
	ShankS	NRMSE (%)	8.0 (1.8)	10.1 (1.5)	12.0 (1.5)
		Pearson's r	0.94 (0.04)	0.81 (0.13)	0.84 (0.05)
	ShankP	NRMSE (%)	4.8 (1.2)	5.8 (0.7)	12.5 (2.0)
		Pearson's r	0.98 (0.01)	0.97 (0.01)	0.87 (0.04)
BCoM	Whole Body	NRMSE (%)	15.4 (2.5)	11.8 (1.3)	8.7 (0.5)
		Pearson's r	0.93 (0.01)	0.94 (0.02)	0.95 (0.01)

b. Sensitivity analysis

i. Sensitivity of SCoM accelerations estimations

Choice of the polynomial model's complexity

Residual variances achieved by the polynomial models developed for the ML component of the SCoM acceleration of each segment are presented in **Table 13**. Residual variances of the same order of magnitude were observed for the other components of the acceleration. Both the quadratic and multilinear models with interactions presented low residual variances for all segments and axes (σ^2 ≤ 0.159, except for the prosthetic shank in the vertical direction - σ^2 ≤ 0.662) with the lowest values for the quadratic models (**Table 13**).

Table 13: Residual variances σ^2 of the linear model with interactions and quadratic model for each segment in the mediolateral direction

Model	σ^2 (Trunk)	σ^2 (ThighS)	σ^2 (ThighP)	σ^2 (ShankS)	σ^2 (ShankP)
Linear + interactions	0.095	0.147	0.044	0.143	0.065
Quadratic	< 0.001	0.001	0.001	0.002	<0.001

Based on these results, the linear model with interactions was considered as an optimal compromise between accuracy and simplicity. Indeed, the achieved maximal residual variance with the multilinear models (0.662) represents a standard deviation of $\sigma = 0.8\%$ which, compared to NRMSE of the order of 10% (**Table 12**), was considered as largely acceptable. The model complexity

corresponding to a first order polynomial model with interactions was selected for all MIMUs and all acceleration components. Therefore, all results presented hereafter were obtained using models with this complexity.

Quantification of the sensitivities

The results of the sensitivity analysis for each SCoM acceleration component (AP, ML, V) are summed up in **Figure 42**.
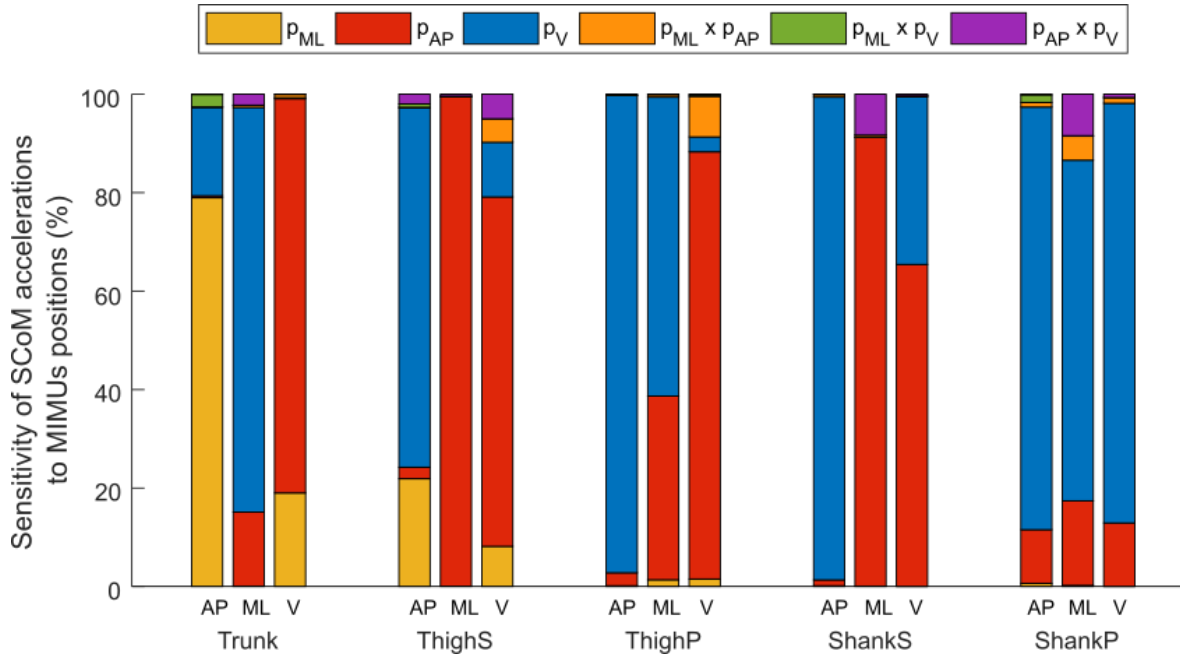
Figure 42: Sensitivities of the SCoM accelerations to each factor x_i and interactions between factors ($x_i * x_j$) with x_i ={p_{AP},p_{ML},p_V} expressed in percent of the total variance. For each MIMU location, the sensitivities of each component of the SCoM acceleration (AP, ML, V) to the factors are displayed

For the lower limbs, **p_{AP}** was found to be the major influencer for the ML and V components of SCoM acceleration, whereas **p_V** was the one for the AP component. Regarding the prosthetic shank, however, the influence of **p_V** dominated that of **p_{AP}** in all three directions. The trunk segment displayed a different behavior with respect to the other segments and was the only one where the MIMU mediolateral position **p_{ML}** displayed a prominent role. Finally, the interactions between factors showed minor influences on the accelerations' estimations. The most important influence of interaction factors was obtained for the prosthetic shank where the interactions between pML and pAP and between pAP and pV explained 15.1 % of the total variance of the rRMSE in the mediolateral direction.

The range of variation of the estimation accuracy Δ_{rRMSE_i} (%) caused by simulated errors in the identification of the MIMU positions over all the simulations are presented in **Table 14** for each component of SCoM acceleration (AP, ML, V). Errors in the identification of the MIMU positions resulted in modification of the estimation accuracy of SCoMs acceleration between $-1.6\ \% <$ $\Delta_{rRMSE_{AP}} < +1.7\ \%$ in AP, $-1.5\ \% <\ \Delta_{rRMSE_{ML}} < +1.6\ \%$ in ML and $-5.6\ \% <\ \Delta_{rRMSE_V} < +\ 6.8\ \%$ in V compared to the NRMSE obtained when these MIMUs positions were correctly identified (**Table 12**).

107

Table 14: Range of variation of the SCoM estimation accuracy Δ_{rRMSE_i} (%) caused by errors in the identification of the corresponding MIMU positions over all the simulations. Results are presented for each component of SCoM acceleration (AP, ML, V).

Trunk

	AP	ML	V
Lower range of Δ_{rRMSE_i} (%)	- 0.2	- 0.7	- 0.4
Upper range of Δ_{rRMSE_i} (%)	+ 0.2	+ 1.1	+ 0.6

Sound Thigh

	AP	ML	V
Lower range of Δ_{rRMSE_i} (%)	- 0.5	- 0.6	- 1.1
Upper range of Δ_{rRMSE_i} (%)	+ 0.3	+ 0.7	+ 1.1

Prosthetic Thigh

	AP	ML	V
Lower range of Δ_{rRMSE_i} (%)	- 1.6	- 1.4	- 1.1
Upper range of Δ_{rRMSE_i} (%)	+ 1.4	+ 1.5	+ 1.2

Sound Shank

	AP	ML	V
Lower range of Δ_{rRMSE_i} (%)	- 1.6	- 1.5	- 4.2
Upper range of Δ_{rRMSE_i} (%)	+ 1.7	+ 1.6	+ 3.7

Prosthetic Shank

	AP	ML	V
Lower range of Δ_{rRMSE_i} (%)	- 1.1	- 0.5	- 5.6
Upper range of Δ_{rRMSE_i} (%)	+ 1.1	+ 0.8	+ 6.9

ii. Sensitivity of BCoM acceleration estimations

Choice of the polynomial model's complexity

The three multilinear models including interactions developed for the sensitivity analysis of the BCoM acceleration presented low residual variances values ($\sigma^2 \leq 10^{-3}$) (**Table 15**).

Table 15: Residual variances σ^2 of the linear model with interactions for each BCoM component

Model	**σ^2 (AP)**	**σ^2(ML)**	**σ^2 (V)**
Linear+ interactions	< 0 .001	0.001	< 0 .001

Consequently, a two-level factorial design was considered to be sufficient to emulate the mechanical models corresponding to the BCoM acceleration. The sensitivity analysis was subsequently performed with the 15 factors of the models resulting in 2^{15} simulations.

Figure 43 highlights the factors that have the most influence on the accuracy of the estimation of each component (AP, ML, V) of the BCoM acceleration. For better readability and clarity, only the factors accounting for more than 1 % of the total variance are shown in the figure. The BCoM acceleration appears to be mostly sensitive to trunk, sound thigh and sound shank factors, particularly to the anteroposterior and vertical localizations of the MIMUs mounted on these segments. Indeed, all together, p_{AP} **Trunk, p_V Trunk, p_{AP} ThighS, p_V ThighS, p_{AP} ShankS**, and **p_V ShankS** explain 92 %, 77 % and 79% of the sensitivity of the estimation of the AP, ML, V BCoM acceleration components respectively. It should be noted that the anteroposterior localization of the trunk MIMU only as a significant impact on the mediolateral component of the BCoM acceleration (accounting for 10.5 % of the total variance).

Similarly to the SCoM analysis, the NRMSE ranges of the variation Δ_{rRMSE_i} (%) obtained over all the simulations, when simulating an error in the identification of MIMUs positions was computed (**Table 16**). The different combinations of errors in the identification of the MIMUs positions resulted in modification of the estimation accuracy of the BCoM acceleration between − 3.4% and + 2.8 % compared to the NRMSE obtained when these MIMUs positions were correctly identified (**Table 16**).
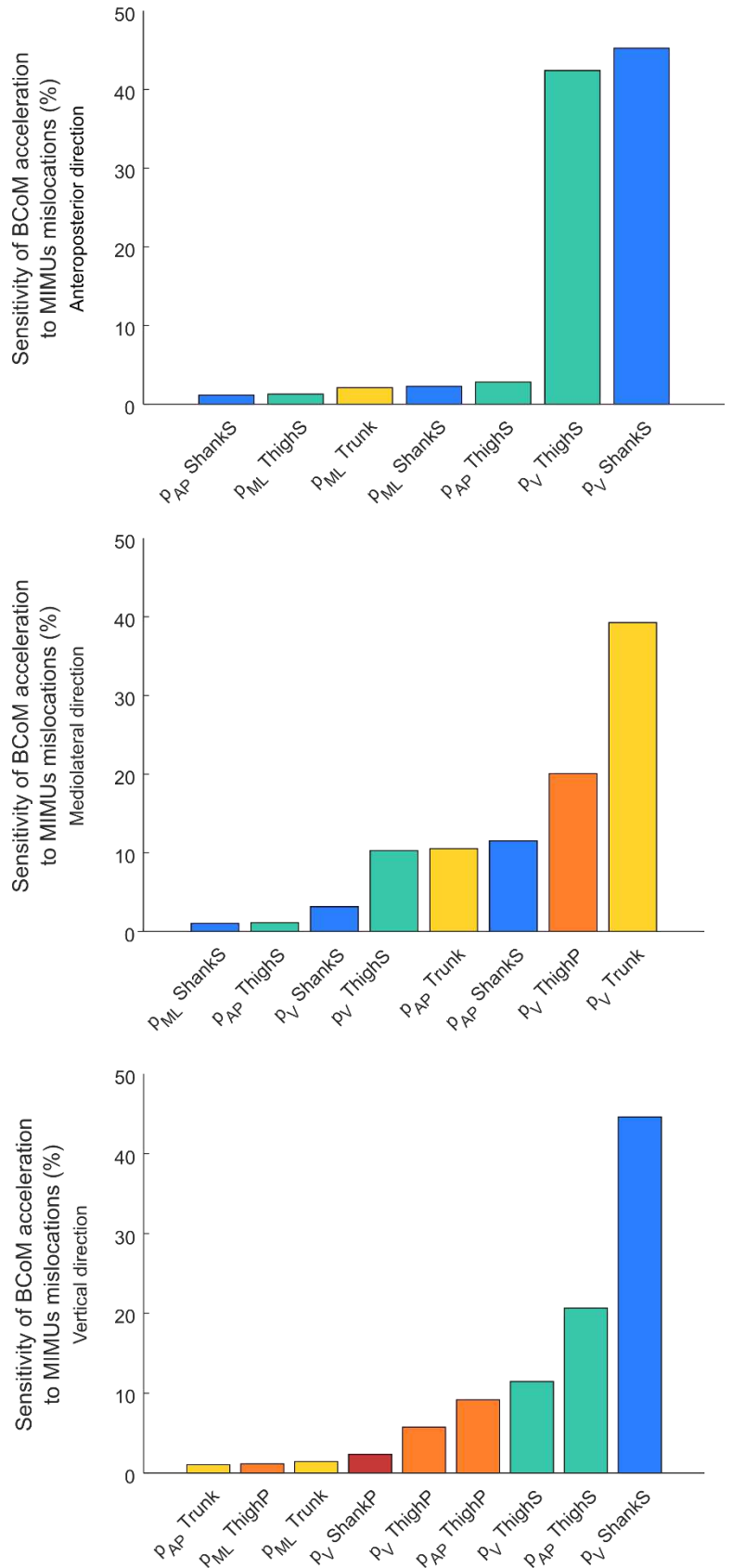
Figure 43: Barplot of the results of the sensitivity analysis expressed in % of total variance for each BCoM acceleration component (ML, AP, V). Sensitivities are presented here for the factors x_i and interactions between factors ($x_i * x_j$) that account for more than 1% of the total variance.

Table 16: Maximum range of variation of the estimation accuracy Δ_{rRMSE_i} (%) caused by errors in the identification of the MIMUs positions over all the simulations. Results are presented for each component of BCoM acceleration (ML, AP, V).

	AP	ML	V
Lower limit for Δ_{rRMSE_i} (%)	- 3.4	- 2.2	- 1.0
Upper limit for Δ_{rRMSE_i} (%)	+ 2.8	+ 2.3	+1.4

4.2.3. Discussion

The present work investigated the impact of the incorrect identification of the position of five segment-mounted MIMUs on the estimation of the corresponding SCoM and BCoM accelerations.

a. Reference and MIMU-based accelerations

The implemented MIMU-based framework for the estimations of SCoM and BCoM accelerations provided relatively accurate results (high agreement: r > 0.77, and low errors: < 15.4 % in AP, < 11.8 % in ML, < 12.5 % in V) compared to reference-based acceleration. Overall, SCoM acceleration estimations showed higher agreements at the prosthetic limbs than at the sound limbs. This can be due, in part, to the fact that MIMUs positioned on the prosthetic limb are not affected by soft-tissues artefacts contrary to those positioned on the sound limbs.

b. Sensitivity Analysis

Using an experimental design methodology, the sensitivity of each component of the SCoM and BCoM accelerations to errors in the identification of each MIMU position was estimated using optimal polynomial models.

i. Sensitivity of SCoM acceleration estimations

Quantification of the sensitivities

The sensitivity analysis allowed to identify the factors having the greatest influence on the accuracy of the estimations of the accelerations of each SCoM. For the lower limbs, incorrect location along the anteroposterior axis mainly influences the vertical component of the acceleration, whereas incorrect location along the vertical axis impacts mainly the mediolateral and anteroposterior acceleration components. It is worth noting that for the prosthetic shank, the vertical localization of the MIMU displays a dominant role over the anteroposterior one even for the vertical component of the acceleration. The localization of MIMUs along the mediolateral direction was shown not to have a major impact on the estimation of their corresponding SCoM acceleration, except for the trunk and to a lesser extent for the sound thigh. This may be explained by the fact that, during gait, the angular velocity of the lower limbs is mainly directed around the mediolateral axis and has a very low magnitude around the vertical axis. Consequently, modifications of the MIMU positions along the flexion-extension axis of the lower-limb segments are not expected to have a major impact on SCoM accelerations (see equation (1) and the properties of the cross-product). This observation shows that the influence of errors in the identified position of MIMUs depends on the considered segment / motion. This has to be particularly taken into consideration in altered gait patterns such as those of people with amputation.

Importantly, erroneous identification of MIMU positions of ± 0.02 m triggered errors between − 5.6 % < Δ_{NRMSE} < +6.9 % for all SCoMs and all acceleration components considered, but only between

- 1.6 % < Δ_{NRMSE} < +1.7 % when the shanks are not considered. Considering NRMSE of the order of 10 % between MIMU-based measurement and reference values, these variations cannot be considered negligible, especially for the shanks. The higher impact of erroneous position identification of shank-mounted MIMUs on the estimated accelerations of their respective SCoM could be explained by the high angular velocity of the shanks compared to the other segments considered. Taken together, these observations suggest that specific attention must be given to the correct identification of the sensor positions, especially for the AP and V directions and for the shank-mounted MIMUs, in order to limit the resulting errors.

ii.   Sensitivity of BCoM acceleration estimations

Quantification of the sensitivities

The results observed for the sensitivity of SCoM acceleration estimations clearly impacted those related to the BCoM acceleration. For a given segment, the direction of the MIMU localization error (AP, ML, V) that was shown to be the most influent for the SCoM acceleration estimation accuracy also played a role in the accuracy of the BCoM acceleration estimate. For instance, erroneous identification of the positions of sound shank-mounted MIMU along the vertical direction was found to greatly influence the BCoM acceleration estimates in the AP direction as was observed for the SCoM (**Figure 43**, **Figure 42**).

Variations in NRMSE of up to 2.8 %, 2.3 % and 1.4 % were observed in AP, ML and V directions respectively. The higher NRMSE variations for the AP and ML components might be explained by the lower amplitude of BCoM acceleration along these directions compared to that along the vertical direction (**Figure 41**). These variations should also be interpreted at the light of the accuracy obtained between MIMU- and reference-based acceleration estimation, namely NRMSE of the order of 15 % in ML and AP, and 5 % in V (**Table 12**). It is interesting to note that the BCoM acceleration was more affected that the SCoM accelerations in the AP and ML direction but not in the vertical direction. This may be due to the fact that for the SCoM, the maximal variations of NRMSE along the vertical direction were obtained for the shank segments, which have a lower mass compared to that of the thighs and trunk, especially for the prosthetic side. Therefore, when computing the BCoM acceleration from a weighted sum of the SCoM acceleration, the variability in the shanks SCoM acceleration accuracy had a lower impact on the BCoM.

Comparison of the present results with the existing literature must be performed with caution due to the different methodologies and target parameters. Specifically, Tan and coworkers (Tan *et al.*, 2019) used a one-at-a-time sensitivity analysis to assess the impact of MIMU placement errors on the estimation of ground reaction force (GRF). In this case, interactions of several MIMU placement errors were not considered. The authors reported that, when a single sensor was misplaced, the accuracy of GRF estimation was decreased by up to 0.9 %, 2.2 %, and 1.1 % in the AP, ML and V directions respectively. It is interesting to stress that in (Tan *et al.*, 2019), no sensor was revealed as having a significantly dominant impact on the accuracy of the GRF estimation. This may be due to the fact that the authors implemented a machine learning framework for the estimation of GRF from raw data of segment-mounted MIMUs, without *a priori* attributing more weight to specific sensors. This machine learning framework may also explain the fact that the magnitude of positioning errors (0.1 m vs 0.02 m) had a negligible influence on the accuracy of the GRF estimation.

The results of the sensitivity analysis performed on BCoM accelerations in the present study advocate the need for an accurate detection of MIMUs positions, especially for the trunk , sound thigh and shank along both the vertical and anteroposterior directions. The important influence of the localization of the trunk and sound thigh might be explained by the fact that they are the heaviest segments of the body and that BCoM acceleration is estimated using a weighted average of SCoM acceleration based on their mass. The sound shank influence may therefore result from the higher angular velocity of shanks segments (almost twice that of the other included segments) while walking and the relatively high mass of the sound shank compared to prosthetic segments. Limiting the errors in the estimations of SCoM accelerations, especially at the shank, is expected to have a positive impact on the accuracy of the whole-body CoM acceleration estimates. Indeed, if a particular attention is given to the identification of the positions of these three MIMUs in the AP and V directions, the variations in NRMSE previously observed may be reduced from 2.8 %, 2.3 % and 1.4 % to 0.9 %, 0.7 %, 0.6 % in AP, ML and V directions, respectively.

c. Limitations and perspectives

The generalizability of the discussed results must be interpreted at the light of the following considerations: first, a larger cohort of participants are needed to confirm present findings. Second, simulated errors in the identification of MIMUs positions were introduced along the axes of the reference frame R_{OMC}, therefore, results could be different if MIMUs were misplaced along the axes of the segments anatomical frames. However, the errors introduced in the simulations covered a cubic zone centered on the correct location of the MIMU's origin. Furthermore, the static calibration phase was performed with the patient standing in an upright posture facing the direction of progression so that segment anatomical axes were assumed to be aligned with those of the global frame R_{OMC} (one axis aligned with the gravity and one axis with the direction of progression). It can be thus assumed that, in case the anatomical frame should be considered instead of R_{OMC}, the position identification errors would cover a similar cubic zone, leading to negligible variations in the obtained sensitivities. Moreover, it is worth underlining that the 0.02 m range of errors in the identification of MIMU positions is a conservative value, being the maximum error observed (see section 4.1), and thus representing a worst-case scenario presumably covering the range of errors that would be observed in practice. Finally, in the present study, the impact of MIMU orientation errors was not investigated despite the latter was found to critically impact the accuracy of GRF estimation (Tan *et al.*, 2019). It should be considered, however, that in (Tan *et al.*, 2019) raw MIMU signals were used as inputs of a machine learning model and were not expressed in a global or anatomical reference frame. Conversely, in the MIMU-based framework proposed in the present study, the SCoM accelerations were expressed in a global reference frame before being summed to estimate the BCoM acceleration. Errors typical of sensor-fusion filters used to obtain MIMU 3D orientation remain to be considered. However, these errors are expected to have a minor impact with respect to what reported in (Tan *et al.*, 2019). Further studies should verify this hypothesis and quantify the impact of orientation errors on both SCoM and BCoM accelerations.

4.2.4. Conclusion

The present study investigated the impact of an erroneous identification of the positions of a set of body-mounted MIMUs on the estimation accuracy of SCoM and BCoM accelerations during walking

in a subject with transfemoral amputation. An optical motion capture system and force plates were used as reference for SCoM and BCoM accelerations estimates, respectively. The performed sensitivity analyses allowed to identify the MIMUs whose localization along certain axes allowed to reduce the variation of errors in the estimated SCoM and BCoM accelerations. Specifically, an accurate identification of MIMUs positioned on the trunk and sound lower limbs along the anteroposterior and vertical axes was proved to limit the variability of the accuracy of the estimated BCoM acceleration below 1 %. These preliminary results need to be confirmed on a larger cohort. Future works are also required in order to consider also the impact of MIMU orientation errors on the estimated accelerations.

Conclusion

This part of the thesis aimed at contributing to the development of a wearable gait analysis protocol for the estimation of 3D body center of mass (BCoM) motion.

Several strategies have emerged from the literature (chapter 1) to estimate BCoM acceleration, velocity or displacement, using one to several MIMUs. While single-sensor approaches may overestimate BCoM motion, in particular in people with lower-limb amputation, finding a balance between accuracy and the number of MIMUs is crucial for the application of wearable protocols in the clinical field. Therefore, in chapter 2, the contributions of each segment to the BCoM acceleration were investigated in order to identify the optimal locations for sensor positioning. Several optimal sensor networks (OSN), including three to six segments, appeared relevant for the estimation of BCoM acceleration in people with transfemoral amputation. However, the study was implemented with optical motion capture data of ten people with transfemoral amputation. When using MIMUs mounted on body segments, obtaining the acceleration of segments centers of mass in a global reference frame is not direct. Furthermore, MIMUs cannot always be positioned on bony landmarks and may therefore be more subjected to soft tissue artefacts. As a result, the identified OSN may not be as successful when using wearable sensors. The aim of chapter 3 was therefore to investigate the suitability of MIMUs for the estimation of 3D BCoM motion, and was further divided in three objectives: *i)* introducing a fully wearable framework for gait analysis, *ii)* verifying that the OSN identified in chapter 2 were indeed relevant when using wearable sensors and *iii)* investigating the suitability of the identified OSN and developed framework for the estimation of instantaneous BCoM velocity. A set of 5 MIMUs positioned on the thighs, shanks and trunk were shown to allow an accurate estimation of these quantities. It has to be noted that, if the output measure of interest is BCoM acceleration in the anteroposterior and/or vertical directions, the thigh-mounted sensors can be removed while increasing the accuracy. The developed framework was thus successful in allowing the accurate estimation of BCoM acceleration and instantaneous velocity from a limited number of sensors (NRMSE ≤ 16.7 %, 14.0 % and 7.7% in the anteroposterior, mediolateral and vertical directions). The results obtained in chapter 3 should be confirmed on a larger cohort in order to further validate the relevance of MIMUs as an alternative to lab-based instruments for the retrieval and analysis of 3D BCoM motion in people with transfemoral amputation. Furthermore, the framework currently requires the use of an optoelectronic system. However, a wearable alternative could be easily developed in order to facilitate its implementation outside of dedicated laboratories: it could easily rely on either a 3D body scan or a camera associated with a simple calibration device. The dependency of the results on the identification of MIMUs positions relative to the segments center of mass would still be an issue. Therefore, in chapter 4, a sensitivity analysis was performed to investigate the impact of erroneous identification of MIMUs' positions on the estimation of the BCoM acceleration estimated using the OSN consisting of trunk, thighs, and shanks mounted MIMUs. Imprecisions in positioning of each MIMU of up to 2 cm in any direction induced a decrease of BCoM acceleration accuracy of up to 3.9 %, 4.6 % and 2.6 % in the anteroposterior, mediolateral and vertical direction respectively. Sensors located at the trunk and the sound thigh and shank were shown to explain most of the observed variance (more than 80 %, 81 % and 66 % in the anteroposterior, mediolateral and vertical directions respectively). A precise positioning of these sensors appears crucial for an accurate estimation of BCoM acceleration as it allows to reduce the decrease of accuracy of the BCoM acceleration estimate to 1.5%, 1.7% and 1.2%

in the anteroposterior, mediolateral and vertical directions respectively. The conclusions could differ when using other segment models. However, as the sound leg and the trunk represent the heaviest segments of the body, their influence on BCoM acceleration accuracy is expected to be prominent in other OSN including these segments. The methodology proposed in this chapter could also be applied to other BCoM derived parameters, such as the instantaneous velocity of the center of mass.

All in all, the work achieved in this direction tend to indicate that MIMUs are a valid alternative for the estimation of 3D BCoM motion in people with transfemoral amputation. Results should be confirmed on a larger cohort and validation should be extended to other BCoM-derived parameters such as 3D BCoM displacement or power. The former would require a supplementary integration step and the knowledge of the initial absolute position of the BCoM. Regarding the latter, further developments are needed since BCoM power can be estimated from the sum of the scalar product of instantaneous BCoM velocity with the ground reaction force under each foot. Several algorithms have been proposed for the smooth distribution of the ground reaction force between both feet, but they may not be adapted to people with lower-limb amputation.

Part 3: Characterization of gait quality in people with lower-limb amputation using concise parameters issued from wearable signal processing

In the previous part, the feasibility of using wearable sensors to derive biomechanical parameters, such as the instantaneous body center of mass acceleration and velocity, has been demonstrated. As illustrated in the literature review of Part 1, wearable sensors have also been proposed to characterize gait using parameters computed through simple signal processing or through the identification of features in raw signals, without requiring the development of complex biomechanical models of the human body. As for parameters based on biomechanical models, these signal-processing-based gait descriptors must also be validated for a specific population and use. The aim of this third part is, therefore, to target these parameters in order to investigate whether wearable sensors could be used to obtain intelligible and clinically relevant quantitative information. This could be done without long set-up and processing times that are often required to characterize and monitor the gait of people with lower-limb amputation along their rehabilitation.

In particular, the overview of the literature in Part 1 allowed to identify several parameters for the quantitative assessment of gait symmetry and balance control during gait that require neither a large number of sensors nor a complex modeling of the human body, making them more mature for a transfer to clinical environment. Indeed, monitoring gait symmetry and assessing the risk of falling are both crucial elements of the rehabilitation of a person with lower-limb amputation as these aspects were shown to lead to the development of comorbidities and have an impact on the activity or social participation level after discharge from the rehabilitation center (Gailey *et al.*, 2008; Highsmith *et al.*, 2016). Furthermore, tracking and quantifying gait (a)symmetry along the rehabilitation process can assist clinicians in refocusing rehabilitation strategies and targets (Cutti *et al.*, 2018). While some aspects of gait (a)symmetry can be visually identified by observing the gait pattern and paying attention to feet placement while walking, other aspects, such as loading asymmetry (see Part 1, section 2.3.3.a.i) or poor balance are difficult to quantify with the naked eye. All these gait deficiencies are hardly tracked accurately in the clinical routine due to the lack of ecological and quantitative assessment tools.

Falling risk might be assessed through aggregate scores, such as the Berg Balance Scale or through clinical walking tests. The Berg Balance Scale consists in 14 balance/mobility exercises rated from 0 to 4 depending on the time required to accomplish the task. Although this aggregate score was shown to be valid for fall risk assessment in people with lower limb amputation, it was not able to distinguish people at greater risk of falling and may therefore lack of sensitivity (Major *et al.*, 2013). Furthermore, the Berg Balance Scales requires fifteen to twenty minutes for administration, which compromises its frequent use during the rehabilitation. Clinical walking tests on the other hand are easily performed in the rehabilitation due to the simple short set-up and acquisition time, but they result in a single quantitative data, characterizing the performance in realizing the test through the measure of the time needed or distance covered during the test. The achieved score allows to characterize the overall gait performance but does not capture the way this performance is obtained: a higher score could for example be achieved by someone walking faster although with increased gait asymmetry. Since

117

asymmetry may lead to comorbidities, improvement in performance should be interpreted with caution. Due to the sensitivity and rapidity of administration of these standardized clinical walking tests, it appears relevant to instrument them with wearable sensors in order to retrieve additional objective and quantitative metrics allowing the simultaneous characterization of both gait performance and quality in the clinical field.

With wearable sensors, gait symmetry can be quantified by comparing the duration of the sound and prosthetic limb stance phases, which is possible once gait events are detected with pressure insoles (by using a threshold on the estimated vertical component of the ground reaction force) or IMUs (by identifying features in IMU signals indicative of a gait event). In the latter case, a large number of algorithms have been proposed using IMUs on the shanks, feet or on the pelvis for gait event detection with no indications regarding the most suited to transfemoral prosthetic gait. Furthermore, the algorithms were validated in the literature for the detection of gait events and for the estimation of temporal parameters but their accuracy in estimating temporal asymmetry was not verified. Therefore, a complete comparative analysis of the algorithms developed for the people with lower-limb amputation appears relevant.

Other parameters quantifying gait symmetry have been proposed by computing metrics based on signal processing. As an example, the improved harmonic ratio, computed using the Fourier decomposition of the acceleration measured by a pelvis-mounted MIMU, has been largely adopted in recent years to describe overall gait symmetry (see Part 1, section 3.2.3.a.i). This parameter offers the advantages of requiring a single IMU and of providing a global score for the symmetry of locomotion. However, its interpretation may not be straightforward as it does not provide indications relative to the origin(s) of the detected asymmetry.

Regarding balance control assessment during gait, several authors have proposed to equip the upper body with three IMUs located at pelvis, sternum and head levels. The ratio of the root mean square of the measured acceleration at two subsequent levels are computed in order to investigate the transmission of accelerations from the lower limbs to the head (Summa *et al.*, 2016; Bergamini *et al.*, 2017; Belluscio *et al.*, 2018; Paradisi *et al.*, 2019). The underlying idea is that, in typical gait, accelerations are attenuated from lower to upper body levels in order to stabilize the optic flow, allow for a more effective processing of the vestibular system signals, and a consequent control of equilibrium (Berthoz and Pozzo, 1994). Therefore, assessing the acceleration pattern as well as their attenuation from the lower limbs to the head seems relevant for the assessment of fall risk.

The validity, accuracy and reliability of the above-mentioned parameters quantifying symmetry or dynamic balance retrieved using IMUs and pressure insoles should be investigated in people with lower-limb amputation, so as to verify their relevance for clinical assessment during the rehabilitation. In particular, it should be verified that the above-mentioned parameters do measure what they are intended to measure (the "construct") and that they allow to discriminate people with different level of the construct (here, it would be the ability to discriminate within people with lower-limb amputation those who are at a higher risk of falling or those who present higher gait asymmetry) (Portney and Watkins, 2015). The reliability of a parameter refers to the level of consistency between two measurements of the same parameter in the same circumstances. It allows to determine the minimal detectable change, that is, the minimal difference observable that can be considered as reflecting a real change in the parameter and not as measurement error or inherent variability. This value must be

118

confronted with the minimal clinically important difference which reflects when a change in the value of the parameter reflects a positive or negative change from a clinical point of view. Quantifying all these aspects requires a large amount of research and represents the first crucial step towards the transfer of these wearable gait quality indices from research to the clinical field (Portney and Watkins, 2015).

This part of the thesis aims at contributing to gaining insight on these concise parameters and algorithms in the prospect of using these parameters for gait quality assessment during the rehabilitation of people with lower-limb amputation. The feasibility and validity of characterizing gait symmetry and balance control in people with lower-limb amputation using these parameters will be explored. In the first chapter, the feasibility of assessing temporal symmetry in people with transfemoral amputation using IMUs and various gait event detection algorithms will be investigated by comparing state-of-the-art algorithms retrieved in the literature. Then, in a second chapter, the relevance of using symmetry or balance descriptors derived from signal processing of wearable sensors during the rehabilitation will be investigated on a cohort of nine people with transtibial amputation and nine asymptomatic subjects. A special focus on the improved harmonic ratio will be proposed in this chapter in order to overcome limitations in its computation and interpretability.

Chapter 1 – Feasibility of determining temporal symmetry from MIMUs in people with transfemoral amputation

In recent years, inertial measurement units (designated as IMUs in this chapter, since no magnetometer is required) have been proposed as an alternative to force platforms and pressure sensors for the detection of gait events (i.e. initial and final contacts). Gait event detection is indeed crucial for gait analysis as it allows gait cycle segmentation, which is often necessary for the analysis of biomechanical features within kinematic or kinetic data or even for the computation of stride-related parameters. Furthermore, the time interval between different gait events allows to define the different phases of the gait cycle and therefore to compute spatiotemporal parameters. While multiple algorithms have been developed in the literature (see Pacini Panebianco et al. 2018), no recommendation on the most suited algorithm for transfemoral prosthetic gait could be retrieved in the literature. Furthermore, despite the clinical importance of (a)symmetry quantification in lower-limb amputee gait, the impact of gait event timing errors on gait (a)symmetry has never been investigated in people with transfemoral amputation walking freely on level ground.

Therefore, the aim of this study was to implement and compare five algorithms taken from the literature to assess their accuracy in providing temporal parameters and estimating gait asymmetry in people with transfemoral amputation during level walking.

This study was published in the review *Medical & Biological Engineering & Computing:*

E. Simonetti, E. Bergamini, C. Villa, J. Bascou, G. Vannozzi, H. Pillet. **Gait events detection using inertial measurement units in people with transfemoral amputation: a comparative study**, Medical & Biological Engineering & Computing, 58:461–470 (2020).

1.1. Introduction

The accurate detection of gait events (GEs) is crucial for the biomechanical assessment of gait function in people with pathological walking patterns (Perry, 1992). The identification of initial contact (IC) or final contact (FC) events, respectively marking stance initiation and termination, allows for gait cycle segmentation and is essential to extract and interpret relevant features from biomechanical and physiological gait variables such as joint angles or muscle activity (Perry, 1992).

In people with lower-limb amputation, whose gait is known to be highly asymmetrical due to joint function loss (Nolan *et al.*, 2003; Bastas *et al.*, 2018), the identification of gait phases is particularly relevant for both prosthetic design and rehabilitation fields. For example, micro-processor-controlled prostheses generally adopt different behaviors according to the gait cycle phase (Ledoux, 2018). Furthermore, stance or swing phase durations and temporal symmetry indices are widely used to evaluate gait in the clinical field. Quantifying these parameters can indeed assist therapists in decision-making during rehabilitation, as well as in prosthetics prescription, fitting and alignment (Aminian *et al.*, 2002; Cutti *et al.*, 2015; Bastas *et al.*, 2018).

In recent years, wearable sensors, such as pressure insoles or inertial measurement units (IMUs), have been proposed as a portable and low-cost alternative to force platforms, instrumented mats or treadmills for the detection of GEs. While some specific pressure insoles have been validated against force platforms (Barnett *et al.*, 2001; Loiret *et al.*, 2019), their use is limited to the obtention of GEs

and vertical ground reaction forces. On the other hand, IMUs, which include accelerometers and gyroscopes, can provide kinematic information in addition to GE detection. Thus, multiple algorithms have been developed for IC and FC identification from linear accelerations and/or angular velocities measured by IMUs (Pacini Panebianco *et al.*, 2018). Many authors have recommended the use of a single sensor at pelvis level to minimize invasiveness and gait alteration (Zijlstra and Hof, 2003; González *et al.*, 2010; Bonnet *et al.*, 2012; Köse *et al.*, 2012; Bastas *et al.*, 2018). However, in pathological gait, a robust detection of both IC and FC events is compromised because of gait inherent variability and stronger attenuation of feet-ground impacts at trunk level (Trojaniello *et al.*, 2015; Pacini Panebianco *et al.*, 2018). Consequently, algorithms based on the use of two IMUs located on both shanks (Salarian *et al.*, 2004; Selles *et al.*, 2005; Jasiewicz *et al.*, 2006; Catalfamo *et al.*, 2010; Greene *et al.*, 2010; Trojaniello, Cereatti, Pelosin, *et al.*, 2014; Maqbool *et al.*, 2017; Bertoli *et al.*, 2018; Ledoux, 2018) or feet (Sabatini *et al.*, 2005; Jasiewicz *et al.*, 2006; Mariani *et al.*, 2013) have been developed and are generally considered to be more accurate (Trojaniello, Cereatti, Pelosin, *et al.*, 2014; Trojaniello *et al.*, 2015; Pacini Panebianco *et al.*, 2018).

Given the number of available algorithms, the comparison of their accuracy in GE detection is relevant. However, most studies differ in their acquisition protocol, in the population investigated and in the reported results, which makes the comparison challenging. Indeed, while the accuracy of the timings of detected GEs is always discussed, the ability of the algorithms to detect all GEs without false positives, or the consequence of the timing errors on clinically relevant parameters, such as cycle durations or symmetry indices, is not always disclosed. Although there have been some attempts in performing comparative studies in the literature (Jasiewicz *et al.*, 2006; Trojaniello, Cereatti and Della Croce, 2014; Trojaniello *et al.*, 2015; Storm *et al.*, 2016), none focused on people with transfemoral amputation (TF). In addition, as most algorithms rely on the extraction of specific features from IMU signals, some may not be relevant for the population of TF because of deviations in their gait pattern, such as hip hiking, vaulting, delayed knee flexion, and temporal and spatial asymmetries (Nolan *et al.*, 2003; Loiret *et al.*, 2019).

This work aimed at comparing the performance of different state-of-the-art algorithms in TF walking freely on level ground. Performance was quantified in terms of i) sensitivity and positive predictive value of GE detection, ii) accuracy of GEs timings and iii) accuracy of derived temporal parameters and of stance phase duration Absolute Symmetry Index (SPD-ASI) values. Furthermore, the robustness to different walking speeds was also investigated. Data from pressure insoles validated against force platforms in people with transfemoral amputation (Loiret *et al.*, 2019) were used for reference values assessment.

1.2. Material and methods

1.2.1. Participants

The study was designed according to the Declaration of Helsinki, and was granted ethical approval (CPP IDF VI, N° 2014-A01938-39). Seven TF (age: 47.3 ± 9.9 years, 5 males, mass: 74.5 ± 11.9 kg; height: 1.80 ± 0.10 m) gave written informed consent to participate in the study (**Table 17**). Inclusion criteria were people with transfemoral unilateral amputation due to trauma or tumor, fitted with a definitive prosthesis, able to walk at various speeds without any assistance. The participants walked with their

usual passive microprocessor-controlled knee with an energy storing and return foot, the alignment of which was controlled by a prosthetist prior to data collection.

	Age (years)	Height (m)	Mass (kg)	Gender	Etiology	Time since amputation (years)	Prosthetic Knee	Prosthetic foot	Average self-selected walking speeds (m.s^{-1})		
									Slow	Comfortable	Fast
TF01	47	1.54	72	F	Tumor	35	Rheo Knee	Variflex LP	0.72	1.02	1.25
TF02	52	1.69	75	M	Trauma	34	Rheo Knee	Variflex XC	0.92	1.13	1.48
TF03	34	1.70	51	F	Tumor	27	C-Leg	Trias	0.92	1.04	1.40
TF04	43	1.90	82	M	Trauma	5	C-Leg	Triton	1.00	1.16	1.35
TF05	64	1.84	86	M	Trauma	6	Rheo Knee	Talux	0.49	0.76	0.96
TF06	39	1.79	85	M	Trauma	3	C-Leg	Triton	0.89	1.06	1.25
TF07	52	1.84	72	M	Trauma	23	C-Leg	Pro-Flex	0.89	1.20	1.61

Table 17: Participants characteristics.
The prosthetic devices are from Ottobock (C-Leg, Triton, and Trias) and from Ossür (Rheo Knee, Variflex LP, Variflex XC, Talux and Pro-Flex)

1.2.2. Measurement protocol

Three IMUs (MTw xSens, Netherlands, 100 samples·s-1), embedding a tri-axial accelerometer (± 16 g) and a tri-axial gyroscope (± 2000 deg/s), were used and positioned on the lower trunk (L4/L5 level) and on both shanks (laterally, below the tibial tuberosity level) of each participant (**Figure 44**). IMUs were manually aligned with the anatomical axes of the underlying segments. Reference GE were obtained using pressure insoles (Loadsol, Novel, Germany, 100 samples·s-1). These insoles have been reported to be reliable and to accurately estimate both vertical ground reaction force and stance phase duration in TF (Loiret *et al.*, 2019) and were, thus, considered a valid gold standard.
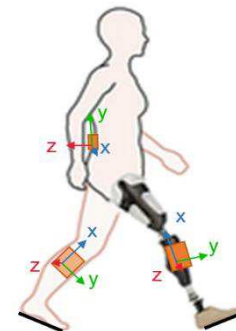
Figure 44: Placement of the inertial measurement units and their associated local frames

Participants walked freely along an 8-meter level walkway, at three self-selected speeds (slow, comfortable and fast), measured with a stopwatch. At least three trials of each condition were recorded. The average walking speeds of each participant are reported in **Table 17**. Participants were asked to stand upright for at least 3 seconds at the beginning and at the end of each trial, and to perform a downward kicking motion with the heel of their sound foot to synchronize the IMUs with the insoles.

1.2.3. Data processing

IMUs and insoles data were post-processed using MATLAB® software (The MathWorks Inc., MA, US). Synchronization was performed semi-automatically by aligning the kicking-motion peaks in the sound-limb shank vertical acceleration and insole signals.

a. IC and FC events detection

Reference IC and FC events were identified using a 20 N threshold on the insoles' ground reaction force signals (Selles *et al.*, 2005; Loiret *et al.*, 2019).

Regarding the IMUs' signals, five GE detection algorithms were selected based on a literature review. The first three algorithms were the only one retrieved that were specifically designed for people with lower-limb amputation. The two remaining algorithms were selected as they are representative of the state-of-the-art and appeared to be promising candidates in TF. Indeed, one of them was validated on an extensive cohort of people with different pathologies that significantly affected gait, and the second one used only one sensor, which is an interesting perspective for clinical applications. The algorithms, designated by the acronyms M-N, with N the initial(s) of the first author's name, are introduced hereafter:

1) M-S: based on shank vertical and anteroposterior acceleration signals, validated against force platform data in ten people with transtibial amputation (TT) (Selles *et al.*, 2005),

2) M-M: based on shank mediolateral angular velocity, validated using footswitches in eight asymptomatic subjects and in two people with lower-limb amputation (one TT and one TF) (Maqbool *et al.*, 2017),

3) M-L: based on shank mediolateral angular velocity, flexion-extension angle and axial acceleration, validated on five TF walking on an instrumented treadmill (Ledoux, 2018),

4) M-T: based on shank mediolateral angular velocity and accelerations, validated against pressure mat data on an extensive cohort consisting of 80 elderly, 125 people with Parkinson's Disease, 31 people with mild cognitive impairment and on ten persons with hemiparesis (Trojaniello, Cereatti, Pelosin, *et al.*, 2014; Bertoli *et al.*, 2018) as well as in ten asymptomatic subjects in an urban environment using pressure insoles (Storm *et al.*, 2016),

5) M-MC: based on pelvis vertical acceleration and angular velocity signals, validated in asymptomatic subjects compared to instrumented mat data (McCamley *et al.*, 2012) and in 30 people with pathological gait in a former comparative study (Trojaniello *et al.*, 2015).

M-L, M-MC, M-S, M-M and M-T were implemented based on their descriptions in the literature (Selles *et al.*, 2005; McCamley *et al.*, 2012; Maqbool *et al.*, 2017; Bertoli *et al.*, 2018; Ledoux, 2018), using only the target sensor signals as inputs. A brief description of the operating principles of each algorithm is reported in **Table 18**. Additional details can be found in the original articles. For M-MC, the pelvis angular velocity failed to discriminate between left- and right-side events, supposedly due to the asymmetrical gait pattern of TF (Goujon-Pillet *et al.*, 2008). Therefore, the mediolateral acceleration was used instead.

Algorithm	Signal used for IC	Signal used for FC	General Principle
M-S (Selles *et al.*, 2005)	Vertical acceleration of the shank	Vertical and AP acceleration of the shank	Gait is segmented into approximate strides by identifying the minima in the low-pass filtered shank vertical acceleration. Within each identified stride, the vertical acceleration is low-pass filtered with a cut-off frequency depending on the estimated stride duration. Peaks identified in the filtered signal enable to define intervals in which to look for gait events. ICs are then identified as maxima in the vertical acceleration and FCs are identified as minima in the AP acceleration in their respective intervals.
M-M (Maqbool *et al.*, 2017)	Shank ML angular velocity		Mid-swing instants are detected as maxima in the filtered ML shank angular velocity. ICs are then defined as the first or subsequent negative local minima following mid-swing, associated with negative slope and FCs are defined as local minima occurring at least 300 ms after ICs, with speed lower than a set threshold
M-L (Ledoux, 2018)	Shank vertical acceleration, ML angular velocity, and flexion/extension angle		This state-machine algorithm uses the shank ML angular velocity, the shank vertical acceleration, and the shank angle (obtained using a complementary filter of the shank acceleration and angular velocity) as inputs to detect transitions between the "swing" state and the "stance" state. Stance is detected at zero-crossings in the vertical acceleration, if the angular velocity is negative and the shank angle is above a threshold. It should occur after at least 200 ms of swing. Swing is detected when the vertical acceleration is increasing above a negative threshold, the angular velocity is negative, and the shank angle is below a negative threshold. It occurs after at least 400ms of stance. A set of similar conditions enable to identify the first transition to swing (FC) or stance (IC).
M-T (Bertoli *et al.*, 2018)	Shank sagittal angular velocity and AP acceleration		Peak identification in the ML angular velocity signal enables to define intervals in which to look for gait events. In these intervals, ICs are identified as the minima in ML angular velocity preceding a maximum AP acceleration and FCs are identified as minima in the AP acceleration preceding the last maximum in AP acceleration.
M-MC (McCamley *et al.*, 2012)	Vertical & ML acceleration of the pelvis		The vertical acceleration is filtered with a Gaussian continuous wavelet transform. ICs are identified as the minima in the filtered acceleration. FCs are identified as the maxima in the differentiated signal. In this study, the ML acceleration was used to distinguish right and left gait events occurrence, while the vertical angular velocity was used in the original study.

Table 18: Description of the operating principle of the implemented algorithms.
AP = Anteroposterior; ML = Mediolateral; IC = Initial Contact event; FC = Final Contact event

b. Temporal parameters and symmetry index computation

The following temporal parameters were estimated for each trial and method (insoles- and IMU-based algorithms):

- Stride duration (time between two consecutive ICs of the same foot), computed based on prosthetic ICs;
- Prosthetic and sound limb stance phase duration (time between an IC and the subsequent FC of the same foot);
- Prosthetic and sound limb initial double support duration (time between an IC and the subsequent FC of the contralateral foot), further referred to as prosthetic or sound limb double support duration.

Stance phase duration symmetry between the prosthetic and sound limbs was also assessed for each stride using the Absolute Symmetry Index (ASI): $ASI = \frac{S-P}{0.5\,(S+P)} \times 100$, where S and P are the stance phase durations for the sound and prosthetic limbs respectively (Nolan *et al.*, 2003).

1.2.4. Algorithms performance assessment

a. GE detection rate

Sensitivity, defined as the number of correctly detected algorithm-derived GEs divided by the number of reference GEs, and positive predictive value (PPV), i.e. the number of correctly detected algorithm-derived GEs divided by the total number of detected GEs (including extra events), are often used in the literature to assess algorithms' performance in terms of detection rate (Salarian *et al.*, 2004; Trojaniello *et al.*, 2015). However, the criterion used to classify an algorithm-detected event as either correct, missed or extra is usually missing. In this work, we propose to compute the number of algorithm-detected events such that $|\,t_{rGE} - t_{aGE}| \leq \frac{1}{2}\,StD_{ref}$ (1) with:

- t_{rGE} the timing of a reference GE,
- t_{aGE} the timing of algorithm-derived GEs,
- StD_{ref} the median stride duration computed from reference ICs.

If no algorithm-detected event fulfilled condition (1), an event was missed. Conversely, if several algorithm-detected events fulfilled condition (1), only the closest to the reference event was considered as correctly detected, and the others were discarded as extra events.

Sensitivity and PPV were computed for all the algorithms to compare their GE detection rate. While the occurrence of a missed event can be detected based on the duration between successive detected events, the identification of a correct event among several possible candidates is not possible without a reference. Therefore, to be used in real-life settings, an algorithm must be extremely robust in this respect. Consequently, for the subsequent accuracy analysis, only the algorithms scoring a PPV above 99%, representing a negligible number of extra events, were considered.

For each algorithm, PPV and sensitivity were quantified for the entire trials in order to assess the algorithm ability to detect all events, including those of the first and last steps which mark gait initiation and termination. For the rest of the analysis, the initiation and termination steps were not considered for the sake of comparison with the literature.

b. Accuracy of GEs timings

For each algorithm, the difference between the timing of each IMU-based and the corresponding reference GE was computed. Positive and negative errors respectively indicate delayed and anticipated event detection.

c. Impact of GEs timings errors on estimates of gait temporal parameters and symmetry index

For each algorithm, stride, stance and double support durations, as well as symmetry derived from IMU-based GEs were computed. IMU-based temporal parameter estimates errors were expressed in seconds and in percentage of the reference parameter, with positive and negative values indicating, respectively, overestimation and underestimation of temporal parameters.

125

1.2.5.   *Statistical analysis*

Descriptive statistics (medians and interquartile ranges [IQR]) were computed over all participants for each walking speed for reference GE timings and temporal parameters, for IMU-based GE and temporal parameter errors as well as for SPD-ASI derived from the insoles and the algorithms.

Normality of the median values was verified using the Shapiro-Wilk test and, according to the test result, either a Friedman test or a one-way repeated-measure ANOVA was performed to investigate the effect of the "walking speed" factor on the errors. Post-hoc pairwise comparisons (Wilcoxon signed-rank tests or t-tests depending on the normality of the data) with Holm-Bonferroni correction were then performed where any difference was found.

If the main effect of "walking speed" persisted, pairwise comparisons were used to investigate the presence of significant differences between each pair of methods, for each level of walking speed, considering separately prosthetic- and sound-limb parameters when relevant. Conversely, if no main effect of "walking speed" was found, medians and IQR were computed over all three walking speeds for each participant and method, and pairwise comparisons were then executed on this new dataset.

Wilcoxon signed-rank tests were used to investigate the effect of the limb considered, that is, to determine whether errors where significantly different at the sound and prosthetic side for each parameter and each algorithm.

The statistical analysis was performed using SPSS (IBM SPSS Statistics 23, NY, USA). The level of significance was set to 0.05 for all statistical tests.

1.3.   Results

Due to technical issues with the insoles, GEs of two participants had to be discarded at the sound limb, leaving a total of 454 sound steps for 623 prosthetic steps considered in the analysis. **Table 19** reports the descriptive statistics of the temporal parameters derived from the insoles.

Table 19: Reference temporal parameters derived from insoles data.
* Stride durations were estimated based on prosthetic IC timings

Walking speed level	Gait velocity (m.s-1) med (IQR)	Stride duration (s)* med (IQR)	Side	Stance phase duration		Double support duration	
				(s) med (IQR)	(% stride) med (IQR)	(s) med (IQR)	(% stride) med (IQR)
Slow	0.89 (0.12)	1.33 (0.14)	Sound	0.91 (0.14)	68.9 (5.2)	0.17 (0.04)	13.2 (2.4)
			Prosthetic	0.81 (0.11)	60.9 (2.4)	0.22 (0.06)	16.4 (4.0)
Comfortable	1.06 (0.12)	1.16 (0.13)	Sound	0.77 (0.10)	67.0 (3.4)	0.14 (0.02)	12.1 (2.2)
			Prosthetic	0.68 (0.08)	58.7 (3.3)	0.16 (0.04)	13.3 (2.1)
Fast	1.35 (0.19)	1.00 (0.13)	Sound	0.65 (0.12)	64.7 (4.9)	0.10 (0.03)	10.5 (1.4)
			Prosthetic	0.56 (0.07)	56.9 (2.6)	0.12 (0.04)	11.6 (3.4)

a. GE detection rate

Sensitivity and PPV for each algorithm are reported in **Table 20**. Only M-T and M-L showed a PPV higher than 99% and were further analyzed. Both algorithms had extra and missed detections, however those of M-T never occurred outside of the first and last steps of gait.

Table 20: Sensitivity and positive predictive value of the five IMU-based algorithms in gait event detection

Method	Sensitivity				Positive Predictive Value			
	Prosthetic limb		Sound limb		Prosthetic limb		Sound limb	
	Initial contact	Final contact	Initial contact	Final contact	Initial contact	Final contact	Initial contact	Final contact
M-S	93.4%	92.7%	94.0%	92.8%	99.1%	97.3%	95.2%	95.7%
M-M	98.6%	98.8%	97.4%	98.2%	99.7%	100.0%	98.3%	99.8%
M-L	88.4%	88.8%	84.2%	85.0%	100.0%	100.0%	100.0%	100.0%
M-T	99.1%	99.1%	98.8%	98.8%	100.0%	100.0%	99.8%	99.8%
M-MC	93.4%	91.9%	91.2%	90.6%	97.1%	96.0%	96.1%	96.1%

b. Accuracy of GEs timings

No significant effect of the "walking speed" factor was found on the errors obtained for GE timings, neither for M-T nor for M-L. GEs were generally detected with a small anticipation with M-L and with a short delay using M-T (**Figure 45**). There was no effect of the "limb" on the IC timings estimated with
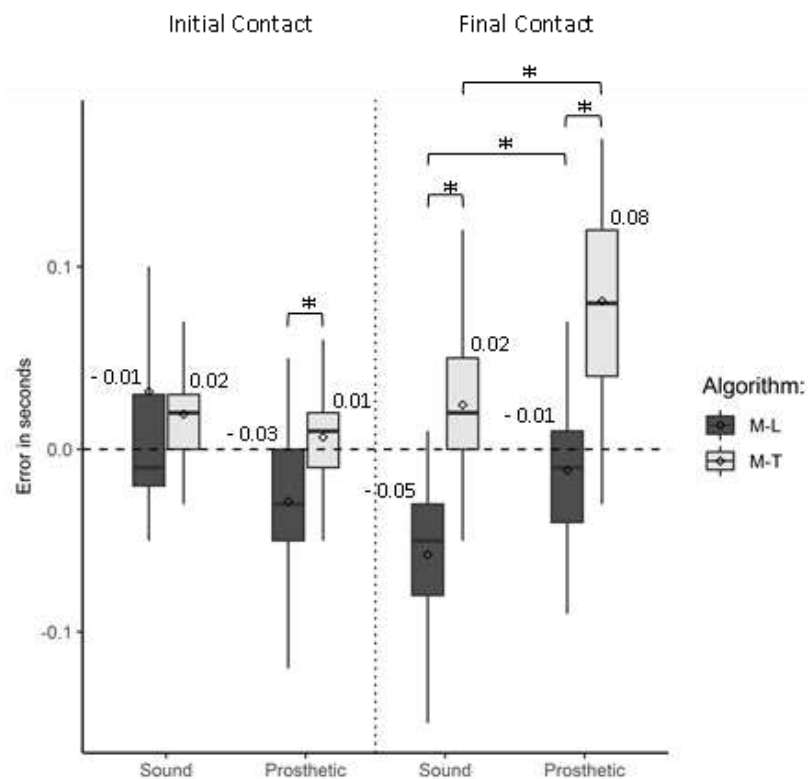
Figure 45: Errors [ms] of IC and FC timings obtained with M-T and M-L algorithms at all speeds with respect to reference events estimated with the insoles. Mean values are indicated with a diamond-shaped point and median values are reported above each boxplot. Significant differences ($p < 0.05$) are marked with an asterisk*. Outliers are not represented. In general, M-T and M-L resulted in a low number of outliers (< 3 %), but M-L resulted in 8.02% of outliers for sound IC.

either algorithm. Conversely, FC timings estimated with M-T were significantly more accurate (t(4) = -3.626, *p-value* = 0.022) at the sound limb than at the prosthetic limb while the contrary was observed with M-L (t(4) = -5.171, *p-value* = 0.007).

When comparing the algorithms in terms of errors, M-T was found to be less accurate than M-L for prosthetic FC detection (t(6)=4.890, *p-value* = 0.003), but more accurate for both prosthetic IC (Z = - 2.214, *p-value* = 0.027) and sound FC detection (t(4)= 6.674 *p-value* = 0.003).

c. Impact of GEs timings errors on estimates of gait temporal parameters and symmetry index

There was no effect of the "walking speed" factor on the median errors of gait temporal parameter estimates. While there was no difference between the algorithms for the stride duration, statistically significant differences were obtained for stance phase and double support duration estimates (**Figure 46** and **Table 21**). Furthermore, a significant effect of the "limb" was observed for stance phase durations for both algorithms (M-T: t(4) = -3.940, p-value = 0.017 ; M-L: t(4) = -2.781, p-value = 0.05) and for double support duration for M-T (t(4) = 4.877, p-value = 0.008).

Table 21: Errors [ms] of gait temporal parameters estimated with M-T and M-L compared to insoles. Results of the statistical tests are reported, with significant differences between M-T and M-L values marked with asterisks (*: p-value ≤ 0.05)

Temporal parameter (in milliseconds)	M-T		M-L		Statistical tests (on % values)	
	median	(IQR)	median	(IQR)	p-value	score
Stride duration	0	(20)	0	(20)	0.317	Z = - 1.000
Sound stance phase duration	10	(40)	-40	(70)	0.017 *	t(4) = 3.927
Prosthetic stance phase duration	70	(60)	0	(40)	0.003 *	t(6) = 4.817
Sound double support duration	70	(53)	0	(60)	0.009 *	t(4) = -4.788
Prosthetic double support duration	10	(40)	-40	(40)	0.001 *	t(4)= -8.953

Median SPD-ASI values were averaged across all participants and walking speeds for each method (insoles, M-T and M-L) as no significant effect of the "walking speed" factor was found. SPD-ASI estimates obtained with M-T and M-L were found to be significantly different than those derived from the insoles (**Table 22**).

Table 22: Mean and standard deviation over all participants of the median stance phase duration ASI derived from insoles and obtained with M-T and M-L algorithms. Results of the statistical tests are reported, with significant differences between insoles- or IMU-based ASI values marked with an asterisk*

Algorithm	ASI Algorithm		ASI Insoles		T-test	
	mean	(sd)	mean	(sd)	p-value	score
M-L	6.72 %	(3.44 %)	12.79 %	(2.85 %)	0.048 *	t(4) = 2.807
M-T	4.16 %	(5.05 %)			0.013 *	t(4) = 4.274
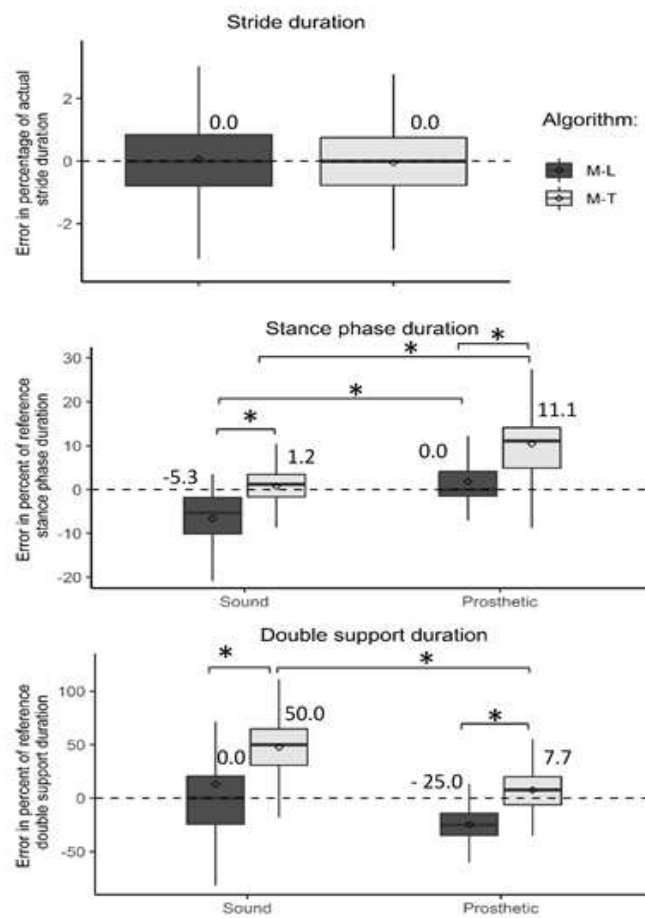
Figure 46: Errors [%] of gait temporal parameters estimated with M-T and M-L expressed in percentage of the actual gait temporal parameters derived from the insoles data, at all speeds. From top to bottom: stride duration, stance phase duration, double support duration.

Mean values are indicated with a diamond-shaped point and median values are reported above each boxplot. Significant differences (p < 0.05) are marked with an asterisk*. Outliers are not represented. In general, M-T and M-L resulted in a low number of outliers (< 4.5 %), except for strides for M-T (13.7% of outliers) and for sound double support estimates for M-L (9.1 % of outliers)

1.4.   Discussion

This study aimed at i) comparing the accuracy of state-of-the-art IMU-based algorithms in detecting both IC and FC events and ii) assessing the impact of GE timing errors on the estimation of gait temporal parameters and symmetry in TF.

Gait temporal parameters and walking speeds obtained with pressure insoles were similar to those reported in the literature for the considered population (Goujon *et al.*, 2006; Goujon-Pillet *et al.*, 2008).

a.   GE detection rate

To be relevant in an ecological context, GE detection algorithms must not detect extra events as they would be impossible to identify without a reference. Given their PPV values inferior to 99%, two

of the algorithms developed for lower-limb amputees (M-S and M-M) and the single-sensor-based algorithm (M-MC) were discarded from the analysis[4].

The modification applied to M-MC algorithm allowed to improve the discrimination between right and left side events, thus reducing the number of extra events (less than 4% of extra FC in our data, while up to 11.2% of extra FC were found in hemiparetic patients in a former study (Trojaniello *et al.*, 2015)), although not sufficiently. However, the number of missed events was higher than in the literature (McCamley *et al.*, 2012; Trojaniello *et al.*, 2015), which might be due to specific gait alterations of prosthetic gait, such as the lack of propulsion inherent to prosthetic components (Nolan *et al.*, 2003).

Neither missed or extra events were reported by the authors of the two other algorithms M-S and M-M. However, it should be noted M-S was designed and validated in TT, whose gait pattern differs from that of TF. Furthermore, while all steps were considered in our analysis, including transition, acceleration, and deceleration steps, Selles and coworkers only analyzed steps that occurred on a force platform, ensuring to consider only steady-state steps (Selles *et al.*, 2005).

Maqbool and coworkers reported a 100% detection rate by comparing the absolute number of events detected by M-M and by footswitches, without considering an objective criterion to ensure that each detected event would correspond to a footswitch event (Maqbool *et al.*, 2017). Furthermore, the algorithm was developed and validated on asymptomatic subjects and on only one TF and one TT who might have presented very few gait alterations, thus preventing the generalization of their results to the population of lower-limb amputees.

In what follows, only results obtained with M-L and M-T algorithms will be discussed.

A surprisingly high number of events were missed by M-L in the present study, despite its reported excellent sensitivity in TFs (Ledoux, 2018). The thresholds originally proposed in (Ledoux, 2018) were specifically devised for treadmill ambulation, which was shown to reduce gait inherent inter-stride variability compared to level ground ambulation (Hollman *et al.*, 2016). This may have hindered the algorithm's capacity to detect all events when walking in a less constraining situation. Furthermore, if an event is undetected by the algorithm, the following event will also be missed because of the state-machine design of M-L. Regarding M-T, no extra or missed events occurred in the steady phase of gait, as reported in former studies (Trojaniello, Cereatti, Pelosin, *et al.*, 2014; Bertoli *et al.*, 2018). This directly results from the efficient design of M-T: the algorithm first detects maxima in the shank angular velocity and uses this information at both sides to segment gait into cycles and to identify restrained intervals of time where one and only one event (either an IC or a FC) has to occur. For all the investigated parameters, both algorithms were found to be robust to various self-selected walking speeds, confirming results reported for M-T (Trojaniello, Cereatti, Pelosin, *et al.*, 2014; Bertoli *et al.*, 2018).

---

[4] Due to high positive predictive values, close to the criterion chosen for this study, the algorithm M-M was further investigated as well. However, the algorithm displayed a poor accuracy and repeatability in detecting gait events, and therefore in estimating temporal parameters. See Appendix B – Comparative assessment of M-M algorithm for more details.

b. GE detection accuracy

Prosthetic IC and FC detections with M-L were as accurate as those reported in the original study (Ledoux, 2018), but slightly less precise. This may also result from the higher gait variability of overground- compared to treadmill-walking. Estimated FC timings were less accurate for the sound limb than the prosthetic limb, likely due to the adoption of identical thresholds for both limbs, as reported by the author (Ledoux, 2018). Defining limb-specific thresholds was beyond the scope of this study, but it might improve sound FC timing accuracy.

M-T achieved similar or even improved GE timing accuracy compared to that reported using other algorithms specifically designed for people with lower-limb amputation (Selles *et al.*, 2005; Maqbool *et al.*, 2017). Furthermore, the achieved accuracy for IC detection in our participants is comparable to that of people with Parkinson's Disease (Trojaniello, Cereatti, Pelosin, *et al.*, 2014). Both these results corroborate previous statements that M-T might be suitable for clinical routine detection of gait events (Trojaniello, Cereatti, Pelosin, *et al.*, 2014; Bertoli *et al.*, 2018). All in all, M-T achieved equivalent or higher accuracy than M-L in GE detection except for prosthetic FC. The algorithms differ not only in the signals that are used as inputs, but also in their design: M-T is based on peak-detection while M-L is a threshold-based algorithm. The latter strategy might be more efficient for prosthetic FC detection: the smoother movement occurring at FC compared to IC (Trojaniello, Cereatti and Della Croce, 2014) and the attenuated propulsion at the prosthetic limb (Nolan *et al.*, 2003) might result in a smoothed signal, detrimental to the peak-identification strategy.

It should be noted that the sampling frequency (100 Hz) might have induced a delay of up to 10 ms between algorithms-derived and insoles-detected events. This constant delay has however no impact on the estimated durations.

c. Impact of GEs timings errors on estimates of gait temporal parameters and symmetry index

Both algorithms provide stride duration estimates acceptable for clinical use (Trojaniello, Cereatti and Della Croce, 2014), with null median errors and IQR of 20 ms.

Regarding stance and double support durations, errors result from the discrepancy between IC and FC timing errors. In our study, temporal parameters errors were mostly driven by relatively high errors in FC detection at the sound limb for M-L and at the prosthetic limb for M-T compared to IC.

The errors achieved for stance phase duration are acceptable at the prosthetic limb with M-L and at the sound limb with M-T (Trojaniello, Cereatti and Della Croce, 2014), with a similar accuracy to that of the original article (Trojaniello, Cereatti, Pelosin, *et al.*, 2014). Furthermore, the achieved errors with either algorithm at either limb are inferior to the minimal change detectable by pressure insoles in people with lower limb amputation (Timmermans *et al.*, 2019). Combining both algorithms by using M-T approach for gait segmentation and interval identification, and then taking advantage of either M-T or M-L detection approaches for the sound or prosthetic limb respectively, might provide more accurate estimates of stance phase duration at both limbs. This would in turn enable a long-term monitoring of a patient's progress during his rehabilitation, but test-retest reliability should be evaluated prior to using the combined algorithm in a clinical setting for longitudinal monitoring.

Regarding double support duration, percentage errors achieved high values and variability at both sides with both algorithms. Therefore, although double support duration is a clinically relevant

131

parameter reflecting stability and weight shifting ability in TF (Goujon *et al.*, 2006; Kendell *et al.*, 2010), the use of either M-T or M-L algorithms for its estimation is not recommended.

Regarding temporal gait symmetry, the discrepancy between sound and prosthetic stance phase duration errors explains the observed SPD-ASI inaccuracy. The algorithms tend to significantly underestimate sound stance-phase duration or to overestimate prosthetic stance-phase duration, resulting in a falsely low asymmetry index. Thus, neither M-T nor M-L can be safely used to assess stance phase duration asymmetry between the prosthetic and the sound limb.

This confirms the need of a more robust algorithm at both the prosthetic and sound limbs for temporal parameters, which in turn would enable to obtain reliable SPD-ASI estimates in TF.

Although the participants of the study were found to be representative of the population with TF (Goujon *et al.*, 2006; Goujon-Pillet *et al.*, 2008), the small sample size in this study should be considered prior to results generalization.

1.5.   Conclusions

This study analyzed the performance of different IMU-based algorithms and gives indications about their accuracy for GE detection in people with transfemoral amputation. Two of the investigated algorithms, using one IMU on each shank, provide acceptable estimates of stride and stance phase durations considering the minimal detectable change of these parameters by pressure insoles. However, test-retest reliability of the IMU-derived estimates remains to be evaluated prior to using these algorithms for longitudinal monitoring of gait. Furthermore, both algorithms lack in accuracy when estimating either double support duration or the temporal asymmetry index. A new algorithm, combining the strengths of M-T and M-L should be devised to improve gait event detection and temporal parameters estimation in people with transfemoral amputation. The results of the present study support the use of *a priori* gait cycle segmentation using the shank mediolateral angular velocity and tend to indicate that threshold-based detection should be preferred to peak-based detection at the prosthetic limb, at least for FC event detection.

Chapter 2 – Investigation of the relevance of gait quality indices issued from wearable gait analysis during the rehabilitation of people with lower-limb amputation

As briefly discussed in the introduction of Part 3, several parameters have been proposed in the literature to quantify gait symmetry and the balance using wearable sensors. The aim of this chapter is to investigate the feasibility and relevance of tracking such parameters during the rehabilitation of people with lower-limb amputation.

Gait Symmetry

In the previous chapter, state-of-the-art algorithms for IMU-based gait event detection were shown not to allow an accurate estimation of stance-phase duration symmetry in people with transfemoral amputation. However, other wearable sensors – namely, pressure insoles – have been validated and used for the quantification of temporal and loading asymmetry in transtibial and transfemoral amputees (Nolan *et al.*, 2003; Cutti *et al.*, 2018; Loiret *et al.*, 2019). Pressure insoles are more expensive than IMUs and necessitate to be bought in a large range of sizes so as to fit most people shoe sizes. Furthermore, insoles require to be calibrated for each patient and are sensitive to temperature changes (Herbert-Copley *et al.*, 2013), which imposes to prepare insoles up to fifteen minutes prior to the acquisition time. The calibration process requires to alternatively load each insole with the full weight of the tested person without external support. Loss of proprioception in the prosthetic leg may jeopardize a successful calibration of insoles as it disrupts balance, compromising the accuracy of insole-based measures (Loiret *et al.*, 2019). For all these reasons, and although temporal and loading symmetry indices can rapidly be retrieved from insoles signals, pressure insoles can be considered more constraining for gait monitoring during the rehabilitation of people with lower-limb amputation than IMUs.

In the literature, several parameters have been proposed to quantify gait symmetry from acceleration signals measured by a trunk or pelvis mounted IMU. In particular, the harmonic ratio (HR), or its improved version, the iHR, has been widely used in research in recent years (Bellanca *et al.*, 2013; Iosa *et al.*, 2014; Riva *et al.*, 2014; Pasciuto *et al.*, 2017; Belluscio *et al.*, 2018; Buckley *et al.*, 2018). Based on the frequential analysis of the accelerations measured by a single IMU at pelvis level, this parameter allows to rapidly quantify step-to-step symmetry (Bellanca *et al.*, 2013; Pasciuto *et al.*, 2017). The advantage of this parameter over temporal and loading asymmetry indices is that it relies on the use of a single IMU, which is interchangeable across any participant (as it is independent of any anthropometric measurement). Interestingly, the HR/iHR is generally computed stride per stride, but several authors have proposed to compute it over a complete gait trial to avoid the propagation of errors due to erroneous gait segmentation methods (Riva *et al.*, 2013; Howcroft, Kofman, *et al.*, 2016). While several standardized guidelines have been proposed in the literature for its computation (Buckley *et al.*, 2017; Pasciuto *et al.*, 2017), the impact of the segmentation method (or absence thereof) was never investigated. More importantly, how this parameter relates to usual symmetry indices is not clear and may hinder its interpretation by clinicians. In order to gain insight on this recent symmetry index, it appears therefore relevant *i)* to analyze the impact on the iHR values of different segmentation methods and of the absence of segmentation at all, and *ii)* to comparatively assess usual parameters of temporal and loading symmetry and the iHR in the same population of lower-limb

133

amputees. To the authors knowledge, this was never done in any population and the iHR was never computed in people with transtibial amputation.

Balance control during gait

People with balance impairment have been shown in the literature to be less able than sound subjects to maintain a steady optical flow and vestibular system while walking, due to the transmission of oscillations from the lower limbs to the upper body (Mazzà *et al.*, 2008; Iosa, Picerno, *et al.*, 2016). Therefore, balance control has been quantified in wearable gait analysis literature by studying the oscillations transmitted to the head by the lower-limbs during gait (Menz *et al.*, 2003; Mazzà *et al.*, 2008; Iosa, Picerno, *et al.*, 2016; Bergamini *et al.*, 2017). Two parameters issued from the measured raw acceleration signals have been described to this end: the root mean square of acceleration (RMSa) and the attenuation coefficients (AC). RMSa provides a measure of the amplitude of dispersion of the acceleration, which has been shown to increase with walking speed (Menz *et al.*, 2003; Iosa, Picerno, *et al.*, 2016) and, when normalized to walking speed, with the level of impairment in pathological gait (Bergamini *et al.*, 2017). The ratio of RMSa signals at different levels of the upper body (pelvis/sternum, sternum/head or pelvis/head) have been used to evaluate the transmission of oscillations from the lower limbs to the head (Mazzà *et al.*, 2008). Both these parameters have been studied in the population of people with transtibial amputation (Paradisi *et al.*, 2019). In that study, the participants were required to perform three successive 10-m walking test and the average values of the RMSa and AC at the three levels were computed and compared between 20 transtibial amputees and 20 asymptomatic subjects. A few number of strides as typically walked within a 10-m pathway may not allow to obtain reliable measures of variability (Riva *et al.*, 2014). Therefore, it would be interesting to assess the reliability of these parameters in the population of people with lower-limb amputation before providing reference values in this population.

Gap analysis and aim of the chapter

The aim of this chapter was to contribute filling the following observed gaps from the literature:

- Parameters have been proposed for assessing gait symmetry and balance from IMUs and were investigated in people with lower-limb amputation, but their reliability was not assessed prior to providing reference values;
- While RMSa, AC, and temporal or loading symmetry indices were evaluated in people with transtibial amputation, the iHR was never quantified in this population. Furthermore, these parameters were never assessed simultaneously in the same sample of transtibial amputees, compromising a complete description of their gait using these parameters. Similar remarks apply to the gait of transfemoral amputees;
- While the iHR is increasingly used in clinical research, no consensus exists about the need for stride segmentation or not. In addition, this parameter was never compared to more standard symmetry indices such as the Absolute Symmetry Index (ASI) of stance-phase duration (temporal symmetry) or of the vertical ground reaction force peak occurring in early stance (loading symmetry) (Nolan *et al.*, 2003; Loiret *et al.*, 2019).

The chapter is organized in two sections in order to contribute filling these gaps. The first section aims at investigating whether RMSa, AC, iHR and temporal and loading ASI are likely to be reliable and relevant for gait monitoring along the rehabilitation of people with transtibial amputation. To do so, these gait quality indices were assessed during two repetitions of the two-minute walking test (2MWT) in people with transtibial amputation and sound participants. This work was performed in

collaboration with Julie Durand, physiotherapist at Institution Nationale des Invalides, during her master internship. Her implication in the data collection and analysis is duly acknowledged. In the second section, a special focus on the computation and interpretation of the iHR will be proposed. First, the iHR will be computed using different segmentation methods and no segmentation in order to clarify the uncertainties regarding its computation. Then, the relation between the iHR and both temporal and loading ASI will be investigated using the data collected in the course of Julie Durand's internship.

2.1. Feasibility and relevance of gait quality monitoring from IMUs- and insoles-derived parameters in people with lower-limb amputation

Gait quality represents a crucial aspect of gait and is therefore monitored during the rehabilitation of people suffering from motor impairment. In particular, monitoring gait symmetry and assessing the risk of falling are crucial elements of the rehabilitation of a person with transtibial amputation as these aspects were shown to lead to the development of comorbidities and have an impact on the activity or social participation level after discharge from the rehabilitation center (Gailey *et al.*, 2008; Highsmith *et al.*, 2016). Few tools are available in the clinical field to quantitatively and objectively monitor the evolution of gait symmetry and fall risk along the rehabilitation process. Optical motion capture systems are not always available and are not adapted to frequent assessment due to the long set up and complex post-processing. On the other hand, clinical walking tests, which are quick to administer, provide a single metric of performance which is not sufficient to gain insight into the way a performance is obtained and, thus, to effectively targeting rehabilitation (Deathe *et al.*, 2009).

Recently, the development of small and affordable wearable sensors for gait analysis such as inertial measurement units (IMUs) and pressure insoles has allowed the introduction of new parameters for the in-field quantification of gait balance and symmetry (Iosa, Picerno, *et al.*, 2016). Pressure insoles allow to estimate the load exerted on each lower limb through the measure of the pressure applied on each insole. This allows to quantify two aspects of gait symmetry, namely loading and temporal symmetry (Nolan *et al.*, 2003). Similarly, IMUs positioned on the upper body (pelvis, lower trunk and head) have been proposed to quantify gait symmetry and stability through the analysis of the frequency content and dispersion of the accelerations measured at these locations (Menz *et al.*, 2003; Mazzà *et al.*, 2008; Pasciuto *et al.*, 2017). Several authors have therefore proposed multi-sensor protocols for the assessment of balance in various pathological populations by computing gait quality indices over a few steps taken while walking in straight line (Summa *et al.*, 2016; Bergamini *et al.*, 2017; Paradisi *et al.*, 2019). Poorer gait balance was shown to be associated with decreased gait symmetry, increased values of acceleration signals, lower average walking speed and inability to attenuate the accelerations transmitted from the lower limbs to the head, highlighting the construct validity of the proposed indices (Iosa, Bini, *et al.*, 2016; Bergamini *et al.*, 2017; Buckley *et al.*, 2018). None of these studies evaluated the reliability of the proposed multi-sensor wearable protocols. Yet, quantifying the minimal detectable change obtained for a parameter using a defined protocol is paramount to verify the relevance and feasibility of monitoring the evolution of this parameter along the rehabilitation process (Portney and Watkins, 2015). Furthermore, previous studies evidenced that acceleration-based gait quality indices often require to be computed over a large number of steps in order to be reliable (Riva *et al.*, 2014; Pasciuto *et al.*, 2017). Therefore, computing gait quality indices over few

strides may not allow to achieve sufficient reliability. In this respect, instrumenting the two-minute walking test (2MWT) with wearable sensors would allow to capture a great number of straight-line strides along a standardized protocol, often administered in clinical practice. The 2MWT appears to be particularly relevant for gait assessment of people with transtibial amputation as it was shown to be a valid indicator of mobility in this population, to be related to fall risk, and is compatible with frequent assessment along the rehabilitation as it is sufficiently brief so as to perform other rehabilitation exercises and allows the use of assistive devices (Brooks *et al.*, 2001; Major *et al.*, 2013; Reid *et al.*, 2015; Gaunaurd *et al.*, 2020).

The aim of this study was therefore to contribute filling the identified gaps by *i)* identifying the parameters that are repeatable within-participant and within-session when performing two repetitions of the 2MWT, *ii)* providing reference values for people with lower-limb amputation and sound participants in order to comparatively characterize both populations and to obtain target values for the rehabilitation, *iii)* providing an estimate of the minimal detectable change by each parameter using this protocol, in order to identify parameters susceptible to be relevant for the rehabilitation.

2.1.1.   Material and methods

a.   Participants

The study was designed according to the Declaration of Helsinki and was granted ethical approval (CPP N° 2018-A03477-48). Nine people with transtibial amputation (age: 51.2 ± 10.5 years, 8 males, mass: 78.6 ± 17.3 kg; height: 1.73 ± 0.09 m, time since amputation: 3.5 ± 6.0 years) and nine asymptomatic participants (age: 30.1 ± 11.1 years, 7 males, mass: 80.9 ± 22.3 kg; height: 1.80 ± 0.13 m) gave written informed consent to participate in the study. Both groups were matched for gender, height and mass. Inclusion criteria for lower-limb amputees were people with unilateral transtibial amputation due to trauma or tumor, fitted with a definitive prosthesis worn on a daily basis, able to walk two minutes without any assistance. The amputee participants walked with their usual prosthesis. Exclusion criteria for both populations were the concomitance of an orthopedic or neurologic pathology.

b.   Acquisition protocol

Each participant was equipped with a pair of pressure insoles (Loadsol, Novel, Germany, 100 samples·s-1) matching his/her shoe sizes and with three IMUs (MTw xSens, Netherlands, 100 samples·s-1), embedding a tri-axial accelerometer (± 16 g) and a tri-axial gyroscope (± 2000 deg/s), positioned on the lower trunk (L4/L5 level), on the center of the sternum and on the occipital bone of the head (**Figure 48**). Insoles were calibrated following the instructions of the manufacturer, by alternatively loading each IMU with the full body weight after a minimum of fifteen minutes of wear for sensors warm-up (Loiret *et al.*,

Figure 48: Participant equipment with IMUs and insoles. For the acquisitions, IMUs on the pelvis, sternum, and head were positioned under the Velcro straps to prevent sensors sliding.

2019). Each participant was given some time to get used to the sensors and to ensure that they did not hinder his/her motion.

Afterwards, each participant was asked to perform two repetitions of the 2MWT. Participants were instructed to walk as far as possible along a corridor or squared path including straight lines of at least 25 m within the two minutes, but were not encouraged during the test, in accordance with the test administration guidelines (Brooks *et al.*, 2001). For synchronization purpose between IMUs and insoles, each repetition of the 2MWT was followed by a 10-s recording of wearable sensors signals during which each participant was standing in a static posture and was asked to strike the ground with his/her prosthetic leg. The distance covered during the test was measured using graduations present in the corridor and a tap meter. Following the first trial, the participant could rest as long as necessary.

c. Data processing

IMUs and insoles data were post-processed using MATLAB® software (The MathWorks Inc., MA, US). Synchronization was performed semi-automatically by aligning the kicking-motion peaks occurring at the end of the 2MWT trial in the pelvis vertical acceleration and insole signals. Synchronization delays had been *a priori* evaluated to be within 1 frame at 100 Hz using an electronic trigger in a motion analysis laboratory to synchronize IMUs, insoles and force plates data. For each 2MWT, the average velocity of progression was computed as the ratio of the distance covered during the test divided by the test duration, i.e. two minutes.

Proper alignment of the IMUs with craniocaudal (CC), anteroposterior (AP), and mediolateral (ML) anatomical axes was ensured through a verticalization procedure during the initial static posture of each 2MWT (Bergamini et al., 2014). Only steady state straight-walking strides were considered within each test for the computation of gait quality indices. Turning strides were identified using the yaw angular velocity measured by the pelvis IMU and were discarded from the analysis.

Gait segmentation was performed using a 20 N threshold on the insoles' ground reaction force signals (Loiret *et al.*, 2019). Gait quality indices were then computed for each stride:

- **Temporal and loading asymmetry** were quantified using, respectively, the stance phase duration (SPD) of each lower limb and the magnitude of the weight acceptance peak (Fz1) in early stance with the absolute symmetry index:

  $ASI = \frac{S-P}{0.5\,(S+P)} \times 100$, where S and P are the SPD or Fz1 values for the sound and prosthetic limbs respectively (Nolan *et al.*, 2003).

- **The improved Harmonic Ratio (iHR)** was computed for each of the 3 acceleration components measured at the pelvis level (Pasciuto et al., 2017). Its computation is based on a spectral analysis of the acceleration and yields values between 0% (step-to-step asymmetry) and 100% (perfect step-to-step symmetry): $iHR = \sum_{1\le j\le n} \frac{P_i^j}{P_e^j + P_i^j} \cdot 100$

  where P_i^j and P_e^j respectively refer to the power associated with the intrinsic harmonics (contributing to gait symmetry) and extrinsic harmonics (leading to deviation from a symmetrical pattern) of the acceleration signal (Cappozzo, 1981)

- After mean subtraction of the complete acceleration signals, **root mean square of the accelerations (RMS)** were computed for each stride and each IMU along the three anatomical axes of the underlying segment. RMS values were then divided by the average

137

walking speed in order to mitigate the dependency of accelerations with velocity and will be designated hereafter as RMSa.

- The capacity to minimize the oscillations transferred from the lower to the upper body was quantified through the **attenuation coefficients (AC)** between each level pair of the body (AC_{PS}, AC_{PH}, and AC_{SH} between pelvis/sternum, pelvis/head and sternum/head respectively), and for each acceleration component (Paradisi et al., 2019):

$$AC_{XY} = 1 - \frac{RMSa_Y}{RMSa_X}.$$

Attenuation of the accelerations from lower to upper body levels corresponds to positive coefficients, while amplification yields negative coefficients.

For each 2MWT of each patient, the median and interquartile range (IQR) of each of the gait quality index was computed over all the analyzed strides, yielding 23 quantitative parameters in addition to the distance covered during the test.

d. Statistical analysis

For each gait quality index, normality of the median values was verified using the Shapiro-Wilk test. According to the test result, either parametric tests (paired t-tests) or non-parametric tests (Wilcoxon signed-rank tests) were implemented to compare the outcomes of the two repetitions of the 2MWT within each population. This step allowed to identify gait quality indices that were repeatable within-session for each population. The repeatability coefficient of each gait quality index was computed following Bland and Altman as twice the standard deviation of the differences between the two repetitions of the 2MWT (Bland and Altman, 1986). Since the standard deviation of the differences allows to estimate the standard error of measurement, the repeatability coefficient is an estimate of the minimal detectable change with a 95% confidence interval, and is expressed in the same units as the original index (Weir, 2005).

Then, for the parameters that were found to be repeatable in both the asymptomatic and transtibial amputee populations, descriptive statistics (medians, IQR) were computed over the gait quality indices for each population. Either parametric tests or non-parametric unpaired tests (respectively, t-tests or Wilcoxon tests) were implemented to compare the outcomes of the first repetition of the 2MWT across both populations.

The statistical analysis was performed using R® version 3.5.1. The alpha level of significance was set to 0.05 for all statistical tests.

2.1.2. Results

i. Identification of within-session repeatable gait quality indices and estimation of the minimally detectable change

Table 23 provides a visual representation of the results of the statistical tests comparing the outcomes of the two repetitions of 2MWT within each population. Two parameters displayed a statistically significant difference within session: the attenuation coefficients between the pelvis and sternum in the vertical direction in the asymptomatic population and the RMSa measured at sternum level in the anteroposterior direction in the transtibial amputee population. Therefore, both these parameters will be discarded from further analysis.

Gait quality indices	Asymptomatic participants			Transtibial amputee participants		
	Anteroposterior	Mediolateral	Vertical	Anteroposterior	Mediolateral	Vertical
iHR						
RMSa pelvis						
RMSa sternum				*		
RMSa head						
AC pelvis/sternum			*			
AC pelvis/head						
AC sternum/head						

	Asymptomatic participants	Transtibial amputees
Temporal ASI		
Loading ASI		
2MWT distance		

The repeatability coefficients, which represent an estimate of the minimal detectable difference were computed for each population and each parameter except the two that displayed within-session difference (**Table 24**). Higher repeatability coefficients were observed in people with transtibial amputation except for the stance-phase duration ASI and the covered distance.

		iHR (%)	RMSa pelvis (s^{-1})	RMSa sternum (s^{-1})	RMSa head (s^{-1})	AC pelvis / sternum	AC pelvis / head	AC sternum / head	Temporal ASI (%)	Loading ASI (%)	Distance (m)
Transtibial amputees	AP	7.4	0.50	/	0.55	0.58	0.53	0.54	2.8	10.0	14.6
	ML	10.2	0.32	0.73	0.22	0.58	0.17	0.42			
	V	8.3	0.53	0.50	0.62	/	0.18	0.15			
Sound participants	AP	1.0	0.20	/	0.31	0.18	0.25	0.48	3.3	3.3	17.4
	ML	4.3	0.08	0.05	0.14	0.08	0.16	0.15			
	V	1.3	0.26	0.15	0.21	/	0.08	0.07			

ii.   Description of the transtibial and asymptomatic populations using gait quality indices

The median values of each gait quality index and the covered distance obtained during the first repetition of the 2MWT for both populations were assessed and compared (**Table 25**). In addition to the covered distance, ten out of the 21 remaining gait quality indices were shown to be statistically different between the populations of asymptomatic participants and transtibial amputees.

Table 25: Median and interquartile range (IQR) of the median scores achieved during the first repetition of the 2-minute walking test (2MWT) by the sound participants and the transtibial amputees. Significant difference (Sig.) between both populations are indicated using an asterisk (α-level of significance = 0.05).
iHR = improved Harmonic Ratio; RMSa = Root Mean Square of Accelerations divided by the average walkng speed; AC = Attenuation Coefficient; ASI = Absolute Symmetry Index

	Anteroposterior Median (IQR)			Mediolateral Median (IQR)			Vertical Median (IQR)		
	Sound participants	Transtibial amputees	Sig.	Sound participants	Transtibial amputees	Sig.	Sound participants	Transtibial amputees	Sig.
iHR (%)	**96.9 (2.1)**	**85.9 (6.5)**	*	**85.2 (11.1)**	**71.4 (8.4)**	*	**97.6 (1.5)**	**89.1 (6.6)**	*
RMSa pelvis (s⁻¹)	2.05 (0.93)	1.78 (0.88)		**1.77 (1.19)**	**1.60 (0.70)**	*	3.13 (0.76)	2.47 (1.41)	
RMSa sternum (s⁻¹)	/	/		**1.09 (0.51)**	**1.27 (0.39)**	*	3.37 (1.29)	2.56 (1.24)	
RMSa head (s⁻¹)	**1.17 (0.58)**	**1.69 (0.75)**	*	**1.00 (0.27)**	**1.53 (0.30)**	*	3.35 (1.07)	2.55 (1.20)	
AC pelvis/sternum	0.35 (0.29)	0.19 (0.29)		0.31 (0.45)	0.27 (0.25)		/	/	
AC pelvis/head	**0.50 (0.38)**	**-0.03 (0.69)**	*	0.20 (0.47)	0.05 (0.20)		-0.01 (0.12)	-0.01 (0.15)	
AC sternum/head	**0.26 (0.52)**	**-0.39 (0.91)**	*	**0.03 (0.15)**	**-0.20 (0.23)**	*	0.01 (0.09)	0.00 (0.12)	

	Sound participants	Transtibial amputees	Sig.
Temporal ASI (%)	-1.4 (3.58)	8.8 (9.3)	
Loading ASI (%)	0.6 (12.2)	5.6 (21.3)	
2MWT distance (m)	192 (16)	140 (35)	*

The RMSa measured at the pelvis level along the three directions was lower in amputee people compared to sound participants, although this difference was significant only for the mediolateral component. To the contrary, RMSa was significantly higher in amputees compared to sound participants in the mediolateral direction for the sternum and in both mediolateral and anteroposterior directions for the head. For all three levels of the upper body, RMSa along the vertical direction were lower in transtibial amputees although not significantly.

The symmetry indices (iHR, temporal and loading ASI) indicated a trend of reduced symmetry in people with transtibial amputation compared to sound participants, but only the iHR differences proved to be statistically significant between populations.

Attenuation coefficients were similar across both populations in the vertical direction. Conversely, people with transtibial amputation exhibited lower coefficients, sometimes negative, in the anteroposterior and mediolateral directions for the pelvis-to-head and pelvis-to-sternum coefficients.

2.1.3. Discussion

The aim of this study was to investigate the relevance and feasibility of monitoring gait quality using indices obtained using wearable sensors such as IMUs and pressure insoles. First, the repeatability intra-session of the identified gait quality indices was investigated in both populations of transtibial and sound participants. Eleven out of the 22 repeatable indices (including the distance covered during a 2MWT) were shown to allow to discriminate transtibial amputees from sound subjects.

Except for the attenuation coefficients between the pelvis and sternum in the vertical direction in the asymptomatic population and the RMSa measured at sternum level in the anteroposterior direction in the transtibial amputee population, no gait quality index displayed a statistically significant difference between both repetitions of the 2MWT. It was thus decided to discard these indices from further analysis. Indeed, they were considered less susceptible of detecting subtle changes within a population.

Conversely, the parameters included in the analysis were deemed repeatable as no difference was detected between both repetitions of the 2MWT. However, the present results must be interpreted in the light of the following two considerations: first, it is possible that no difference was detected due to the small samples included in this study. Second, the repeatability coefficients obtained in this study are likely to underestimate the minimal detectable change by each pair of sensor and gait quality index. Indeed, these indices were acquired within the same session, without removing and repositioning the sensors. A different positioning of sensors would have affected the measured signals, and hence, the values of the retrieved parameters. Similarly, inherent day-to-day variability within participants could have contributed in the increase of the repeatability coefficients.

Except for the distance covered within a 2MWT, no prior study reports repeatability coefficients or minimal detectable changes for the parameters and the population investigated in this study. Therefore, for the gait quality indices obtained with wearable sensors, it is not possible to compare the computed repeatability coefficients with the literature. Regarding the distance, Resnik and coworkers evaluated the test-retest reliability of the 2MWT in a sample constituted with 44 lower-limb amputees, including 19 (43.2%) people with transtibial amputation and 25 (56.8%) people with transfemoral or though-knee amputation, who performed a 2MWT twice within a week. The minimal detectable change with a 90% confident interval reported in their study is 34.3 m against 14.6 m with a 95% confidence interval in the present study (Resnik and Borgia, 2011). Since the distance measurement is not affected by sensor relocation, it is expected that the study design is not accountable for most of the observed difference. In the study retrieved from the literature, the participants could use mobility aids (although it is not mentioned if any of the participants did require any assistance when performing the test), participants were older than in the current study (mean age: 66 ± 13 years) and a little more than half of them were amputated at a higher level, while age and level of amputation have been shown to be associated with decreased functional capacities. Therefore, we assume that the results achieved in the present study are more susceptible to represent the population of experienced walkers with transtibial amputation. According to our results, the 2MWT is thus able to detect score changes as low as 15 m. A between-session configurations should nevertheless be implemented to confirm our results on a bigger sample size.

In general, higher repeatability coefficients (and thus, higher minimal detectable changes) were observed in people with transtibial amputation compared to sound participants, except for the stance-phase duration ASI and the distance (**Table 24**). This reflects a higher inter-subject variability within the population of people with transtibial amputation compared to sound subjects. The different prostheses used by the recruited participants and the large range of durations since amputation may explain the observed variability in this population. The values of the repeatability coefficients provide

trends regarding the possible minimal detectable changes in people with transtibial amputation and in sound participants. However, in order to interpret if a gait quality index obtained following the presented protocol can detect sufficiently subtle changes to track patients' progression during the rehabilitation, baseline values and values achieved during the rehabilitation are required. Therefore, a study involving a regular follow-up of people with transtibial amputation undergoing rehabilitation is necessary. Comparing the repeatability coefficients to the 2MWT score changes observed between baseline and follow-up / discharge would allow to conclude on the relevance of the selected parameters for rehabilitation monitoring.

ii. Description of the transtibial and asymptomatic populations using gait quality indices

Apart from the iHR, all the gait quality indices reported in the present study had already been investigated in the population of people with transtibial amputation in the literature, although never concomitantly.

The distance covered during the 2MWT by both populations is consistent with the values reported in the literature for both sound adults (Bohannon *et al.*, 2015) and people with transtibial amputation (Gaunaurd *et al.*, 2020). Furthermore, this confirms that self-selected speed of people with transtibial amputation is lower than that of sound participants. This reduced walking speed might not only be the sign of higher metabolic cost of walking (Waters *et al.*, 1976) but also of decreased stability as it was shown to be one of the mechanisms allowing to increase the margin of stability (Hak *et al.*, 2014).

Sound participants achieved similar iHR scores as those reported in the literature (Bergamini *et al.*, 2017; Pasciuto *et al.*, 2017). Regarding the scores achieved by people with transtibial amputation, while no reference value could be retrieved in the literature, results seem consistent. Indeed, the achieved iHR scores by people with transtibial amputation in this study were closer to those of asymptomatic population than people with transfemoral amputation (Pasciuto *et al.*, 2017), who were previously shown to have a more asymmetrical gait pattern than people with transtibial amputation (Nolan *et al.*, 2003; Iosa *et al.*, 2014; Cutti *et al.*, 2018). Iosa and coworkers have evaluated the HR in people with transtibial and transfemoral amputation at dismissal of the rehabilitation center (Iosa *et al.*, 2014). The HR was shown to be less reliable and more difficult to interpret than its improved version (Pasciuto *et al.*, 2017) and therefore was not investigated in the present study. However, the authors in (Iosa *et al.*, 2014) observed the same trend as retrieved here: the gait of transtibial amputees was shown to be statistically more asymmetrical than that of sound participants.

Asymmetry was also quantified in the present study using the ASI computed based on the stance-phase duration (temporal ASI) and the vertical acceptance peak occurring in the first half of the stance phase (loading ASI). These parameters have been described in (Nolan *et al.*, 2003) in a population of four people with transtibial amputation, four people with transfemoral amputation and six sound subjects walking along a straight line at various speeds. Similarly as in (Nolan *et al.*, 2003), people with transtibial amputation were shown to spend more time and put more weight on their sound leg than on the prosthetic leg. The asymmetries observed in the present study were less important than those reported in (Nolan *et al.*, 2003), which might be explained by the higher distance and number of steps covered in the present study, allowing to select strides pertaining to the steady state of gait. Although people with transtibial amputation exhibited more temporal and loading asymmetries than sound participants, the difference between both populations was not found to be significant.

It is interesting to note that among the 3 different kind of parameters quantifying gait (a)symmetry, the iHR displayed less between-subjects variability than the conventional asymmetry parameters and was the only index allowing to discriminate people with transtibial amputation from sound participants (**Table 25**).

Interestingly, RMSa measured at the pelvis level was lower in the group of transtibial amputees than in sound participants in all directions, even if the difference was only statistically significant for the mediolateral acceleration. In the literature, pelvis RMS values were higher in pathological gait than in normal gait at pelvis level when normalized to walking speed (Summa *et al.*, 2016; Bergamini *et al.*, 2017; Belluscio *et al.*, 2019). In (Paradisi *et al.*, 2019), RMS accelerations at the pelvis level were found to be significantly higher in the transtibial amputation group than in the control group in the mediolateral direction, but the RMS was not normalized to walking speed while the former was shown to be significantly more important in the control group. Another reason for this difference might again lie in the reduced time since amputation in the population investigated in the present study compared to that recruited in (Paradisi *et al.*, 2019). Indeed, in (Iosa *et al.*, 2014), lower-limb amputees evaluated at discharge from the rehabilitation exhibited significantly lower RMS values at the pelvis level along the anteroposterior and mediolateral directions compared to the control group. The less time spent walking with a prosthesis may contribute to a lower trust in the prosthesis, resulting in voluntarily restraining motion at the pelvis level to enhance control over the prosthesis.

Conversely, sternum and head RMSa were significantly higher in amputees compared to sound participants in both the mediolateral and anteroposterior directions. Attenuations of the accelerations from pelvis to sternum in the anteroposterior and mediolateral directions were insufficient to regulate the RMSa at the sternum level in the transtibial amputee group. The higher RMSa at the sternum in the mediolateral direction may result from gait compensations involving the trunk in the frontal plane of people with transtibial amputation (Michaud *et al.*, 2000). In the amputee group, negative attenuation coefficients were observed from the sternum to the head, thus leading to an amplification of the accelerations and increased RMSa at head level compared to sternum level, confirming results from the literature (Paradisi *et al.*, 2019). Similarly, reduced attenuations of accelerations from the pelvis-to-head accelerations were observed in our sample of amputees compared to sound participants or even to the transtibial amputees described in (Paradisi *et al.*, 2019). This seems to indicate a lower stability of the transtibial amputees recruited in the present study, which might be explained by the reduced time interval since amputation of some participants. The difficulty to attenuate accelerations from the lower limbs in the anteroposterior and mediolateral directions may result from the reduced counter-rotation of pelvis and trunk segments in the transverse plane observed in people with lower-limb amputation (Goujon-Pillet *et al.*, 2008) and was also observed in patients with subacute stroke (Bergamini *et al.*, 2017). This may lead to instability of the head, thus compromising a steady optical flow and vestibular proprioception, which in turn may lead to an increased fall risk.

All in all, the quantified parameters during the 2MWT tended to indicate a decreased dynamic balance in people with transtibial amputation compared to sound participants, even if only eleven of the twenty-two remaining parameters (including the distance) allowed to discriminate the two populations. It should be noted that this study doesn't allow to conclude on the most relevant parameters for rehabilitation monitoring in people with lower-limb amputation. Indeed, the eleven parameters that differ between populations may not display a progression during the rehabilitation

143

and therefore, may not be responsive to change. In particular, the attenuation coefficients were shown not to display a significative difference between assessments occurring before and after vestibular rehabilitation training in people with stroke (Tramontano *et al.*, 2018). Conversely, the parameters that were not found to be statistically different in sound participants and people with transtibial amputation that have terminated their rehabilitation may display a wide margin of progression during the rehabilitation. Therefore, obtaining baseline values at the beginning of – or in the course of – rehabilitation is paramount to draw conclusions on the relevance of the considered parameters. However, some assumptions can be drawn by comparing the values of the repeatability coefficients of each gait index with the median values achieved in rehabilitated transtibial amputees. For instance, the high variability of attenuation coefficients within the population of people with transtibial amputation leads to repeatability coefficients that are way higher than the achieved median values as well as than the difference of median values between transtibial amputees and sound participants. As a consequence, these parameters are not expected to capture subtle changes that may occur during the rehabilitation of people with transtibial amputation. Conversely, the repeatability coefficients of the three components of the iHR are very low compared to the median iHR values of people with transtibial amputation while being lower than the observed difference between both populations. It therefore appears that the iHR could allow the detection of subtle improvements in the symmetry of transtibial amputee gait. These hypotheses should be verified in a study involving transtibial amputees undergoing rehabilitation, which, in turn, would allow to quantify and compare gait quality indices measured at several periods of the rehabilitation.

This study allowed to demonstrate the feasibility of instrumenting people with transtibial amputation during their rehabilitation to quantify gait quality indices. The latter were acquired by a physiotherapist during a 2MWT, which is a clinical test easy to implement and usually performed in clinical practice. The participants reported no discomfort or motion hindrance due to the sensors. In order to facilitate the implementation of the protocol in the clinical routine, automation of the post-processing is required (in particular, sensors synchronization) as it would allow to obtain an immediate report at the end of the rehabilitation session.

2.1.4.   Conclusions

This study investigated the feasibility and relevance of tracking gait quality indices derived from IMUs or pressure insoles signals during two-minute walking tests (2MWT) performed by people with transtibial amputation. Most of the investigated gait quality indices (improved harmonic ratio, root mean square of head, sternum and pelvis accelerations, loading and temporal gait symmetry and attenuation coefficients from the lower-limbs to the upper-body) were shown to be repeatable within session, and therefore to be good candidates for such a monitoring. Furthermore, ten out of the twenty-three investigated indices showed that people with transtibial amputation exhibited an asymmetrical gait pattern and were more prone to falling than asymptomatic people. A between-session test-retest reliability study should be implemented to confirm the observed trends regarding the reliability of the gait quality indices derived from wearable sensors in transtibial amputee gait. A study allowing to retrieve baseline values of the indices at the beginning and during the rehabilitation must be implemented in order to identify the indices that allow to detect a progression of the participants during the rehabilitation and therefore to confirm the relevance of the instrumented 2MWT for the follow-up of people with transtibial amputation along their rehabilitation.

2.2. Computation and interpretation of the improved harmonic ratio in people with lower-limb amputation

Despite its wide use for gait symmetry quantification in the recent literature, the computation and interpretation of the improved harmonic ratio (iHR) retains some uncertainties.

This section will therefore be divided in two subsections. The first subsection aims at clarifying whether the iHR must be computed on segmented gait cycles or if it could be computed on the whole gait signal without segmentation, and if the segmentation method has an impact on the computed score. This study was presented at the 2019 congress of the Société de Biomécanique and uses the data described in the first chapter of Part 3. The second subsection aims at investigating the relationship between the iHR and traditional temporal and loading asymmetry indices, which are used in the clinical practice and are easily interpretable. Indeed, while the iHR was shown to discriminate people with transtibial amputation from sound participants, where commonly used temporal or loading asymmetry indices failed (see section 2.1 above), its interpretation in terms of the (a)symmetry origin or causes remains questionable. This study uses the data collected on nine people with transtibial amputation, presented in the preceding section.

2.2.1. Investigating symmetry in amputee gait through the Improved Harmonic Ratio: influence of the stride segmentation method

a. Introduction

The quantification of gait symmetry is extremely important in several clinical contexts. Among the many indices used to describe gait symmetry, the Harmonic Ratio (HR), which is based on a stride-by-stride spectral analysis of trunk accelerations, is often used (Bellanca *et al.*, 2013). Recently, an improved version of this index (iHR) has been proposed, relying on a rigorous mathematical definition and on values ranging from 0 to 100% (Pasciuto *et al.*, 2017). The influence of acceleration realignment procedures (Buckley *et al.*, 2017), as well as of the number of considered strides and harmonics on HR and/or iHR values have been assessed in the literature, and standardized guidelines have been proposed in this respect (minimum of 20 strides and 20 harmonics should be considered) (Riva *et al.*, 2014; Pasciuto *et al.*, 2017). Concerning stride segmentation approaches, several methods are usually adopted in the literature, based on different signals (ground reaction forces, pelvis or shank accelerations or angular velocities), thus corresponding to different instants of time within the gait cycle. The whole signal has also been considered, to avoid the propagation of errors due to inaccurate segmentation (Riva *et al.*, 2013). Nevertheless, despite its role in the computation of iHR, the impact of the stride segmentation method has never been adressed, especially in people characterized by high gait asymmetry, such as people with lower-limb amputation. Thus, the aim of this study was to investigate the influence of different stride segmentation methods and of the absence thereof on iHR values obtained during gait in people with transfemoral amputation.

b. Methods

i. Participants & protocol

This study was granted ethical approval (CPP IDF VI, N° 2014-A01938-39) and seven people with transfemoral amputation (5 males, age: 47.3± 9.9 years, mass: 74.5±11.9 kg) gave written informed

145

consent prior to their participation. They were instrumented with a pair of pressure insoles (Novel, 100 Hz) and two inertial measurement units (Xsens, 100 Hz) located on their lower trunk (L4/L5 level) and prosthetic shank. Participants walked a minimum of three times at their self-selected speed along an 8-meter linear pathway. At the beginning of each trial, they were required to stay in a static posture for 3 seconds and to perform a kicking task for synchronization purpose.

ii.   Data processing

Proper alignment of the trunk unit with craniocaudal (CC), anteroposterior (AP), and mediolateral (ML) anatomical axes was ensured through a verticalization procedure during the initial static posture of each trial (Bergamini *et al.*, 2014). Only steady state strides were considered by discarding the first and last strides of each trial. The iHR was then computed, for each stride and each anatomical axis, using four different segmentation methods, representative of the state of the art:

- Insoles (REF) (used as a reference): based on the timings of initial foot contacts, determined using a 20 N threshold on the insole signals;
- Shank (TIB): based on local maxima in the measured ML shank angular velocity signals, roughly corresponding to the middle of the swing phase;
- Pelvis (PEL): based on the local maxima in the measured ML lower-trunk angular velocity signals, occurring slightly after initial contacts;
- Zijlstra (ZS): based on an algorithm which identifies initial contacts in the AP acceleration measured at the lower-trunk (Zijlstra and Hof, 2003).

In addition, no stride segmentation (ABS) was also considered, corresponding to the calculation of the iHR on the whole signal for each gait trial, from the first to the last initial contacts detected by the insoles.

For each patient and each segmentation method, the medians and interquartile ranges (IQRs) of the iHR were computed. The IQR/median ratio (IMR) was also calculated to estimate the iHR reliability.

iii.   Statistics

A Shapiro-Wilk test was performed on the iHR medians and IMR. According to the results of this test, a one-way Repeated Measures ANOVA, or a Friedman test, was performed to investigate if significant differences existed between REF and the other methods (TIB, PEL, ZS, ABS). Pairwise comparisons were analyzed using *post-hoc* paired t-tests or Wilcoxon signed-rank tests and considering a Holm-Bonferroni correction. Finally, Pearson's or Spearman's correlations were used to investigate correlations between iHR values obtained with IS and the other four methods. The significance level (α) was set to 0.05 for all statistical tests.

c.   Results and discussion

A total of 405 strides pertaining to the steady-state phase of gait were analyzed.

Regarding the iHR obtained with IS, results were consistent with those obtained in the literature for the same population (Pasciuto *et al.*, 2017) (**Figure 49**). Only iHR scores obtained without segmentation (ABS) were significantly different to those obtained using insoles (REF), for all three axes (**Figure 49** – p < 0.0125 ; **Figure 50**). Furthermore, iHR scores derived from TIB, PEL, and ZS were very strongly and significantly correlated with the reference iHR (r>0.97, p<0.05). Conversely, correlations

between REF- and ABS-based iHRs were only moderate and not significant in two out of three directions.
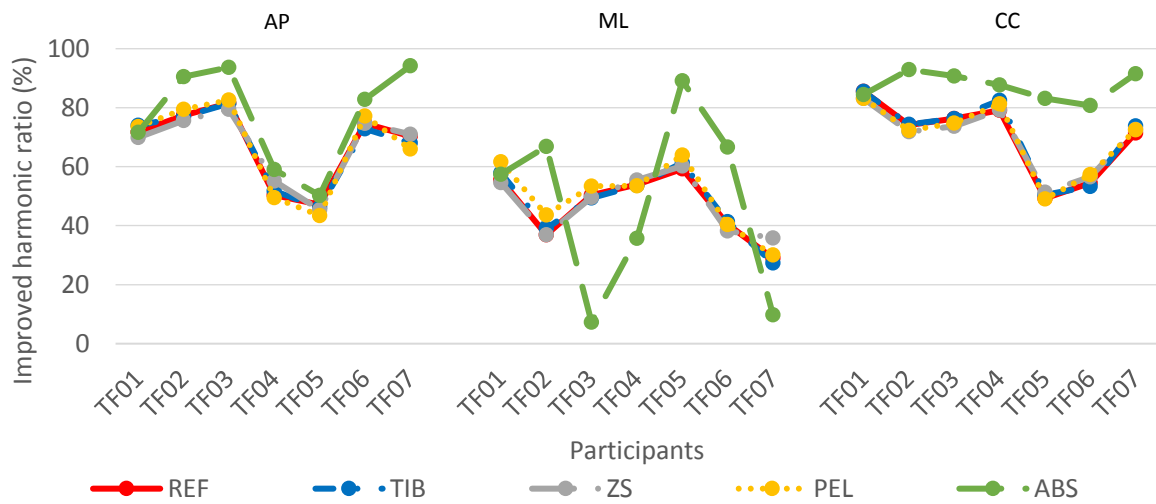
Figure 49: Median values of the iHR scores for each segmentation method (REF = reference, insole-based method; TIB = shank-based segmentation ; ZS = segmentation based on Zijlstra's algorithm, PEL = lower-trunk based segmentation) and in the absence thereof (ABS = no segmentation) and each participant along all three anatomical axes : anteroposterior (AP), mediolateral (ML), vertical (CC).
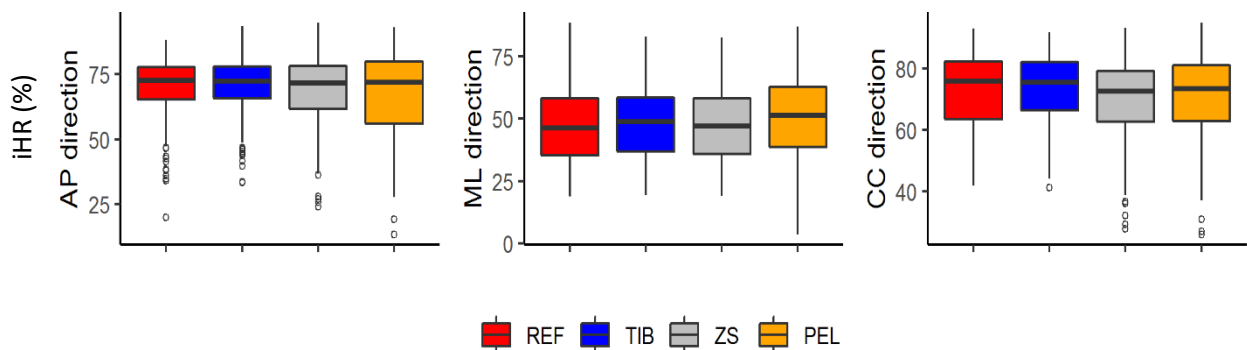
Figure 50: Median and interquartile range values over all participants for all the segmentation methods (REF = reference, insole-based method; TIB = shank-based segmentation ; ZS = segmentation based on Zijlstra's algorithm, PEL = lower-trunk based segmentation) along all three anatomical axes : anteroposterior (AP), mediolateral (ML), vertical (CC).

Concerning the iHR reliability, consistently with previous findings (Pasciuto *et al.*, 2017), IMR values were found to be higher in the ML than in AP or CC direction (**Table 26**). No statistically significant difference was found between IMRs obtained with IS and any other methods, for each axis. Nevertheless, TS-based iHR IMRs tended to be higher than those obtained with the other segmentation methods.

147

Table 26: Mean and standard deviations of the iHR IMRs (ratio of the interquartile range and median), for each segmentation method (REF = reference, insole-based method; TIB = shank-based segmentation ; ZS = segmentation based on Zijlstra's algorithm, PEL = lower-trunk based segmentation) and in the absence thereof (ABS = no segmentation) for the different anatomical axis (anteroposterior [AP], mediolateral [ML], vertical [CC]).

| | | iHR IMR values [%] | | |
		AP	ML	CC
Segmentation method	REF	11.3 ± 5.9	21.4 ± 9.7	12.7 ± 5.6
	TIB	11.3 ± 2.0	28.1 ± 22.9	7.2 ± 4.4
	ZS	12.7 ± 7.4	29.4 ± 8.4	13.1 ± 3.5
	PEL	12.6 ± 8.1	34.6 ± 16.0	15.4 ± 5.8
	ABS	6.9 ± 32.2	49.8 ± 60.4	5.6 ± 14.0

d. Conclusions

This study showed that computing iHR on the whole acceleration signal provides significantly different results than using any of the assessed stride segmentation method. When using stride segmentation methods, care should be taken to ensure that the method chosen provides a reliable segmentation for the specific population under study. In particular, special attention must be paid when using pelvis accelerations due to feet impacts attenuation and inherent signal variability at trunk level (Trojaniello *et al.*, 2015).

2.2.2. Investigating symmetry in amputee gait through the Improved Harmonic Ratio: comparison with commonly used loading and temporal symmetry indices

In order to investigate the relationship between the iHR and conventional gait symmetry indices, the data previously collected during a 2MWT performed by nine sound participants and nine people with transtibial amputation were used (see section 2.1.1). The median iHR values along the three directions and the median absolute symmetry indices (ASI) of stance-phase duration (temporal symmetry) or of the vertical ground reaction force peak occurring in early stance (loading symmetry) (Nolan *et al.*, 2003) of each participant were retrieved during the first repetition of the 2MWT. Spearman correlations were then computed between the temporal and loading ASI and the iHR computed in all three directions, for the population of transtibial amputees and for the sound population. The level of significance was set to 0.05.

The achieved correlations between the iHR and the ASI are reported in **Table 27**.

Table 27: Spearman's correlations (ρ) and associate *p*-values between the improved harmonic ratio (iHR) computed in the anteroposterior (AP), mediolateral (ML) and vertical (V) directions and the temporal and loading absolute symmetry index (ASI) in nine people with transtibial amputation and nine asymptomatic participants.

| | Sound participants (n = 9) | | | | Transtibial amputee participants (n = 9) | | | |
| | Loading ASI | | Temporal ASI | | Loading ASI | | Temporal ASI | |
	ρ	*p*-value	ρ	*p*-value	ρ	*p*-value	ρ	*p*-value
iHR AP	0.15	> 0.05	-0.17	> 0.05	0.15	> 0.05	-0.03	> 0.05
iHR ML	0.18	> 0.05	0.48	> 0.05	-0.08	> 0.05	0.05	> 0.05
iHR V	0.60	> 0.05	0.58	> 0.05	0.43	> 0.05	-0.17	> 0.05

None of the correlations were found to be significant (*p*-value > 0.05). Furthermore, the strength of the correlations between each pair of iHR component and ASI were shown to differ across

148

populations (see for instance the correlation between the iHR in the mediolateral direction and the temporal ASI in both populations in **Table 27**). Therefore, it can be concluded that the iHR components are not associated with either gait temporal or loading symmetry.

The former indices are easier to interpret than the iHR but were shown not to allow the discrimination between people with transtibial amputation and sound participants. Therefore, they may not allow to detect changes within patients or to detect the differences between transtibial amputees displaying different levels of asymmetry. Conversely, the iHR allowed to discriminate people with transtibial amputation from sound participants and displayed small repeatability coefficients, indicating that it may allow the detection of subtle changes of (a)symmetry within participants. Furthermore, the iHR is computed from the acceleration signals of one sensor positioned at the pelvis, which doesn't require to be calibrated. It therefore provides a more ecological measure than the ASI derived from pressure insoles data. However, it should be noted that the pelvis is chosen as a point to emulate the body center of mass. The validity of this assumption when computing the iHR should however be verified in pathological gait, as it was shown that the pelvis acceleration does not accurately emulate the body center of mass acceleration in people with transfemoral amputation for instance (see chapter 2, part 3). Furthermore, the clinical interpretation of the iHR is not straightforward. It seems to identify overall gait (a)symmetry and, based on its definition, it is likely influenced by asymmetrical gait pattern of contralateral limbs. However, it is not currently possible to conclude on the origin(s) of the detected asymmetries. Further investigations are therefore required to shed light on the interpretation of the iHR in people with lower-limb amputation. It might be relevant to investigate the impact of asymmetries in joint patterns on the iHR values in order to better further understand this parameter.

Conclusion

This part of the thesis aimed at investigating the feasibility, relevance and intra-session reliability of using wearable sensors to describe gait quality using parameters derived from direct signal processing, which neither require a biomechanical model of the human nor of the performed motion. These parameters can be retrieved from a low number of sensors by instrumenting clinical walking tests, making them particularly relevant for an ecological monitoring of rehabilitation.

In the first chapter, the feasibility of deriving temporal parameters from gait events identified in the signals of a single or two segment-mounted IMUs was investigated. Five algorithms taken from the literature were implemented and tested using gait data of people with transfemoral amputation. Two algorithms were found to allow an accurate detection of initial and final contact events. However, they tended to either underestimate the sound stance phase or to overestimate the prosthetic stance phase durations, which prevents their use for the quantification of temporal asymmetry. Further work is required to improve the algorithms in order to use them for temporal asymmetry monitoring in people with transfemoral amputation. The adequacy of the developed algorithms to the gait of people with transtibial amputation, which does not exhibit the same compensations as that of transfemoral amputees, should also be investigated. Although IMUs do not appear to be mature yet for temporal parameters tracking in people with transfemoral amputation, pressure insoles represent a valid wearable alternative (Loiret *et al.*, 2019).

In the second chapter, the feasibility and relevance of tracking gait quality indices in people with transtibial amputation undergoing rehabilitation by instrumenting the two-minute walking test (2MWT) with pressure insoles and IMUs was investigated. In order to fulfill this aim, gait quality indices (improved harmonic ratio [iHR], root mean square of accelerations [RMSa] and attenuation coefficients between the pelvis, sternum and head) were computed in both rehabilitated people with transtibial amputation and sound participants. The study therefore allowed to obtain reference values for the population of transtibial amputees and to characterize the risk of falling and gait asymmetry of this population by comparison to sound participants with the above-mentioned gait quality indices. In particular, this study was the first to provide values for the iHR in people with transtibial amputation. The first step conducted in this study is necessary in order to obtain target values during the rehabilitation. Furthermore, the participants were asked to perform two repetitions of the 2MWT, which allowed to obtain a first estimate of the minimal detectable change by each pair of sensor/gait index. Although the retrieved repeatability coefficients may underestimate the actual minimal detectable changes, this study was the first proposing to assess the intra-session reliability of gait quality indices acquired during a clinical test. However, without knowing the values taken by these gait quality indices by people undergoing rehabilitation, the feasibility of actually detecting a gait quality improvement or deterioration using the proposed protocol cannot be confirmed yet. However, it is worth noting that the protocol presented in this study proved to be compatible with clinical context and could be directly implemented during the rehabilitation of patients.

Furthermore, although ten of the investigated gait quality indices corroborated the literature regarding the higher risk of falling and reduced gait symmetry of people with transtibial amputation compared to the asymptomatic population, there is still a lack of hindsight on these gait descriptors, making their interpretation difficult. As an example, the iHR, computed from pelvis acceleration

signals, indicates overall gait (a)symmetry, but does not provide any indication regarding the origin of the asymmetry. In particular, this index was found not to be correlated with either temporal or loading symmetry computed with the absolute symmetry index. It is believed that kinematic asymmetries, such as an asymmetric knee flexion during gait, might have repercussions on the iHR, but the protocol implemented did not allow to verify this hypothesis. Computing the iHR on the trajectory of the pelvis or body center of mass may facilitate its interpretation but would considerably complexify its computation from IMUs.

To conclude, wearable sensors offer the opportunity of easily tracking gait while being minimally invasive. Multiple indices have been proposed in the literature to describe segments and body motion from the analysis of raw signals extracted from these sensors. For instance, the root mean square of the acceleration within a stride computed at different levels of the upper body has been proposed to describe the transmission and attenuations of oscillations from the lower limbs to the head while walking. Although the methodology is interesting, work has to be done in order to gain insight to interpret these parameters. This study contributed to a better understanding and mastering of wearable-based gait quality indices, advancing towards providing better tools for therapeutic follow up. In order to further enhance the understanding of these parameters, future studies should focus on establishing reference values on larger samples of pathological or asymptomatic populations while comparing the wearable-based gait quality indices to gold standards. This will facilitate the clinical interpretation of the retrieved gait quality indices and therefore will promote the clinical transfer of wearable gait quality analysis, thus having an actual impact on the clinical decision making.

General conclusion

The aim of this thesis was to contribute to the development of a wearable framework to support the in-field assessment of people with lower-limb amputation during their functional rehabilitation.

The first step to achieve this aim was to identify clinically relevant parameters that could be quantified using wearable sensor data. Therefore, the **first part** of the thesis aimed at providing an overview of the literature with regards to lower-limb amputee care (chapter 1), biomechanical parameters usually retrieved in lower-limb amputee gait analysis (chapter 2), and opportunities offered by wearable sensors through a presentation of the different technologies and the derived parameters from wearable sensor data analysis (chapter 3). In that last chapter, a special focus on pressure insoles and magneto-inertial measurement units (MIMUs) was developed, since these technologies were found to allow capturing a wide variety of gait descriptors, including a set of parameters that are usually retrieved to describe the gait of people with lower-limb amputation. Interestingly, since wearable sensors rely on different technologies compared to the gold standard optical motion capture systems or force platforms, the output parameters derived from wearable gait analysis may differ from those of usual laboratory-based gait analysis. In fact, two different approaches have emerged from the literature when dealing with wearable sensors, and most particularly with MIMUs. A first approach consists in developing biomechanical models of the human body or the motion (e.g. inertial model, inverted pendulum, kinematic chains) in order to retrieve biomechanically-founded parameters, similar to those that could be obtained (often more quickly and easily) with laboratory-based instruments. A second approach consists in identifying patterns in the signals measured by wearable sensors to extract new features describing a specific motion or pathology, to learn the relationship between the observed features and a relevant reference gait descriptor, or to link features in the signal to observed events. In this second approach, an *a priori* model of the human body or motion is not necessary, and the post-processing may seem closer to signal processing than biomechanical analysis. Both these complementary approaches were deemed relevant and were therefore implemented in the course of the thesis, with the aim to retrieve global descriptors of the lower-limb amputee gait allowing to quantify gait deficiencies and to relate those to mechanical parameters. The overview of the literature presented in the first part of the manuscript allowed to identify such global descriptors as being the kinematics of the center of mass and synthetic descriptors of balance and symmetry.

The **second part** of the manuscript, then, proposed a framework for wearable gait analysis based on a biomechanical model-based approach. This framework aimed at providing an accurate estimation of body center of mass kinematics from a minimal number of sensors, in order to be compatible with the clinical routine. First, optimal sensor locations were identified through the analysis of the contributions of fifteen segments (head, trunk, upper arms, forearms, hands, pelvis, thighs, shanks and feet) to the total body center of mass acceleration in ten people with transfemoral amputation, using a full-body inertial model and an optical motion capture system (chapter 2). In the third chapter, an almost fully wearable framework was proposed to retrieve body center of mass motion from inertial measurement units positioned on the identified segments. The framework allowed to estimate both body center of mass acceleration and instantaneous velocity from only five sensors located on the

trunk, thighs and shanks with high agreement compared to reference laboratory-based instruments in one person with transfemoral amputation (Pearson's coefficients of correlation r > 0.89 for the acceleration components and r > 0.94 for the instantaneous velocity). To the authors' knowledge, this is the first study that allowed to estimate the instantaneous velocity of the body center of mass in an inertial Earth-fixed reference frame from wearable sensors, without having formulated the hypothesis that the center of mass of the body lies in the pelvis reference frame. The same methodology could be applied in sound or other pathological gait to develop appropriate optimal sensor networks for these populations. Finally, an original study was proposed in chapter 4 to investigate the robustness of the developed framework to erroneous identification of sensors positions. The methodology proposed in this chapter could be easily adapted to other sensor networks or other biomechanical parameters (for instance, the instantaneous velocity). It could also be implemented to investigate the impact of errors resulting from the proposed static calibration and assumptions in the computed MIMUs orientations in a common global reference frame. It is therefore a precious tool to investigate the impact of sensor positioning or localization on a parameter of interest.

The work achieved in this framework has, however, some limitations, the most obvious being that the original algorithms and methods proposed in chapter 3 and 4 were developed and validated on the data from a single person with transfemoral amputation, partly due to the pandemic situation in 2020. More patients should be recruited in order to confirm the validity and relevance of the framework for body center of mass motion tracking. A second important limitation is that the wearable framework proposed in this work is quite cumbersome due to the need of multiple sensing modalities. The protocol could be simplified and made 100% wearable by using a 3D body scanner instead of calibrated photographs and an optical motion capture system. However, the accuracy of the scan-based geometric inertial model and of MIMUs positions retrieved from the scan should be evaluated. A few tracks for improvement regarding the framework consist in improving the identification of MIMUs location by positioning MIMUs on top of the stretch Velcro bands and/or by positioning colored stickers on top of the location of MIMUs origin. This could pave the way for the development of an algorithm that would automatically detect the position of MIMUs origins on the photograph or textured mesh issued from the 3D body scan in order to reduce the intervention of the operator. Eventually, the development of a kinematic model of the lower limbs and/or pelvis could allow to further reduce the number of required sensors.

In parallel with these improvements, the framework could be expanded to propose the quantification of other clinically relevant parameters. For instance, the instantaneous body center of mass velocity could further be integrated to estimate the body center of mass displacement or excursion, which was used for instance to quantify inter-limb symmetry in prosthetic gait (Askew *et al.*, 2019). Another parameter of great interest, especially for the rehabilitation of people with lower-limb amputation (Cutti *et al.*, 2018; Loiret *et al.*, 2019) is the ground reaction force under each foot while walking. Several models have been proposed but they generally use the assumption of symmetrical gait to distribute the force during the double stance phase of gait (Ancillao *et al.*, 2018), which is obviously not applicable in people with lower-limb amputation. Last but not least, combining the estimation of the ground reaction force under each foot with the instantaneous velocity of the body center of mass would allow to investigate mechanical energy exchanges with the individual limb method (Donelan *et al.*, 2002b), therefore providing relevant information regarding the effect of a

rehabilitation procedure or a prosthetic component on gait efficiency (Bonnet *et al.*, 2014; Askew *et al.*, 2019).

In the **third part** of the manuscript, the relevance and feasibility of the second wearable gait analysis approach – which consists in identifying features or computing metrics from the signals of wearable sensors without the use of biomechanical modelling – was investigated in people with lower-limb amputation, with the perspective of a clinical transfer for rehabilitation monitoring.

First, the accuracy of state-of-the-art methods for temporal parameter estimation using IMUs was assessed in people with amputation. To this aim, five inertial-measurement-units-based gait event detection algorithms were implemented and tested in people with transfemoral amputation. Although two of the five algorithms displayed a good accuracy in the timing of occurrence of initial and final contact events, validating their use for gait cycle segmentation, they tended to either underestimate the sound stance phase duration or to overestimate the prosthetic stance phase duration, resulting in the underestimation of stance phase duration asymmetry. This comparative analysis thus highlighted the need for the development and extended validation of algorithms that are specific to people with transfemoral amputation ambulating overground. It however provided a few tracks to enhance the current algorithms in order to further improve gait event detection.

In the second chapter, a protocol consisting in the instrumentation of the two-minute walking test (2MWT) with three inertial measurement units and two pressure insoles was proposed. It allowed to quantify recent gait quality indices in a group of transtibial amputees and of sound participants and was proved to be compatible with the rehabilitation. The investigated indices allowed to quantify either gait symmetry or the ability to attenuate acceleration from the lower limbs to the upper body, which was described in the literature as a pre-requisite to stabilize the head while walking and therefore, avoid falling. The study allowed to comparatively assess the population of transtibial amputees and of sound participants, and showed that people with transtibial amputation walk with a more asymmetrical gait than young and healthy participants (as evidenced by a lower improved harmonic ratio) and were more prone to falling (as evidenced by the higher root mean square accelerations at the head and sternum level and the low-to-negative attenuation coefficients exhibited by people with transtibial amputation). The study was the first to propose an estimation of the reliability of the investigated gait quality indices in both people with transtibial amputation and healthy participants. However, the participants were tested twice within the same session, which limited the influence of intra-participant variability and prevented to consider errors which could occur while setting up or calibrating sensors in the repeatability analysis. Therefore, the estimated minimal detectable changes found in this study are to be carefully interpreted as they may be underestimated. Still, the results obtained allowed to provide original reference values for these indices in rehabilitated people with transtibial amputation. In order to complete these results and advance towards clinical transfer of the protocol, future studies should focus on retrieving the values of these gait quality indices during the rehabilitation. Only then would it be possible to confirm the relevance of a gait quality index for monitoring gait symmetry and/or assessing the risk of falling during the rehabilitation. Lastly, there is still a lack of hindsight on the investigated gait quality indices, especially the improved harmonic ratio, which makes their interpretation difficult and compromise their use in the clinical field for clinical gait assessment. Concomitantly assessing the investigated gait quality indices with wearable

sensors and kinematic and balance biomechanical parameters issued from laboratory-based instruments may provide relevant information regarding how to interpret these parameters and how to benefit from these indices in the rehabilitation pathway. Furthermore, standardized protocols across laboratories may allow to develop a database to better characterize different populations using these parameters.

All in all, the work achieved during this thesis allowed to investigate two complementary approaches for the wearable gait analysis of people with lower-limb amputation. The first approach allowed to develop a comprehensive method based on a biomechanical model that allows to characterize the kinematics of the body center of mass with promising results, which should be confirmed on larger cohorts. This method could be used to adapt and monitor the effects of rehabilitation protocols as the retrieved synthetic global parameter (the instantaneous velocity or acceleration of the body center of mass) is directly linked to segmental motion. More development is required to improve the usability of wearable gait analysis in the clinical field (user-friendly acquisition system, quick post-processing, easy interpretation) and other synthetic parameters could be retrieved based on the proposed protocol. The second approach allowed to further validate a wearable framework that is mature for in-the-field quantification of gait quality indices that are intelligible to both the patients and the clinicians and allow to evaluate gait symmetry and balance. More work is required to further understand the implications of the different gait quality indices, notably the improved harmonic ratio, in order to propose rehabilitation protocols targeting these aspects of gait.

It is worth noting that all the methodologies that were proposed in this framework and developed for people with lower-limb amputation could be adapted to other pathologies as well. It should however be kept in mind that if the methodologies are transferable, most of the proposed algorithms rely on specificities of the gait of people with lower-limb amputation and may require some specific development for other populations.

Appendix A – Marker set used in Part 2

In the second part of the present manuscript, the participants were equipped with a full-body marker set as displayed in the following figures (**Figure appendix 1**, **Figure appendix 2**).

The marker clusters on the thorax (markers THOXX) and feet (PHXX and PBXX) were only present on the patient equipped with inertial measurement units (see chapters 3 and 4):
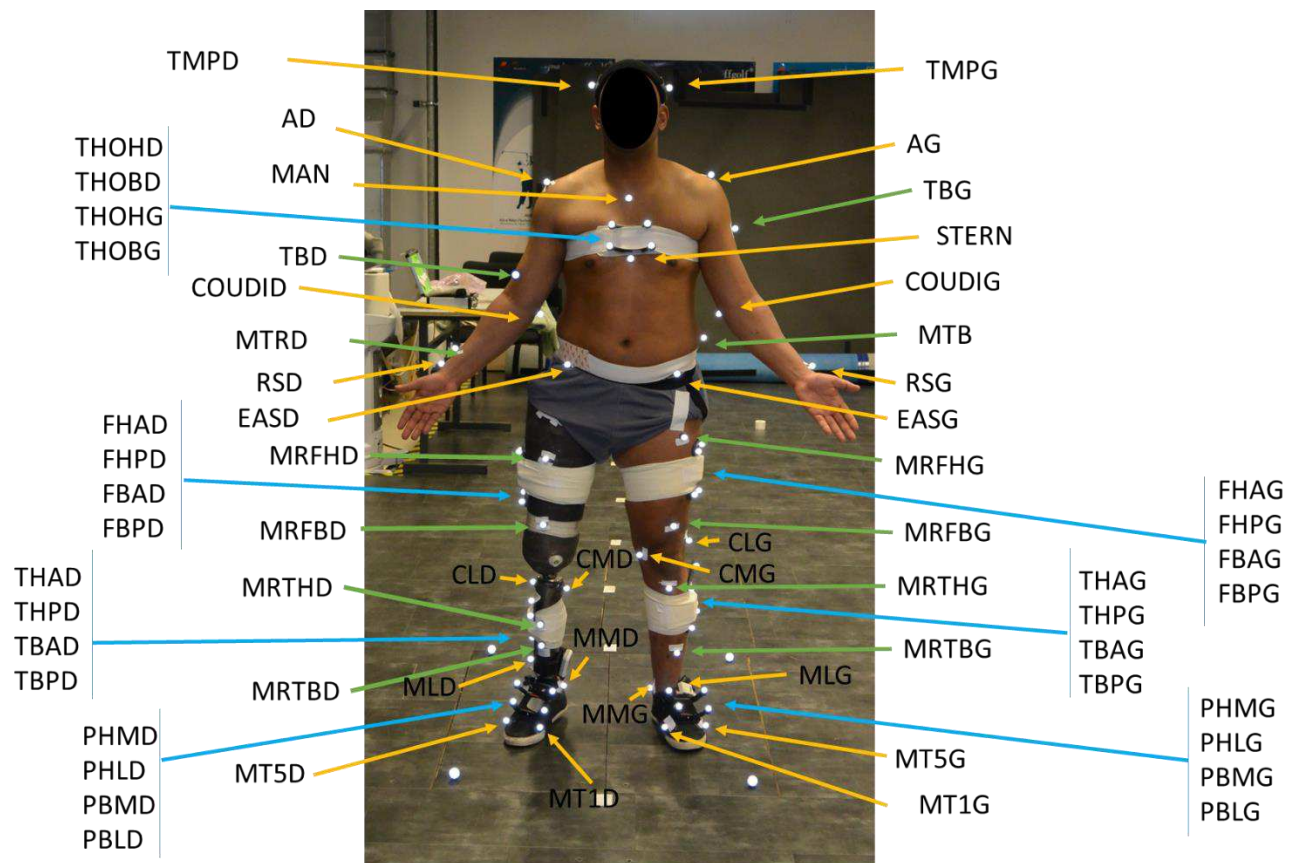

**Figure appendix 1** - Full-body marker set (face view)
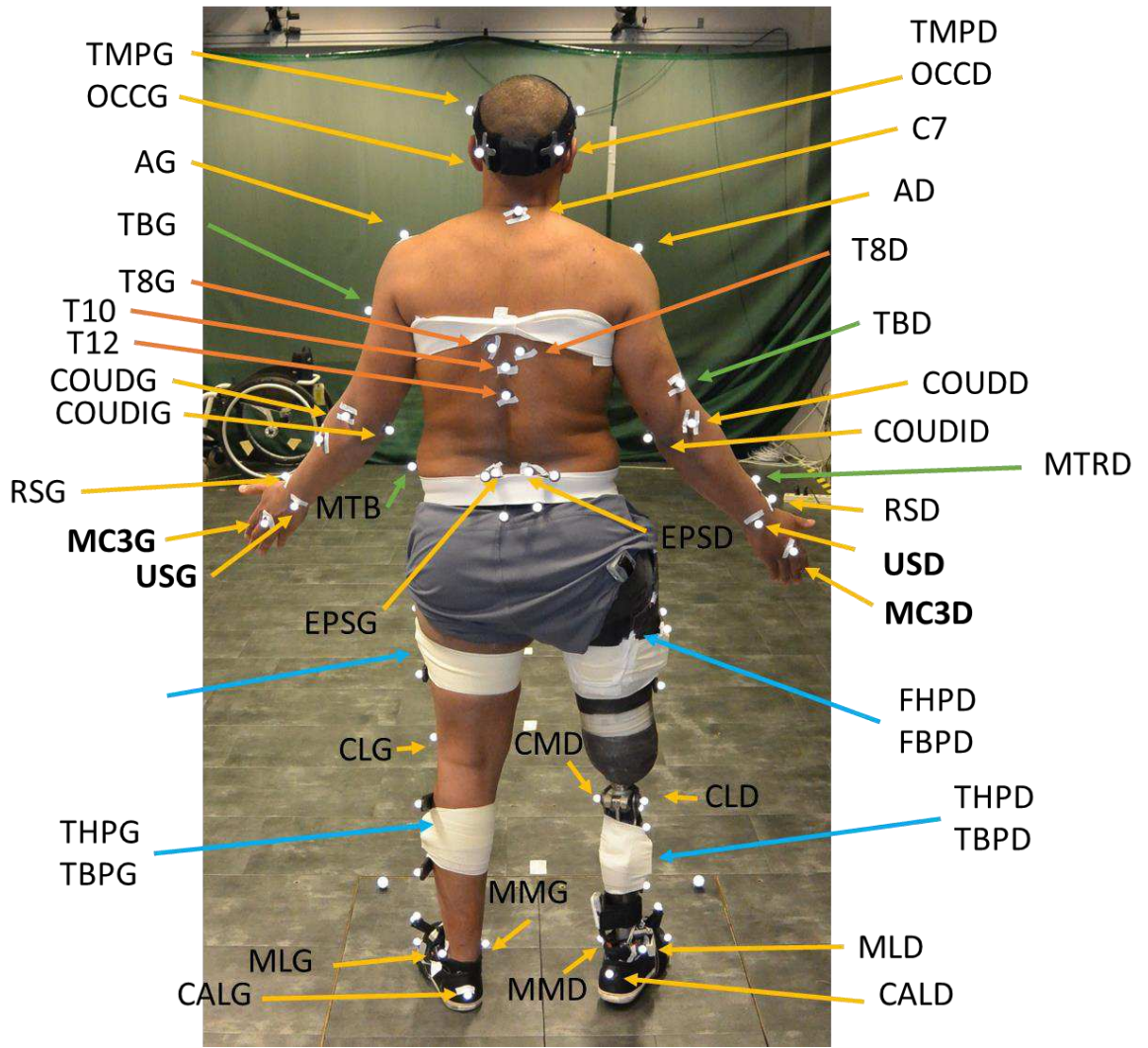
Figure appendix 2 - Full-body marker set (back view)

Appendix B – Comparative assessment of M-M algorithm

Given that M-M algorithm had both a very good sensitivity and high positive predictive values (PPV), close to that set as a criterion for further investigation, the possibility to decrease the PPV threshold criterion was considered.

Therefore, the accuracy achieved by this algorithm in detecting gait events and estimating temporal parameters was investigated.

However, results obtained with M-M are very poor compared to the other two algorithms, with a large dispersion of timing errors for gait event detection, and a data distribution far from the normality (as evidenced by a mean very different than the median) (see **Figure appendix 3**).

In the authors' opinion, due to the huge variability of its results, the M-M algorithm cannot be adopted in an actual clinical context and therefore, providing its results in the core of the manuscript was thought not to add significant/useful information to the study. Last but not least, making a clear graphical representation of the results was jeopardized by this error variability, as can be seen in the figures below (gait event detection timing in **Figure appendix 3** and temporal parameters errors in **Figure appendix 4**). For all these reasons, we finally decided to strictly respect the PPV threshold and to restrain the analysis to M-L and M-T algorithms.
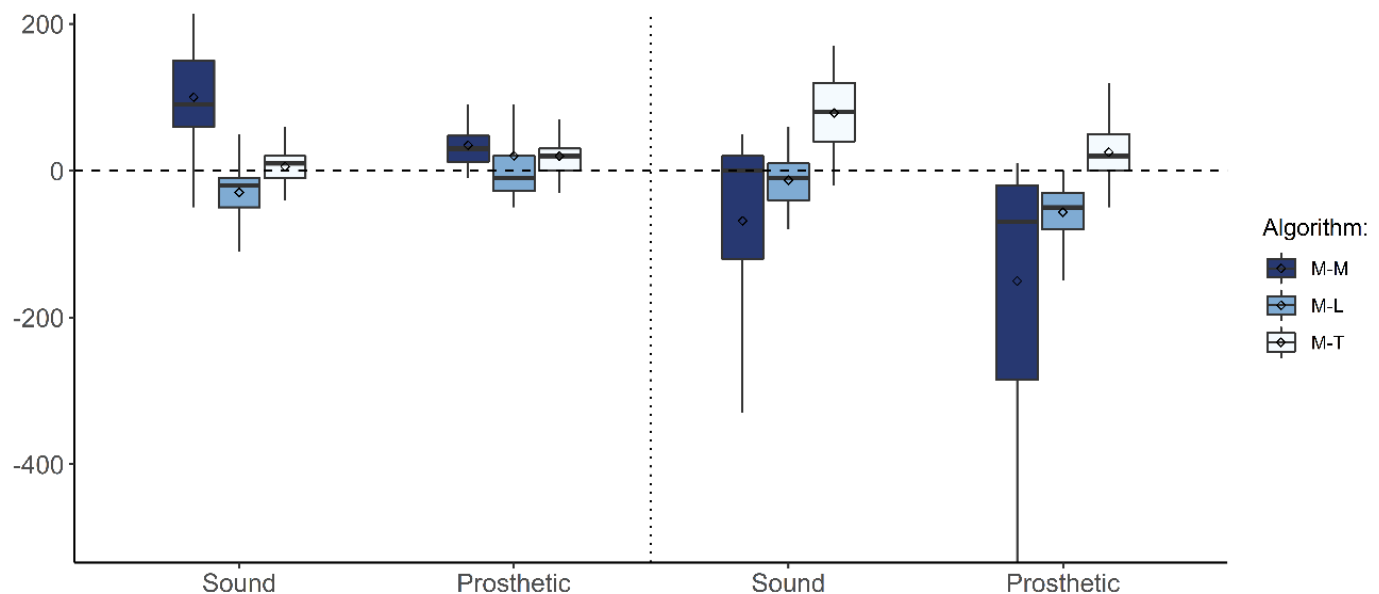
Figure appendix 3: Gait event timing errors with M-M, M-L and M-T (ms). Mean values are indicated with the diamond shape within the boxplot.

159
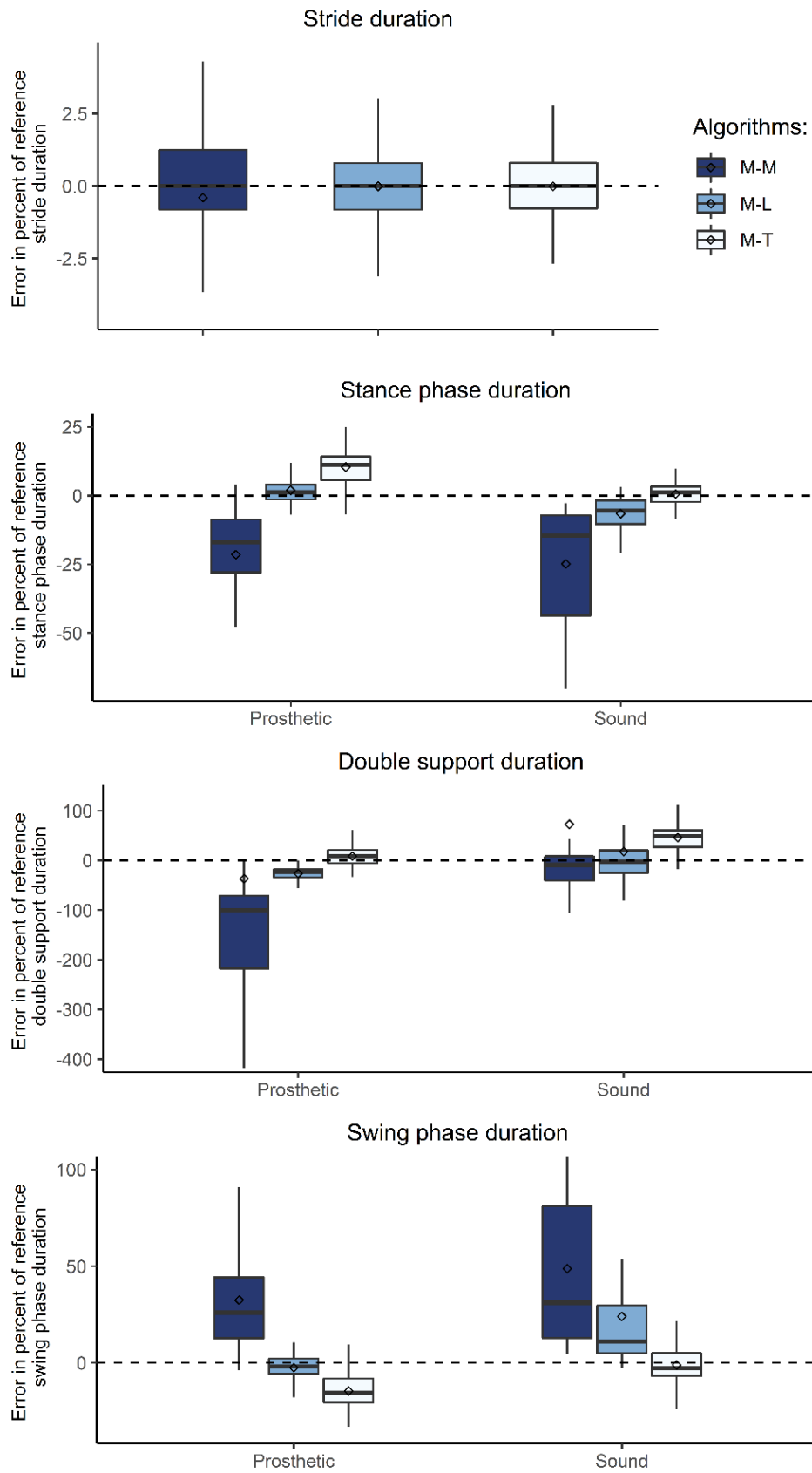
Figure appendix 4: Temporal parameters errors in % as obtained with M-M, M-L, M-T

Résumé détaillé de la thèse en français

1. Introduction et objectifs de la thèse

1.1. Objectifs et déroulement de la rééducation des personnes amputées de membre inférieur

L'amputation d'un membre inférieur a un impact définitif sur les capacités locomotrices et la qualité de vie des personnes amputées (Gailey *et al.*, 2008; Samuelsson *et al.*, 2012). Après l'amputation, les patients sont pris en charge par une équipe multidisciplinaire constituée d'un médecin MPR (Médecine Physique et de Réadaptation), de kinésithérapeutes et ergothérapeutes, d'un orthoprothésiste, et de tout autre personnel soignant jugé nécessaire (pour assurer, par exemple, un suivi psychologique). Cette équipe en charge de la rééducation a vocation à assurer le retour du patient à son domicile avec la meilleure qualité de vie possible. Pour ce faire, la rééducation a pour objectif de réduire les limitations fonctionnelles induites par l'amputation. Lorsque les capacités du patient le lui permettent, un appareillage peut être proposé. Dès lors, la rééducation s'attache à restaurer l'équilibre postural et de la marche ainsi qu'à restituer une marche la plus physiologique possible. En effet, les compensations et asymétries mises en place par la personne amputée appareillée peuvent conduire au développement de comorbidités (arthrose, lombalgie chronique…) notamment du fait des sur-sollicitations des articulations controlatérales qu'elles entrainent (Sawers and Hafner, 2013; Villa, Bascou, *et al.*, 2017).

Pour suivre l'évolution du patient pendant la rééducation, des évaluations régulières sont nécessaires. En clinique, celles-ci s'appuient principalement sur les observations des cliniciens ainsi que sur le ressenti du patient à propos de sa prothèse (notamment inconfort et douleurs) (Cuesta-Vargas *et al.*, 2010; Hafner and Sanders, 2014). Des indicateurs de performance peuvent être attribués par les cliniciens lors de la réalisation de tâches motrices spécifiques, telles que définies par des tests ou scores cliniques. Souvent, ces indicateurs sont en partie subjectifs car dépendent de l'appréciation et de l'expérience du clinicien. Certains tests cliniques, tels que le Timed-Up-and-Go test ou le test de deux minutes, consistent à réaliser une tâche locomotrice bien définie visant à évaluer la mobilité. Ces tests reposent alors sur une mesure quantitative objective telle que la durée nécessaire pour la réalisation de la tâche ou la distance parcourue pendant la durée de la tâche. Typiquement, ces deux tests ont été validés chez les personnes amputées de membre inférieur (Deathe *et al.*, 2009) et sont ainsi régulièrement réalisés lors de la rééducation afin d'obtenir une donnée quantitative d'évaluation de la performance lors de la marche. Toutefois, une bonne performance ne traduit pas nécessairement une bonne qualité de marche (Calmels *et al.*, 2002). Ainsi, l'évaluation de la rééducation doit prendre en compte d'autres aspects, tels que la symétrie et la régularité de la marche, l'occurrence de perte d'équilibre, etc.

1.2. Intérêts et limites des laboratoires d'analyse du mouvement

Les laboratoires d'analyse du mouvement, constitués en général de plateformes de force et d'un système optoélectronique, permettent d'obtenir de très nombreuses données quantitatives de la marche (Cappozzo *et al.*, 2005; Goujon, 2006). Ils ont largement été utilisés en recherche pour

161

caractériser la locomotion des personnes amputées de membre inférieur (Goujon-Pillet *et al.*, 2008; Houdijk *et al.*, 2009; Sagawa *et al.*, 2011; Villa, Loiret, *et al.*, 2017).

Les paramètres spatiotemporels de la marche font partie des paramètres les plus étudiés en, laboratoire d'analyse du mouvement chez les personnes amputées de membre inférieur (Sagawa *et al.*, 2011). Ils peuvent être calculés à partir de la trajectoire de marqueurs optoélectroniques au niveau des pieds et/ou de l'instant de dépassement de seuil d'effort détecté sur les plateformes de force. Les paramètres spatiotemporels permettent notamment de calculer la vitesse de marche, indicateur associé à la qualité de vie et au niveau fonctionnel d'une personne (Perry, 1992; Batten *et al.*, 2019), ainsi que les asymétries de durée d'appui ou de longueur de pas, mises en évidence chez les personnes amputées (Jaegers *et al.*, 1995; Goujon *et al.*, 2006; Roerdink *et al.*, 2012) et pouvant traduire une instabilité à la marche (Hof *et al.*, 2005; Hak *et al.*, 2014).

Les systèmes optoélectroniques permettent de décrire les trajectoires de segments ou articulations du corps pendant la marche et, lorsqu'associés à un modèle inertiel représentant le corps comme un ensemble de solides indéformables, d'obtenir la cinématique du centre de masse du corps (analyse segmentaire). Les asymétries du schéma de marche que l'on retrouve chez les personnes amputées de membre inférieur au niveau segmentaire ou articulaire ont des répercussions sur la trajectoire ou la vitesse du centre de masse du corps (Tesio *et al.*, 1998; Agrawal *et al.*, 2009; Askew *et al.*, 2019; Strutzenberger *et al.*, 2019). Ainsi, l'analyse de la cinématique du centre de masse issue des laboratoires d'analyse du mouvement permet de s'affranchir de l'analyse de la cinématique de chaque articulation ou segment tout en mettant en évidence la présence de compensations ou asymétries lors de la marche.

Les plateformes de force, quant à elles, fournissent des informations sur les efforts et moments de réaction au sol qui s'appliquent au corps au cours de la marche. Par application de la seconde loi de Newton, la somme des efforts de réaction au sol permet ainsi de calculer la cinématique du centre de masse lorsqu'aucun autre effort externe n'est appliqué au corps. Les efforts de réaction au sol sous chaque pied présentent un intérêt non négligeable lors de la rééducation des personnes amputées de membre inférieur en quantifiant la mise en charge de la prothèse et les éventuelles asymétries de charge entre le membre sain et prothétique (Loiret *et al.*, 2019). Par ailleurs, en combinant les efforts de réaction au sol et les informations de la cinématique articulaire, il est possible de calculer les efforts et moments articulaires. Enfin, lorsqu'associés à la vitesse instantanée du centre de masse, les efforts de réaction au sol sous chaque pied fournissent des informations sur le coût énergétique de la marche, à travers les échanges d'énergie mécanique (Donelan *et al.*, 2002a; Bonnet *et al.*, 2014)

La quantification de tous ces aspects biomécaniques de la marche est pertinente lors de la rééducation des personnes amputées de membre inférieur. Elle fournit en effet des renseignements à la fois sur la qualité et la performance de la marche. Par ailleurs, elle permet de fournir des données objectives et quantitatives d'évaluation de la marche, ce qui est de plus en plus attendu en pratique clinique avec l'émergence de « la pratique fondée sur la preuve » (« *evidence-based practice* »), notamment pour prescrire des composants prothétiques les plus adaptés possibles à un patient ou pour en justifier le remboursement (Hafner and Sanders, 2014; Agrawal, 2016; Hawkins and Riddick, 2018). En revanche, les laboratoires d'analyse du mouvement sont très coûteux, nécessitent un technicien/ingénieur formé et imposent une prise de mesure uniquement en laboratoire, ce qui limite leur utilisation en routine clinique (Loiret *et al.*, 2005). Par ailleurs, les données issues des laboratoires

d'analyse du mouvement, certes complètes et précises, sont très nombreuses, ce qui peut allonger et complexifier l'interprétation des mesures pour le clinicien. C'est pourquoi, l'utilisation de systèmes d'acquisition de données alternatifs, moins coûteux et permettant une évaluation globale de la marche, est attractive pour la rééducation.

1.3. *Emergence des capteurs embarqués et opportunités pour la rééducation des personnes amputées de membre inférieur*

La miniaturisation de capteurs et l'émergence de solutions embarquées abordables pour l'analyse du mouvement ces dernières années offrent de nombreuses opportunités de prise de mesure quantitative en situation écologique (Wong *et al.*, 2007, 2015; Iosa, Picerno, *et al.*, 2016; Benson *et al.*, 2018). Ainsi, les technologies embarquées telles que les centrales inertielles ou les semelles de pression pourraient permettre d'obtenir des données quantitatives de la marche, sans perturber celle-ci, au cours d'exercices de rééducation. Ceci complèterait le suivi actuel de la rééducation grâce à des données quantitatives et objectives acquises au cours de séances avec les praticiens, mais également en télé-rééducation. A terme, l'utilisation de la technologie embarquée au cours de la rééducation pourrait également bénéficier au système de santé publique en réduisant les coûts globaux de la rééducation (Hafner and Sanders, 2014). Cependant, le transfert en clinique de ces outils n'est pas immédiat (Cutti *et al.*, 2015; Iosa, Picerno, *et al.*, 2016). En effet, les technologies sous-jacentes des capteurs embarqués diffèrent de celles des laboratoires d'analyse de mouvement.

Les centrales inertielles (*magneto-inertial measurement units*, ou MIMU en anglais) fournissent des données quantifiant le mouvement (accélération et vitesse angulaire) ainsi que le champ magnétique terrestre dans un repère inertiel associé au boîtier du capteur (en mouvement). Par ailleurs, l'orientation des centrales inertielles dans un repère inertiel terrestre (fixe), comprenant un axe aligné avec l'accélération de gravité (verticale) et un axe aligné avec le nord magnétique (Roetenberg, 2006; Sabatini, 2011) est obtenue par fusion des informations des différents capteurs qui la composent (accéléromètre, gyroscope et éventuellement magnétomètre, **Figure 51**) (Sabatini, 2011; Bergamini *et al.*, 2014; Ligorio *et al.*, 2020). En revanche, la position de la centrale inertielle dans ce repère ne peut pas être obtenue directement. L'intégration de la vitesse angulaire ou de l'accélération mesurée par la centrale, après soustraction de l'accélération de la gravité, permettent d'obtenir respectivement les déplacements angulaires et linéaires de la centrale. On retrouve alors, aux conditions initiales près, les paramètres qui sont directement issus des systèmes optoélectroniques mais ceux-ci sont soumis à une
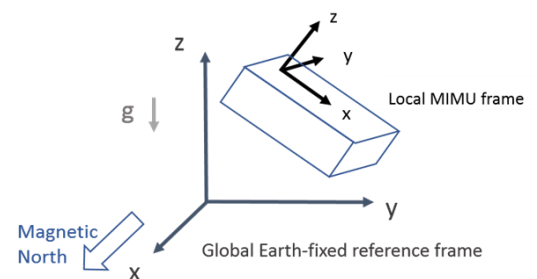
Figure 51 : Orientation du repère local d'une centrale inertielle (local MIMU frame) dans le repère terrestre de référence (Earth-fixed reference frame) perçu par la centrale (axe z vertical aligné avec l'accélération de gravité g et axe x dirigé vers le nord magnétique)
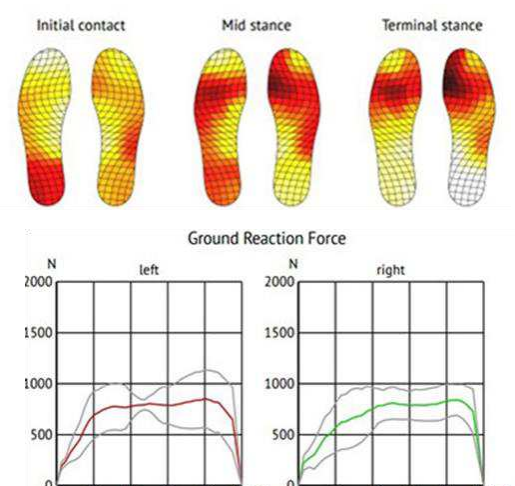
Figure 52: Semelle de pression fournissant la distribution des pressions au cours de l'appui (en haut) et la composante normale des efforts de réaction au sol (en bas).
Tiré de https://peakpodiatry.com.au

dérive du fait du bruit contenu dans les signaux bruts des capteurs (Iosa, Picerno, *et al.*, 2016; Hannink *et al.*, 2017). De nombreuses études se sont alors attachées à développer des algorithmes permettant d'obtenir des paramètres biomécaniques éprouvés tels que les angles articulaires (Picerno, 2017; Poitras *et al.*, 2019; Pacher *et al.*, 2020). Ceux-ci nécessitent toutefois de connaître l'orientation relative de la centrale et du segment sous-jacent, ce qui requiert de procéder à des calibrations fonctionnelles ou anatomiques pouvant allonger le temps d'acquisition (Pacher *et al.*, 2020). A l'inverse, de nombreux paramètres obtenus directement à partir des données brutes des capteurs, en particulier des accélérations, ont émergé et sont utilisés pour caractériser notamment l'équilibre et la symétrie de la marche (Iosa, Picerno, *et al.*, 2016; Benson *et al.*, 2018; Ghislieri *et al.*, 2019).

Les semelles de pression peuvent fournir la composante verticale de l'effort de réaction du sol s'appliquant sur la semelle, ce qui permet de caractériser la symétrie temporelle ou de charge lors de la marche (Nolan et al. 2003; Cutti et al. 2018; Loiret et al. 2019 - **Figure 52**). Toutefois, les autres composantes de l'effort de réaction du sol ou le moment de réaction au sol obtenues avec les plateformes de force ne peuvent être obtenu directement à partir des semelles de pression.

Ainsi, dans le but d'accompagner la rééducation avec des capteurs embarqués, il apparaît donc nécessaire d'identifier les paramètres biomécaniques pertinents qui puissent être caractérisés à l'aide de ces capteurs et de développer des algorithmes spécifiques aux technologies embarquées pour les obtenir. Il faut par ailleurs noter que, pour faciliter l'utilisation en clinique de la technologie embarquée, l'acquisition de données doit être la plus courte et la moins invasive possible, les cliniciens ayant souvent peu de temps à passer avec leurs patients. Ainsi, limiter le nombre de capteurs nécessaires et simplifier au maximum les protocoles d'acquisitions de données est primordial. Enfin, les altérations du schéma de marche des personnes amputées se reflétant dans les signaux mesurés par les capteurs positionnés sur ces personnes, il est nécessaire de s'assurer que les algorithmes développés prennent en compte les spécificités de la marche des personnes amputées et soient validés pour cette population.

1.4. Objectif de la thèse

L'objectif de cette thèse est donc de contribuer au développement d'outils ou protocoles embarqués permettant de quantifier la marche des personnes amputées de membre inférieur au cours de leur rééducation. Les protocoles développés devront permettre d'obtenir rapidement des données quantitatives pertinentes. Suite à la revue de littérature présentée dans les sections précédentes, l'acquisition d'indicateurs décrivant la qualité de la marche (symétrie, équilibre) et la cinématique du centre de masse (qui permet notamment d'identifier des altérations du schéma de marche et donne des informations sur l'efficacité énergétique de celle-ci) semble particulièrement pertinente. Une attention particulière sera portée à la compatibilité de ces protocoles à une utilisation en clinique. En outre, des données pertinentes devront pouvoir être obtenues à partir d'un nombre minimal de capteurs, soit à partir de données acquises rapidement en quelques pas, soit en instrumentant des tests cliniques éprouvés et validés chez les personnes amputées de membre inférieur, tel que le test de deux minutes, afin de ne pas perturber la rééducation.

Afin de répondre à ces objectifs, deux approches complémentaires ont été implémentées et suivies au cours de cette thèse.

La seconde partie de la thèse présentera donc une première approche, qui consiste à extraire des paramètres biomécaniques pertinents et éprouvés à partir des données des capteurs embarqués. Cette approche s'appuie sur le développement d'algorithmes parfois complexes, nécessitant de modéliser le corps et/ou le mouvement. La seconde partie de la thèse aura donc pour but de proposer un protocole embarqué et un algorithme original permettant d'estimer l'accélération et la vitesse instantanée du centre de masse d'une personne amputée au niveau transfémoral à partir d'un nombre limité de centrales inertielles.

Dans la troisième partie de la thèse, une approche alternative sera mise en place. La seconde approche consiste en effet à extraire des paramètres des signaux bruts des capteurs, sans avoir recours à une modélisation complexe du corps ou du mouvement. Les signaux bruts des capteurs embarqués étant différents de ceux issus des instruments présents dans les laboratoires d'analyse du mouvement, la pertinence du suivi de paramètres issus de ces capteurs pour la caractérisation de la marche des personnes amputées de membre inférieur n'est pas établie. Ainsi, la troisième partie de la thèse a pour objectif d'examiner la faisabilité et la pertinence clinique de l'utilisation des capteurs embarqués pour la caractérisation de la symétrie et de l'équilibre de la marche chez les personnes amputées de membre inférieur.

2. Approche biomécanique : développement d'un protocole embarqué pour l'acquisition de la cinématique du centre de masse chez les personnes amputées au niveau transfémoral

La pertinence de l'acquisition de la cinématique du centre de masse a été mise en évidence dans la revue de littérature restituée dans l'état de l'art de la partie précédente. Ainsi, cette partie de la thèse a pour objectif de proposer un protocole et un algorithme permettant d'acquérir la cinématique du centre de masse à l'aide de capteurs embarqués. Dans la littérature, plusieurs méthodes ont été proposées dans ce but et validées chez des sujets sains. Elles peuvent être catégorisées en deux typologies selon le nombre de centrales inertielles utilisées.

La première typologie de méthodes est basée sur l'hypothèse qu'un unique capteur positionné au niveau du bassin permet d'acquérir la cinématique du centre de masse (Esser *et al.*, 2009; Floor-Westerdijk *et al.*, 2012) et peut s'assimiler à la méthode du marqueur sacral avec des systèmes optoélectroniques (Gard *et al.*, 2004; Pavei *et al.*, 2017). Lorsque la tâche étudiée implique des mouvements importants du haut du corps ou dans le cas d'une marche asymétrique, les méthodes à capteur/marqueur unique au niveau du bassin ont montré une tendance à surestimer l'excursion du centre de masse (Eames *et al.*, 1999; Meichtry *et al.*, 2007; Myklebust *et al.*, 2015; Huntley *et al.*, 2017; Pavei *et al.*, 2017; Mohamed Refai *et al.*, 2020). Pour cette raison, ces méthodes, bien que très attractives par leur simplicité (Huntley *et al.*, 2017; Jeong *et al.*, 2018), ne semblent pas pertinentes pour étudier la cinématique du centre de masse chez les personnes amputées de membre inférieur. Une seconde catégorie de méthodes consiste alors à estimer la trajectoire (ou vitesse ou accélération) du centre de masse du corps à l'aide d'une moyenne pondérée de la trajectoire (ou vitesse ou accélération) des centres de masse des segments du corps, comme ce qui est fait à l'aide de systèmes optoélectroniques et d'un modèle inertiel par analyse segmentaire. Dans le cas de cette méthode multi-segmentaire, deux approches sont proposées dans la littérature : soit les accélérations des centres de masse des segments sont directement estimées à l'aide des centrales inertielles

165

positionnées sur lesdits segments (Lintmeijer *et al.*, 2018; Shahabpoor *et al.*, 2018), soit les positions des centres de masse des segments sont estimées de manière récursive en utilisant une chaîne cinématique et l'estimation de l'orientation de chaque segment donnée par la centrale inertielle positionnée sur celui-ci (Fasel, Sporri, *et al.*, 2017; Karatsidis *et al.*, 2017). Une phase d'intégration ou de dérivation peut être alors nécessaire selon que l'on recherche la trajectoire ou l'accélération du centre de masse. Ces deux approches impliquent d'utiliser de nombreux capteurs (11 à 17 capteurs d'après les méthodes retrouvées dans la littérature - Karatsidis et al. 2017; Pavei et al. 2017; Fasel et al. 2017), limitant l'utilisabilité de la méthode en clinique.

Plusieurs auteurs ont envisagé de diminuer le nombre de capteurs nécessaires (Zijlstra *et al.*, 2010; Fasel, Spörri, *et al.*, 2017; Shahabpoor *et al.*, 2018).

Dans le cas de la chaîne cinématique, des capteurs doivent toutefois être positionnés sur tous les segments de la chaîne, limitant ainsi la réduction possible du nombre de capteurs (7 au lieu de 11, en enlevant les capteurs positionnés sur les bras dans (Fasel, Spörri, *et al.*, 2017) par exemple). Par ailleurs, cette approche implique de connaître précisément l'orientation relative entre les repères locaux des centrales inertielles et les repères anatomiques des segments (Kianifar *et al.*, 2019), ce qui peut être chronophage et nécessiter des instruments additionnels (Picerno *et al.*, 2008; Cutti *et al.*, 2010; Pacher *et al.*, 2020).

En ce qui concerne l'approche qui repose sur la moyenne pondérée des accélérations des centres de masse de segments, une méthode intéressante a été proposée pour déterminer les localisations optimales de capteurs pour l'estimation de l'accélération du centre de masse au cours de la marche chez des sujets sains, et pourrait être adaptée aux personnes amputées (Shahabpoor *et al.*, 2018). Les auteurs ont montré que l'accélération du centre de masse pouvait être estimée à l'aide des accélérations des centres de masse des segments du tronc, du bassin et de la cuisse chez les sujets sains (erreur quadratique moyenne - RMSE < 18 % dans les trois directions - Shahabpoor et al. 2018).

On peut également noter l'existence d'une méthode reposant sur le principe de la chaîne cinématique, mais faisant l'hypothèse que le centre de masse est fixe dans le repère anatomique du bassin (Yuan and I. Chen, 2014). Cette méthode permet de réduire les erreurs induites par l'intégration directe de l'accélération d'une centrale positionnée au bassin, mais repose sur la même hypothèse d'immobilité du centre de masse du corps par rapport au bassin que la méthode sacrale et est ainsi tout autant susceptible de surestimer les excursions du centre de masse.

Cette analyse de la littérature nous a alors conduit à nous diriger vers une approche multi-segmentaire, ne reposant pas sur le principe de la chaîne cinématique. Dans un premier temps, suivant la méthodologie proposée par (Shahabpoor *et al.*, 2018), une analyse des contributions segmentaires dans l'accélération du centre de masse du corps a été menée à l'aide d'un système optoélectronique afin d'identifier les localisations optimales de centrales inertielles pour l'estimation de l'accélération du centre de masse du corps chez les personnes amputées transfémorales se déplaçant sur sol plan. Ceci a permis d'identifier différents modèles optimaux permettant d'estimer l'accélération du centre de masse du corps à l'aide d'un nombre restreint de centrales inertielles (section 2.1). Dans un second temps, cette approche a été transférée et validée en embarqué sur les données de marche d'une personne amputée transfémorale. Un protocole original permettant d'obtenir les accélérations des centres de masse segmentaires puis du corps à partir d'un nombre minimal de centrales inertielles a ainsi été proposé (section 2.2). Pour finir, la précision des accélérations des centres de masse des

segments étant dépendante de la précision avec laquelle la position relative des centrales inertielles et des centres de masse des segments est obtenue, l'influence des erreurs dans la localisation des centrales inertielles sur l'estimation des accélérations des centres de masse des segments et du corps a été explorée à l'aide d'une analyse de sensibilité (section 2.3).

2.1. Identification des contributions des segments et estimation de l'accélération du centre de masse du corps à partir d'un nombre restreint de segments

L'objectif de cette première étude était d'une part, d'identifier les segments contribuant le plus à l'accélération du centre de masse du corps chez les personnes amputées transfémorales, et d'autre part, d'évaluer différents modèles d'estimation de l'accélération du centre de masse du corps à partir des accélérations des centres de masse des segments préalablement identifiés (« accélérations segmentaires »).

Dix personnes amputées au niveau transfémoral (âge : 41,5 ± 11,3 ans ; masse : 68,8 ± 15,2 kg ; taille : 1,73 ± 0,07 m ; 8 hommes et 2 femmes) ont participé à cette étude. Chaque participant a été équipé de marqueurs optoélectroniques sur le corps complet selon (Al Abiad *et al.*, 2020). Lors d'une phase statique en position debout, les positions des marqueurs ont été enregistrées avec un système optoélectronique (VICON, Oxford, UK, 200 Hz) simultanément à la prise de photos de face et profil. A la suite de cette acquisition, les participants ont effectué plusieurs allers à vitesse confortable dans la salle d'analyse du mouvement selon une ligne rectiligne de 8 m au milieu de laquelle se trouvaient trois plateformes de force (AMTI, 1000 Hz). Dans le cadre de cette étude, seuls les essais pour lesquels trois appuis consécutifs sur les plateformes de force étaient détectés ont été conservés afin d'isoler un cycle complet sur les plateformes. Les paramètres inertiels segmentaires (masse des segments et positions des centres de masse dans les repères anatomiques segmentaires) ont été définis à l'aide d'un modèle inertiel comprenant 15 segments, personnalisé selon (Pillet *et al.*, 2010) à partir des photographies de face et profil des participants. Les accélérations des centres de masse des segments (SCoM) et du centre de masse du corps (BCoM) ont alors été obtenues.

Les contributions des segments dans l'accélération du centre de masse du corps ont été calculées selon deux critères, définis dans (Shahabpoor *et al.*, 2018):

- Le « poids » des accélérations segmentaires dans l'accélération du centre de masse du corps, ($\boldsymbol{Contrib_{seg_i}} = \frac{m_{seg_i}}{m_{body}} \, \boldsymbol{a_{SCoM_i}}$ avec m_{seg_i} la masse du segment, m_{body} la masse du corps et $\boldsymbol{a_{SCoM_i}}$ l'accélération du centre de masse du segment obtenue par double dérivation)
- La similarité des accélérations segmentaires à celle du centre de masse du corps exprimée à l'aide du coefficient de corrélation de Pearson selon les directions antéropostérieure (AP), médio-latérale (ML) et verticale (V).

Les contributions moyennes de chaque segment ont été obtenues en prenant la moyenne sur l'ensemble des participants.

Une fois les contributeurs les plus importants identifiés, deux types de réseaux de segments optimaux (OSN) ont été proposés pour estimer l'accélération du centre de masse du corps à partir d'un nombre restreint de segments (≤ 6) :

167

OSN de type 1 :
$$a_{BCoM,OSN_1} = \sum_{i=1}^{N} Contrib_{seg_i} = \sum_{i=1}^{N} \frac{m_{seg_i}}{\sum_{j=1}^{N} m_{seg_j}} a_{SCoM_i}$$

OSN de type 2 :
$$a_{BCoM,OSN_2} = \sum_{i=1}^{N} \alpha_i \, Contrib_{seg_i} = \sum_{i=1}^{N} \frac{m_{seg_i} + \sum_{j=1}^{15-N} r_{j,i} m_{seg_j}}{m_{body}} a_{SCoM_i}$$

Le deuxième type de réseau de segments correspond au modèle proposé dans (Shahabpoor *et al.*, 2018). Il requiert le calcul de la matrice de corrélation croisée entre chaque paire d'accélérations segmentaires. La masse de chacun des segments j non inclus est alors redistribuée au segment k inclus qui présente le coefficient de corrélation le plus élevé ($r_{j,i=k} = 1$ et $r_{j,i\neq k} = 0$ dans l'équation ci-dessus).

Les accélérations du BCoM obtenues à l'aide des deux types d'OSN ont ensuite été comparées à l'accélération de référence du BCoM ($a_{BCoM,ref}$), calculée à partir des efforts mesurés par les plateformes de force. La précision des accélérations estimées a été évaluée à l'aide du coefficient de corrélation de Pearson et des erreurs moyennes quadratiques (NRMSE, exprimée en % de l'amplitude de l'accélération de référence). Les modèles incluant uniquement le segment du tronc ou du bassin ont également été investigués (par exemple, $a_{BCoM} = a_{SCoM,bassin}$).

Les « poids » moyens des contributions segmentaires sont représentés sur la **Figure 53**. Celle-ci permet de mettre en avant que les segments contribuant le plus dans l'accélération du centre de masse du corps en termes de « poids » sont le tronc, le bassin, les cuisses ainsi que la tête. Les bras contribuent pour moins de 10 % dans l'accélération du centre de masse du corps et ont des contributions opposées selon l'axe antéropostérieur. Les autres segments jambiers (tibia, pied) sont également des contributeurs importants.

Les similarités des accélérations segmentaires avec l'accélération du centre de masse du corps, quantifiées à travers les corrélations de Pearson (non représentées dans ce résumé), permettent de mettre en évidence des corrélations significatives et importantes entre le centre de masse du corps et le tronc, le bassin, les cuisses et les tibias. Les accélérations des tibias sont également fortement et significativement corrélées avec celles des pieds. L'accélération de la tête n'est pas systématiquement significativement corrélée à celle du centre de masse du corps, ce qui peut être dû à des mouvements volontairement décorrélés de la tête par rapport au reste du corps.

Finalement, le tronc, le bassin, ainsi que les segments des membres inférieurs apparaissent comme des contributeurs majeurs de l'accélération du centre de masse du corps.
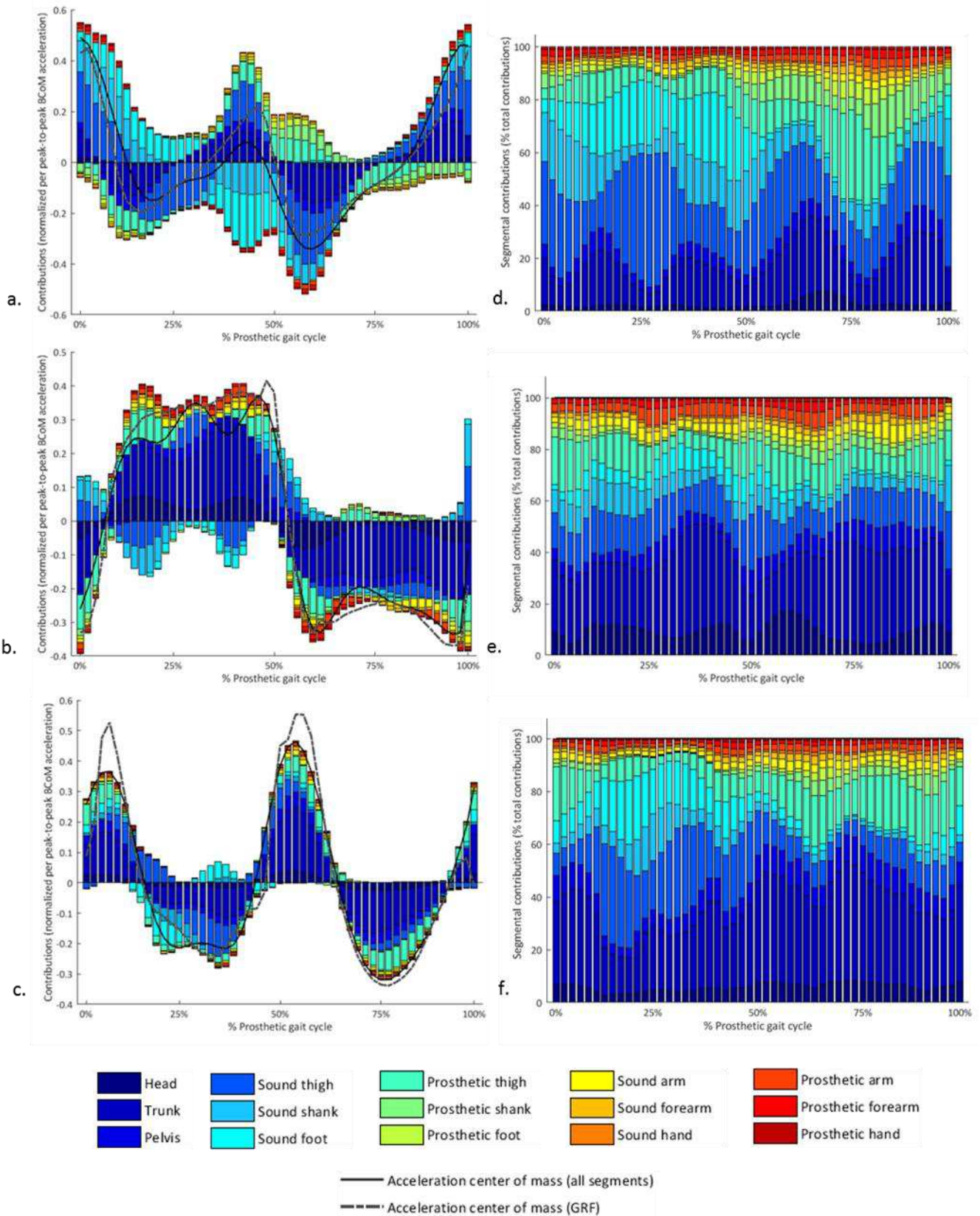
Figure 53: Contributions segmentaires à l'accélération du centre de masse du corps (BCoM) comparées à la contribution totale issue du modèle inertiel (ligne noire) et/ou à l'accélération de référence issue des plateformes de force (GRF – ligne pointillée) dans les directions antéropostérieure (a.et d.), médio-latérale (b. et e.) et verticale (c. et f.).
(a.-c.) Contributions segmentaires axiales normalisées par l'amplitude des contributions totales (accélération du modèle inertiel);
(d.-f.) Contributions segmentaires exprimées en pourcentage de la contribution totale

169

Plusieurs OSN ont ainsi été construits incluant 3 à 6 segments parmi le tronc, bassin, les cuisses ainsi que les tibias ou les pieds (**Figure 54**).
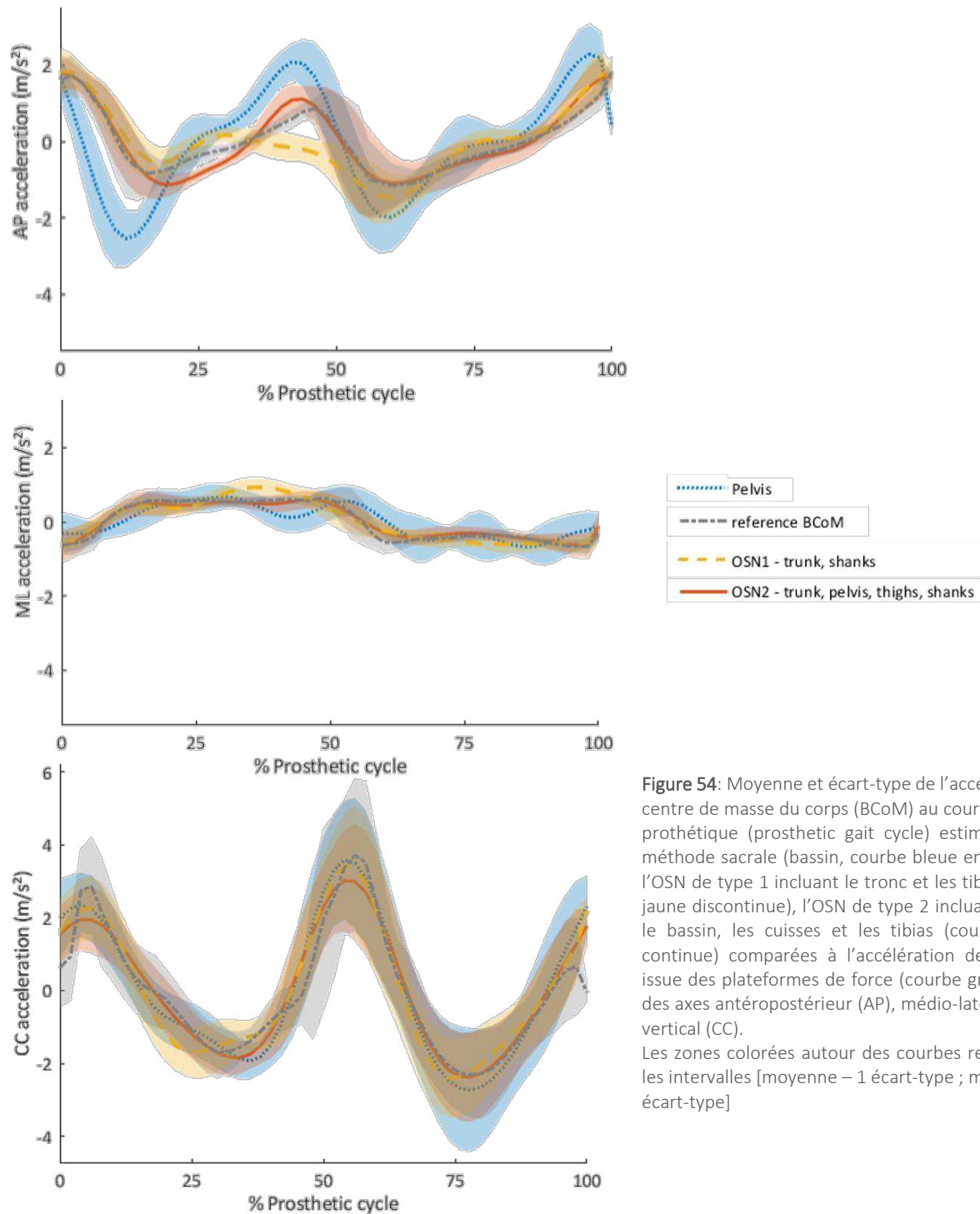
Figure 54: Moyenne et écart-type de l'accélération du centre de masse du corps (BCoM) au cours d'un cycle prothétique (prosthetic gait cycle) estimée avec la méthode sacrale (bassin, courbe bleue en pointillés), l'OSN de type 1 incluant le tronc et les tibias (courbe jaune discontinue), l'OSN de type 2 incluant le tronc, le bassin, les cuisses et les tibias (courbe orange continue) comparées à l'accélération de référence issue des plateformes de force (courbe grise) le long des axes antéropostérieur (AP), médio-latéral (ML) et vertical (CC).
Les zones colorées autour des courbes représentent les intervalles [moyenne – 1 écart-type ; moyenne + 1 écart-type]

La comparaison de l'accélération de référence aux accélérations issues des OSN, ainsi qu'à celles issues des deux modèles n'incluant que le tronc ou que le bassin comme segment, ont permis de mettre en évidence plusieurs éléments :

- Une approche multi-segmentaire permet d'estimer avec une plus grande précision l'accélération du BCoM

- L'inclusion du segment tronc, plus grand contributeur à l'accélération du corps, est à privilégier plutôt que celle du segment bassin pour les modèles OSN
- Un modèle OSN de type 1 à trois segments, incluant le tronc et les deux tibias, permet d'estimer l'accélération du BCoM avec plus grande précision (NRMSE < 16.3%, coefficient de Pearson r > 0,82) que le modèle à 3 segments proposé dans (Shahabpoor *et al.*, 2018) pour les sujets sains
- Les modèles OSN incluant 5 segments (tronc, cuisse et tibias ou pieds) permettent d'estimer l'accélération du centre de masse du corps avec précision (NRMSE < 14%, coefficient de Pearson r > 0,89)
- Les OSN de type 2, plus complexes car requérant notamment le calcul des matrices de corrélation croisées entre les différentes accélérations segmentaires, n'améliorent généralement pas l'estimation de l'accélération du BCoM par rapport aux OSN de type 1. Ces derniers sont donc à privilégier.

Il est à noter que la comparaison de l'accélération de référence du BCoM à celle issue du modèle inertiel à partir duquel les modèles OSN ont été construits fournit des erreurs de l'ordre de 11 % dans les trois plans, ce qui peut expliquer pourquoi les modèles OSN fournissent des erreurs minimales de l'ordre de 10,5 %.

Les modèles OSN proposés dans cette étude ont été construits et validés à partir de données obtenues à l'aide de marqueurs optoélectroniques. La validité de l'utilisation de centrales inertielles pour estimer l'accélération du centre de masse du corps reste donc à démontrer.

2.2. Développement d'un protocole embarqué pour l'estimation de l'accélération et de la vitesse instantanée du centre de masse des personnes amputées transfémorales

L'objectif de cette seconde étude était ainsi de vérifier que la méthodologie et les OSN de type 1 identifiés lors de l'étude précédente peuvent être utilisés avec des centrales inertielles pour l'estimation de l'accélération du centre de masse du corps a_{BCoM,OSN_1}^{G} dans un repère global R_G selon l'équation (1) ci-dessous :

$$a_{BCoM,OSN_1}^{G} = \sum_{i=1}^{N} \frac{m_{seg_i}}{\sum_{j=1}^{N} m_{seg_j}} \, a_{SCoM_i}^{G} \ (1)$$

où m_{seg_i} et $a_{SCoM_i}^{G}$ désignent respectivement la masse et l'accélération du centre de masse du $i^{ème}$ segment inclut dans le modèle OSN.

Plusieurs difficultés sont rencontrées lorsque l'on utilise des centrales inertielles. Tout d'abord, chaque centrale inertielle fournit une mesure de l'accélération à l'origine du repère local de la centrale, qui doit être transférée au centre de masse du segment (SCoM). Pour appliquer la loi de distribution des accélérations dans un solide rigide indéformable, il est alors nécessaire de connaitre la position relative entre le SCoM et la centrale inertielle :

171

$$a_{sCoM_i}^{MIMU_i} = a_{oIMU_i}^{MIMU_i} + \Omega_{oIMU_i}^{MIMU_i} \wedge \left(\Omega_{oIMU_i}^{MIMU_i} \wedge r_{oIMU_i - sCoM_i}^{MIMU_i}\right) + \left(\Omega_{oIMU_i}^{\dot{MIMU_i}}\right) \wedge r_{oIMU_i - sCoM_i}^{MIMU_i} \quad (2)$$

Dans l'équation (2), toutes les quantités sont exprimées dans le repère local de la centrale inertielle R_{MIMU_i} et :

$\begin{cases} a_{sCoM_i}^{MIMU_i} \text{ est l'accélération du } i^{\text{ème}} \text{ SCoM} \\[2mm] a_{oIMU_i}^{MIMU_i} \text{ est l'accélération mesurée par la } i^{\text{ème}} \text{ centrale, attachée rigidement au } i^{\text{ème}} \text{ segment} \\[2mm] \Omega_{oIMU_i}^{MIMU_i} \text{ est la vitesse angulaire mesurée par la } i^{\text{ème}} \text{centrale} \\[2mm] \left(\Omega_{oIMU_i}^{\dot{MIMU_i}}\right) \text{ est l'accélération angulaire obtenue par différentation de } \Omega_{oIMU_i}^{MIMU_i} \\[2mm] r_{oIMU_i - sCoM_i}^{MIMU_i} \text{ est le vecteur de translation reliant l'origine de la } i^{\text{ème}} \text{centrale au SCoM sous-jacent} \end{cases}$

Dans la littérature, certains auteurs ont proposé de positionner les centrales inertielles au niveau des SCoM (Lintmeijer *et al.*, 2018; Shahabpoor *et al.*, 2018) et d'utiliser directement la mesure de l'accélération de la centrale comme une estimation de celle du SCoM correspondant, afin de s'affranchir de la détermination de la position relative entre une centrale inertielle et le SCoM sous-jacent. Ceci peut conduire à une erreur d'estimation importante de l'accélération selon les segments considérés et les mouvements effectués. En effet, cela revient à considérer la distance relative entre la centrale inertielle et le SCoM comme étant nulle lorsque l'on applique la formule de distribution des accélérations (équation 2) et donc à négliger la vitesse angulaire du segment. Cependant, déterminer précisément la position relative entre une centrale et le SCoM du segment sur lequel elle est rigidement attachée n'est pas immédiat car les données issues des centrales inertielles ne permettent pas de remonter à leur position absolue. Plusieurs auteurs ont donc proposé d'utiliser des photographies calibrées ou un système optoélectronique afin d'estimer la position absolue de centrales inertielles dans un repère global lors d'une calibration statique (Dejnabadi *et al.*, 2006; Teufl *et al.*, 2018; Guaitolini *et al.*, 2019). Ces méthodes pourraient être adaptées pour obtenir à la fois la position absolue de la centrale et du SCoM sous-jacent.

Une fois les accélérations des SCoM estimées dans les repères locaux des centrales R_{MIMU_i} à l'aide de l'équation (2), il est nécessaire de les exprimer dans un repère global commun R_G avant de pouvoir utiliser l'équation (1) pour estimer l'accélération du BCoM :

$$a_{SCoM_i}^G = P_{G - MIMU_i} \, a_{SCoM_i}^{MIMU_i} \quad (3)$$

(avec $P_{G - MIMU_i}$, l'orientation relative entre le repère R_G et le repère R_{MIMU_i})

Or, si les capteurs contenus dans une centrale inertielle peuvent être, en théorie, fusionnés pour estimer l'orientation de la centrale dans un repère global comprenant un axe aligné avec la verticale et un axe aligné avec le nord magnétique, ces capteurs sont, en pratique, impactés différemment par des distorsions locales dans le champ magnétique mesuré par la centrale. Il en résulte que les repères de référence R_{GF} perçus par différentes centrales peuvent être incohérents (Picerno et al. 2011; Lebel et al. 2018; Guaitolini et al. 2019 - **Figure 5**). Il est donc nécessaire de définir un repère global commun dans lequel exprimer les accélérations des SCoM.
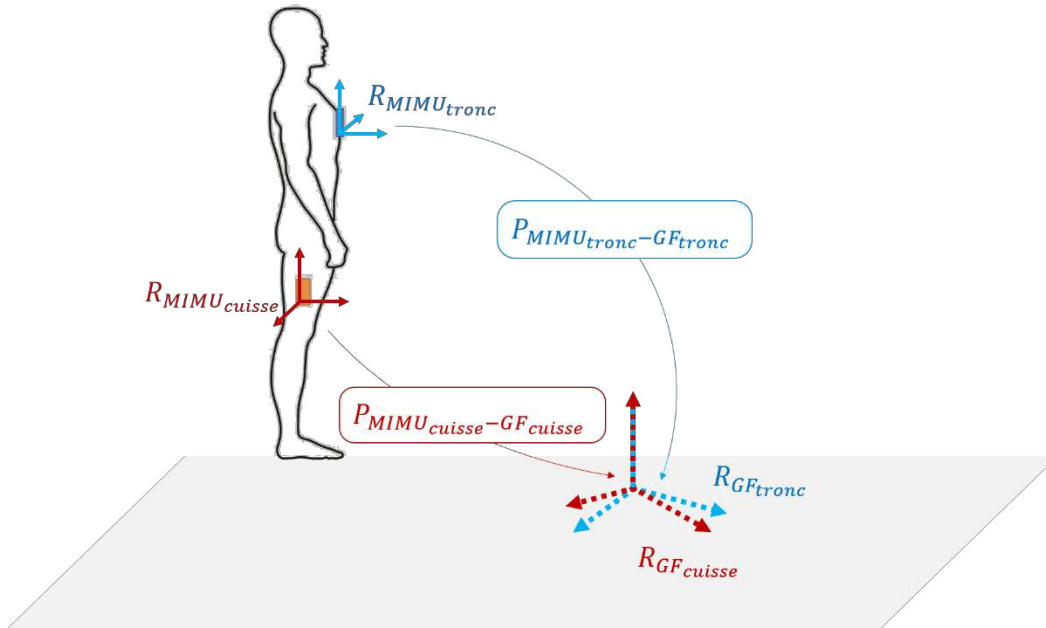
Figure 55 : Incohérence entre les repères de référence perçus par deux centrales inertielles – Exemple pour des centrales positionnées au niveau du tronc et de la cuisse
R_{MIMU_i}, le repère local de la centrale i, $P_{MIMU_i-GF_i}$ la matrice de transformation entre le repère local et le repère de référence R_{GF_i} perçu par la centrale ($i = tronc, cuisse$)

Enfin, une fois l'accélération du BCoM obtenue dans un repère global, il semble pertinent de chercher à exprimer la vitesse instantanée du BCoM. Celle-ci peut être décomposée en une composante cyclique et une composante moyenne. La vitesse de marche moyenne est en effet utilisée en clinique pour décrire le statut fonctionnel global d'un patient (Batten *et al.*, 2019), et la vitesse instantanée (composant cyclique et moyenne) peut être utilisée pour obtenir des informations sur le coût énergétique (Donelan *et al.*, 2002b; Detrembleur *et al.*, 2005) ou sur l'équilibre dynamique (Hof *et al.*, 2005, 2007) de la marche. L'intégration directe de l'accélération du BCoM obtenue à l'aide des centrales inertielles peut dériver du fait de la présence de bruit dans les signaux des centrales. Pour limiter cette dérive, la vitesse instantanée du BCoM peut être obtenue en deux temps, en calculant d'une part la composante moyenne sur un cycle de marche et d'autre part la composante cyclique. La première peut être estimée via le ratio de la distance parcourue par le tibia pendant un pas et la durée du pas (obtenue par exemple en utilisant le modèle cinématique du tibia proposé dans (Duraffourg *et al.*, 2019)), tandis que la seconde peut être estimée par intégration directe de l'accélération, suivie de l'application d'un filtre passe-haut pour enlever la composante moyenne et le bruit du signal (Steins *et al.*, 2014).

L'objectif de cette étude était donc de proposer un protocole permettant d'estimer l'accélération et la vitesse instantanée du BCoM à partir de centrales inertielles montées sur des segments, en utilisant des réseaux optimaux de capteurs (OSN), via l'estimation de l'accélération des SCoM dans un repère global commun et l'intégration de l'accélération du BCoM.

Une personne amputée transfémorale (83kg, 1,69m, homme) ayant participé à l'étude décrite dans la section précédente a été équipée, en plus des marqueurs optoélectroniques, de 7 centrales inertielles positionnées sur le tronc, les cuisses, les tibias et les pieds.

173

Tout comme dans l'étude précédente, les photographies prises pendant la phase statique de l'acquisition sont calibrées à l'aide du système optoélectronique et sont utilisées pour définir un modèle inertiel personnalisé selon (Pillet *et al.*, 2010). Ceci permet d'obtenir les positions des SCoM dans le repère global du système optoélectronique R_{OMCS}. L'identification des positions des centrales inertielles dans ce même repère est alors possible par DLT (*Direct Linear Transform*) en cliquant sur les photographies calibrées. Ceci permet de calculer la position relative des centrales inertielles et des SCoM dans le repère R_{OMCS}. Il est alors nécessaire d'obtenir la matrice de passage entre le repère local de chaque centrale inertielle R_{MIMU_i} et le repère R_{OMCS} pour exprimer la position relative de la centrale et du SCoM dans le repère local de la centrale.

Comme indiqué plus haut, il n'est pas possible d'utiliser directement les matrices d'orientation fournies par les centrales inertielles, celles-ci étant susceptibles de fournir l'orientation des centrales dans des repères globaux différents. En revanche, des hypothèses sur l'alignement manuel des centrales sur les segments et sur l'alignement des segments en position debout peuvent être utilisées pour estimer l'orientation relative $P_{OMCS-MIMU_i}$ entre les centrales et le repère global du système optoélectronique (Ligorio *et al.*, 2020). On peut en effet supposer dans un premier temps que pendant l'acquisition statique en position debout, deux des axes anatomiques des segments sont alignés avec la verticale et la direction de progression. Si les centrales sont parfaitement alignées sur les segments, on obtient donc une première estimation de l'orientation relative $P_{OMCS-MIMU_i}$. En pratique, l'alignement manuel des centrales peut comprendre des erreurs. Cette hypothèse forte peut donc être corrigée en utilisant l'orientation de la centrale par rapport à la verticale (donnée par la centrale inertielle et non perturbée par les distorsions magnétiques) pour obtenir une nouvelle estimation plus correcte de $P_{OMCS-MIMU_i}$. La **Figure 56** détaille les étapes d'obtention de cette matrice pour la centrale située sur le tronc.
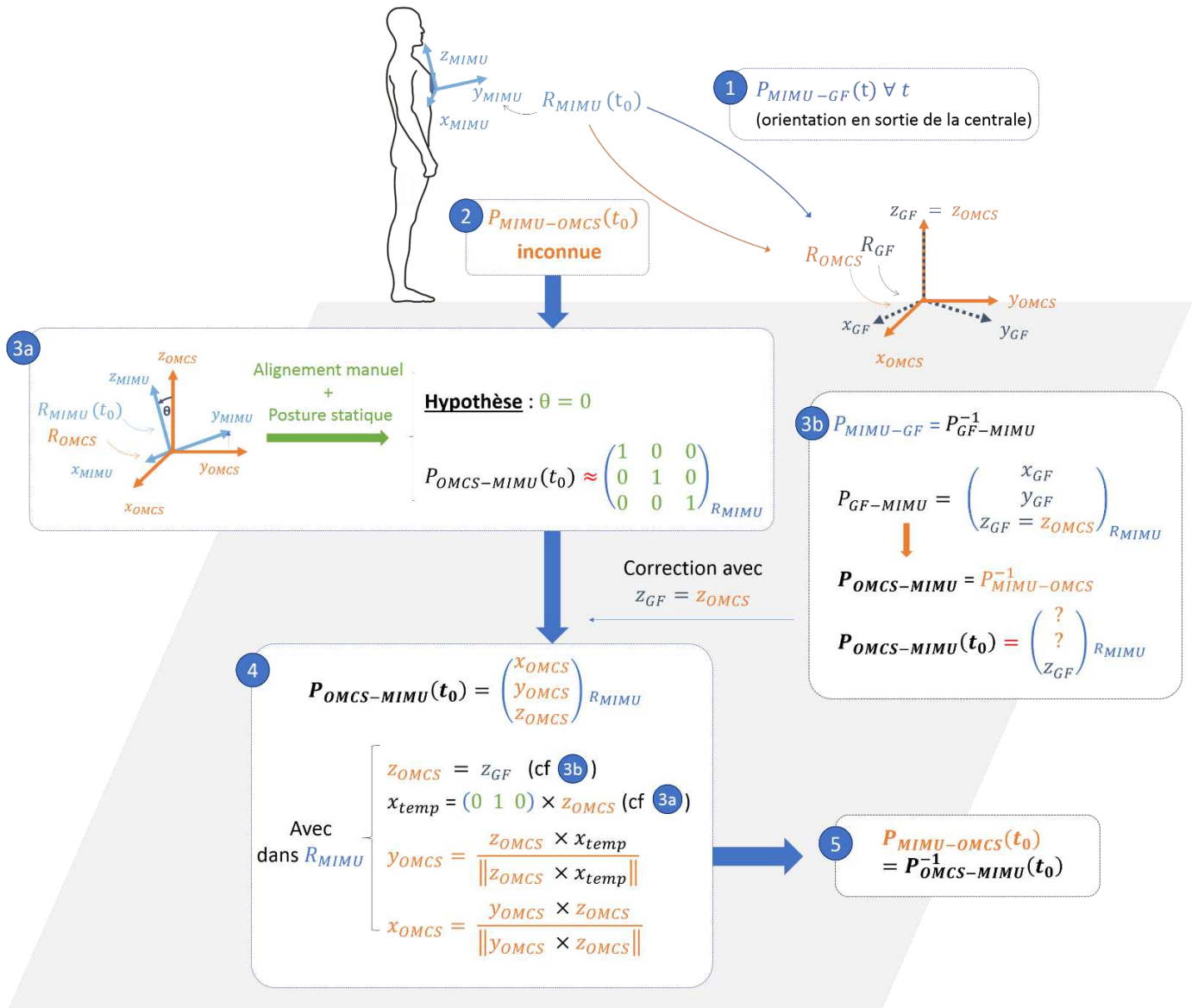
Figure 56: Approximation de l'orientation du repère local d'une centrale inertielle R_{MIMU} dans le repère du système optoélectronique (R_{OMCS}) pendant l'acquisition statique en posture debout à $t = t_0$ – Exemple pour la centrale du tronc.
- La matrice $P_{MIMU-GF}$ est directement obtenue en sortie de la centrale à $t = t_0$ (1)
- La matrice $P_{MIMU-OMCS}$ est inconnue à $t = t_0$ (2) mais peut être estimée en utilisant (3a) + (3b) :
  Une première approximation de la matrice de transformation du repère global R_{OMCS} vers le repère local de la MIMU $P_{OMCS-MIMU}$ est obtenue en utilisant des hypothèses concernant l'alignement manuelle de la centrale positionnée sur le tronc dans R_{OMCS} (3a). Ensuite, en utilisant la détection de la direction verticale par la centrale, robuste car indépendante du magnétomètre (l'axe z_{GF} du repère de référence perçu par la centrale est confondu avec l'axe vertical z_{OMCS} de R_{OMCS}), une seconde approximation peut être calculée (4).
- Enfin, $P_{MIMU-OMCS}$ est obtenue à $t = t_0$ en prenant l'inverse de $P_{OMCS-MIMU}$ (5)

La calibration statique permet d'obtenir pour chaque centrale inertielle :

- Son orientation dans le repère de la photographie calibrée, ici le repère R_{OMCS}, à l'instant t_0 de la statique : $P_{OMCS-MIMU_i}(t_0)$

- L'orientation relative (constante) des repères perçus par deux centrales inertielles différentes $P_{GF_i-GF_j}$. En effet, celle-ci s'obtient à l'aide de l'orientation directement fournie par les centrales dans leur repère global ($P_{GF_k-MIMU_k}$) et par leur matrice d'orientation dans le repère R_{OMCS} ($P_{OMCS-MIMU_k}$) ou leurs inverses :
  - $P_{GF_i-GF_j} = P_{GF_i-MIMU_i}(t_0) \times P_{MIMU_i-OMCS}(t_0) \times P_{OMCS-MIMU_j}(t_0) \times P_{MIMU_j-GF_j}(t_0)$

Pour les essais dynamiques, le repère de référence perçu par la centrale du tronc $R_{GF_{tronc}}$, tourné pour avoir un axe orienté selon la direction de progression (**Figure 57**) est utilisé comme repère global commun à toutes les centrales R_G : $P_{GF_{tronc}-G} = R_z(\theta)$
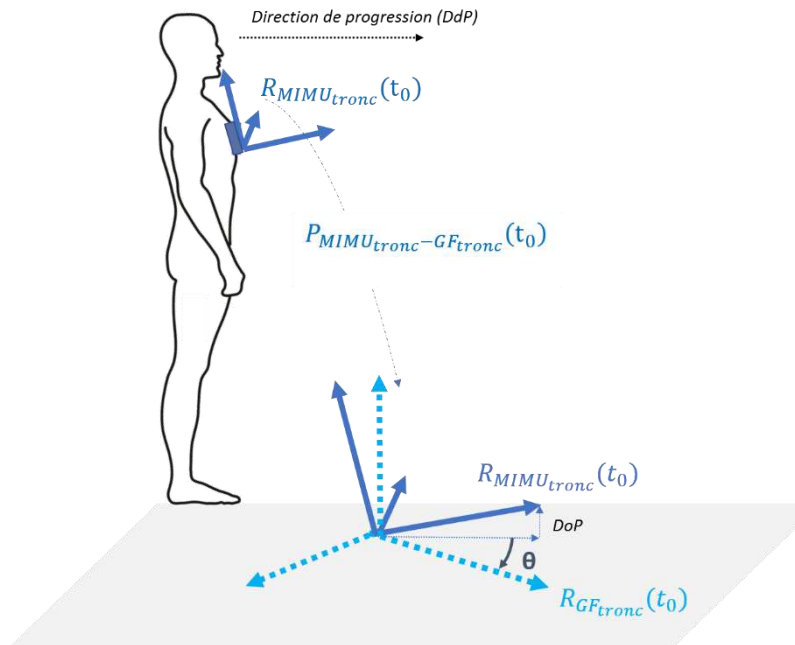
Figure 57: Rotation $R_z(\theta)$ du repère de référence perçu par la centrale du tronc ($R_{GF_{tronc}}$) pour aligner l'un des axes du repère de référence à la direction de progression. La rotation nécessaire est déterminée à l'aide de l'orientation du repère local de la centrale $R_{MIMU_{tronc}}$) dans son repère global. En effet, la centrale est positionnée sur le corps du participant tel qu'un des axes pointe vers la direction de progression.

On obtient alors, à tout instant t, l'orientation d'une centrale inertielle $MIMU_i$ dans ce nouveau repère global de référence comme suit : $P_{MIMU_i-G}(t) = P_{MIMU_i-GF_i}(t) \times P_{GF_i-GF_{tronc}} \times P_{GF_{tronc}-G}$

En somme :

- La calibration statique permet d'obtenir la position relative entre chaque centrale inertielle et SCoM sous-jacent dans le repère R_{OMCS} puis dans celui de la centrale R_{MIMU_i} : $r_{oIMU_i-sCoM_i}^{MIMU_i}$

- On peut utiliser cette position relative, constante dans le repère de la centrale au cours des acquisitions, pour déterminer l'accélération de chacun des SCoM dans le repère local de la centrale qui lui est associée : $a_{SCoM_i}^{MIMU_i}$ (équation 2)

- On peut finalement utiliser l'orientation donnée en sortie de la centrale inertielle $P_{MIMU_i-GF_i}(t)$ et l'orientation relative entre le repère de référence associé à la centrale et

le repère global commun obtenu à partir de la centrale du tronc P_{GF_i-G} pour estimer l'accélération du SCoM dans le repère global : $a^G_{SCoM_i}$ (équation 3)

- On peut utiliser les OSN pour estimer l'accélération du BCoM dans le repère global à partir d'une moyenne pondérée des accélérations des SCoM : a^G_{BCoM} (équation 1)
- Enfin, on peut estimer pour chaque cycle de marche la vitesse instantanée du BCoM en décomposant la vitesse en une composante moyenne et une composante cyclique.

Le protocole décrit ci-avant a été mis en place pour tester et valider l'utilisation de différents réseaux de capteurs tels qu'indiqués dans le **Tableau 1** pour l'estimation de l'accélération et la vitesse instantanée du centre de masse du corps. La précision de l'estimation de l'accélération et de la vitesse à l'aide d'une centrale unique au niveau du tronc a également été étudiée.

Tableau 1: Liste des réseaux de capteurs testés

Nombre de segments	Segments inclus
5	Tronc, cuisses, tibias
5	Tronc, cuisses, pieds
3	Tronc, tibias
1	Tronc

Les accélérations des SCoM et du BCoM ainsi que la vitesse instantanée du BCoM obtenues à l'aide des centrales inertielles ont été comparées aux accélérations et vitesse de référence obtenues à l'aide des plateformes de force (accélération du BCoM) ou du modèle inertiel du corps complet (accélération des SCoM et vitesse du BCoM). La précision des estimations a été évaluée à l'aide des coefficients de corrélation de Pearson (r), des erreurs quadratiques moyennes (RMSE), des RMSE normalisées par l'amplitude de la valeur de référence (NRMSE) et, pour la vitesse moyenne, de la RMSE exprimée en pourcentage de la vitesse moyenne de référence.

Les résultats obtenus dans cette étude sont encourageants et suggèrent que les centrales inertielles sont une alternative valide aux instruments des laboratoires d'analyse du mouvement pour l'obtention de l'accélération et de la vitesse instantanée du centre de masse chez les personnes amputées au niveau transfémoral. L'utilisation de cinq centrales inertielles situées au niveau du tronc, des deux cuisses et des deux tibias permet d'estimer avec précision l'accélération et la vitesse du centre de masse obtenues avec les plateformes de force et le système optoélectronique (coefficients de Pearson r > 0.89 et r > 0.94 respectivement, NRMSE = 11,6 ± 2,1 % ; 14,0 ± 2,1 % ; 7,7 ± 0,4 % pour l'accélération et 16,7 ± 5,1 % ; 13,2 ± 3,0 % ; 6,0 ± 0,8 % pour la vitesse dans les directions antéropostérieure, médio-latérale et verticale respectivement – voir **Figure 58**). La vitesse moyenne de marche est notamment estimée avec une précision de 0,05 m/s (RMSE) correspondant à 4,1 % de la vitesse nominale. Seules deux études dans la littérature ont permis une estimation de la vitesse de marche avec une précision similaire ou accrue, chez des sujets sains (Mariani *et al.*, 2010; Yang and Li, 2012a). Dans le futur, plus de sujets devront être recrutés afin de confirmer les résultats obtenus avec ce protocole et ce réseau de capteurs chez les personnes amputées transfémorales. Par ailleurs, le protocole devra être adapté afin de permettre une acquisition en embarqué, sans nécessiter un

système optoélectronique. Pour cela, un système de calibration simplifié ou l'utilisation d'un scanner 3D est envisagé. Ces méthodes reposeront toujours sur l'estimation a posteriori de la position relative des centrales et des centres de masse de segments. C'est pourquoi l'impact des erreurs de localisation des centrales inertielles sur l'estimation de l'accélération ou de la vitesse du centre de masse doit être étudiée.
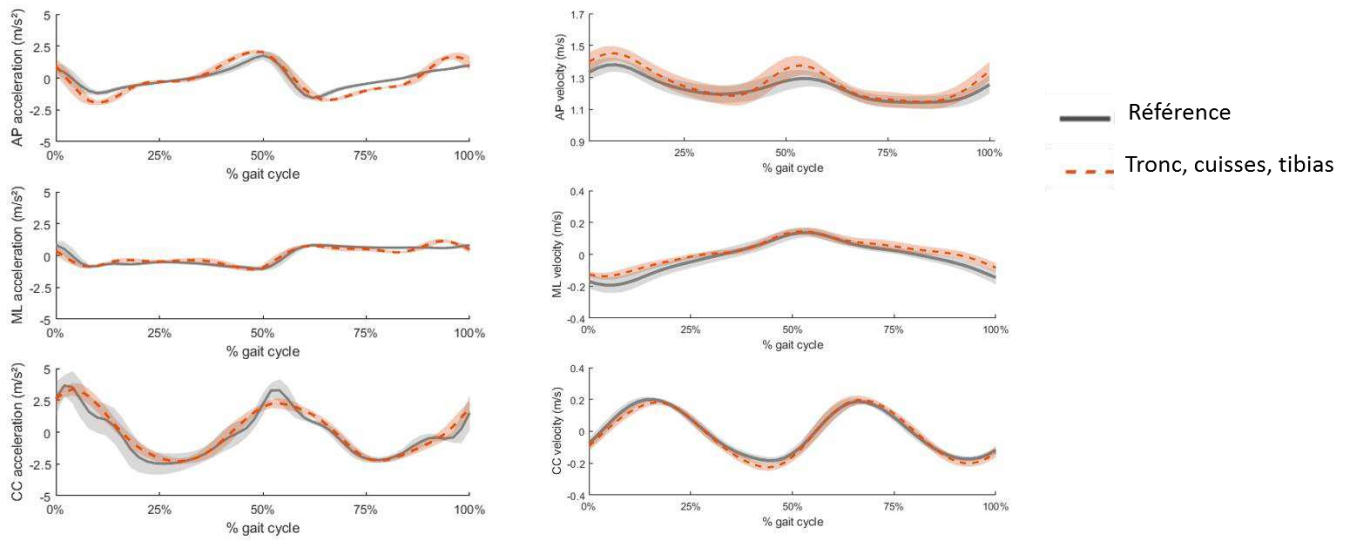

Figure 58: Accélération (à gauche) et vitesse instantanée (à droite) du centre de masse du corps obtenues à l'aide de cinq centrales inertielles situées sur le tronc, les cuisses et les tibias (courbe orange discontinue) comparé à la référence (courbe grise)

2.3. Analyse de sensibilité de l'accélération du centre de masse du corps aux erreurs de localisation des centrales inertielles

L'objectif de cette étude était d'étudier l'impact de l'erreur d'estimation de la localisation des centrales inertielles sur l'accélération du centre de masse obtenue à l'aide du protocole précédent et de cinq centrales inertielles situées sur le tronc, les cuisses et les tibias.

Une analyse de sensibilité a été menée pour répondre à cette problématique, en utilisant les données de l'étude précédente. Dans un premier temps, l'amplitude maximale d'erreur possible sur la localisation des centrales inertielles a été estimée. Les centrales étaient insérées dans des supports rigides imprimés en 3D contenant quatre marqueurs optoélectroniques et permettant ainsi d'obtenir l'orientation et la position des centrales dans le repère du système optoélectronique. Pour estimer l'amplitude d'erreurs de localisation possible avec le protocole décrit dans la section précédente, deux opérateurs ont calibré les photographies de face, dos et profils du participant en posture statique et ont cliqué sur les positions des origines des centrales inertielles à cinq reprises chacun. Les positions obtenues en cliquant sur les photos ont été comparées aux valeurs de référence fournies par le système optoélectronique. Des erreurs allant jusque 2 cm ont ainsi été mises en évidence.

Les accélérations des centres de masse des segments (SCoM) et du centre de masse du corps (BCoM) ont ensuite été estimées en simulant une mauvaise localisation des centrales, c'est-à-dire, une erreur dans l'estimation du vecteur $r_{oIMU_i-sCoM_i}^{MIMU_i}$ (cf équation 2 de la section précédente), pouvant aller jusque 2 cm dans chacune des directions de l'espace (antéropostérieur, médio-latérale et verticale, selon les axes du repère R_{OMCS}). Afin de quantifier uniquement les erreurs liées à une

178

mauvaise localisation des centrales, les orientations des centrales inertielles étaient déterminées dans le repère R_{OMCS} à l'aide des marqueurs positionnés sur les ancillaires les contenant, plutôt qu'en utilisant la méthode décrite dans l'étude précédente (**Figure 59**).
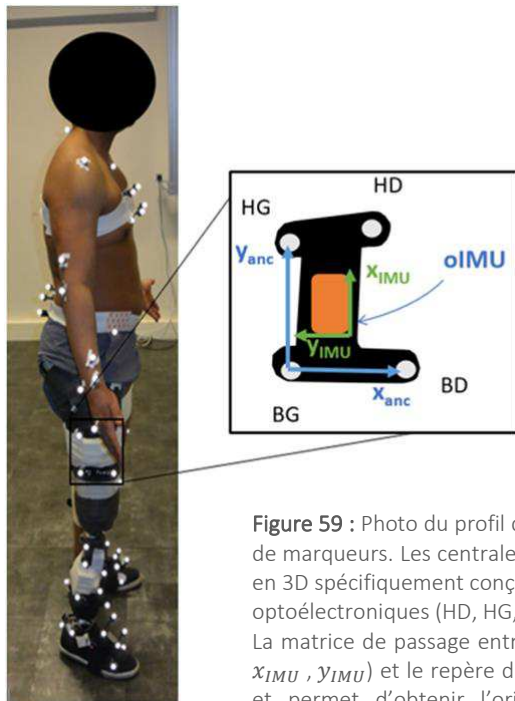
Figure 59 : Photo du profil droit du participant équipé de centrales inertielles et de marqueurs. Les centrales sont insérées dans des ancillaires rigides imprimés en 3D spécifiquement conçus pour cette application et équipés de 4 marqueurs optoélectroniques (HD, HG, BD, BG).
La matrice de passage entre le repère local de la centrale (origine oIMU, axes x_{IMU}, y_{IMU}) et le repère de l'ancillaire (x_{anc}, y_{anc}) est connue par conception et permet d'obtenir l'orientation de l'IMU dans le repère du système optoélectronique.

En utilisant la théorie des plans d'expériences (Goupy, 2016), tous les cas possibles d'erreurs de positionnement, simultanées ou non, des cinq centrales inertielles ont été simulés. L'erreur entre les accélérations des SCoM et du BCoM simulées à l'aide des données des centrales inertielles et les accélérations de références (modèle inertiel pour le SCoM et plateformes de force pour le BCoM) a été calculée. Par ailleurs, pour chacun des composants des accélérations, un modèle polynomial multilinéaire avec interactions a été proposé pour décrire la relation entre les erreurs de localisation de chaque centrale selon les axes du repère R_{OMCS} et la précision de l'estimation (en termes de NRMSE) de l'accélération obtenue à l'aide des centrales inertielles. L'étude des variances associées aux différents termes du polynôme permet d'estimer le pourcentage de variance dans la précision de l'estimation de l'accélération (NRMSE) expliqué par chacune des erreurs de localisation (Goupy, 2016).

Les erreurs de localisation des centrales inertielles engendrent des variations dans la précision de l'estimation des accélérations des centres de masse des segments entre - 5.6 % et 6.9 % (tous segments et axes confondus) et entre - 1.6 % et 1.7 % en ne considérant que le tronc et les cuisses. Les plus grandes variations de l'erreur identifiées pour les tibias dans les directions antéropostérieure et verticale peuvent s'expliquer par la plus grande vitesse angulaire du tibia dans le plan sagittal par rapport aux autres segments. La précision des accélérations des SCoM des membres inférieurs est principalement affectée par les erreurs de localisation des centrales selon les axes antéropostérieur et vertical. Les erreurs de position selon la direction médio-latérale ont une influence prépondérante uniquement sur la précision de l'accélération du tronc dans la direction antéropostérieure et dans une moindre mesure, dans la direction verticale ainsi que sur la précision de l'accélération de la cuisse dans la direction antéropostérieure (**Figure 61**). Ces différences entre les segments peuvent s'expliquer par

179

les différents mouvements des segments lors de la marche (tronc vs segments des membres inférieurs).

Concernant l'estimation de l'accélération du BCoM, l'analyse de sensibilité a permis de mettre en évidence qu'une localisation précise des centrales inertielles du tronc, de la cuisse saine et du tibia sain selon les directions antéropostérieure et verticale permet de réduire la variabilité de l'estimation de l'accélération du centre de masse du corps (**Figure 60** – exemple pour la composante antéropostérieure du BCoM). En effet, des erreurs dans les localisations de ces centrales selon ces directions expliquent 92 %, 77 % et 79 % de la variation de la précision de l'estimation de l'accélération du BCoM dans les directions antéropostérieure, médio-latérale et verticale respectivement.
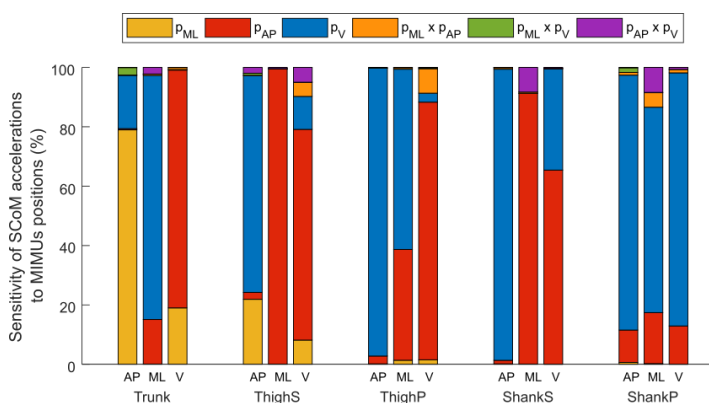
Figure 61 : Sensibilité de la précision des accélérations des segments (S = sain ; P = prothétique) selon les directions médio-latérales (ML), antéro-postérieures (AP) et verticales (V) en fonction des erreurs de localisation pX des centrales et de leurs interactions pX*pY (X, Y = AP, ML, V)
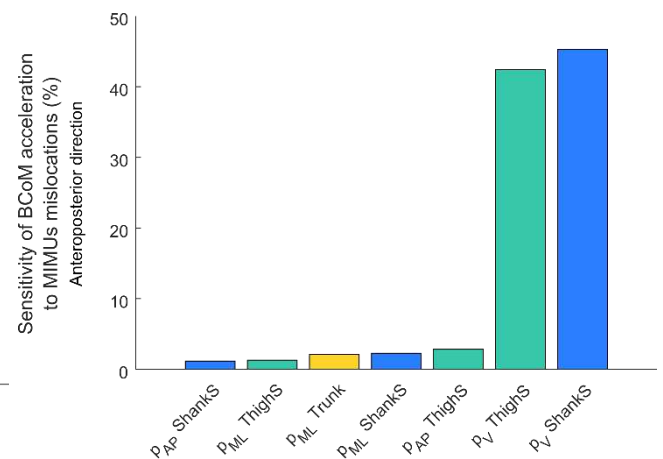
Figure 60: Sensibilité de la précision de la composante antéropostérieure de l'accélération du centre de masse du corps au positionnement antéropostérieur (pAP), médiolatéral (pML) ou vertical (pV) des segments (tibia sain : ShankS, tronc : Trunk, cuisse saine : ThighS)

La variabilité de la précision de l'accélération du BCoM estimée à l'aide de la méthodologie présentée ici peut être maintenue à moins de 1 % en identifiant correctement les localisations antéropostérieure et verticale des centrales du tronc ainsi que des tibia et cuisse du côté sain. Le rôle prépondérant de ces centrales peut s'expliquer par la masse prépondérante du tronc et de la jambe saine par rapport aux autres segments chez une personne amputé au niveau transfémoral ainsi que par la plus grande vitesse des tibias dans le plan sagittal au cours de la marche.

La présente analyse de sensibilité ne s'est pas intéressée à l'impact des erreurs d'orientation des centrales inertielles, contrairement à ce qui a pu être fait dans (Tan *et al.*, 2019). Dans l'analyse de sensibilité implémentée ici, les accélérations des SCoM sont estimées dans un repère global avant d'être fusionnées pour estimer l'accélération du BCoM. Ainsi, en utilisant le protocole proposé dans cette étude, un mauvais alignement manuel de la centrale avec les axes anatomiques des segments ne devrait pas conduire à une erreur prépondérante dans l'estimation des accélérations. Au contraire, dans l'étude de (Tan *et al.*, 2019), l'accélération du BCoM est estimée à l'aide d'une approche d'apprentissage machine prenant en entrées les données brutes de centrales inertielles, ce qui peut expliquer la forte influence des erreurs d'orientation des centrales sur la sortie du modèle. Dans le protocole implémenté ici, seules des erreurs d'orientation des centrales dans le repère de référence commun aux centrales devraient avoir un impact, supposé négligeable. Cette hypothèse devra être vérifiée dans de prochaines études.

180

3. Deuxième approche : faisabilité et pertinence clinique de la caractérisation de la qualité de la marche (équilibre, symétrie) à l'aide de capteurs embarqués

Dans cette partie, la faisabilité et la pertinence clinique de l'utilisation de centrales inertielles et/ou de semelles de pression pour caractériser la symétrie et l'équilibre de la marche des personnes amputées sont explorées.

Une première étude avait pour objectif de déterminer si les algorithmes de détection des événements de la marche à partir de centrales inertielles peuvent être utilisés pour estimer la symétrie temporelle de la marche chez les personnes amputées de membre inférieur (section 3.1). La seconde étude explore la faisabilité d'utiliser des indices de qualité de la marche issus du traitement des signaux de capteurs embarqués pour suivre l'évolution de personnes amputées de membre inférieur au cours de leur rééducation à l'aide de l'instrumentation du test de deux minutes (section 3.2).

3.1. Utilisation des centrales inertielles pour l'estimation de la symétrie de durée d'appui chez les personnes amputées transfémorales

De très nombreux algorithmes ont été proposés dans la littérature afin d'identifier les événements du cycle de marche, notamment les instants de début et de fin de contact du pied au sol, à partir de centrales inertielles. Le foisonnement de la littérature rend difficile la sélection d'un algorithme pour une certaine population et une situation donnée. Ainsi, le but de cette étude était de comparer cinq algorithmes de détection des événements de la marche issus de la littérature afin d'évaluer la faisabilité d'utiliser des centrales inertielles pour estimer des paramètres temporels et l'asymétrie de durée de phase d'appui chez les personnes amputées transfémorales.

Trois des algorithmes, utilisant deux centrales inertielles au niveau de chaque tibia, ont été choisis car ils ont été développés et validés sur les données de marche de personnes amputées de membre inférieur (Selles *et al.*, 2005; Maqbool *et al.*, 2017; Ledoux, 2018). Un algorithme utilisant une unique centrale au niveau du tronc (McCamley *et al.*, 2012), jamais testé chez les personnes amputées, a également été sélectionné car une étude comparative dans la littérature l'avait identifié comme l'algorithme utilisant une seule centrale le plus performant pour la détection d'événements de la marche dans des populations pathologiques (Trojaniello *et al.*, 2015). Enfin, un dernier algorithme utilisant deux centrales au niveau des tibias a également été implémenté (Trojaniello, Cereatti, Pelosin, *et al.*, 2014). Ce dernier algorithme a été très largement validé sur une population importante de sujets pathologiques (236 patients parmi lesquels 125 Parkinsoniens et 31 hémi-parétiques – Bertoli et al. 2018). La performance des algorithmes a été appréciée au regard de la fréquence de détection des événements, de la précision de l'estimation des paramètres temporels et enfin de la précision de l'estimation de l'asymétrie de durée de phase d'appui. Des semelles de pression, validées chez les personnes amputées transfémorales (Loiret *et al.*, 2019), ont été utilisées comme référence.

Sept personnes amputées au niveau transfémoral (âge : 47,3 ± 9,9 ans ; masse : 74,5 ± 11,9 kg ; taille : 1,80 ± 0,10 m ; 5 hommes) ont participé à cette étude et ont réalisé plusieurs passages de marche sur sol plan horizontal à vitesse confortable, rapide et lente. Au total, 454 pas sains et 623 pas prothétiques ont été considérés dans l'analyse.

Seuls deux des cinq algorithmes présentaient une valeur positive prédictive de plus de 99 % (taux de faux positifs < 1 %) pour la détection des instants de contact initial et final pour les pas prothétiques et sains (Trojaniello, Cereatti, Pelosin, *et al.*, 2014; Ledoux, 2018). Un faible taux de faux positif est

181

primordial pour une utilisation de ces algorithmes sans méthode de référence, ainsi, seuls ces algorithmes sont étudiés en détails. Ces deux algorithmes permettent la détection des instants de contact du pied au sol avec une précision suffisante. Toutefois, la divergence des erreurs de détection des événements de contact final pour le pied sain (Ledoux, 2018) ou le pied prothétique (Trojaniello, Cereatti, Pelosin, *et al.*, 2014) contribue à la surestimation systématique du temps d'appui prothétique ou à la sous-estimation du temps d'appui sain, qui conduit finalement à la sous-estimation de l'asymétrie de durée de phase d'appui avec chacun des deux algorithmes. De même, une trop grande variabilité dans la détection des événements nuit à la précision de l'estimation de la durée de double d'appui, pourtant pertinente pour juger de l'équilibre dynamique des personnes amputées au niveau transfémoral (Goujon *et al.*, 2006; Kendell *et al.*, 2010).

En conclusion, cette étude a démontré que, si les instants de contact initial identifiés à l'aide des algorithmes de détection des événements de la marche peuvent être utilisés pour segmenter la marche des personnes amputées transfémorales de manière robuste, des développements complémentaires sont nécessaires pour les utiliser en clinique pour suivre l'asymétrie temporelle de la marche.

3.2. Pertinence clinique du suivi des indices d'équilibre et de symétrie de la marche obtenus à l'aide des capteurs embarqués chez les personnes amputées de membre inférieur

Ces dernières années, de très nombreuses études se sont intéressées à la caractérisation de la symétrie de la marche et de l'équilibre dynamique à l'aide d'indices dérivés des signaux de centrales inertielles portées sur le haut du corps (Mazzà *et al.*, 2008; Iosa *et al.*, 2014; Summa *et al.*, 2016; Bergamini *et al.*, 2017; Pasciuto *et al.*, 2017; Belluscio *et al.*, 2018) ou de semelles de pression (Nolan *et al.*, 2003; Cutti *et al.*, 2018; Loiret *et al.*, 2019), dans de diverses pathologies. Ces indices de qualité de la marche comprennent :

- Les symétries de durée d'appui et de charge quantifiées à l'aide de semelles de pression et de l'Absolute Symmetry Index ou ASI (**Figure 62**).

- $ASI = \frac{S-P}{0.5\,(S+P)} \times 100$, avec S et P les valeurs de la durée de la phase d'appui ou du pic d'effort Fz1 pour les jambes saines et prothétiques respectivement (Nolan *et al.*, 2003).
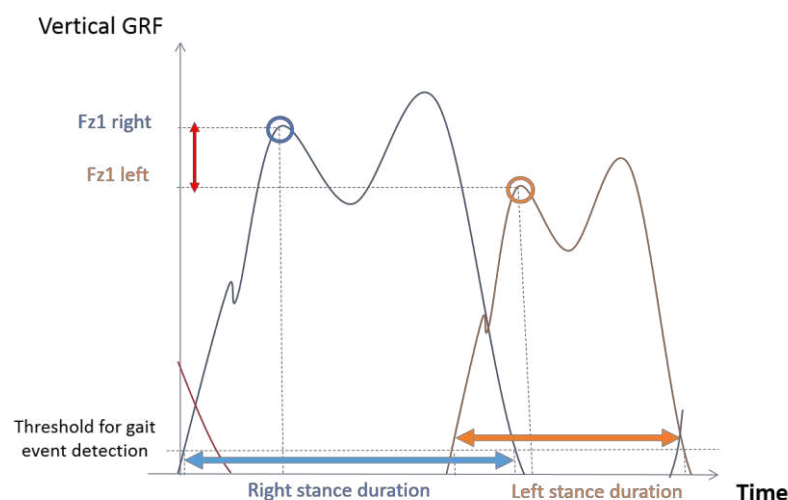

Figure 62 : Durée de phase d'appui (stance duration) et pic d'effort de début d'appui (Fz1) dérivé de la composante normale des efforts de réaction au sol (Vertical GRF) avec des semelles de pression droite (Right – courbe bleue) et gauche (Left – courbe orange)

- Le ratio harmonique, selon sa plus récente définition, le iHR, calculé à partir d'une analyse fréquentielle des accélérations mesurées par une centrale au niveau du bassin selon les trois directions de l'espace (Pasciuto et al., 2017).

$$iHR = \sum_{1 \leq j \leq n} \frac{P_i^j}{P_e^j + P_i^j} \cdot 100$$ avec P_i^j et P_e^j la puissance associée, respectivement, aux harmoniques intrinsèques (contribuant à la symétrie de la marche) ou extrinsèques (traduisant une déviation d'un schéma de marche symétrique) de l'accélération (Cappozzo, 1981)

- Les valeurs efficaces des accélérations ou RMS, calculées au niveau du bassin, du sternum et de la tête selon les trois directions de l'espace. A vitesse égale, une plus grande valeur de RMS traduit une instabilité du segment auquel elle est mesurée.
- Les coefficients d'atténuation entre le bassin et le sternum, le sternum et la tête et le bassin et la tête, calculés à partir du ratio des RMS des accélérations entre deux niveaux successifs du haut du corps (Paradisi et al., 2019) : $AC_{XY} = 1 - \frac{RMSa_Y}{RMSa_X}$.
  - Un coefficient positif indique une atténuation des accélérations du niveau bas vers le niveau haut alors qu'un coefficient négatif indique une amplification des accélérations. Cette définition repose sur l'idée que, dans un schéma de marche physiologique, les accélérations dues au mouvement des jambes sont transmises vers le haut du corps en étant atténuées pour assurer un flux optique stable et une interprétation efficace des signaux du système vestibulaire

Ces 23 indices ont été calculés dans diverses populations, y compris chez les personnes amputées au niveau transtibial, à l'exception de l'iHR. Toutefois, les protocoles d'acquisition des données diffèrent d'une étude à une autre, et aucune ne donne une vue d'ensemble de ces indices dans un même échantillon de personnes amputées. Par ailleurs, aucune étude n'a examiné la répétabilité des indices de qualité de la marche, ce qui est essentiel pour caractériser la sensibilité des indices à détecter une évolution réelle de la qualité de la marche.

Cette étude avait donc pour objectif de répondre à ces limitations en étudiant simultanément tous les indices sus-cités chez neuf sujets sains et neuf sujets amputés au niveau transtibial au cours de deux tests de deux minutes, instrumentés avec trois centrales inertielles au niveau du bassin, du sternum et de la tête, et équipés d'une paire de semelles de pression. Par ailleurs, les valeurs de l'iHR obtenues au cours des tests ont été comparées aux indices d'asymétrie obtenus avec les semelles (ASI) à l'aide du coefficient de corrélation de Pearson dans le but de clarifier le sens de ce paramètre de symétrie globale.

Les indices répétables d'un test à l'autre ont d'abord été identifiés puis ont été utilisés pour caractériser les populations de sujets sains et d'amputés transtibiaux. Ensuite, la différence minimale détectable par chacun des indices a été estimée à l'aide du coefficient de répétabilité proposé par (Bland and Altman, 1986).

Sur les 23 indices étudiés, 21 indices ne présentent pas de différences significatives entre le premier et le second test de deux minutes pour les deux populations. De même, la distance parcourue est similaire entre les deux tests. Les deux indices présentant des différences significatives ont donc été écartés de l'analyse car ne semblent pas pouvoir caractériser de manière fiable une population à l'aide d'un test de deux minutes. Pour les autres indices, des valeurs cohérentes avec la littérature ont été retrouvées. Les 21 indices restants ainsi que la distance parcourue pendant le test de deux minutes

ont alors été utilisés pour caractériser les populations saine et amputée. Seuls onze des paramètres (y compris la distance parcourue) permettent de distinguer les personnes amputées transtibiales des sujets sains et démontrent un moins bon équilibre dynamique et une asymétrie accrue des personnes amputées par rapport aux sujets sains (**Tableau 2**).

Tableau 2 : Médiane et écart interquartile (IQR) des valeurs des indices de qualité de la marche quantifiés lors du premier test de deux minutes pour les sujets sains et amputés. Les différences significatives entre les deux populations (valeur p < 0,05) sont identifiées par la présence d'un astérisque dans la colonne Sig. (significativité)

	Anteropostérieur Médiane (IQR)			Médio-latéral Médiane (IQR)			Vertical Médiane (IQR)		
	Sujets sains	Amputés transtibiaux	Sig.	Sujets sains	Amputés transtibiaux	Sig.	Sujets sains	Amputés transtibiaux	Sig.
iHR (%)	**96,9 (2,1)**	**85,9 (6,5)**	*	**85,2 (11,1)**	**71,4 (8,4)**	*	**97,6 (1,5)**	**89,1 (6,6)**	*
RMSa pelvis (s^{-1})	2,05 (0,93)	1,78 (0,88)		**1,77 (1,19)**	**1,60 (0,70)**	*	3,13 (0,76)	2,47 (1,41)	
RMSa sternum (s^{-1})	/	/		**1,09 (0,51)**	**1,27 (0,39)**	*	3,37 (1,29)	2,56 (1,24)	
RMSa tête (s^{-1})	**1,17 (0,58)**	**1,69 (0,75)**	*	**1,00 (0,27)**	**1,53 (0,30)**	*	3,35 (1,07)	2,55 (1,20)	
AC pelvis/sternum	0,35 (0,29)	0,19 (0,29)		0,31 (0,45)	0,27 (0,25)		/	/	
AC pelvis/tête	**0,50 (0,38)**	**-0,03 (0,69)**	*	0,20 (0,47)	0,05 (0,20)		-0,01 (0,12)	-0,01 (0,15)	
AC sternum/tête	**0,26 (0,52)**	**-0,39 (0,91)**	*	**0,03 (0,15)**	**-0,20 (0,23)**	*	0,01 (0,09)	0,00 (0,12)	

	Sujets sains	Amputés transtibiaux	Sig.
ASI temporelle (%)	-1,4 (3,58)	8,8 (9,3)	
ASI charge (%)	0,6 (12,2)	5,6 (21,3)	
Distance test (m)	**192 (16)**	**140 (35)**	*

Il est intéressant de noter que l'iHR est le seul des trois paramètres de symétrie qui présente une différence significative entre les deux populations. Des études plus poussées sur l'interprétation de l'iHR sont nécessaires : en effet, cet indice de symétrie ne présente aucune corrélation avec les ASI caractérisant la symétrie temporelle et de charge ni chez les sujets sains ni chez les personnes amputées au niveau transtibial. Si dix des paramètres ne permettent pas de différencier les sujets sains des sujets amputés, ils ne sont pour autant pas nécessairement à écarter lors du suivi des patients en cours de rééducation. Il est en effet tout à fait possible qu'une différence existe en début de rééducation et qu'elle soit comblée au cours de la rééducation fonctionnelle des personnes amputées. Seule une étude permettant d'obtenir les valeurs caractérisant les personnes amputées en cours de rééducation peut permettre de conclure sur l'intérêt des indices pour le suivi en cours de rééducation. En effet, la comparaison des valeurs des indices au cours de la rééducation et à la fin de celle-ci avec la différence minimale détectable permettrait de juger si les indices sont sensibles aux évolutions de la marche et donc pertinents pour suivre les progrès des patients au cours de leur rééducation. Il est toutefois intéressant de noter qu'au regard des valeurs élevées des différences minimales détectables des coefficients d'atténuation trouvées dans cette étude, il est probable que ceux-ci ne permettent pas de détecter une évolution des patients au cours de la rééducation.

Cette étude a contribué à améliorer la compréhension des indices de qualité de la marche. La faisabilité de la caractérisation de ces indices en clinique lors du test de deux minutes, validé chez les personnes amputées, a par ailleurs été démontrée. Afin de conclure sur la pertinence du suivi de ces indices, il est nécessaire d'obtenir des valeurs de référence en cours de rééducation. Ceci permettra

de mettre en évidence si les indices sont suffisamment sensibles pour détecter une évolution de la qualité de la marche au cours de la rééducation, et ainsi de conclure sur leur pertinence clinique.

4. Conclusion générale

L'objectif de cette thèse était de contribuer au développement d'outils et protocoles embarqués permettant l'évaluation quantitative des personnes amputées de membre inférieur pendant leur rééducation.

La première partie de la thèse a permis d'identifier les paramètres biomécaniques et cliniques pertinents, potentiellement quantifiables à l'aide de centrales inertielles ou de semelles de pression. Deux approches complémentaires ont alors été implémentées pour développer des algorithmes originaux ou valider, chez les personnes amputées de membre inférieur, des outils existants permettant de quantifier la cinématique du centre de masse, la symétrie de la marche et l'équilibre dynamique.

La première approche, fondée sur la modélisation biomécanique du corps, a été implémentée dans la seconde partie de la thèse (section 2 du résumé). Un algorithme original permettant d'estimer avec précision l'accélération et la vitesse instantanée du centre de masse à l'aide de cinq centrales inertielles a pu ainsi être proposé et validé chez une personne amputée transfémorale. La robustesse du protocole aux erreurs de localisation des centrales inertielles pour l'estimation de l'accélération du centre de masse du corps a été étudiée à travers une étude de sensibilité. Cette analyse pourrait être complétée par une étude de l'impact des erreurs d'orientation héritées des hypothèses d'alignement des centrales pour la définition d'un repère global commun. Le travail effectué dans ce cadre n'est pas exempt de limites. L'analyse de sensibilité et le protocole ont été développé et validé sur les données d'une unique personne amputée. Davantage de patients devraient être recrutés afin de confirmer la validité et la pertinence du protocole proposé. Par ailleurs, en l'état, le protocole repose sur l'utilisation d'un système optoélectronique pour la calibration des photographies nécessaires à l'obtention du modèle inertiel personnalisé et la position absolue des centrales inertielles. Des développements et un travail de validation sont donc nécessaires pour se passer de l'utilisation du système opto-électronique, par exemple, en utilisant des scanners 3D. Enfin, le protocole pourrait être adapté pour permettre d'acquérir d'autres paramètres biomécaniques pertinents tels que le déplacement du centre de masse et les efforts de réaction au sol sous chaque pied.

La seconde approche, fondée sur l'exploitation des signaux des capteurs embarqués pour identifier des indices caractérisant le mouvement, a été implémentée dans la troisième partie de la thèse (section 3 du résumé) dans le but d'examiner la pertinence d'algorithmes ou d'indices de qualité de la marche déjà proposés dans la littérature pour le suivi de la rééducation des personnes amputées de membre inférieur. Une première étude avait pour objectif d'évaluer la faisabilité de l'utilisation des centrales inertielles pour caractériser l'asymétrie temporelle de la marche. Si deux des cinq algorithmes de détection des événements de la marche permettent d'identifier avec suffisamment de précision les instants d'occurrence des événements de contact initial et final, une tendance à sous-estimer l'asymétrie de durée de phase d'appui a été mise en évidence, proscrivant l'usage des algorithmes dans ce but. Dans une deuxième étude, l'instrumentation du test de deux minutes avec des centrales inertielles sur le haut du corps et des semelles de pression a été proposée. Cette étude a permis de démontrer la faisabilité de caractériser, en milieu clinique, la qualité de la marche des

185

personnes amputées transtibiales en termes d'équilibre dynamique et de symétrie à l'aide d'indices issus des capteurs embarqués. La pertinence des indices a été explorée à l'aide d'une étude de répétabilité intra-session, dont les résultats devront être confirmés sur une étude de répétabilité inter-session avec une cohorte de personnes amputées plus importante. Par ailleurs, il est nécessaire de comparer les valeurs de référence obtenues au cours de l'étude aux valeurs prises par les indices au cours de la rééducation afin de vérifier la sensibilité au changement des indices et de conclure sur leur utilité pour le suivi clinique de patients pendant la rééducation.

Les deux approches implémentées dans cette thèse ont donc contribué, chacune à leur échelle, au transfert vers la clinique des capteurs embarqués. La première a, en effet, exploré de nouvelles pistes d'utilisation des capteurs embarqués chez les personnes amputées de membre inférieur tandis que la seconde a approfondi les connaissances et le degré de validation d'indices de qualité de la marche chez les personnes amputées. Des travaux complémentaires de validation sont toutefois nécessaires avant de pouvoir implémenter les protocoles proposés en clinique. Il est intéressant de noter que les algorithmes et protocoles proposés dans cette thèse pourraient également servir à évaluer la marche d'autres populations que celle des personnes amputées de membre inférieur, mais de légères adaptations des algorithmes pourraient être nécessaires (par exemple, concernant le choix des segments à instrumenter pour la cinématique du centre de masse) et la validation des indicateurs ou algorithmes devra être vérifiée au préalable dans la population visée.

References

Abdul Razak, A. H., Zayegh, A., Begg, R. K. and Wahab, Y. (2012) 'Foot plantar pressure measurement system: A review', Sensors (Switzerland), 12(7), pp. 9884–9912.

Al Abiad, N., Pillet, H. and Watier, B. (2020) 'A mechanical descriptor of instability in human locomotion: Experimental findings in control subjects and people with transfemoral amputation', Applied Sciences (Switzerland), 10(3).

Agrawal, V. (2016) 'Clinical Outcome Measures for Rehabilitation of Amputees – A Review', Physical Medicine and Rehabilitation Int, 3(2), pp. 01–04.

Agrawal, V., Gailey, R., O'Toole, C., Gaunaurd, I. and Dowell, T. (2009) 'Symmetry in external work (SEW): a novel method of quantifying gait differences between prosthetic feet.', Prosthetics and orthotics international, 33(2), pp. 148–56.

Al-Jawad, A., Barlit, A., Romanovas, M., Traechtler, M. and Manoli, Y. (2013) 'The Use of an Orientation Kalman Filter for the Static Postural Sway Analysis', APCBEE Procedia, 7, pp. 93–102.

Amin, M. S., Reaz, M. B. I., Nasir, S. S., Bhuiyan, M. A. S. and Ali, M. A. M. (2014) 'A Novel Vehicle Stationary Detection Utilizing Map Matching and IMU Sensors', Scientific World Journal, 2014(September).

Aminian, K., Najafi, B., Büla, C., Leyvraz, P.-F. and Robert, P. (2002) 'Spatio-temporal parameters of gait measured by an ambulatory system using miniature gyroscopes', Journal of Biomechanics, 35(5), pp. 689–699.

Ancillao, A., Tedesco, S., Barton, J. and O'flynn, B. (2018) 'Indirect measurement of ground reaction forces and moments by means of wearable inertial sensors: A systematic review', Sensors (Switzerland), 18(8).

Arch, E. S., Erol, O., Bortz, C., Madden, C., Galbraith, M., Rossi, A., Lewis, J., Higginson, J. S., Buckley, J. M. and Horne, J. (2016) 'Real-World Walking Performance of Individuals with Lower-Limb Amputation Classified as Medicare Functional Classification Level 2 and 3', Journal of Prosthetics and Orthotics, 28(2), pp. 51–57.

Arumukhom Revi, D., Alvarez, A. M., Walsh, C. J., De Rossi, S. M. M. and Awad, L. N. (2020) 'Indirect measurement of anterior-posterior ground reaction forces using a minimal set of wearable inertial sensors: from healthy to hemiparetic walking', Journal of NeuroEngineering and Rehabilitation, 17(1), p. 82.

Arvin, M., Mazaheri, M., Hoozemans, M. J. M., Pijnappels, M., Burger, B. J., Verschueren, S. M. P. and van Dieën, J. H. (2016) 'Effects of narrow base gait on mediolateral balance control in young and older adults.', Journal of biomechanics, 49(7), pp. 1264–1267.

Askew, G. N., McFarlane, L. A., Minetti, A. E. and Buckley, J. G. (2019) 'Energy cost of ambulation in trans-tibial amputees using a dynamic-response foot with hydraulic versus rigid "ankle": Insights from body centre of mass dynamics', Journal of NeuroEngineering and Rehabilitation, 16(1), pp. 1–12.

Barnett, S., Cunningham, J. L. J. and West, S. (2001) 'A comparison of vertical force and temporal parameters produced by an in-shoe pressure measuring system and a force platform', Clinical Biomechanics, 16(4), pp. 353–357.

Bastas, G., Fleck, J. J., Peters, R. A. and Zelik, K. E. (2018) 'IMU-based gait analysis in lower limb prosthesis users : Comparison of step demarcation algorithms', Gait & Posture, 64(May), pp. 30–37.

Batten, H. R., McPhail, S. M., Mandrusiak, A. M., Varghese, P. N. and Kuys, S. S. (2019) 'Gait speed as an indicator of prosthetic walking potential following lower limb amputation', Prosthetics and Orthotics International, 43(2), pp. 196–203.

Bellanca, J. L., Lowry, K. A., VanSwearingen, J. M., Brach, J. S. and Redfern, M. S. (2013) 'Harmonic ratios: A quantification of step to step symmetry', Journal of Biomechanics, 46(4), pp. 828–831.

Belluscio, V. (2020) From the lab to the field: the use of wearable inertial sensors for quantifying movements disorders. Rapport de thèse - Università degli Studi di Roma "Foro Italico".

Belluscio, V., Bergamini, E., Iosa, M., Tramontano, M., Morone, G. and Vannozzi, G. (2018) 'The iFST: An instrumented version of the Fukuda Stepping Test for balance assessment', Gait and Posture, 60(November 2017), pp. 203–208.

Belluscio, V., Bergamini, E., Salatino, G., Marro, T., Gentili, P., Iosa, M., Morelli, D. and Vannozzi, G. (2019) 'Dynamic balance assessment during gait in children with Down and Prader-Willi syndromes using inertial sensors', Human Movement Science, 63, pp. 53–61.

Benson, L. C., Clermont, C. A., Bosnjak, E. and Ferber, R. (2018) 'The use of wearable devices for walking and running gait analysis outside of the lab: a systematic review', Gait & Posture, 63(April), pp. 124–138.

Bergamini, E. (2011) Biomechanics of sprint running: a methodological contribution. Rapport de thèse - Università degli Studi di Roma "Foro Italico".

Bergamini, E., Iosa, M., Belluscio, V., Morone, G., Tramontano, M. and Vannozzi, G. (2017) 'Multi-sensor assessment of dynamic balance during gait in patients with subacute stroke', Journal of Biomechanics, 61, pp. 208–215.

Bergamini, E., Ligorio, G., Summa, A., Vannozzi, G., Cappozzo, A. and Sabatini, A. M. (2014) 'Estimating Orientation Using Magnetic and Inertial Sensors and Different Sensor Fusion Approaches: Accuracy Assessment in Manual and Locomotion Tasks', Sensors, 14(10), pp. 18625–18649.

Berthoz, A. and Pozzo, T. (1994) 'Head and Body Coordination during Locomotion and Complex Movements', in Interlimb Coordination. Elsevier, pp. 147–165.

Bertoli, M., Cereatti, A., Trojaniello, D., Avanzino, L., Pelosin, E., Del Din, S., Rochester, L., Ginis, P., Bekkers, E. M. J., Mirelman, A., et al. (2018) 'Estimation of spatio-temporal parameters of gait from magneto-inertial measurement units: multicenter validation among Parkinson, mildly cognitively impaired and healthy older adults.', Biomedical engineering online, 17(1), p. 58.

Betker, A. L., Szturm, T. and Moussavi, Z. (2006) 'Center of mass approximation during walking as a function of trunk and swing leg acceleration', Annual International Conference of the IEEE Engineering in Medicine and Biology - Proceedings, 53(4), pp. 3435–3438.

Bland, J. and Altman, D. (1986) 'Statistical methods for assessing agreement between two methods of clinical measurement', The lancet, pp. 307–310.

Bohannon, R. W., Wang, Y. C. and Gershon, R. C. (2015) 'Two-minute walk test performance by adults 18 to 85 years: Normative values, reliability, and responsiveness', Archives of Physical Medicine and Rehabilitation, 96(3), pp. 472–477.

Bonnet, V., McCamley, J., Mazza, C. and Cappozzo, A. (2012) 'Trunk orientation estimate during walking using gyroscope sensors', in 2012 4th IEEE RAS & EMBS International Conference on Biomedical Robotics and Biomechatronics (BioRob). IEEE, pp. 367–372.

Bonnet, X. (2009) Mise en situation numérique et expérimentale de composants prothétiques pour l'appareillage de personnes amputées du membre inférieur. Rapport de thèse - Arts et Métiers ParisTech.

Bonnet, X., Villa, C., Fodé, P., Lavaste, F. and Pillet, H. (2014) 'Mechanical work performed by individual limbs of transfemoral amputees during step-to-step transitions: Effect of walking velocity', Proceedings of the Institution of Mechanical Engineers, Part H: Journal of Engineering in Medicine, 228(1), pp. 60–66.

Boone, D. A., Kobayashi, T., Chou, T. G. ., Arabian, A. K., Coleman, K. L., Orendurff, M. S. and Zhang, M. (2012) 'Perception of socket alignment perturbations in amputees with transtibial prostheses', The Journal of Rehabilitation Research and Development, p. 843.

Brooks, D., Parsons, J., Hunter, J. P., Devlin, M. and Walker, J. (2001) 'The 2-minute walk test as a measure of functional improvement in persons with lower limb amputation', Archives of Physical

Medicine and Rehabilitation, 82(10), pp. 1478–1483.

Bruijn, S. M., Meijer, O. G., Beek, P. J. and van Dieen, J. H. (2013) 'Assessing the stability of human locomotion: a review of current measures', Journal of The Royal Society Interface, 10(83), pp. 20120999–20120999.

Buckley, C., Galna, B., Rochester, L. and Mazzà, C. (2017) 'Quantification of upper body movements during gait in older adults and in those with Parkinson's disease: impact of acceleration realignment methodologies', Gait and Posture, 52, pp. 265–271.

Buckley, C., Galna, B., Rochester, L. and Mazzà, C. (2018) 'Upper body accelerations as a biomarker of gait impairment in the early stages of Parkinson's disease', Gait and Posture, (in press), pp. 1–7.

Calmels, P., Béthoux, F., Le-Quang, B., Chagnon, P. Y. and Rigal, F. (2002) 'Échelles D˙évaluation Fonctionnelle Et Amputation Du Membre Inférieur', Annales de Réadaptation et de Médecine Physique, 44(8), pp. 499–507.

Cappozzo, A. (1981) 'Analysis of the linear displacement of the head and trunk during walking at different speeds', Journal of Biomechanics, 14(6), pp. 411–425.

Cappozzo, A. (1984) 'Gait Analysis Methodology', Human Movement Science, 3, pp. 27–50.

Cappozzo, A., Della Croce, U., Leardini, A. and Chiari, L. (2005) 'Human movement analysis using stereophotogrammetry. Part 1: Theoretical background', Gait and Posture, 21(2), pp. 186–196.

Carmona, G. A., Lacraz, A., Hoffmeyer, P. and Assal, M. (2014) 'Incidence de l'amputation majeure des membres inférieurs à Genève : Vingt-et-un ans d'observation', Revue Medicale Suisse, 10(447), pp. 1997–2001.

Caruso, M., Sabatini, A. M., Knaflitz, M., Gazzoni, M., Croce, U. Della and Cereatti, A. (2019) 'Accuracy of the Orientation Estimate Obtained Using Four Sensor Fusion Filters Applied to Recordings of Magneto-Inertial Sensors Moving at Three Rotation Rates', Proceedings of the Annual International Conference of the IEEE Engineering in Medicine and Biology Society, EMBS, pp. 2053–2058.

Catalfamo, P., Ghoussayni, S. and Ewins, D. (2010) 'Gait event detection on level ground and incline walking using a rate gyroscope', Sensors, 10(6), pp. 5683–5702.

Catena, R. D., Chen, S. H. and Chou, L. S. (2017) 'Does the anthropometric model influence whole-body center of mass calculations in gait?', Journal of Biomechanics, 59, pp. 23–28.

Choe, N., Zhao, H., Qiu, S. and So, Y. (2019) 'A sensor-to-segment calibration method for motion capture system based on low cost MIMU', Measurement: Journal of the International Measurement Confederation, 131, pp. 490–500.

Condie, E., Scott, H. and Treweek, S. (2006) 'Lower Limb Prosthetic Outcome Measures: A Review of the Literature 1995 to 2005', Journal of Prosthetics and Orthotics, 18(1), pp. 13–45.

Cuesta-Vargas, A. I., Galán-Mercant, A. and Williams, J. M. (2010) 'The use of inertial sensors system for human motion analysis', Physical Therapy Reviews, 15(6), pp. 462–473.

Cutti, A. G., Ferrari, A. A. A. A. A. A., Garofalo, P., Raggi, M., Cappello, A. and Ferrari, A. A. A. A. A. A. (2010) '"Outwalk": a protocol for clinical gait analysis based on inertial and magnetic sensors.', Medical & biological engineering & computing, 48(1), pp. 17–25.

Cutti, A. G., Raggi, M., Andreoni, G. and Sacchetti, R. (2015) 'Clinical gait analysis for amputees: Innovation wishlist and the perspectives offered by the outwalk protocol', Giornale Italiano di Medicina del Lavoro ed Ergonomia, 37(July), pp. 45–48.

Cutti, A. G., Verni, G., Migliore, G. L., Amoresano, A. and Raggi, M. (2018) 'Reference values for gait temporal and loading symmetry of lower-limb amputees can help in refocusing rehabilitation targets', Journal of NeuroEngineering and Rehabilitation, 15(Suppl 1).

Dadashi, F., Mariani, B., Rochat, S., Büla, C. J., Santos-Eggimann, B. and Aminian, K. (2013) 'Gait and foot clearance parameters obtained using shoe-worn inertial sensors in a large-population sample of older adults', Sensors (Switzerland), 14(1), pp. 443–457.

189

Dauriac, B. (2018) Contribution à la mise en oeuvre et l'évaluation de technologies embaquées pour l'appareillage de personnes amputées de membre inférieur. Rapport de thèse - Arts et Métiers ParisTech.

Dauriac, B., Bonnet, X., Pillet, H. and Lavaste, F. (2019) 'Estimation of the walking speed of individuals with transfemoral amputation from a single prosthetic shank-mounted IMU', Proceedings of the Institution of Mechanical Engineers, Part H: Journal of Engineering in Medicine, 233(9), pp. 931–937.

Deathe, A. B., Wolfe, D. L., Devlin, M., Hebert, J. S., Miller, W. C. and Pallaveshi, L. (2009) 'Selection of outcome measures in lower extremity amputation rehabilitation: ICF activities', Disability and Rehabilitation, 31(18), pp. 1455–1473.

Dejnabadi, H., Jolles, B. M., Casanova, E., Fua, P. and Aminian, K. (2006) 'Estimation and visualization of sagittal kinematics of lower limbs orientation using body-fixed sensors', IEEE Transactions on Biomedical Engineering, 53(7), pp. 1385–1393.

Detrembleur, C., Vanmarsenille, J. M., De Cuyper, F. and Dierick, F. (2005) 'Relationship between energy cost, gait speed, vertical displacement of centre of body mass and efficiency of pendulum-like mechanism in unilateral amputee gait', Gait and Posture, 21(3), pp. 333–340.

Detrembleur, D. ucl ac be, van den Hecke, A. and Dierick, F. (2000) 'Motion of the body centre of gravity as a summary indicator of the mechanics of human pathological gait', Gait and posture, 12(3), pp. 243–250.

Dingwell, J. B., Davis, B. L. and Frazier, D. M. (1996) 'Use of an instrumented treadmill for real-time gait symmetry evaluation and feedback in normal and trans-tibial amputee subjects', Prosthetics and Orthotics International, 20(2), pp. 101–110.

Donelan, J. M., Kram, R. and Kuo, A. D. (2002a) 'Mechanical work for step-to-step transitions is a major determinant of the metabolic cost of human walking.', The Journal of experimental biology, 205(Pt 23), pp. 3717–27.

Donelan, J. M., Kram, R. and Kuo, A. D. (2002b) 'Simultaneous positive and negative external mechanical work in human walking.', Journal of biomechanics, 35(1), pp. 117–24.

Dorschky, E., Nitschke, M., Martindale, C. F., van den Bogert, A. J., Koelewijn, A. D. and Eskofier, B. M. (2020) 'CNN-Based Estimation of Sagittal Plane Walking and Running Biomechanics From Measured and Simulated Inertial Sensor Data', Frontiers in Bioengineering and Biotechnology, 8, pp. 1–20.

Dorschky, E., Nitschke, M., Seifer, A. K., van den Bogert, A. J. and Eskofier, B. M. (2019) 'Estimation of gait kinematics and kinetics from inertial sensor data using optimal control of musculoskeletal models', Journal of Biomechanics, 95, p. 109278.

Drevelle, X., Villa, C., Bonnet, X., Loiret, I., Fodé, P. and Pillet, H. (2014) 'Vaulting quantification during level walking of transfemoral amputees.', Clinical biomechanics (Bristol, Avon), 29(6), pp. 679–83.

Dumas, R., Chèze, L. and Verriest, J. P. (2007) 'Adjustments to McConville et al. and Young et al. body segment inertial parameters', Journal of Biomechanics, 40(3), pp. 543–553.

Duraffourg, C., Bonnet, X., Dauriac, B. and Pillet, H. (2019) 'Real time estimation of the pose of a lower limb prosthesis from a single shank mounted IMU', Sensors (Switzerland), 19(13), pp. 1–11.

Eames, M. H. A., Cosgrove, A. and Baker, R. (1999) 'Comparing methods of estimating the total body centre of mass in three-dimensions in normal and pathological gaits', Human Movement Science, 18, pp. 637–646.

Esposito, E. R., Whitehead, J. M. A. and Wilken, J. M. (2015) 'Clinical Biomechanics Sound limb loading in individuals with unilateral transfemoral amputation across a range of walking velocities ☆', JCLB, 30(10), pp. 1049–1055.

Esquenazi, A. and DiGiacomo, R. (2001) 'Rehabilitation after amputation', Journal of the American Podiatric Medical Association, 91(1), pp. 13–22.

190

Esser, P., Dawes, H., Collett, J. and Howells, K. (2009) IMU: Inertial sensing of vertical CoM movement, Journal of Biomechanics.

Faber, G. S., Chang, C. C., Kingma, I., Dennerlein, J. T. and van Dieën, J. H. (2016) 'Estimating 3D L5/S1 moments and ground reaction forces during trunk bending using a full-body ambulatory inertial motion capture system', Journal of Biomechanics, 49(6), pp. 904–912.

Fasel, B., Sporri, J., Chardonnens, J., Kroll, J., Muller, E. and Aminian, K. (2017) 'Joint Inertial Sensor Orientation Drift Reduction for Highly Dynamic Movements', IEEE Journal of Biomedical and Health Informatics, 22(1), pp. 77–86.

Fasel, B., Spörri, J., Schütz, P., Lorenzetti, S. and Aminian, K. (2017) 'An Inertial Sensor-Based Method for Estimating the Athlete's Relative Joint Center Positions and Center of Mass Kinematics in Alpine Ski Racing.', Frontiers in physiology, 8, p. 850.

Favre, J., Jolles, B. M., Aissaoui, R. and Aminian, K. (2008) 'Ambulatory measurement of 3D knee joint angle.', Journal of biomechanics, 41(5), pp. 1029–35.

Fino, P. C., Horak, F. B. and Curtze, C. (2020) 'Inertial Sensor-Based Centripetal Acceleration as a Correlate for Lateral Margin of Stability During Walking and Turning', IEEE Transactions on Neural Systems and Rehabilitation Engineering, 28(3), pp. 629–636.

Fleury, A., Sugar, M. and Chau, T. (2015) 'E-textiles in Clinical Rehabilitation: A Scoping Review', Electronics, 4(1), pp. 173–203.

Floor-Westerdijk, M. J., Schepers, H. M., Veltink, P. H., van Asseldonk, E. H. F. and Buurke, J. H. (2012) 'Use of inertial sensors for ambulatory assessment of center-of-mass displacements during walking.', IEEE transactions on bio-medical engineering, 59(7), pp. 2080–4.

Frengopoulos, C., Payne, M. W. C., Holmes, J. D., Viana, R. and Hunter, S. W. (2018) 'Comparing the Effects of Dual-Task Gait Testing in New and Established Ambulators With Lower Extremity Amputations', PM and R, 10(10), pp. 1012–1019.

Frigo, C. and Crenna, P. (2009) 'Multichannel SEMG in clinical gait analysis: A review and state-of-the-art', Clinical Biomechanics, 24(3), pp. 236–245.

Fritz, S. and Lusardi, M. (2009) 'White paper: "walking speed: The sixth vital sign"', Journal of Geriatric Physical Therapy, 32(2), pp. 2–5.

Gailey, R., Allen, K., Castles, J., Kucharik, J. and Roeder, M. (2008) 'Review of secondary physical conditions associated with lower-limb amputation and long-term prosthesis use.', Journal of rehabilitation research and development, 45(1), pp. 15–29.

Gard, S. A., Miff, S. C. and Kuo, A. D. (2004) 'Comparison of kinematic and kinetic methods for computing the vertical motion of the body center of mass during walking', Human Movement Science, 22(6), pp. 597–610.

Gardner, D. W., Redd, C. B., Cagle, J. C., Hafner, B. J., Sanders, J. E., Msme, D. W., Mse, C. B., Bse, J. C., Brian, J., Joan, E., et al. (2016) 'Monitoring Prosthesis User Activity and Doffing Using an Activity Monitor and Proximity Sensors', Journal of Prosthetics and Orthotics, 28(2), pp. 68–77.

Garofalo, P. (2010) Development of motion analysis protocols based on inertial sensors. Rapport de thèse - Université de Bologne.

Gaunaurd, I., Kristal, A., Horn, A., Krueger, C., Muro, O., Rosenberg, A., Gruben, K., Kirk-Sanchez, N., Pasquina, P. and Gailey, R. (2020) 'The Utility of the 2-Minute Walk Test as a Measure of Mobility in People With Lower Limb Amputation', Archives of Physical Medicine and Rehabilitation, 101(7), pp. 1183–1189.

Ghillebert, J., De Bock, S., Flynn, L., Geeroms, J., Tassignon, B., Roelands, B., Lefeber, D., Vanderborght, B., Meeusen, R. and De Pauw, K. (2019) 'Guidelines and Recommendations to Investigate the Efficacy of a Lower-Limb Prosthetic Device: A Systematic Review', IEEE Transactions on Medical Robotics and Bionics, 1(4), pp. 279–296.

Ghislieri, M., Gastaldi, L., Pastorelli, S., Tadano, S. and Agostini, V. (2019) 'Wearable inertial sensors

to assess standing balance: a systematic review', Sensors (Switzerland), 19(19), pp. 1–25.

Gillet, C., Duboy, J., Barbier, F., Armand, S., Jeddi, R., Lepoutre, F. X. and Allard, P. (2003) 'Contribution of accelerated body masses to able-bodied gait', American Journal of Physical Medicine and Rehabilitation, 82(2), pp. 101–109.

Gitter, A., Czerniecki, J. and Weaver, K. (1995) 'A reassessment of center-of-mass dynamics as a determinate of the metabolic inefficiency of above-knee amputee ambulation', American Journal of Physical Medicine and Rehabilitation, pp. 332–338.

González, R. C., López, A. M., Rodriguez-Uría, J., Álvarez, D. and Alvarez, J. C. (2010) 'Real-time gait event detection for normal subjects from lower trunk accelerations', Gait and Posture, 31(3), pp. 322–325.

Goujon-Pillet, H., Sapin, E., Fodé, P. and Lavaste, F. (2008) 'Three-Dimensional Motions of Trunk and Pelvis During Transfemoral Amputee Gait', Archives of Physical Medicine and Rehabilitation, 89(1), pp. 87–94.

Goujon, H. (2006) Analyse de la marche de l'amputé fémoral. Rapport de thèse - Arts et Métiers ParisTech.

Goujon, H., Bonnet, X., Sautreuil, P., Maurisset, M., Darmon, L., Fode, P. and Lavaste, F. (2006) 'A functional evaluation of prosthetic foot kinematics during lower-limb amputee gait.', Prosthetics and orthotics international, 30(2), pp. 213–223.

Goupy, J. (2016) 'Modélisation par les plans d'expériences', Techniques de l'ingénieur Méthodes de mesure, p. 275.

Greene, B. R., McGrath, D., O'Neill, R., O'Donovan, K. J., Burns, A. and Caulfield, B. (2010) 'An adaptive gyroscope-based algorithm for temporal gait analysis', Medical & Biological Engineering & Computing, 48(12), pp. 1251–1260.

Guaitolini, M., Aprigliano, F., Mannini, A., Micera, S., Monaco, V. and Sabatini, A. M. (2019) 'Ambulatory Assessment of the Dynamic Margin of Stability Using an Inertial Sensor Network', Sensors, 19(19), p. 4117.

Guo, Y., Storm, F., Zhao, Y., Billings, S. A., Pavic, A., Mazzà, C. and Guo, L. Z. (2017) 'A new proxy measurement algorithm with application to the estimation of vertical ground reaction forces using wearable sensors', Sensors, 17(10), p. 2181.

Hafner, B. J. and Askew, R. L. (2015) 'Physical performance and self-report outcomes associated with use of passive, adaptive, and active prosthetic knees in persons with unilateral, transfemoral amputation: Randomized crossover trial', Journal of Rehabilitation Research and Development, 52(6), pp. 677–700.

Hafner, B. J. and Sanders, J. E. (2014) 'Considerations for development of sensing and monitoring tools to facilitate treatment and care of persons with lower-limb loss: A review', Journal of Rehabilitation Research and Development, 51(1), pp. 1–14.

Hak, L., van Dieen, J. H., van der Wurff, P. and Houdijk, H. (2014) 'Stepping assymmetry among people with Limb Loss Might Be Functional in Terms of Gait Stability', Journal of Physical Therapy, 94(10).

Hannink, J., Ollenschläger, M., Kluge, F., Roth, N., Klucken, J. and Eskofier, B. M. (2017) 'Benchmarking foot trajectory estimation methods for mobile gait analysis', Sensors, 17(9), p. 1940.

Hansen, A. H., Childress, D. S. and Knox, E. H. (2000) 'Prosthetic foot roll-over shapes with implications for alignment of trans-tibial prostheses', Prosthetics and Orthotics International, 24(3), pp. 205–215.

Hansen, A. H., Childress, D. S. and Miff, S. C. (2004) 'Roll-over characteristics of human walking on inclined surfaces', Human Movement Science, 23(6), pp. 807–821.

Hausdorff, J. M., Ashkenazy, Y., Peng, C. K., Ivanov, P. C., Stanley, H. E. and Goldberger, A. L. (2001) 'When human walking becomes random walking: Fractal analysis and modeling of gait rhythm

fluctuations', Physica A: Statistical Mechanics and its Applications, 302(1–4), pp. 138–147.

Hawkins, A. T., Henry, A. J., Crandell, D. M. and Nguyen, L. L. (2014) 'A systematic review of functional and quality of life assessment after major lower extremity amputation', Annals of Vascular Surgery, 28(3), pp. 763–780.

Hawkins, E. J. and Riddick, W. (2018) 'Reliability, Validity, and Responsiveness of Clinical Performance-Based Outcome Measures of Walking for Individuals With Lower Limb Amputations: A Systematic Review', Physical therapy, 98(12), pp. 1037–1045.

Hayot, C., Sakka, S. and Lacouture, P. (2013) 'Contribution of the six major gait determinants on the vertical center of mass trajectory and the vertical ground reaction force', Human Movement Science, 32(2), pp. 279–289.

Heinemann, A. W., Connelly, L., Ehrlich-Jones, L. S. and Fatone, S. (2014) 'Outcome instruments for prosthetics : Clinical Applications', 25, pp. 179–198.

Herbert-Copley, A. G., Sinitski, E. H., Lemaire, E. D. and Baddour, N. (2013) 'Temperature and measurement changes over time for F-Scan sensors', MeMeA 2013 - IEEE International Symposium on Medical Measurements and Applications, Proceedings, pp. 265–267.

Herr, H. and Popovic, M. (2008) 'Angular momentum in human walking', Journal of Experimental Biology, 211(4), pp. 467–481.

Highsmith, M. J., Andrews, C. R., Millman, C., Fuller, A., Kahle, J. T., Klenow, T. D., Lewis, K. L., Bradley, R. C. and Orriola, J. J. (2016) 'Gait Training Interventions for Lower Extremity Amputees: A Systematic Literature Review', Technology & Innovation, 18(2), pp. 99–113.

Hof, A. L., van Bockel, R. M., Schoppen, T. and Postema, K. (2007) 'Control of lateral balance in walking. Experimental findings in normal subjects and above-knee amputees', Gait and Posture, 25(2), pp. 250–258.

Hof, A. L., Gazendam, M. G. J. and Sinke, W. E. (2005) 'The condition for dynamic stability', Journal of Biomechanics, 38(1), pp. 1–8.

Hollman, J. H., Watkins, M. K., Imhoff, A. C., Braun, C. E., Akervik, K. A. and Ness, D. K. (2016) 'A comparison of variability in spatiotemporal gait parameters between treadmill and overground walking conditions', Gait & Posture, 43, pp. 204–209.

Houdijk, H., Appelman, F. M., Van Velzen, J. M., Van der Woude, L. H. V and Van Bennekom, C. A. M. (2008) 'Validity of DynaPort GaitMonitor for assessment of spatiotemporal parameters in amputee gait.', The Journal of Rehabilitation Research and Development, 45(9), p. 1335.

Houdijk, H., Pollmann, E., Groenewold, M., Wiggerts, H. and Polomski, W. (2009) 'The energy cost for the step-to-step transition in amputee walking', Gait and Posture, 30(1), pp. 35–40.

Howcroft, J., Kofman, J. and Lemaire, E. D. (2013) 'Review of fall risk assessment in geriatric populations using inertial sensors', Journal of NeuroEngineering and Rehabilitation, 10(1), p. 1.

Howcroft, J., Kofman, J., Lemaire, E. D. and McIlroy, W. E. (2016) 'Analysis of dual-task elderly gait in fallers and non-fallers using wearable sensors', Journal of Biomechanics, 49(7), pp. 992–1001.

Howcroft, J., Lemaire, E. D., Kofman, J. and Kendell, C. (2015) 'Understanding dynamic stability from pelvis accelerometer data and the relationship to balance and mobility in transtibial amputees', Gait & Posture, 41(3), pp. 808–812.

Howcroft, J., Lemaire, E. D., Kofman, J. and Kendell, C. (2016) 'Understanding responses to gait instability from plantar pressure measurement and the relationship to balance and mobility in lower-limb amputees', Clinical Biomechanics, 32, pp. 241–248.

Hsu, Y.-L., Chung, P.-C. J., Wang, W.-H., Pai, M.-C., Wang, C.-Y., Lin, C.-W., Wu, H.-L. and Wang, J.-S. (2014) 'Gait and balance analysis for patients with Alzheimer's disease using an inertial-sensor-based wearable instrument.', IEEE journal of biomedical and health informatics, 18(6), pp. 1822–30.

Hunter, S. W., Frengopoulos, C., Viana, R. and Payne, M. W. C. (2018) 'Dual-task related gait changes in individuals with trans-tibial lower extremity amputation', Gait & Posture, 61(January), pp.

403–407.

Huntley, A. H., Schinkel-Ivy, A., Aqui, A. and Mansfield, A. (2017) 'Validation of simplified centre of mass models during gait in individuals with chronic stroke', Clinical Biomechanics, 48, pp. 97–102.

Iosa, M., Bini, F., Marinozzi, F., Fusco, A., Morone, G., Koch, G., Martino Cinnera, A., Bonnì, S. and Paolucci, S. (2016) 'Stability and Harmony of Gait in Patients with Subacute Stroke', Journal of Medical and Biological Engineering, 36(5), pp. 635–643.

Iosa, M., Paradisi, F., Brunelli, S., Delussu, A. S., Pellegrini, R., Zenardi, D., Paolucci, S. and Traballesi, M. (2014) 'Assessment of gait stability, harmony, and symmetry in subjects with lower-limb amputation evaluated by trunk accelerations', Journal of Rehabilitation Research and Development, 51(4), pp. 623–634.

Iosa, M., Picerno, P., Paolucci, S. and Morone, G. (2016) 'Wearable inertial sensors for human movement analysis', Expert Review of Medical Devices, 13(7), pp. 641–659.

Jaegers, S. M. H. J., Arendzen, J. H. and de Jongh, H. J. (1995) 'Prosthetic gait of unilateral transfemoral amputees: A kinematic study', Archives of Physical Medicine and Rehabilitation, 76(8), pp. 736–743.

Jasiewicz, J. M., Allum, J. H. J., Middleton, J. W., Barriskill, A., Condie, P., Purcell, B. and Li, R. C. T. (2006) 'Gait event detection using linear accelerometers or angular velocity transducers in able-bodied and spinal-cord injured individuals', Gait and Posture, 24(4), pp. 502–509.

Jeong, B., Ko, C. Y., Chang, Y., Ryu, J. and Kim, G. (2018) 'Comparison of segmental analysis and sacral marker methods for determining the center of mass during level and slope walking', Gait and Posture, 62(July 2017), pp. 333–341.

Karatsidis, A., Bellusci, G., Schepers, H. M., de Zee, M., Andersen, M. S. and Veltink, P. H. (2017) 'Estimation of ground reaction forces and moments during gait using only inertial motion capture', Sensors (Switzerland), 17(1), pp. 1–22.

Karatsidis, A., Jung, M., Schepers, H. M., Bellusci, G., de Zee, M., Veltink, P. H. and Andersen, M. S. (2019) 'Musculoskeletal model-based inverse dynamic analysis under ambulatory conditions using inertial motion capture', Medical Engineering & Physics, 65, pp. 68–77.

Kavanagh, J. J. and Menz, H. B. (2008) 'Accelerometry: A technique for quantifying movement patterns during walking', Gait & Posture, 28(1), pp. 1–15.

Kendell, C., Lemaire, E. D., Dudek, N. L. and Kofman, J. (2010) 'Indicators of dynamic stability in transtibial prosthesis users', Gait and Posture, 31(3), pp. 375–379.

Kendell, C., Lemaire, E. D., Kofman, J. and Dudek, N. (2016) 'Gait adaptations of transfemoral prosthesis users across multiple walking tasks.', Prosthetics and orthotics international, 40(1), pp. 89–95.

Khurelbaatar, T., Kim, K., Lee, S. K. and Kim, Y. H. (2015) 'Consistent accuracy in whole-body joint kinetics during gait using wearable inertial motion sensors and in-shoe pressure sensors', Gait and Posture, 42(1), pp. 65–69.

Kianifar, R., Joukov, V., Lee, A., Raina, S. and Kulić, D. (2019) 'Inertial measurement unit-based pose estimation: Analyzing and reducing sensitivity to sensor placement and body measures', Journal of Rehabilitation and Assistive Technologies Engineering, 6, p. 205566831881345.

Kitagawa, N. and Ogihara, N. (2016) 'Estimation of foot trajectory during human walking by a wearable inertial measurement unit mounted to the foot', Gait and Posture, 45, pp. 110–114.

Köse, A., Cereatti, A. and Della Croce, U. (2012) 'Bilateral step length estimation using a single inertial measurement unit attached to the pelvis', Journal of NeuroEngineering and Rehabilitation, 9(1), pp. 1–10.

Kovač, I., Kauzlarić, N., Živković, O., Mužić, V., Abramović, M., Vuletić, Z., Vukić, T., Ištvanović, N. and Livaković, B. (2015) 'Rehabilitation of lower limb amputees', Periodicum Biologorum, 117(1), pp. 147–159.

Ladlow, P., Nightingale, T. E., McGuigan, M. P., Bennett, A. N., Phillip, R. and Bilzon, J. L. J. J. (2017) 'Impact of anatomical placement of an accelerometer on prediction of physical activity energy expenditure in lower-limb amputees', PLos ONE, 12(10), pp. 1–15.

Lamandé, F., Dupré, J.-C., Baudin, O., Cécile, F., Frison, V. and Mangin, C. (2011) 'Rééducation de la personne amputée de membre inférieur', EMC - Kinésithérapie - Médecine physique - Réadaptation, 7(3), pp. 1–20.

Lamoth, C. J. C., Ainsworth, E., Polomski, W. and Houdijk, H. (2010) 'Variability and stability analysis of walking of transfemoral amputees.', Medical engineering & physics, 32(9), pp. 1009–14.

Lebel, K., Boissy, P., Hamel, M. and Duval, C. (2015) 'Inertial measures of motion for clinical biomechanics: Comparative assessment of accuracy under controlled conditions - Changes in accuracy over time', PLoS ONE, 10(3), pp. 1–12.

Lebel, K., Boissy, P., Nguyen, H. and Duval, C. (2017) 'Inertial measurement systems for segments and joints kinematics assessment: Towards an understanding of the variations in sensors accuracy', BioMedical Engineering OnLine, 16(1), p. 56.

Lebel, K., Hamel, M., Duval, C., Nguyen, H. and Boissy, P. (2018) 'Camera pose estimation to improve accuracy and reliability of joint angles assessed with attitude and heading reference systems', Gait and Posture, 59(March 2017), pp. 199–205.

Ledoux, E. (2018) 'Inertial Sensing for Gait Event Detection and Transfemoral Prosthesis Control Strategy', IEEE Transactions on Biomedical Engineering, 9294(c).

Lemaire, E. D., Biswas, A. and Kofman, J. (2006) 'Plantar Pressure Parameters for Dynamic Gait Stability Analysis', in 2006 International Conference of the IEEE Engineering in Medicine and Biology Society. IEEE, pp. 4465–4468.

Leporace, G., Batista, L. A., Metsavaht, L. and Nadal, J. (2015) 'Residual analysis of ground reaction forces simulation during gait using neural networks with different configurations', Proceedings of the Annual International Conference of the IEEE Engineering in Medicine and Biology Society, EMBS, 2015-Novem, pp. 2812–2815.

Li, Q., Young, M., Naing, V. and Donelan, J. M. M. (2010) 'Walking speed estimation using a shank-mounted inertial measurement unit', Journal of Biomechanics, 43(8), pp. 1640–1643.

Ligorio, G., Bergamini, E., Pasciuto, I., Vannozzi, G., Cappozzo, A. and Sabatini, A. M. (2016) 'Assessing the performance of sensor fusion methods: Application to magnetic-inertial-based human body tracking', Sensors (Switzerland), 16(2).

Ligorio, G., Bergamini, E., Truppa, L., Guaitolini, M., Raggi, M., Mannini, A., Sabatini, A. M., Vannozzi, G. and Garofalo, P. (2020) 'A Wearable Magnetometer-Free Motion Capture System: Innovative Solutions for Real-World Applications', IEEE Sensors Journal, 20(15), pp. 8844–8857.

Lintmeijer, L. L., Faber, G. S., Kruk, H. R., van Soest, A. J. K. and Hofmijster, M. J. (2018) 'An accurate estimation of the horizontal acceleration of a rower's centre of mass using inertial sensors: a validation', European Journal of Sport Science, 18(7), pp. 940–946.

Liu, T., Inoue, Y., Shibata, K. and Shiojima, K. (2011) 'Three-dimensional lower limb kinematic and kinetic analysis based on a wireless sensor system', in 2011 IEEE International Conference on Robotics and Automation. IEEE, pp. 842–847.

Liu, Y. T., Zhang, Y. A. and Zeng, M. (2019) 'Sensor to segment calibration for magnetic and inertial sensor based motion capture systems', Measurement: Journal of the International Measurement Confederation, 142, pp. 1–9.

Loiret, I. (2016) Gait asymmetry with wearable insoles in lower limb amputees. Rapport de master - BME Paris.

Loiret, I., Paysant, J., Martinet, N. and André, J. M. (2005) 'Evaluation of amputees', Annales de Readaptation et de Medecine Physique, 48(6), pp. 307–316.

Loiret, I., Villa, C., Dauriac, B., Bonnet, X., Martinet, N., Paysant, J. and Pillet, H. (2019) 'Are wearable

195

insoles a validated tool for quantifying transfemoral amputee gait asymmetry ?', Prosthetics and Orthotics International, 43(5), pp. 492–499.

Lopez-Nava, I. H. and Angelica, M. M. (2016) 'Wearable Inertial Sensors for Human Motion Analysis: A review', IEEE Sensors Journal, PP(99).

Madgwick, S. O. H., Harrison, A. J. L. and Vaidyanathan, A. (2011) 'Estimation of IMU and MARG orientation using a gradient descent algorithm.', IEEE International Conference on Rehabilitation Robotics, 2011, p. 5975346.

Major, M. J., Fatone, S., Hons, B. P. O. and Roth, E. J. (2013) 'Validity and Reliability of the Berg Balance Scale for Community-Dwelling Persons With Lower-Limb Amputation', YAPMR, 94(11), pp. 2194–2202.

Mancini, M., Salarian, A., Carlson-Kuhta, P., Zampieri, C., King, L., Chiari, L. and Horak, F. B. (2012) 'ISway: A sensitive, valid and reliable measure of postural control', Journal of NeuroEngineering and Rehabilitation, 9(1), pp. 1–8.

Maqbool, H. F., Husman, M. A. B., Awad, M. I., Abouhossein, A. and Dehghani-Sanij, A. A. (2015) 'Real-time gait event detection for transfemoral amputees during ramp ascending and descending.', Conf Proc IEEE Eng Med Biol Soc, 2015, pp. 4785–8.

Maqbool, H. F., Husman, M. A. B., Awad, M. I., Abouhossein, A., Iqbal, N. and Dehghani-Sanij, A. A. (2017) 'A Real-Time Gait Event Detection for Lower Limb Prosthesis Control and Evaluation.', IEEE transactions on neural systems and rehabilitation engineering, 25(9), pp. 1500–1509.

Mariani, B., Hoskovec, C., Rochat, S., Büla, C., Penders, J. and Aminian, K. (2010) '3D gait assessment in young and elderly subjects using foot-worn inertial sensors', Journal of Biomechanics, 43(15), pp. 2999–3006.

Mariani, B., Rouhani, H., Crevoisier, X. and Aminian, K. (2013) 'Quantitative estimation of foot-flat and stance phase of gait using foot-worn inertial sensors', Gait and Posture, 37(2), pp. 229–234.

Mazzà, C., Iosa, M., Pecoraro, F. and Cappozzo, A. (2008) 'Control of the upper body accelerations in young and elderly women during level walking', Journal of NeuroEngineering and Rehabilitation, 5, pp. 1–10.

Mazzà, C., Iosa, M., Picerno, P. and Cappozzo, A. (2009) 'Gender differences in the control of the upper body accelerations during level walking', Gait and Posture, 29(2), pp. 300–303.

McCamley, J., Donati, M., Grimpampi, E. and Mazzà, C. (2012) 'An enhanced estimate of initial contact and final contact instants of time using lower trunk inertial sensor data', Gait and Posture, 36(2), pp. 316–318.

Meichtry, A., Romkes, J., Gobelet, C., Brunner, R. and Müller, R. (2007) 'Criterion validity of 3D trunk accelerations to assess external work and power in able-bodied gait', Gait and Posture, 25(1), pp. 25–32.

Menz, H. B., Lord, S. R. and Fitzpatrick, R. C. (2003) 'Acceleration patterns of the head and pelvis when walking on level and irregular surfaces', Gait and Posture, 18, pp. 35–46.

Michaud, S. B., Gard, S. A. and Childress, D. S. (2000) 'A preliminary investigation of pelvic obliquity patterns during gait in persons with transtibial and transfemoral amputation', Journal of rehabilitation research and development, 37(1), pp. 1–10.

Miezal, M., Taetz, B. and Bleser, G. (2016) 'On inertial body tracking in the presence of model calibration errors', Sensors (Switzerland), 16(7), pp. 1–34.

Miller, W. C., Speechley, M. and Deathe, B. (2001) 'The prevalence and risk factors of falling and fear of falling among lower extremity amputees', Archives of Physical Medicine and Rehabilitation, 82(8), pp. 1031–1037.

Minetti, A. E., Cisotti, C. and Mian, O. S. (2011) 'The mathematical description of the body centre of mass 3D path in human and animal locomotion', Journal of Biomechanics, 44(8), pp. 1471–1477.

Miyazaki, S. (1997) 'Long-term unrestrained measurement of stride length and walking velocity

utilizing a piezoelectric gyroscope', IEEE Transactions on Biomedical Engineering, 44(8), pp. 753–759.

Moe-Nilssen, R. and Helbostad, J. L. (2004) 'Estimation of gait cycle characteristics by trunk accelerometry', Journal of Biomechanics, 37(1), pp. 121–126.

Mohamed, A., Sexton, A., Simonsen, K. and McGibbon, C. A. (2019) 'Development of a mechanistic hypothesis linking compensatory biomechanics and stepping asymmetry during gait of transfemoral amputees', Applied Bionics and Biomechanics, 2019, p. 4769242.

Mohamed Refai, M. I., Van Beijnum, B. J. F., Buurke, J. H. and Veltink, P. H. (2020) 'Portable Gait Lab: Estimating 3D GRF Using a Pelvis IMU in a Foot IMU Defined Frame', IEEE Transactions on Neural Systems and Rehabilitation Engineering, 28(6), pp. 1308–1316.

Mohan Varma, D. S. and Sujatha, S. (2017) 'Segmental contributions to the center of mass movement in normal gait', Applied Mathematical Modelling, 46, pp. 328–338.

Morgan, S. J., Hafner, B. J., Kartin, D. and Kelly, V. E. (2018) 'Dual-task standing and walking in people with lower limb amputation: A structured review', Prosthetics and Orthotics International, 42(6), pp. 652–666.

Muro-de-la-Herran, A., García-Zapirain, B. and Méndez-Zorrilla, A. (2014) 'Gait analysis methods: An overview of wearable and non-wearable systems, highlighting clinical applications', Sensors (Switzerland), 14(2), pp. 3362–3394.

Myklebust, H., Gløersen, Ø. and Hallén, J. (2015) 'Validity of Ski Skating Center-of-Mass Displacement Measured by a Single Inertial Measurement Unit.', Journal of applied biomechanics, 31(6), pp. 492–8.

Najafi, B., Bharara, M., Talal, T. K. and Armstrong, D. G. (2012) 'Advances in balance assessment and balance training for diabetes', Diabetes Management, 2(4), pp. 293–308.

Najafi, B., Lee-Eng, J., Wrobel, J. S. and Goebel, R. (2015) 'Estimation of Center of Mass Trajectory using Wearable Sensors during Golf Swing.', Journal of sports science & medicine, 14(2), pp. 354–63.

Neptune, R. and Vistamehr, A. (2019) 'Dynamic Balance during Human Movement: Measurement and Control Mechanisms', Journal of Biomechanical Engineering, 141(7), p. 070801.

Nguyen, H., Lebel, K., Boissy, P., Bogard, S., Goubault, E. and Duval, C. (2017) 'Auto detection and segmentation of daily living activities during a Timed Up and Go task in people with Parkinson's disease using multiple inertial sensors', Journal of NeuroEngineering and Rehabilitation, 14(1), pp. 1–13.

Noamani, A., Nazarahari, M., Lewicke, J., Vette, A. H. and Rouhani, H. (2020) 'Validity of using wearable inertial sensors for assessing the dynamics of standing balance', Medical Engineering and Physics, (xxxx).

Nolan, L., Wit, A., Dudziñski, K., Lees, A., Lake, M. and Wychowañski, M. (2003) 'Adjustments in gait symmetry with walking speed in trans-femoral and trans-tibial amputees', Gait & posture, 17(2), pp. 142–151.

Nott, C. R., Neptune, R. R. and Kautz, S. A. (2014) 'Relationships between frontal-plane angular momentum and clinical balance measures during post-stroke hemiparetic walking', Gait & Posture, 39(1), pp. 129–134.

Ochoa-Diaz, C. and Padilha L. Bó, A. (2020) 'Symmetry Analysis of Amputee Gait Based on Body Center of Mass Trajectory and Discrete Fourier Transform', Sensors, 20(8), p. 2392.

Pacher, L., Chatellier, C., Vauzelle, R. and Fradet, L. (2020) 'Sensor-to-Segment Calibration Methodologies for Lower - Body Kinematic Analysis with Inertial Sensors : A Systematic Review', Sensors, 20(3322).

Pacini Panebianco, G., Bisi, M. C., Stagni, R. and Fantozzi, S. (2018) 'Analysis of the performance of 17 algorithms from a systematic review: Influence of sensor position, analysed variable and computational approach in gait timing estimation from IMU measurements', Gait and Posture, 66, pp. 76–82.

Palermo, E., Rossi, S., Marini, F., Patanè, F. and Cappa, P. (2014) 'Experimental evaluation of

accuracy and repeatability of a novel body-to-sensor calibration procedure for inertial sensor-based gait analysis', Measurement, 52(1), pp. 145–155.

Paradisi, F. (2016) Motor Ability Assessment in Lower-Limb Amputees.

Paradisi, F., Di Stanislao, E., Summa, A., Brunelli, S., Traballesi, M. and Vannozzi, G. (2019) 'Upper body accelerations during level walking in transtibial amputees', Prosthetics and Orthotics International, 43(2), pp. 204–212.

Pasciuto, I., Bergamini, E., Iosa, M., Vannozzi, G. and Cappozzo, A. (2017) 'Overcoming the limitations of the Harmonic Ratio for the reliable assessment of gait symmetry.', Journal of biomechanics, 53, pp. 84–89.

Patel, S., Park, H., Bonato, P., Chan, L. and Rodgers, M. (2012) 'A review of wearable sensors and systems with application in rehabilitation', Journal of NeuroEngineering and Rehabilitation, 9(1), p. 21.

Pavei, G., Salis, F., Cereatti, A. and Bergamini, E. (2020) 'Body center of mass trajectory and mechanical energy using inertial sensors: a feasible stride?', Gait & Posture, 80, pp. 199–205.

Pavei, G., Seminati, E., Cazzola, D. and Minetti, A. E. (2017) 'On the estimation accuracy of the 3D body center of mass trajectory during human locomotion: Inverse vs. forward dynamics', Frontiers in Physiology, 8(MAR), pp. 1–13.

Perry, J. (1992) Gait Analysis Normal and Pathological Function. Thorofare, NJ, Slack Incorporated.

Pfau, T., Witte, T. H. and Wilson, A. M. (2005) 'A method for deriving displacement data during cyclical movement using an inertial sensor', Journal of Experimental Biology, 208(13), pp. 2503–2514.

Piazza, L., Ferreira, E. G., Minsky, R. C., Pires, G. K. W. and Silva, R. (2017) 'Assesment of physical activity in amputees : Évaluation de l'activité physique chez les amputés : revue', Science et Sports, 32(4), pp. 191–202.

Picerno, P. (2017) '25 years of lower limb joint kinematics by using inertial and magnetic sensors: A review of methodological approaches', Gait and Posture. Elsevier B.V., pp. 239–246.

Picerno, P., Cereatti, A. and Cappozzo, A. (2008) 'Joint kinematics estimate using wearable inertial and magnetic sensing modules', Gait and Posture, 28(4), pp. 588–595.

Picerno, P., Cereatti, A. and Cappozzo, A. (2011) 'A spot check for assessing static orientation consistency of inertial and magnetic sensing units', Gait and Posture, 33(3), pp. 373–378.

Pillet, H., Bonnet, X., Lavaste, F. and Skalli, W. (2010) 'Evaluation of force plate-less estimation of the trajectory of the centre of pressure during gait. Comparison of two anthropometric models', Gait and Posture, 31(2), pp. 147–152.

Poitras, I., Dupuis, F., Bielmann, M., Campeau-Lecours, A., Mercier, C., Bouyer, L. J. and Roy, J. S. (2019) 'Validity and reliability of wearable sensors for joint angle estimation: A systematic review', Sensors (Switzerland), 19(7), pp. 1–17.

Popovic, M., Hofmann, A. and Herr, H. (2004) 'Angular momentum regulation during human walking: biomechanics and control', pp. 2405-2411 Vol.3.

Portney, L. G. and Watkins, M. P. (2015) Foundations of clinical research: applications to practice. 3rd edn. Edited by Pearson. Upper Saddle River, N.J: Pearson/Prentice Hall.

Preece, S. J., Goulermas, J. Y., Kenney, L. P. J. and Howard, D. (2009) 'A comparison of feature extraction methods for the classification of dynamic activities from accelerometer data.', IEEE transactions on bio-medical engineering, 56(3), pp. 871–9.

Prinsen, E. C., Nederhand, M. J. and Rietman, J. S. (2011) 'Adaptation strategies of the lower extremities of patients with a transtibial or transfemoral amputation during level walking: A systematic review', Archives of Physical Medicine and Rehabilitation, 92(8), pp. 1311–1325.

Redfield, M. T., Cagle, J. C., Hafner, B. J. and Sanders, J. E. (2013a) 'amputations', 50(9), pp. 1201–1212.

Redfield, M. T., Cagle, J. C., Hafner, B. J. and Sanders, J. E. (2013b) 'Classifying prosthetic use via

accelerometry in persons with transtibial amputations', Journal of rehabilitation research and development, 50(9), pp. 1201–1212.

Regterschot, G. R. H., Folkersma, M., Zhang, W., Baldus, H., Stevens, M. and Zijlstra, W. (2014) 'Gait & Posture Sensitivity of sensor-based sit-to-stand peak power to the effects of training leg strength , leg power and balance in older adults', Gait & Posture, 39(1), pp. 303–307.

Regterschot, G. R. H., Zhang, W., Baldus, H., Stevens, M. and Zijlstra, W. (2016) 'Accuracy and concurrent validity of a sensor-based analysis of sit-to-stand movements in older adults.', Gait & posture, 45, pp. 198–203.

Reid, L., Thomson, P., Besemann, M. and Dudek, N. (2015) 'Going places: Does the two-minute walk test predict the six-minute walk test in lower extremity amputees?', Journal of Rehabilitation Medicine, 47(3), pp. 256–261.

Ren, L., Jones, R. K. and Howard, D. (2008) 'Whole body inverse dynamics over a complete gait cycle based only on measured kinematics', Journal of Biomechanics, 41(12), pp. 2750–2759.

Resnik, L. and Borgia, M. (2011) 'Reliability of Outcome Measures for People With Lower-Limb Amputations: Distinguishing True Change From Statistical Error', Physical Therapy, 91(4), pp. 555–565.

Richman, J. S. and Randall Moorman, J. (2000) 'Physiological time-series analysis using approximate entropy and sample entropy', Am.J.Physiol Heart Circ Physiol, 278(6), pp. H2039–H2049.

Riva, F., Bisi, M. C. and Stagni, R. (2014) 'Gait variability and stability measures: Minimum number of strides and within-session reliability', Computers in Biology and Medicine, 50, pp. 9–13.

Riva, F., Toebes, M. J. P., Pijnappels, M., Stagni, R. and van Dieën, J. H. (2013) 'Estimating fall risk with inertial sensors using gait stability measures that do not require step detection', Gait & Posture, 38(2), pp. 170–174.

Robert, T., Leborgne, P., Beurier, G. and Dumas, R. (2017) 'Estimation of body segment inertia parameters from 3D body scanner images: a semi-automatic method dedicated to human movement analysis applications', Computer Methods in Biomechanics and Biomedical Engineering, 20(October), pp. 177–178.

Roerdink, M., Roeles, S., van der Pas, S. C. H., Bosboom, O. and Beek, P. J. (2012) 'Evaluating asymmetry in prosthetic gait with step-length asymmetry alone is flawed', Gait and Posture, 35(3), pp. 446–451.

Roetenberg, D. (2006) Inertial and magnetic sensing of human motion.

Rosenbaum Chou, T. G., Webster, J. B., Shahrebani, M., Roberts, T. L., Bloebaum, R. D., Chou, T. G. R., Webster, J. B., Shahrebani, M., Roberts, T. L. and Bloebaum, R. D. (2009) 'Characterization of step count accuracy of actigraph activity monitor in persons with lower limb amputation', Journal of Prosthetics and Orthotics, 21(4), pp. 208–214.

Rueda, F. M., Diego, I. M. A., Sánchez, A. M., Tejada, M. C., Montero, F. M. R. and Page, J. C. M. (2013) 'Knee and hip internal moments and upper-body kinematics in the frontal plane in unilateral transtibial amputees', Gait and Posture, 37(3), pp. 436–439.

Sabatini, A. M. (2011) 'Estimating three-dimensional orientation of human body parts by inertial/magnetic sensing.', Sensors (Basel, Switzerland), 11(2), pp. 1489–525.

Sabatini, A. M., Ligorio, G. and Mannini, A. (2015) 'Fourier-based integration of quasi-periodic gait accelerations for drift-free displacement estimation using inertial sensors', BioMedical Engineering OnLine, 14(1), p. 106.

Sabatini, A. M. and Mannini, A. (2016) 'Ambulatory Assessment of Instantaneous Velocity during Walking Using Inertial Sensor Measurements.', Sensors, 16(12), p. 2206.

Sabatini, A. M., Martelloni, C., Scapellato, S. and Cavallo, F. (2005) 'Assessment of walking features from foot inertial sensing', IEEE Transactions on Biomedical Engineering, 52(3), pp. 486–494.

Sagawa, Y., Turcot, K., Armand, S., Thevenon, A., Vuillerme, N. and Watelain, E. (2011) 'Biomechanics and physiological parameters during gait in lower-limb amputees: A systematic review',

Gait and Posture, 33(4), pp. 511–526.

Salarian, A., Russmann, H., Vingerhoets, F. J. G., Dehollain, C., Blanc, Y., Burkhard, P. R. and Aminian, K. (2004) 'Gait Assessment in Parkinson ' s Disease : Toward an Ambulatory System for Long-Term Monitoring', IEEE Transactions on Biomedical Engineering, 51(8), pp. 1434–1443.

Samuelsen, B. T., Andrews, K. L., Houdek, M. T., Terry, M., Shives, T. C. and Sim, F. H. (2017) 'The Impact of the Immediate Postoperative Prosthesis on Patient Mobility and Quality of Life after Transtibial Amputation', American Journal of Physical Medicine and Rehabilitation, 96(2), pp. 116–119.

Samuelsson, K. A. M., Toytari, O., Salminen, A.-L. A.-L. A.-L. A.-L., Brandt, A., Töytäri, O., Salminen, A.-L. A.-L. A.-L. A.-L., Brandt, A., Toytari, O., Salminen, A.-L. A.-L. A.-L. A.-L. and Brandt, A. (2012) 'Effects of lower limb prosthesis on activity, participation, and quality of life: a systematic review.', Prosthetics and orthotics international, 36(2), pp. 145–158.

Santos-lozano, A., Santin-medeiros, F., Bailón, R., Bergmeir, C., Ruiz, J. R., Lucia, A. and Garatachea, N. (2014) 'Actigraph GT3X : Validation and Determination of Physical Activity Intensity Cut Points Personal pdf file for Actigraph GT3X : Validation and Determination of Physical', (May 2013).

Saunders, J. B., Inman, V. T. and Eberhart, H. D. (1953) 'The major determinants in normal and pathological gait', J Bone Joint Surg, 35-A(3), pp. 543–558.

Sawers, A. B. and Hafner, B. J. (2013) 'Outcomes associated with the use of microprocessor-controlled prosthetic knees among individuals with unilateral transfemoral limb loss: A systematic review', The Journal of Rehabilitation Research and Development, 50(3), p. 273.

Schepers, M., Giuberti, M. and Bellusci, G. (2018) 'Xsens MVN : Consistent Tracking of Human Motion Using Inertial Sensing', Xsens Technologies, (March), pp. 1–8.

Schmalz, T., Blumentritt, S. and Jarasch, R. (2002) 'Energy expenditure and biomechanical characteristics of lower limb amputee gait: The influence of prosthetic alignment and different prosthetic components', Gait & Posture, 16(3), pp. 255–263.

van Schooten, K. S., Rispens, S. M., Pijnappels, M., Daffertshofer, A. and van Dieen, J. H. (2013) 'Assessing gait stability: The influence of state space reconstruction on inter- and intra-day reliability of local dynamic stability during over-ground walking', Journal of Biomechanics, 46(1), pp. 137–141.

Seel, T., Raisch, J. and Schauer, T. (2014) 'IMU-based joint angle measurement for gait analysis.', Sensors (Basel, Switzerland), 14(4), pp. 6891–909.

Selles, R. W., Formanoy, M. A. G., Bussmann, J. B. J., Janssens, P. J. and Stam, H. J. (2005) 'Automated estimation of initial and terminal contact timing using accelerometers; development and validation in transtibial amputees and controls', IEEE Transactions on Neural Systems and Rehabilitation Engineering, 13(1), pp. 81–88.

Seroussi, R. E., Gitter, A., Czerniecki, J. M. and Weaver, K. (1996) 'Mechanical work adaptations of above-knee amputee ambulation', Arc, 77(November).

Shahabpoor, E. and Pavic, A. (2017) Measurement of walking ground reactions in real-life environments: A systematic review of techniques and technologies, Sensors (Switzerland).

Shahabpoor, Erfan and Pavic, A. (2018) 'Estimation of tri-axial walking ground reaction forces of left and right foot from total forces in real-life environments', Sensors (Switzerland), 18(6).

Shahabpoor, E. and Pavic, A. (2018) 'Estimation of vertical walking ground reaction force in real-life environments using single IMU sensor', Journal of Biomechanics, 79, pp. 181–190.

Shahabpoor, E., Pavic, A., Brownjohn, J. M. W., Billings, S. A., Guo, L. Z. and Bocian, M. (2018) 'Real-life measurement of tri-axial walking ground reaction forces using optimal network of wearable inertial measurement units', IEEE Transactions on Neural Systems and Rehabilitation Engineering, 26(6), pp. 1243–1253.

Silverman, A. K., Fey, N. P., Portillo, A., Walden, J. G., Bosker, G. and Neptune, R. R. (2008) 'Compensatory mechanisms in below-knee amputee gait in response to increasing steady-state walking speeds', Gait & posture, 28, pp. 602–609.

Simonetti, E., Bergamini, E., Bascou, J., Vannozzi, G. and Pillet, H. (2020) 'Development of a wearable framework for body center of mass acceleration assessment in people with transfemoral amputation', Computer Methods in Biomechanics and Biomedical Engineering, (accepted).

Smidt, G. L., Arora, J. S. and Johnston, R. C. (1971) 'Accelerographic analysis of several types of walking.', American Journal of Physical Medicine, 50(6), pp. 285–300.

Steins, D., Sheret, I., Dawes, H., Esser, P. and Collett, J. (2014) 'A smart device inertial-sensing method for gait analysis', Journal of Biomechanics, 47(15), pp. 3780–3785.

Storm, F. A., Buckley, C. J. and Mazzà, C. (2016) 'Gait event detection in laboratory and real life settings: Accuracy of ankle and waist sensor based methods', Gait and Posture, 50, pp. 42–46.

Strutzenberger, G., Alexander, N., De Asha, A., Schwameder, H. and Barnett, C. T. (2019) 'Does an inverted pendulum model represent the gait of individuals with unilateral transfemoral amputation while walking over level ground?', Prosthetics and Orthotics International, 43(2), pp. 221–226.

Summa, A., Vannozzi, G., Bergamini, E., Iosa, M., Morelli, D. and Cappozzo, A. (2016) 'Multilevel upper body movement control during gait in children with cerebral palsy', PLoS ONE, 11(3), pp. 1–13.

Tan, T., Chiasson, D. P., Hu, H. and Shull, P. B. (2019) 'Influence of IMU position and orientation placement errors on ground reaction force estimation', Journal of Biomechanics, 97, p. 109416.

Tesio, L., Lanzi, D. and Detrembleur, C. (1998) 'The 3-D motion of the centre of gravity of the human body during level walking. II. Lower limb amputees', Clinical Biomechanics, 13(2), pp. 83–90.

Tesio, L. and Rota, V. (2019) 'The Motion of Body Center of Mass During Walking: A Review Oriented to Clinical Applications', Frontiers in Neurology, 10(September), pp. 1–22.

Teufl, W., Miezal, M., Taetz, B., Fröhlich, M. and Bleser, G. (2018) 'Validity, test-retest reliability and long-term stability of magnetometer free inertial sensor based 3D joint kinematics', Sensors (Switzerland), 18(7).

Teufl, W., Miezal, M., Taetz, B., Frohlichi, M. and Bleser, G. (2019) 'Validity of inertial sensor based 3D joint kinematics of static and dynamic sport and physiotherapy specific movements', PLoS ONE, 14(2), pp. 1–18.

Thomas-Pohl, M., Villa, C., Davot, J., Bonnet, X., Facione, J., Lapeyre, E., Bascou, J. and Pillet, H. (2019) 'Microprocessor prosthetic ankles: comparative biomechanical evaluation of people with transtibial traumatic amputation during standing on level ground and slope', Disability and Rehabilitation: Assistive Technology, pp. 1–10.

Timmermans, C., Cutti, A. G., van Donkersgoed, H. and Roerdink, M. (2019) 'Gaitography on lower-limb amputees: Repeatability and between-methods agreement', Prosthetics and Orthotics International, 43(1), pp. 71–79.

Tramontano, M., Bergamini, E., Iosa, M., Belluscio, V., Vannozzi, G. and Morone, G. (2018) 'Vestibular rehabilitation training in patients with subacute stroke: A preliminary randomized controlled trial', NeuroRehabilitation, 43(2), pp. 247–254.

Trojaniello, D., Cereatti, A. and Della Croce, U. (2014) 'Accuracy, sensitivity and robustness of five different methods for the estimation of gait temporal parameters using a single inertial sensor mounted on the lower trunk.', Gait & posture, 40(4), pp. 487–92.

Trojaniello, D., Cereatti, A., Pelosin, E., Avanzino, L., Mirelman, A., Hausdorff, J. M. and Della Croce, U. (2014) 'Estimation of step-by-step spatio-temporal parameters of normal and impaired gait using shank-mounted magneto-inertial sensors: application to elderly, hemiparetic, parkinsonian and choreic gait.', Journal of neuroengineering and rehabilitation, 11(1), p. 152.

Trojaniello, D., Ravaschio, A., Hausdorff, J. M. and Cereatti, A. (2015) 'Comparative assessment of different methods for the estimation of gait temporal parameters using a single inertial sensor: application to elderly, post-stroke, Parkinson's disease and Huntington's disease subjects.', Gait & posture, 42(3), pp. 310–6.

Tunca, C., Pehlivan, N., Ak, N., Arnrich, B., Salur, G. and Ersoy, C. (2017) 'Inertial sensor-based

robust gait analysis in non-hospital settings for neurological disorders', Sensors (Switzerland), 17(4), pp. 1–29.

Tura, A., Raggi, M., Rocchi, L., Cutti, A. G. and Chiari, L. (2010) 'Gait symmetry and regularity in transfemoral amputees assessed by trunk accelerations', Journal of NeuroEngineering and Rehabilitation, 7(1), p. 4.

Van Velzen, J. M., Van Bennekom, C. A. M., Polomski, W., Slootman, J. R., Van Der Woude, L. H. V. and Houdijk, H. (2006) 'Physical capacity and walking ability after lower limb amputation: A systematic review', Clinical Rehabilitation, 20(11), pp. 999–1016.

Villa, C. (2014) Analyse de la marche des personnes amputées de membre inférieur en situations contraignantes de la vie courante. Rapport de thèse - Arts et Métiers ParisTech.

Villa, C., Bascou, J., Loiret, I., Martinet, N., Bonnet, X. and Pillet, H. (2017) 'Recherches sur la thématique de l ' appareillage de la personne amputée de membre inférieur en rééducation fonctionnelle', in Colloque Jeunes Chercheurs Jeunes Chercheuses, 8 juin 2017, Paris, France.

Villa, C., Loiret, I., Langlois, K., Bonnet, X., Lavaste, F., Fodé, P. and Pillet, H. (2017) 'Cross-Slope and Level Walking Strategies During Swing in Individuals With Lower Limb Amputation', Archives of Physical Medicine and Rehabilitation, 98(6), pp. 1149–1157.

Villeger, D., Costes, A., Watier, B. and Moretto, P. (2014) 'An algorithm to decompose ground reaction forces and moments from a single force platform in walking gait', Medical Engineering and Physics, 36(11), pp. 1530–1535.

Walker, C. R. C., Ingram, R. R., Hullin, M. G. and McCreath, S. W. (1994) 'Lower limb amputation following injury: a survey of long-term functional outcome', Injury, 25(6), pp. 387–392.

van de Walle, P., Hallemans, A., Schwartz, M., Truijen, S., Gosselink, R. and Desloovere, K. (2012) 'Mechanical energy estimation during walking: Validity and sensitivity in typical gait and in children with cerebral palsy', Gait and Posture, 35(2), pp. 231–237.

Waters, R. L. and Mulroy, S. (1999) 'The energy expenditure of normal and pathologic gait', Gait and Posture, 9(3), pp. 207–231.

Waters, R. L., Perry, J., Antonelli, D. and Hislop, H. (1976) 'Energy cost of walking of amputees: the influence of level of amputation', Journal of Bone and Joint Surgery - Series A, 58(1), pp. 42–46.

Weir, J. (2005) 'Quantitative test-retest reliability using the intraclass correlation coefficient and teh SEM', Journal of strength and conditioning research, 19(1), pp. 231–240.

Wentink, E. C., Beijen, S. I., Hermens, H. J., Rietman, J. S. and Veltink, P. H. (2013) 'Intention detection of gait initiation using EMG and kinematic data.', Gait & posture, 37(2), pp. 223–8.

Whittle, M. W. (2007) Gait Analysis - An introduction. Butterwort. Edited by M. W. Whittle. Elsevier.

Wilhoite, S., Williams, S., Cook, J. and Ryan, G. (2019) 'Rehabilitation, Guidelines, and Exercise Prescription for Lower Limb Amputees', Strength and Conditioning Journal, p. 1.

Winter, D. (1995) 'Human balance and posture control during standing and walking', Gait & Posture, 3(4), pp. 193–214.

Wong, C., Zhang, Z. Q., Lo, B. and Yang, G. Z. (2015) 'Wearable Sensing for Solid Biomechanics: A Review', IEEE Sensors Journal, 15(5), pp. 2747–2760.

Wong, W. Y., Wong, M. S. and Lo, K. H. (2007) 'Clinical applications of sensors for human posture and movement analysis: A review', Prosthetics and Orthotics International, 31(1), pp. 62–75.

Yang, E. C. Y. and Mao, M. H. (2015) '3D analysis system for estimating intersegmental forces and moments exerted on human lower limbs during walking motion', Measurement: Journal of the International Measurement Confederation, 73, pp. 171–179.

Yang, L., Dyer, P. S., Carson, R. J., Webster, J. B., Bo Foreman, K. and Bamberg, S. J. M. (2012) 'Utilization of a lower extremity ambulatory feedback system to reduce gait asymmetry in transtibial amputation gait', Gait & Posture, 36(3), pp. 631–634.

Yang, S. and Li, Q. (2012a) 'IMU-based ambulatory walking speed estimation in constrained treadmill and overground walking', Computer Methods in Biomechanics and Biomedical Engineering, 15(3), pp. 313–322.

Yang, S. and Li, Q. (2012b) 'Inertial Sensor-Based Methods in Walking Speed Estimation: A Systematic Review', Sensors, 12(12), pp. 6102–6116.

Yuan, Q. and Chen, I. (2012) 'Physical Human velocity and dynamic behavior tracking method for inertial capture system', 183, pp. 123–131.

Yuan, Q. and Chen, I. (2014) 'Physical Localization and velocity tracking of human via 3 IMU sensors', Sensors & Actuators A : Physical, 212, pp. 25–33.

Yuan, Q. and Chen, I. M. (2014) 'Human Velocity Tracking and Localization Using 3 IMU Sensors', Sensors & Actuators A, 212, pp. 25–33.

Zabat, M., Ababou, A., Ababou, N. and Dumas, R. (2019) 'IMU-based sensor-to-segment multiple calibration for upper limb joint angle measurement—a proof of concept', Medical and Biological Engineering and Computing, 57(11), pp. 2449–2460.

Zhang, T., Bai, X., Liu, F., Ji, R. and Fan, Y. (2020) 'The effect of prosthetic alignment on hip and knee joint kinetics in individuals with transfemoral amputation', Gait and Posture, 76(1), pp. 85–91.

Ziegler-Graham, K., MacKenzie, E. J., Ephraim, P. L., Travison, T. G. and Brookmeyer, R. (2008) 'Estimating the Prevalence of Limb Loss in the United States: 2005 to 2050', Archives of Physical Medicine and Rehabilitation, 89(3), pp. 422–429.

Zijlstra, W., Bisseling, R. W., Schlumbohm, S. and Baldus, H. (2010) 'A body-fixed-sensor-based analysis of power during sit-to-stand movements.', Gait & posture, 31(2), pp. 272–8.

Zijlstra, W. and Hof, A. L. (2003) 'Assessment of spatio-temporal gait parameters from trunk accelerations during human walking', Gait & Posture, 18(2), pp. 1–10.

List of communications and publications

International peer-reviewed journals

E. Simonetti, E. Bergamini, C. Villa, J. Bascou, G. Vannozzi, H. Pillet. Gait events detection using inertial measurement units in people with transfemoral amputation: a comparative study, *Medical & Biological Engineering & Computing*, 58:461–470 (2020). doi: 10.1007/s11517-019-02098-4

Conference proceedings published on International Journals

E. Simonetti, H. Pillet, G. Vannozzi, I. Loiret, C. Villa, J. Bascou & E. Bergamini (2019), Investigating symmetry in amputee gait through the improved harmonic ratio: influence of the stride segmentation method, *Computer Methods in Biomechanics and Biomedical Engineering*, 22:sup1, S221-S223, doi: 10.1080/10255842.2020.1714248, *44th congress of the Société de Biomécanique, 28 - 30 October 2019, Poitiers*

E. Simonetti, E. Bergamini, J. Bascou, G. Vannozzi & H. Pillet (2020), Development of a wearable framework for body center of mass acceleration assessment in people with transfemoral amputation, *Computer Methods in Biomechanics and Biomedical Engineering*, accepted (doi: 10.1080/10255842.2020.1816294), *45th congress of the Société de Biomécanique, 26 - 28 October 2020, Metz*

J. Durand, A. Prat, T. Provot, J. Bascou & **E. Simonetti** (2020), Preliminary study: identification of gait stability indices for the rehabilitation follow-up of people with transtibial amputation, *Computer Methods in Biomechanics and Biomedical Engineering*, accepted (doi: 10.1080/10255842.2020.1812172), *45th congress of the Société de Biomécanique, 26 - 28 October 2020, Metz*

J. Basel, **E. Simonetti**, E. Bergamini, J. Bascou, G. Vannozzi & H. Pillet (2020), Definition of an optimal model based on segments' contribution for the estimation of the acceleration of the center of mass in people with lower-limb amputation, *Computer Methods in Biomechanics and Biomedical Engineering*, accepted (doi: 10.1080/10255842.2020.1811499), *45th congress of the Société de Biomécanique, 26 - 28 October 2020, Metz*

International conference proceedings

E. Simonetti, C. Villa, J. Bascou, I. Loiret, E. Bergamini, G. Vannozzi, H. Pillet, Stance phase duration estimation from inertial sensors in a population of people with transfemoral amputation: comparison of five algorithms, *ISPO 17th World Congress, 5 - 8 october 2019, Kobe, Japan*

National conference proceedings

E. Vacherand, C. Villa, J. Bascou, E. Bergamini, G. Vannozzi, H. Pillet, Capteurs embarqués et rééducation : état de l'art, XXIIème Congrès National Scientifique de l'International Society of Prosthetics and Orthotics, ISPO France, 16 novembre 2018, Lyon, France

E. Simonetti, C. Villa, J. Bascou, E. Bergamini, G. Vannozzi, H. Pillet, Estimation des paramètres temporels de la marche à l'aide de centrales inertielles chez la personne amputée de membre inférieur

204

au niveau transfémoral : une étude comparative, 8ème Congrès de la SOFAMEA, 23 - 25 janvier 2019, Grenoble, France [poster]

E. Simonetti, G. Vannozzi, I. Loiret, C. Villa, J. Bascou, H. Pillet, <u>E. Bergamini</u>, A comparative analysis of gait symmetry indices in people with transfemoral amputation, XX CONGRESSO SIAMOC, Società Italiana di Analisi del Movimento in Clinica, 9-12 October 2019, Bologna, Italy [poster]

Emeline SIMONETTI

Contribution to the development and validation of wearable-sensor-based methodologies for gait assessment and rehabilitation of people with lower limb amputation

Résumé

Un des objectifs majeurs de la rééducation des personnes amputées de membre inférieur appareillées est le retour à une marche physiologique, efficace énergétiquement et minimisant le risque de chutes lié à la perte d'équilibre. Peu d'outils cliniques permettent aujourd'hui de quantifier ces aspects de la locomotion. L'émergence de capteurs embarqués miniaturisés offre des opportunités pour la description quantitative et écologique de la marche. Dans ce contexte, l'objectif de la thèse était de contribuer au développement de protocoles embarqués pour apporter des données quantitatives pertinentes lors de la rééducation à la marche des personnes amputées de membre inférieur. Deux approches complémentaires ont été adoptées. La première approche consiste à utiliser un modèle biomécanique du corps afin d'extraire des descripteurs quantifiés pertinents. Un protocole permettant d'estimer l'accélération et la vitesse instantanée du centre de masse à partir de 5 centrales inertielles a ainsi été proposé à partir d'une analyse préliminaire sur les données de marche de dix personnes amputées transfémorales et a été validé chez une personne amputée transfémorale. La seconde approche consiste à extraire des paramètres concis par traitement du signal des données brutes des capteurs. La fiabilité et la pertinence clinique de la quantification de tels paramètres pour caractériser la symétrie et l'équilibre de la marche ont été étudiées pour la première fois chez les personnes amputées de membre inférieur. L'ensemble des travaux produits au cours de cette thèse contribue ainsi au transfert vers la clinique des outils embarqués d'analyse du mouvement par l'identification de paramètres biomécaniques et cliniques pertinents et la validation d'algorithmes originaux permettant la quantification de la marche des amputés de membre inférieur.

Mots clés : Analyse quantifiée de la marche, capteurs embarqués, centre de masse, équilibre dynamique, symétrie, personnes amputées de membre inférieur

Résumé en anglais

One key objective during the rehabilitation of people with lower-limb amputation fitted with a prosthesis is the restoration of a physiological and energy-efficient gait pattern minimizing falling risks due to the loss of balance. Few practical tools are available to provide quantitative data to assist the follow-up of patients in the clinical routine. The development of wearable sensors offers opportunities to quantitatively and objectively describe gait in ecological situations. In this context, the aim of the thesis is to contribute to the development of wearable tools and protocols to support the functional rehabilitation of lower-limb amputees by providing clinically relevant quantitative data. Two complementary approaches have been implemented. The first approach consists in developing biomechanical models of the human body in order to retrieve biomechanically founded parameters. A protocol allowing to accurately estimate the body center of mass acceleration and instantaneous velocity has therefore been proposed based on gait data of ten people with transfemoral amputation and was validated in one person with transfemoral amputation. The second approach consists in identifying patterns in the signals measured by wearable sensors to extract concise descriptors of gait symmetry and dynamic balance. The clinical relevance and reliability of these descriptors have been investigated for the first time in people with lower-limb amputation. The work produced in the course of this thesis has contributed to the clinical transfer of wearable sensors into the clinical practice through the identification of clinically and biomechanically relevant parameters and the validation of original algorithms allowing to quantitatively describe the gait of lower-limb amputees.

Key words: Quantitative gait analysis, wearable sensors, center of mass, symmetry, dynamic balance, people with lower-limb amputation